

Aus dem Pharmakologischen Institut

Direktor: Prof. Dr. Thomas Worzfeld

des Fachbereichs Medizin der Philipps-Universität Marburg

Mechanisms of Mitotic Spindle Orientation by Plexin-B2

Inaugural-Dissertation

zur Erlangung des Doktorgrades der Naturwissenschaften

Doctor of Natural Sciences

dem Fachbereich Medizin der Philipps-Universität Marburg

vorgelegt von

Javier Fernández Baldovinos

aus Huesca, Spanien

Marburg, 2021

Angenommen vom Fachbereich Medizin der Philipps-Universität Marburg am:

28. Januar 2021

Gedruckt mit Genehmigung des Fachbereichs Medizin

Dekanin: Frau Prof. Dr. D. Hilfiker-Kleiner

Referent: Herr Prof. Dr. T. Worzfeld

1. Korreferent: Herr Prof. Dr. O. Hantschel

Table of contents

List of figures	5
List of tables.....	9
Abbreviations.....	11
Abstract	15
Zusammenfassung.....	16
1. Introduction	19
1.1. Cell polarity	19
1.2. Types of cell polarity	22
1.3. Epithelial cell polarity.....	33
1.4. Mitotic spindle orientation	38
1.5. Semaphorin-plexin signaling.....	46
1.6. CRISPR/Cas9 genome editing.....	56
2. Aim of this study.....	59
3. Materials and Methods	61
3.1. Materials	61
3.2. Methods.....	71
3.2.1. Immunofluorescence staining of murine tissue	71
3.2.2. Cell culture	73
3.2.3. Immunofluorescence staining of 2D and 3D cell cultures	74
3.2.4. Generation of fluorophore-labelled protein constructs in viral plasmids	75
3.2.5. Plexin-B1 and Plexin-B2 expression analysis.....	81
3.2.6. CRISPR/Cas9 genome editing.....	85
3.2.7. Generation of virally-transduced stable cell lines.....	92
3.2.8. Lumen formation assay	95

3.2.9. Cell counting and crystal violet staining.....	96
3.2.10. Cell cycle analysis	97
3.2.11. Spinning disk microscopy	97
4. Results.....	99
4.1. Plexin-B2 and its ligand sema4D localize to the basolateral membrane in the renal epithelium.....	99
4.2. Plexin-B2 localizes to cell-cell contacts in mIMCD-3 cells in 2D and 3D cultures	100
4.3. Plexin-B2 localizes to cell-cell contacts during mitosis in MDCK cysts.....	103
4.4. The basolateral localization of Plexin-B2 is ligand-independent.....	104
4.5. The localization of Plexin-B2 to cell-cell contacts is independent of its intracellular domain in MDCK and mIMCD-3 cells in 2D	105
4.6. The localization of Plexin-B2 to the basolateral membrane in MDCK and mIMCD-3 cysts is dependent on its intracellular domain.....	110
4.7. Identification of a possible motif required for the sorting of Plexin-B2 to the lateral membrane.....	112
4.8. Generation of Plexin-B2-deficient mIMCD-3 cells by CRISPR/Cas9 genome editing	113
4.9. Knockout of Plexin-B2 impairs lumen formation in mIMCD-3 cysts	115
4.10. Knockout of Plexin-B2 does not increase net proliferation of mIMCD-3 cells	118
4.11. Knockout of Plexin-B2 increases the proportion of cells in the S and G2/M phases and aneuploidy in mIMCD-3 cells.....	121
4.12. Knockout of Plexin-B2 does not change LGN and NuMA localization during mitosis.....	122
5. Discussion	127
5.1. Polarized localization of Plexin-B2 in epithelia.....	127
5.2. Plexin-B2 localization during cell division.....	130

Table of contents

5.3. Plexin-B2 localization does not depend on binding to its ligand.....	131
5.4. Identification of a basolateral sorting motif in the cytoplasmic domain of Plexin-B2	132
5.5. Plexin-B2 in mitotic spindle orientation	133
5.6. Plexin-B2 and cell cycle	136
6. Acknowledgements	139
7. List of academic professors	143
8. References	145

List of figures

Figure 1. Polarized cells with different morphologies	19
Figure 2. Generation of a polarity point and delivery of secretory vesicles in <i>S. cerevisiae</i> for budding spore formation	21
Figure 3. Front-rear polarity in migratory cells	23
Figure 4. Components of the “core” planar cell polarity pathway	25
Figure 5. Anterior-posterior axis determination in the <i>C. elegans</i> zygote.....	28
Figure 6. Asymmetric cell division during the development of the nervous system in <i>Drosophila</i>	29
Figure 7. Localization and interactions of polarity proteins in the establishment of apicobasal polarity and its maintenance.....	32
Figure 8. Epithelial polarity	35
Figure 9. Alignment of the mitotic spindle with the anterior-posterior axis in the <i>C. elegans</i> zygote	39
Figure 10. Model of mitotic spindle orientation by the Gai-LGN-NuMA complex.....	40
Figure 11. Mitotic spindle orientation along the apico-basal axis	42
Figure 12. Alignment of the mitotic spindle with the epithelial plane	44
Figure 13. Different mitotic spindle orientation axes during tubular organ morphogenesis	45
Figure 14. Semaphorin and plexin families	46
Figure 15. CRISPR/Cas9 system	56
Figure 16. Principle of the indel PCR	90
Figure 17. Confocal images of immunofluorescence stainings of Plexin-B2, Sema4D, E-cadherin and ZO-1 in embryonic and adult mouse renal epithelium	100
Figure 18. Confocal images of immunofluorescence staining of Plexin-B2 and E-cadherin in mIMCD-3 cells in two-dimensional culture.....	101
Figure 19. Confocal images of immunofluorescence staining of Plexin-B2, E-cadherin and ZO-1 in mIMCD-3 three-dimensional cysts	102
Figure 20. Spinning disk live-cell microscopy images of Plexin-B2-GFP and H2B- mCherry-expressing MDCK cells during mitosis in 3D cell culture.....	104

Figure 21. Confocal images of immunofluorescence staining of Plexin-B2, E-cadherin and ZO-1 in the renal epithelium of Sema4B, Sema4D and Sema4G triple deficient mice	105
Figure 22. Confocal image of an MDCK cyst expressing Plexin-B2 Δ IC-GFP	106
Figure 23. Sequence alignment of mouse Plexin-A3 (residues 1242-1872) and mouse Plexin-B2 (residues 1123-1842).....	107
Figure 24. Domain structure of the EGFP-tagged Plexin-B2 wild type, complete cytoplasmic deletion mutant (Plexin-B2 Δ IC) and C1, RBD and C2 domains deletion mutant (Plexin-B2 Δ C1-RBD-C2).....	108
Figure 25. Confocal images of MDCK cells growing in 2D and expressing the Plexin-B2 constructs	109
Figure 26. Confocal images of mIMCD-3 cells growing in 2D and expressing the Plexin-B2 constructs	109
Figure 27. Confocal images of MDCK cells growing in 3D and expressing the Plexin-B2 constructs	111
Figure 28. Confocal images of mIMCD-3 cells growing in 3D and expressing the Plexin-B2 constructs	111
Figure 29. Potential lateral localization motif in the cytoplasmic domain of Plexin-B2	112
Figure 30. Alignment of all mouse plexins and human Plexin-B2.....	113
Figure 31. Expression levels of the Plexin-B1 and Plexin B2 genes in mIMCD-3 cells growing in 2D and 3D cultures assessed by qPCR	114
Figure 32. Western blot showing Plexin-B2 in mIMCD-3 cells and in control and knockout CRISPR clones	115
Figure 33. Confocal images of mIMCD-3 Plexin-B2 wild type (control) and Plexin-B2 knockout growing in 3D and stained for β -catenin, ZO-1 and DAPI	116
Figure 34. Quantification of normal and abnormal lumen formation in mIMCD-3 Plexin- B2 wild type and Plexin-B2 knockouts transduced with EGFP-NuMA or EGFP-LGN and tubulin-mCherry	117
Figure 35. Growth of mIMCD-3 control cells and Plexin-B2 mutants.....	119
Figure 36. Crystal violet absorbance-based indirect measurement of growth of mIMCD-3 control cells and Plexin-B2 knockouts	120

Figure 37. Aberrant mitosis in a Plexin-B2 knockout mIMCD-3 cell 121

Figure 38. Cell cycle analysis of control and Plexin-B2 knockout mIMCD-3 cells 122

Figure 39. Spinning disk live-cell imaging of wild type and Plexin-B2 knockout cysts expressing EGFP-LGN and tubulin-mCherry during mitosis 124

Figure 40. Spinning disk live-cell imaging of a Plexin-B2 knockout cyst expressing EGFP-NuMA and labelled with SiR-tubulin during mitosis 125

List of tables

Table 1. Immunofluorescence stainings of murine tissue 72

Table 2. Cell lines used in the study with their origin, culture medium and bibliographic reference 73

Table 3. Immunostainings in mIMCD-3 cells growing in 2D and 3D 75

Table 4. Alkaline phosphatase reaction mix 79

Table 5. Initial components of the reverse transcription mix..... 83

Table 6. Final components of the reverse transcription mix 83

Table 7. Program for the reverse transcription 84

Table 8. qPCR mix 84

Table 9. Virally-transduced cell lines stably expressing fluorescently-labelled proteins 93

Abbreviations

Abl	Abelson tyrosine-protein kinase
AE1	Anion exchanger 1
ANKRD6	Ankyrin repeat domain 6
APC	Adenomatous polyposis coli
aPKC	Atypical protein kinase C
APS	Ammonium persulfate
ARE	Apical recycling endosome
ATP	Adenosine triphosphate
AurA	Aurora A
Baz	Bazooka
Bem1	Bud emergence protein 1
BES	N,N-bis(2-hydroxyethyl)-2-aminoethanesulfonic acid
Bni1	Bud neck involved protein 1
Brat	Brain tumour protein
BSA	Bovine serum albumin
cAMP	Cyclic adenosine monophosphate
Cas	CRISPR-associated
CD	Cluster of differentiation
Cdc	Cell division control protein
cDNA	Complementary deoxyribonucleic acid
Cdx2	Caudal type homeobox 2
CELSR	Cadherin EGF LAG seven-pass G-type receptor
cGMP	Cyclic guanosine monophosphate
COUP-TF2	Chicken ovalbumin upstream promoter transcription factor 2
Crb	Crumbs
CRE	Common recycling endosome
CRISPR	Clustered regularly interspaced short palindromic repeats
CRMP2	Collapsin response mediator protein 2
crRNA	CRISPR ribonucleic acid
CSNK-1	Casein kinase 1
CtBP1	C-terminal binding protein 1
DAPI	4',6-Diamidino-2-phenylindole
Dbl3	Diffuse B-cell lymphoma proto-oncogene 3
Dgo	Diego
Dlg	Discs large
Dll4	Delta-like ligand 4
DLX1	Distal-less homeobox 1
DMEM	Dulbecco's modified Eagle medium
DMSO	Dimethyl sulfoxide
dNTP	Deoxynucleotide triphosphate
Ds	Dachsous

Abbreviations

Dsh	See Dvl
Dvl	Dishevelled
EB1	End-binding protein 1
ECL	Enhanced chemiluminescence substrate
EDTA	Ethylenediaminetetracetic acid
EGFP	Enhanced green fluorescent protein
EGFR	Epidermal growth factor receptor
EMT	Epithelial-to-mesenchymal transition
ErbB2	Avian erythroblastic leukemia viral oncogene B homologue 2
FAK	Focal adhesion kinase
FCS	Fetal calf serum
Fj	Four-jointed
Fmi	Flamingo
Ft	Fat
Fz	Frizzled
GAP	GTPase-activating protein
GDP	Guanosine diphosphate
GEF	Guanine nucleotide exchange factor
GoLoco	G $\alpha_{i/o}$ -Loco interaction motif
GPI	Glycosyl-phosphatidyl-inositol
GPR-1/2	G-protein regulator 1/2
Grhl2	Grainhead-like transcription factor 2
GSK3 β	Glycogen synthase kinase-3 β
GTP	Guanosine triphosphate
HA	Influenza haemagglutinin
HEK293	Human embryonic kidney 293 cells
HR	Homologous recombination
HRP	Horseradish peroxidase
IC	Intracellular
IL	Interleukin
ILK	Integrin-linked kinase
Insc	Inscuteable
IP	Immunoprecipitation
KIF	Kinesin family member
KO	Knockout
L1CAM	L1 cell adhesion molecule
LARG	Leukemia-associated RhoGEF
LB	Lysogeny broth
LET-99	Lethal protein 99
Lgl	Lethal giant larvae
LGN	Leu-Gly-Asn repeat-enriched protein
LIMK1	LIM kinase 1
Lin-5/7	Abnormal cell lineage protein 5/7

Abbreviations

Loco	Locomotion defects gene
MCS	Multiple cloning site
MDCK	Madin-Darby Canine Kidney
MEM	Minimum essential medium
Mena	Mammalian enabled variant
MET	Mesenchymal-to-epithelial transition
MEX	Maternally expressed
mIMCD-3	Murine inner medullary collecting duct 3 cells
MT	Microtubule
MTOC	Microtubule organizing centre
Mud	Mushroom body defect gene
NHEJ	Non-homologous end joining
NKCC1	Sodium-potassium-chloride cotransporter 1
NKX2.1	NK2 homeobox 1
NR2F2	Nuclear receptor subfamily 2 group F member 2
Nrp	Neuropilin
NuMA	Nuclear mitotic apparatus protein
Oct4	Octamer-binding transcription factor 4
PAK	P21-activated kinase
Pals1	Protein associated with Lin-7 1
Par	Partitioning defective protein
Patj	Protein associated to tight junctions
Pax-6	Paired box protein 6
PBS	Phosphate buffered saline
PCP	Planar cell polarity
PCR	Polymerase chain reaction
PDZ	PSD95/Dlg/ZO-1 domain
PFA	Paraformaldehyde
PI3K	Phosphoinositide 3 kinase
Pins	Partner of inscuteable
PIP	Phosphatidylinositol
Pk	Prickle
PKD	Protein kinase D
PPK-1	Phosphatidylinositol-4-phosphate 5' kinase 1
Pros	Prospero
PTEN	Phosphatase and tensin homologue
PVDF	Polyvinylidene fluoride
Rac1	Ras-related C3 botulinum toxin substrate 1
Rap1	Ras-related protein 1
RBD	Rho GTPase-binding domain
RGC	Retinal ganglion cell
Robo	Roundabout guidance receptor
ROCK	Rho-associated kinase

Abbreviations

Ron	Recepteur d'origine Nantais
RT	Reverse transcriptase
Scrib	Scribble
SDS	Sodium dodecyl sulfate
SDS-PAGE	Sodium dodecyl sulfate-polyacrylamide gel electrophoresis
Sema	Semaphorin
sgRNA	Single-guide ribonucleic acid
shRNA	Short hairpin ribonucleic acid
siRNA	Small interfering ribonucleic acid
Smurf1	Smad ubiquitination regulatory factor 1
Stbm	Strabismus
SynGAP	Synaptic Ras GTPase activating protein
TBS-T	Tris buffered saline with tween
TE	Tris EDTA buffer
TEMED	Tetramethylethylenediamine
TGF β	Transforming growth factor β
TGN	Trans-Golgi network
Tiam1	T-lymphoma invasion and metastasis-inducing protein 1
TIM2	T-cell immunoglobulin and mucin domain-containing protein 2
TNF α	Tumour necrosis factor α
Trem-2	Triggering receptor expressed on myeloid cells 2
TPR	Tricopeptide repeats
Vang	Van Gogh
Vangl	Van Gogh like
VASP	Vasodilator-stimulated phosphoprotein
VEGF	Vascular endothelial growth factor
VEGFR	Vascular endothelial growth factor receptor
Wnt	Wingless-type MMTV integration site family member
Yap	Yes-associated protein
ZEB-1	Zinc finger E-box binding homeobox 1
ZO-1	Zonula occludens 1
β Pix	PAK-interacting exchange factor β

Abstract

Cells show certain asymmetries in morphology and molecular organization, a characteristic that is known as cell polarity. Polarity is generally regulated by protein complexes and Rho GTPases like Cdc42, Rho or Rac. Epithelial cells are polarized along the apicobasal axis, and this apicobasal polarity influences many cellular processes, including cell division. Polarized mitosis in epithelia is controlled by the orientation of the mitotic spindle. This is crucial in epithelial cells during development for a correct tissue morphogenesis, but also in the adult for maintenance of tissue homeostasis or damage repair. The orientation of the spindle is controlled by a protein complex that includes NuMA, which mediates pulling from the spindle poles and LGN, which links NuMA to the correct regions of the cell cortex.

Semaphorin-Plexin signaling is a cell-cell communication pathway involved in many tissues and processes mainly through regulation of the cytoskeleton and adhesion. It has been shown that Plexin-B2 regulates mitotic spindle orientation in kidney epithelial cells and that this regulation is relevant for kidney morphogenesis and repair. However, the molecular mechanisms through which Plexin-B2 controls spindle orientation are still largely unclear. In this work, I demonstrate that Plexin-B2 localizes to cell-cell contacts in the kidney epithelium and in epithelial cell lines in 2D and 3D. Furthermore, I show that Plexin-B2 remains polarized during mitosis. I add that the basolateral localization of Plexin-B2 in the kidney is independent of its ligands, but depends on its intracellular juxtamembrane domain in 3D cultures. Furthermore, I show that this region contains a unique basolateral targeting motif present in all murine class B plexins and conserved in human Plexin-B2. Using CRISPR-Cas genome editing, I confirm that the deletion of Plexin-B2 impairs correct lumen formation in epithelial cell cysts. Additionally, I show that the lack of Plexin-B2 does not influence growth of these cells, but increases the proportion of cells in the S and G2/M phases of the cell cycle and aneuploidy. Importantly, I demonstrate that the deletion of Plexin-B2 does not have an effect on the normal localization of the spindle regulators LGN and NuMA in 3D cell cultures. Therefore, the role of the polarized expression of Plexin-B2 in its control of mitotic spindle orientation and its possible connection with mitotic spindle regulators need to be further investigated.

Zusammenfassung

Zellen weisen Asymmetrien in ihrer Morphologie und molekularen Organisation auf. Diese Eigenschaft ist als Zellpolarität bekannt. Polarität wird durch Proteinkomplexe und Rho GTPasen wie Cdc42, Rho und Rac reguliert. Epithelzellen sind entlang ihrer apicobasalen Achse polarisiert, und diese apicobasale Polarität beeinflusst zahlreiche zelluläre Prozesse einschließlich der Zellteilung. Die Polarisierung der Mitose wird in Epithelzellen durch die Ausrichtung der Mitosespindel gesteuert. Dies ist sowohl für die korrekte Morphogenese epithelialer Gewebe während der Entwicklung entscheidend, als auch für die Aufrechterhaltung der Gewebshomöostase und für die Gewebereparatur nach einer Schädigung von zentraler Bedeutung. Die Orientierung der Mitosespindel wird durch einen Proteinkomplex kontrolliert. Dieser enthält das Protein NuMA, das die Übertragung von Zugkräften auf die Spindelpole vermittelt, und das Protein LGN, das für die korrekte Lokalisation von NuMA am zellulären Cortex zuständig ist.

Semaphorin-Plexin-Signaling stellt einen Zell-Zell-Kommunikationsweg dar, der in viele Gewebe und zellulären Prozesse involviert ist, hauptsächlich über eine Regulation des Zytoskeletts und der Adhäsion. Es ist gezeigt worden, dass Plexin-B2 die Orientierung der Mitosespindel in Epithelzellen der Niere reguliert, und dass diese Regulation für die Nierenmorphogenese und -reparatur von Bedeutung ist. Die molekularen Mechanismen, über die Plexin-B2 die Ausrichtung der Mitosespindel kontrolliert, sind jedoch weitgehend unklar. In dieser Dissertation zeige ich, dass Plexin-B2 an Zell-Zell-Kontakten im Nierentubulusepithel und in Nierentubulusepithel-Zelllinien in 2D und 3D lokalisiert ist. Des weiteren zeige ich, dass die Plexin-B2-Lokalisation während der Mitose polarisiert bleibt. Zudem beschreibe ich, dass die basolaterale Lokalisation von Plexin-B2 unabhängig von seinen Liganden ist, und von der intrazellulären Juxtamembran-Domäne von Plexin-B2 in 3D-Kulturen abhängt. Darüber hinaus zeige ich, dass diese Region ein einzelnes basolaterales Zielmotiv trägt, das in allen murinen B-Plexinen enthalten ist und in humanem Plexin-B2 konserviert ist. Mit Hilfe von CRISPR-Cas Genom-Editierung bestätige ich, dass die Deletion von Plexin-B2 die korrekte Lumenbildung in epithelialen Zellzysten beeinträchtigt. Zusätzlich zeige ich, dass das Fehlen von Plexin-B2 das Wachstum dieser Zellen nicht beeinträchtigt, aber den Anteil

von Zellen in der S- und G2/M-Phase des Zellzyklus und Aneuploidie steigert. Insbesondere zeige ich, dass die Deletion von Plexin-B2 keinen Effekt auf die normale Lokalisation der Spindelregulatoren LGN und NuMA in 3D Zellkulturen hat. Weitere Studien zur Rolle der polarisierten Expression von Plexin-B2 bei der Kontrolle der Orientierung der Mitosespindel und zur möglichen Verbindung von Plexin-B2 und Mitosespindelregulatoren sind daher notwendig.

1. Introduction

1.1. Cell polarity

A cell is not a simple structure where its components distribute homogeneously. Different cell types can adopt a variety of shapes (Figure 1) and the same cell type can have different shapes at specific times. Besides, their components, such as organelles or molecular complexes, are distributed in an organized manner and located to specific domains of the cell at certain timepoints, which allows for the specific function of each cell type. This asymmetrical shape and unequal distribution of cell components constitute patterns of polarity. For instance, epithelial cells and neurons exemplify how much cell types can differ from one another (Figure 1). Moreover, migrating and non-migrating cells of the same type show that cells can adopt a different organization during certain processes. Neurons have a cell body from which a number of processes emerge in different directions, namely the axon and the dendrites, with different structure and composition (Lodish et al. 2000). Cells in simple epithelia have their apical surface facing a lumen or the exterior of the body, their lateral sides in contact with other cells and their basal surface facing the extracellular matrix, containing different molecules and organelles in each one of these locations (Roignot, Peng, and Mostov 2013). Migrating cells form lamellipodia and filopodia at their leading edge, while retracting their rear edge to drive the movement forward (Ridley et al. 2003).

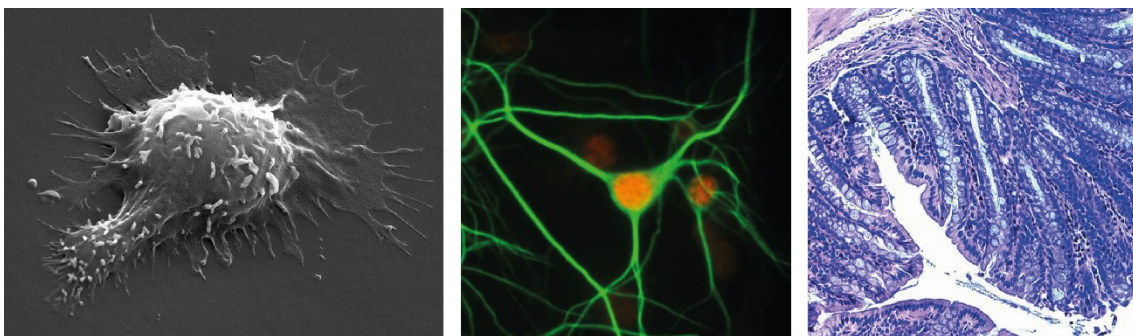


Figure 1. Polarized cells with different morphologies. Left: migratory cell (Saitakis et al. 2017); center: neurons (Seward et al. 2013); right: epithelial cells (Grinberg-Bleyer et al. 2018)

How does this diversity of shapes and polarized composition originate? In yeast, establishment of polarity is controlled by the Rho GTPase Cdc42 (Wedlich-Soldner et al.

2004). Rho GTPases are proteins belonging to the superfamily of Ras, which are small GTPases. They are proteins that act as molecular switches in many signaling processes, including cell polarity. They are active when bound to GTP and inactive when bound to GDP (Hodge and Ridley 2016). Small GTPases are activated by guanine nucleotide exchange factors (GEFs), which stimulate the exchange of GDP for GTP. On the other hand, they become inactive through GTPase activating proteins (GAPs), which catalyze GTP hydrolysis (Lawson and Ridley 2018). One example of how Cdc42 controls polarity in yeast is budding spore formation (Figure 2). In *Saccharomyces cerevisiae*, budding spores are able to break symmetry at a random point (Johnson, Jin, and Lew 2011). The effector proteins of Cdc42 called p21-activated kinases (PAKs) bind the scaffold protein Bem1, which binds a Cdc42 guanine nucleotide exchange factor (Cdc42GEF) called Cdc24 (Bose et al. 2001; Butty et al. 2002). This complex diffuses in the cytoplasm. PAKs also bind active Cdc42 at the membrane, where then GDP-Cdc42 will be locally activated to GTP-Cdc42 through the activity of Cdc24, recruiting even more PAK-scaffold-GEF complexes to this area (Kozubowski et al. 2008). In this way, a stochastic increase in the concentration of GTP-Cdc42 somewhere in the yeast cell is able to create a polarity point by a self-amplifying positive feedback loop (Chiou, Balasubramanian, and Lew 2017).

Moreover, in *S. cerevisiae*, the formin Bni1 is another Cdc42 effector, which nucleates actin filaments that form linear bundles anchored to the polarity site (Figure 2) (Sagot, Klee, and Pellman 2002). These actin bundles allow secretory vesicles to be delivered to the polarity site by type V myosins (Pruyne, Schott, and Bretscher 1998). These vesicles also carry the exocyst, a plasma membrane tethering complex that includes another two Cdc42 effectors (Donovan and Bretscher 2012), which allows the fusion of the vesicles with the plasma membrane in order to form the budding spore. Therefore, the establishment of a polarity point, the delivery of secretory vesicles and their fusion with the plasma membrane are all induced by Cdc42 (Chiou, Balasubramanian, and Lew 2017).

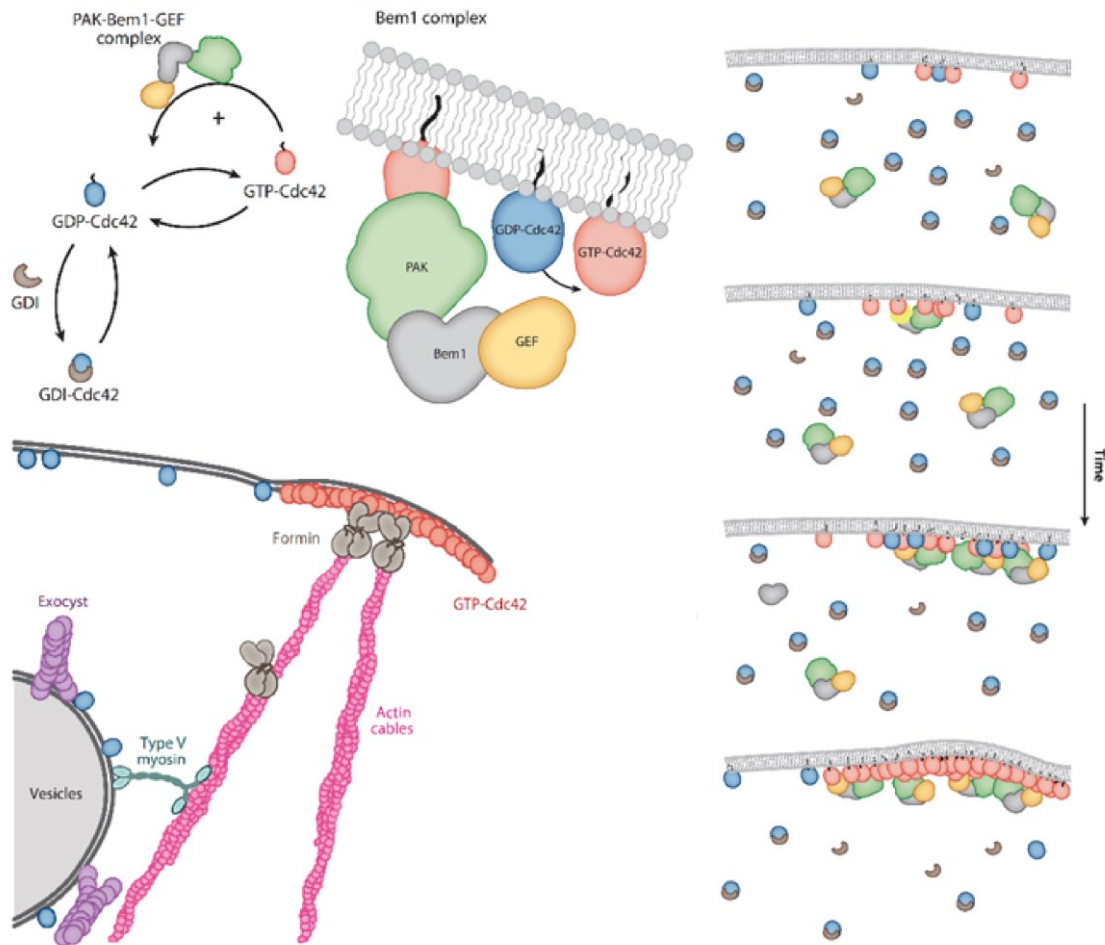


Figure 2. Generation of a polarity point and delivery of secretory vesicles in *S. cerevisiae* for budding spore formation. Top-left: active Cdc42 is able to induce the formation of a PAK-Bem1-Cdc24 complex by a positive feedback loop in the cytoplasm as well as at the cell membrane at the budding point, where GTP-Cdc42 accumulates. Right: time course of Cdc42-PAK-Bem1-Cdc24 complex accumulation at the polarity site. Bottom-left: Nucleation of actin cables by the formin Bni1 and delivery of secretory vesicles containing the exocyst by type V myosins (Chiou, Balasubramanian, and Lew 2017)

In animal cells, there are mainly three complexes involved in the development of polarity: Par, Crumbs and Scribble, which mutually regulate each other and scaffold Rho GTPases to specific membrane domains where they induce polarization (Campanale, Sun, and Montell 2017). In the Par complex, the proteins Par6, Par3 and atypical protein kinase C (aPKC) are of particular importance (St Johnston and Ahringer 2010). The Par complex establishes the border between the apical and basal domains of epithelial cells (Margolis and Borg 2005) and determines the front and rear edges in migratory cells as well as the anterior and posterior poles of the *Caenorhabditis elegans* embryo

(Campanale, Sun, and Montell 2017). The Crumbs complex is required for the generation of an apical domain in epithelial cells and it comprises the transmembrane protein Crumbs (Crb) and the associated cytoplasmic proteins Pals1 and Pals1-associated tight junction protein (Patj) (Tepass, Theres, and Knust 1990; Wodarz et al. 1995; Straight et al. 2004). For the determination of the basolateral plasma membrane domain, a key role is played by the Scribble complex, formed by Scribble (Scrib), lethal giant larvae homologue (Lgl) and discs-large homologue (Dlg), which have a mutual antagonistic relationship with the apical proteins of the Par and Crb complexes (Bilder, Li, and Perrimon 2000; Bilder, Schober, and Perrimon 2003; Tanentzapf and Tepass 2003; Betschinger, Mechtler, and Knoblich 2003).

1.2. Types of cell polarity

There are several types of cell polarity. One of them is the front-rear polarity (Figure 3). Front-rear polarity plays an essential role in migratory cells in order to achieve directional migration. Directional migration is the steady movement of individual cells or groups of cells in a specific direction in response to extracellular cues like growth factors or chemokines and environmental cues like mechanical forces or the extracellular matrix, among others (Lawson and Ridley 2018; Iden and Collard 2008). Directional migration is essential for animal tissue morphogenesis, for physiological functions and during pathological processes like cancer cell invasion and metastasis (Lawson and Ridley 2018; Iden and Collard 2008). Some of these migrating cells originate from epithelial cells that have to redistribute during tissue morphogenesis. They undergo an epithelial-to-mesenchymal transition (EMT), often involving TGF β receptors and resulting in loss of E-cadherin (Iden and Collard 2008; Rodriguez-Boulan and Macara 2014).

Cytoskeletal dynamics are finely controlled by Rho GTPases in migrating cells to drive persistent directional movement, in particular by Cdc42, Rac1 and RhoA (Machacek et al. 2009). Epithelial cells after EMT and other migratory cells like astrocytes and fibroblasts utilize the polarity complexes in order to asymmetrically activate Cdc42 and Rac1 at the front edge to generate protrusions in the direction of the

movement and RhoA at the rear edge to promote detachment and retraction (Campanale, Sun, and Montell 2017). In rat astrocytes, Scribble binds the Cdc42GEF β Pix at the leading edge and together they promote the activation of Cdc42 locally (Figure 3) (Osmani et al. 2006). In fibroblasts and migrating epithelial cells, active Cdc42 locally activates aPKC at the leading edge, probably through Par6 (Iden and Collard 2008). Furthermore, it has been shown that in persistently migrating epithelial cells, Par3 and aPKC form a complex with the Rac1GEF Tiam1 that gets recruited to the leading edge and is responsible for the maintenance of the front-rear polarity, the persistence of directed migration and the response to chemotactic factors through stabilization of microtubules (Pegtel et al. 2007). At the same time, signaling through aPKC downstream of Cdc42-Par6 also recruits the E3 ubiquitin ligase Smurf1 at the leading edge, which targets the protrusion inhibitor RhoA for degradation, therefore restricting its activity to the rear edge (Figure 3) (Wang et al. 2003).

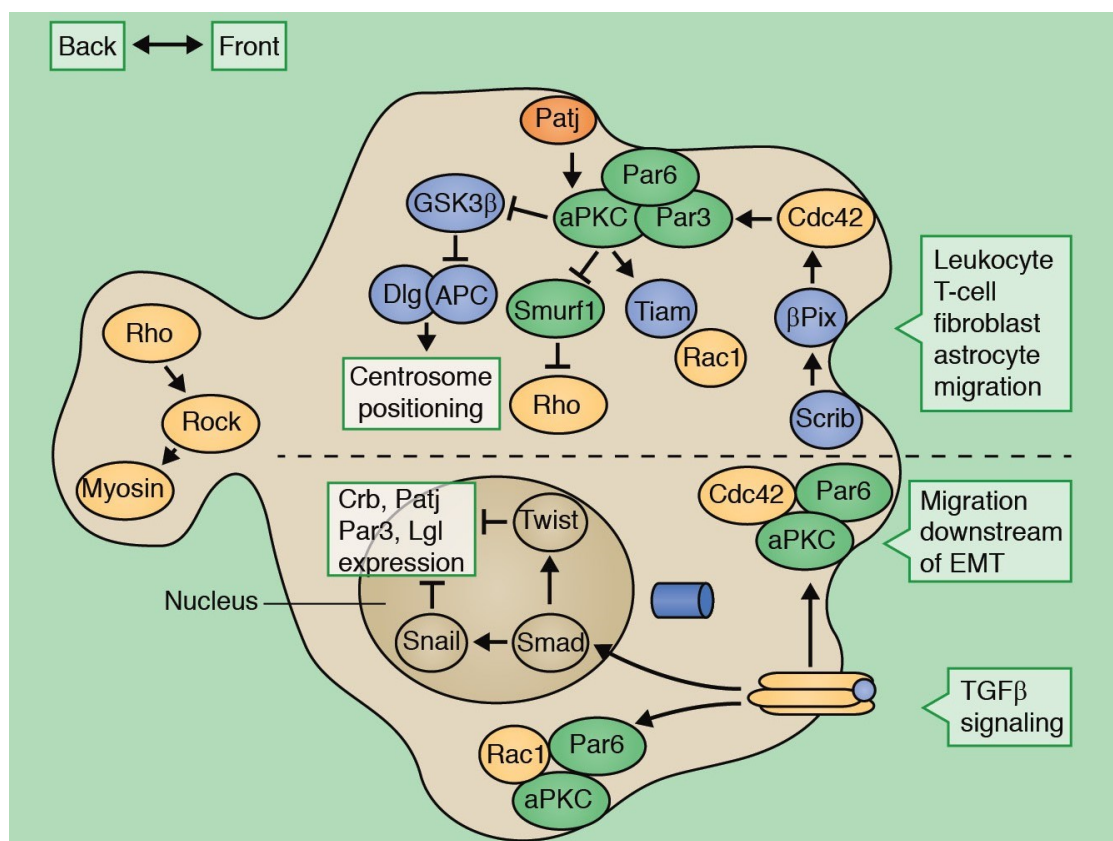


Figure 3. Front-rear polarity in migratory cells. For details, see text (Campanale, Sun, and Montell 2017)

Another type of polarity is planar cell polarity. Planar cell polarity (PCP) is the collective orientation of cells along an axis orthogonal to the apical-basal axis within the epithelial plane (Devenport 2014; Campanale, Sun, and Montell 2017). The PCP machinery is not only relevant in epithelial cells, but also in some mesenchymal cell types during development, where it plays a role in migration and intercalation (Simons and Mlodzik 2008). Communication between cells is essential in order to establish and coordinate PCP (Devenport 2014). PCP was found to be important for the correct orientation of cuticular structures in *Drosophila* (Gubb and García-Bellido 1982) and of ommatidia in the insect retina (Lawrence and Shelton 1975). PCP is also important in vertebrates as it is required for several developmental processes like convergent extension movements during gastrulation (Tada and Smith 2000; Wallingford et al. 2000; Jessen et al. 2002; Simons et al. 2005) and neural tube closure (Kibar et al. 2001; Curtin et al. 2003; Nishimura, Honda, and Takeichi 2012), orientation of hair follicles in the mammalian epidermis (Guo, Hawkins, and Nathans 2004), ciliary beating in the trachea and in the brain ventricles (Vladar et al. 2012; Tissir et al. 2010), mammalian hair cell patterning in the inner ear (Montcouquiol et al. 2003; Curtin et al. 2003), lung branching (Yates et al. 2010) and oriented cell division (Gong, Mo, and Fraser 2004), among other. Defects in PCP have also been associated with human disease. For example, mutations in PCP genes have been found in neural tube defects (Nikolopoulou et al. 2017; Beaumont et al. 2019; Kibar et al. 2007) and heart malformations (Qiao et al. 2016). PCP has also been linked to glomerular disease (Papakrivopoulou et al. 2018) and chronic obstructive pulmonary disease (Poobalasingam et al. 2017). Furthermore, there are studies showing the implications of PCP proteins in cancer (VanderVorst et al. 2018; Daulat and Borg 2017).

This type of polarity relies on two evolutionarily conserved systems that act in parallel: the “core” and the “Fat/Dachsous” PCP pathways (Thomas and Strutt 2012). These two systems seem to influence planar polarity independently of each other (Lawrence, Struhl, and Casal 2007). A shared feature of both is the antagonism of two complexes that locate at opposite poles of the cell (Devenport 2014). The “core” pathway consists of the transmembrane proteins Frizzled (Fz), Van Gogh (Vang, also known as Strabismus, Vangl in vertebrates) and Flamingo (Fmi, also known as Starry

night, in vertebrates known as CELSR), in addition to the cytoplasmic proteins Prickle (Pk), Dishevelled (Dsh, Dvl in mammals) and Diego (Dgo, in vertebrates ANKRD6, also known as Diversin) (Adler 2002; Strutt 2003; Veeman, Axelrod, and Moon 2003; Klein and Mlodzik 2005; Wang and Nathans 2007; Simons and Mlodzik 2008). On one side of the cell localize the proteins Fz, Dsh and Dgo, while on the other reside Vang and Pk (Figure 4); Fmi localizes to both sides and forms homodimeric bridges between neighbouring cells (Usui et al. 1999; Axelrod 2001; Feiguin et al. 2001; Shimada et al. 2001; Tree et al. 2002; Bastock, Strutt, and Strutt 2003). Fz and Dsh are the main PCP signaling proteins, which potentially act through Rho GTPases like Cdc42 and the Rho-associated Kinase ROCK (Wallingford 2012), while the other PCP factors regulate Fz-Dsh complex localization and activity (Simons and Mlodzik 2008).

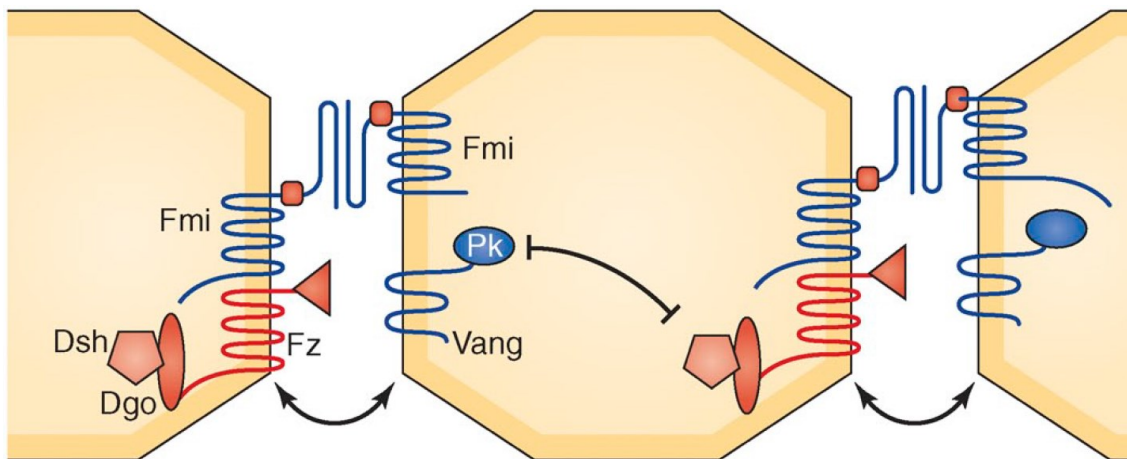


Figure 4. Components of the “core” planar cell polarity pathway. For details, see text (Devenport 2014)

The “Fat/Dachsous” pathway is composed of the atypical large protocadherins Fat (Ft) and Dachsous (Ds), as well as the Golgi-associated transmembrane kinase Four-jointed (Fj) (Matis and Axelrod 2013). Ft and Ds bind heterotypically between neighbouring cells (Matakatsu and Blair 2004). Fj regulates the activity of Ds and its binding to Ft. It phosphorylates the extracellular domain of Ft, which increases its affinity for Ds, while it also phosphorylates the extracellular region of Ds, decreasing its affinity for Ft (Simon et al. 2010; Brittle et al. 2010). Since, Fj is expressed in a gradient in many tissues, this results in the polarized distribution of active Ft and Ds to opposite sides of the cell (Simon 2004).

For a long time, an upstream global cue has been searched that could orient the asymmetric localization of the “core” PCP molecules along an entire tissue. Molecules that distribute in a gradient throughout the tissue are good candidates. The “Fat/Dachsous” pathway has been proposed to fulfil this function, as Ds and Fj are expressed in opposing gradients in the *D.melanogaster* imaginal eye disc and pupal wing (Yang, Axelrod, and Simon 2002; Ma et al. 2003). On the other hand, Fz molecules act as Wnt receptors (Bhanot et al. 1996). Wnt proteins are important signaling molecules that are involved in the specification of primary body axes and cell fate, among other processes, and are frequently found in gradients during development in tissues that exhibit PCP (Sokol 2015). Therefore, they have also been proposed as upstream cues for PCP (Wu et al. 2013; Chu and Sokol 2016). Lastly, mechanical forces, like flow of liquid or tissue strain, have been suggested as potential global upstream cues for PCP as well (Chien et al. 2015; Guirao et al. 2010).

Mitosis is a key process during development, as well as in the adult animal, and asymmetric cell division is another example of a polarized process (Richardson and Portela 2017). Asymmetric cell division is determined by the unequal distribution of extrinsic or intrinsic factors after mitosis (Campanale, Sun, and Montell 2017; Chen, Fingerhut, and Yamashita 2016). Mitotic spindle orientation plays a key role in achieving asymmetric cell division (Morin and Bellaïche 2011). During development, asymmetric cell division positions certain cells at specific locations (Knoblich 2001). This can determine embryonic axis, as in the first division of the *C. elegans* embryo, which determines the anterior-posterior axis (Sulston et al. 1983). It can also specify cell fate, contributing to the cellular diversity observed in the developed organism and it is important in order to give the organs their correct shape during development (Gillies and Cabernard 2011). In the adult, in particular in epithelia, asymmetric cell divisions are important to ensure maintenance of tissue homeostasis. Its disruption could lead to tissue degeneration, hyperplasia or cancer (Chen, Fingerhut, and Yamashita 2016). In the context of epithelia, an asymmetric cell division produces one stem cell and one non-stem cell, while a symmetric cell division gives either two non-stem cells or two stem cells (Yang, Plikus, and Komarova 2015).

In the early *C. elegans* embryo, besides defining the anterior-posterior axis, asymmetric cell division occurs to segregate the somatic (originated from the AB cell) and germ (originated from the P1 cell) lineages (Campanale, Sun, and Montell 2017; Knoblich 2001). The AB cell fate is established by the accumulation of the zinc-finger proteins MEX-5 AND MEX-6 (Schubert et al. 2000), while large cytoplasmic ribonucleoprotein particles called P-granules segregate to the P1 cell, even though their segregation to the posterior cell is not required for germline determination (Gallo et al. 2010). It was in this context that the Par proteins were discovered (Kemphues et al. 1988).

For the segregation of MEX-5 and MEX-6, as well as the P-granules in the *C. elegans* embryo, an anterior complex (aPar) and a posterior complex (pPar) are established (Figure 5). The first is formed by the proteins Par3, Par6 and aPKC (Etemad-Moghadam, Guo, and Kemphues 1995; Hung and Kemphues 1999; Tabuse et al. 1998), while the second is composed mainly of the proteins Par1 and Par2 (Guo and Kemphues 1995; Boyd et al. 1996). At the time of fertilization, the sperm-derived microtubule organizing center (MTOC) is delivered to the zygote in an area that will be the future posterior pole (Campanale, Sun, and Montell 2017). It spawns microtubules that protect Par2 from aPKC phosphorylation, which leads to the recruitment of Par1 and Par2 from the cytoplasm to the cortex near the centrosome. There, Par1 and Par2 antagonize the anterior complex (Motegi et al. 2011). Non-muscle myosin contractions at the anterior-posterior boundary controlled by Par4 promote the flow of the aPar, as well as MEX-5 and MEX-6 proteins to the anterior pole (Cuenca et al. 2003; Munro, Nance, and Priess 2004). In addition, Par5 inhibits cortical localization of the anterior complex proteins in the posterior pole (Morton et al. 2002).

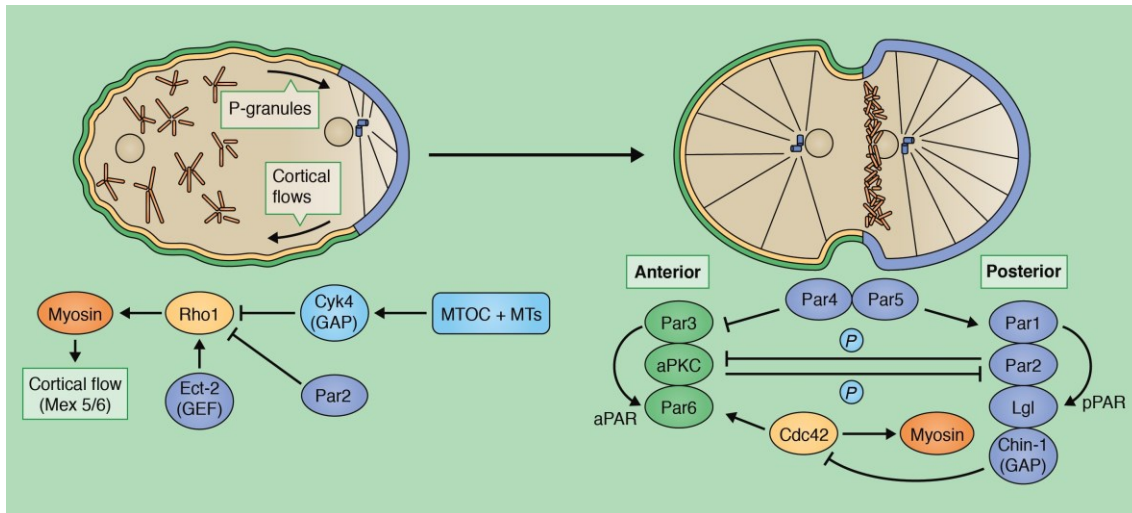


Figure 5. Anterior-posterior axis determination in the *C. elegans* zygote. For details, see text (Campanale, Sun, and Montell 2017)

During the development of the nervous system in *Drosophila*, neuroblasts divide perpendicularly to the neuroectoderm to generate a small differentiating ganglion mother cell, which is placed further deep in the tissue, while retaining a self-renewing neuroblast (Figure 6) (Gillies and Cabernard 2011). In this case, asymmetric cell division is determined by the segregation of cell fate determinants like Miranda, Prospero, Numb, Partner of Numb and Brain Tumor (Spana and Doe 1995; Lee et al. 2006; Lu et al. 1998). Mitotic spindle orientation is critical to ensure this asymmetric cell division (Cabernard and Doe 2009).

Drosophila neuroblasts inherit the apical Par complex from the neuroectoderm epithelial cells (Campanale, Sun, and Montell 2017). At the start of asymmetric cell division, the kinase Aurora A (AurA) phosphorylates Par6 which activates aPKC (Figure 6). This allows the formation of Baz-Par6-aPKC complex (Wirtz-Peitz, Nishimura, and Knoblich 2008). Baz (the *Drosophila* homologue of Par3) then fixes Inscuteable (Insc), which recruits Pins (Yu et al. 2000; Schaefer et al. 2000), a protein belonging to the mitotic spindle orientation machinery, discussed further below (see section 1.4).

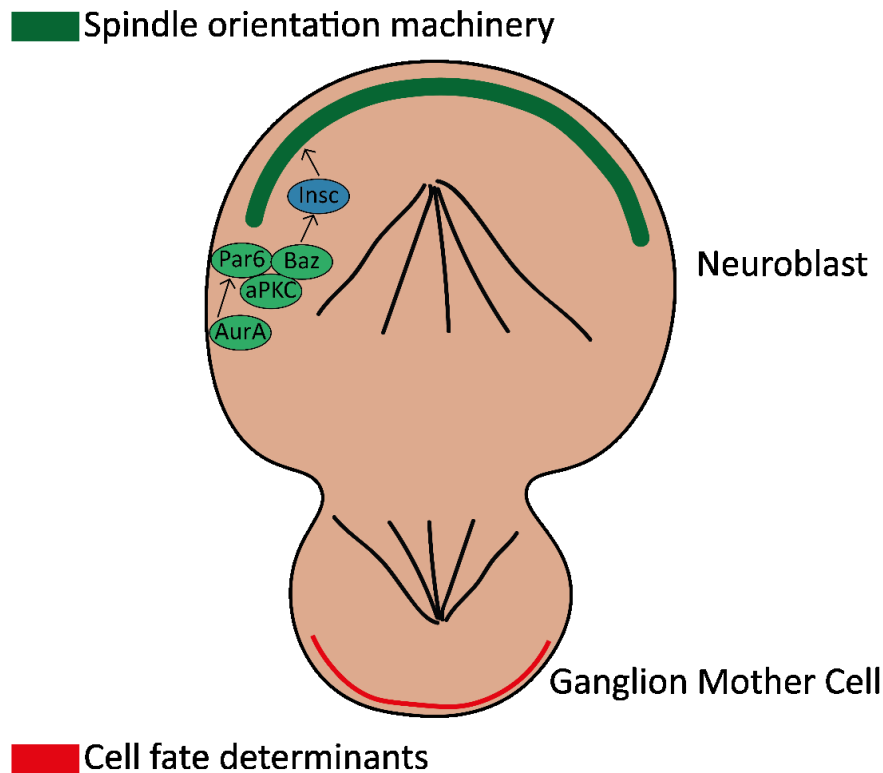


Figure 6. Asymmetric cell division during the development of the nervous system in *Drosophila*. For details, see text

Lastly, cells can also be polarized in the apical-basal axis, a form of polarity in which this work focuses. Apicobasal polarity is a defining characteristic of epithelial cells (Campanale, Sun, and Montell 2017; Rodriguez-Boulan and Macara 2014). It consists on the establishment of distinct opposing cortical domains, named apical and basolateral, with different protein and lipid composition, separated by adherens junctions and occluding *junctions* (named tight junctions in vertebrates and septate junctions in invertebrates), which maintain the identity of each membrane domain (Roignot, Peng, and Mostov 2013). Adherens junctions provide cohesion to the epithelial sheet by keeping neighbouring epithelial cells firmly attached to each other, while occluding junctions form a barrier that blocks the diffusion of molecules between epithelial cells and restricts the free movement of membrane components between the apical and basolateral domains (Riga, Castiglioni, and Boxem 2020). Apicobasal polarity also includes a number of processes that occur aligned to the axis defined by these distinct cortical domains, such as directed vesicle trafficking and secretion, endocytosis or

response to stimuli (Worzfeld and Schwaninger 2016). This kind of polarity is controlled by an epithelial polarity program that includes polarity protein complexes, differential protein targeting, membrane lipid regulators and the cytoskeleton (Rodriguez-Boulan and Macara 2014).

Apicobasal polarity plays a crucial role in many functions of epithelial cells, like epithelial barrier function, tissue morphogenesis, asymmetric cell division and cell migration (Wilson 2011). It has been shown to regulate the Hippo pathway, a proliferation inhibitor pathway that plays a crucial role in epithelial homeostasis (Genevet and Tapon 2011). Apicobasal polarity is important for the correct targeting of proteins during epithelial morphogenesis. For example, in renal tubule epithelial cells, the epithelial sodium channel, the cystic fibrosis chloride transporter, the sodium-potassium antiporter, the proton ATPase and the aquaporin 2 water channel are located at the apical membrane, while the sodium-potassium ATPase, the chloride-bicarbonate cotransporter AE1, the sodium-potassium-chloride cotransporter NKCC1 and the epithelial growth factor receptor (EGFR) localize at the basal membrane (Wilson 2011). Disrupted apicobasal polarity has been associated with human disease. The loss of apicobasal polarity can produce hyperproliferation by inhibition of the Hippo pathway (Genevet and Tapon 2011). This has also been observed in human cancer, where it is associated with disease progression (Lo, Hawrot, and Georgiou 2012). In the kidney, the incorrect sorting of transporters, channels and receptors to the wrong membrane domain has been implicated in several diseases like Autosomal Dominant Polycystic Kidney Disease (Wilson 2011).

Apicobasal polarization starts upon formation of epithelial cell-cell contacts and cell-matrix interaction (Roignot, Peng, and Mostov 2013). Cell-cell adhesion molecules like E-cadherin or nectin and cell-matrix adhesion proteins like integrins start receptor-mediated signaling that recruits polarity proteins (Worzfeld and Schwaninger 2016; Rodriguez-Fraticelli and Martin-Belmonte 2014). Then, polarity proteins interact with each other to help with the maturation of the junctional complexes and the maintenance of polarity (Roignot, Peng, and Mostov 2013). The correct targeting of polarity complexes to the apical or basolateral membrane domains depends on their mutual antagonism (Rodriguez-Boulan and Macara 2014; Roignot, Peng, and Mostov

2013; Riga, Castiglioni, and Boxem 2020). The apical domain is defined by the Par and Crumbs complexes, while the basolateral domain is defined by the Scribble complex (Figure 7).

For the generation of distinct membrane domains, Par3 is recruited first apically (Figure 7) through an unknown mechanism (Riga, Castiglioni, and Boxem 2020), although in *Drosophila* a dynein-dependent transport of Par3 to the site of adherens junction formation has been shown (Harris and Peifer 2005). Then, Par3 interacts with nectins at the developing adherens junctions, where it recruits afadin (an F-actin and nectin binding protein) and together regulate the formation of adherens junctions (Ooshio et al. 2007). Par3 at the apical-lateral border also controls tight junction formation through Rac1 by inhibiting its GEF Tiam1 (Figure 7) (Chen and Macara 2005). Another function of Par3 in the determination of the apical domain is to contribute to the difference in membrane lipid composition (Figure 7). While at the basolateral membrane, the abundance of PIP₃ is increased by the activity of the lipid kinase PI3K on PIP₂ (Peng et al. 2015), at the apical membrane Par3 recruits the phosphoinositide phosphatase PTEN (von Stein et al. 2005; Feng et al. 2008). PTEN converts PIP₃ into PIP₂ at the apical membrane, increasing its abundance, which promotes the recruitment of annexin 2 first, to which then Cdc42 is recruited (Martin-Belmonte et al. 2007). At the apical membrane, Cdc42 is locally activated by Tuba (Figure 7) (Cestra et al. 2005; Bryant et al. 2010; Qin et al. 2010) or Dbp3 (Zihni et al. 2014). The Par6-aPKC complex is thought to be recruited apically by Cdc42 (Hutterer et al. 2004; Nunes de Almeida et al. 2019). On the other hand, it has been shown in *Drosophila* that dyneins drive the transport of Crumbs and its transcripts apically (Li et al. 2008), while being excluded from the basolateral membrane by yurt (Laprise et al. 2009). For the correct localization of the apical-lateral border, Par3 must be excluded from the interaction with Par6-aPKC at the apical membrane (Figure 7), which is achieved by phosphorylation of a conserved serine residue of Par3 by aPKC (Nagai-Tamai et al. 2002; Morais-de-Sá, Mirouse, and St Johnston 2010). This phosphorylation is however not sufficient to exclude Par3 from a complex with Par6-aPKC, being even dispensable in some cell types (Morais-de-Sá, Mirouse, and St Johnston 2010) and it further requires association of Par6 with active Cdc42 and Crb (Morais-de-Sá, Mirouse, and St Johnston 2010; Nunes de Almeida et al.

2019). The binding of the Par6-aPKC cassette to Crb (Figure 7) was at first proposed through binding of Par6 to Crb-bound Stardust/Pals1 (Hurd et al. 2003), but later also demonstrated through direct binding between Par6 and Crb, an interaction that helps both complexes stabilize each other at the apical membrane (Nunes de Almeida et al. 2019). Also, $\beta 1$ integrin signaling upon binding to collagen in the extracellular matrix induces Rac1 activation, which leads to laminin assembly at the basement membrane and definition of the basal side, which orients the direction of apicobasal polarity (O'Brien et al. 2001; Yu et al. 2005). Laminin has been shown to regulate apicobasal polarity *in vivo* (Rasmussen, Reddy, and Priess 2012). However, it seems that the Rac1 regulation of the orientation of apicobasal polarity is cell type-specific and another mechanism has been proposed, in which $\beta 1$ integrins signal through Focal Adhesion Kinases (FAK) and p190a (a RhoA GAP) to downregulate RhoA-ROCK signaling (Bryant et al. 2014).

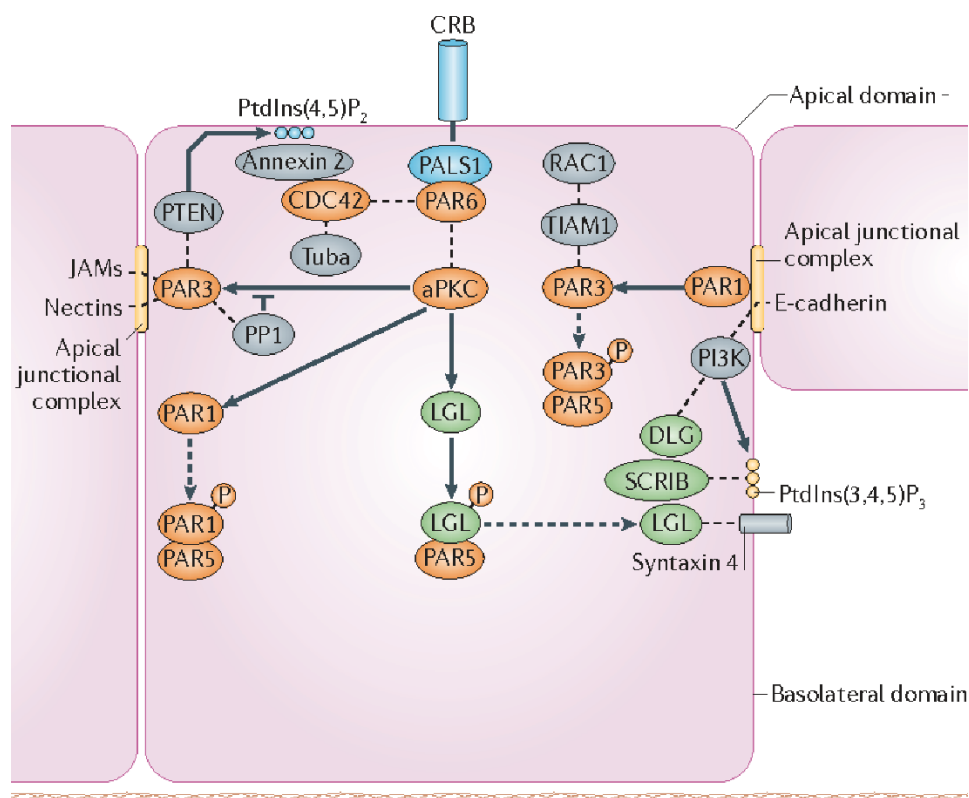


Figure 7. Localization and interactions of polarity proteins in the establishment of apicobasal polarity and its maintenance. Dashed lines show binding interactions. Solid arrows indicate phosphorylation/dephosphorylation. Dashed arrows indicate change in the protein to or from a phosphorylated state. For details, see text (Rodriguez-Boulan and Macara 2014)

After being established, the maintenance of apicobasal polarity depends on reciprocal antagonism and exclusion between apical and basolateral polarity complexes. Lgl and the kinase Par1, two proteins that localize at the basolateral membrane, are phosphorylated by aPKC (Figure 7), excluding them from the apical domain (Yamanaka et al. 2003; Hurov, Watkins, and Piwnica-Worms 2004; Suzuki et al. 2004). In turn, lateral Lgl inhibits basolateral localization of Par6-aPKC (Hutterer et al. 2004). Par3 is excluded from the basolateral membrane by Par1-mediated phosphorylation of two conserved serine residues and subsequent binding to members of the 14-3-3 family of proteins (Figure 7), which prevents its membrane association (Benton and St Johnston 2003).

1.3. Epithelial cell polarity

Epithelial cells appear early during development with the formation of a blastocyst (Ziomek and Johnson 1980). They are especially useful for the formation of tissues and organs because they have a polarized cytoskeleton that allows them to constrict their apical surface, something that is required for morphogenetic processes like gastrulation or tubulogenesis (Sawyer et al. 2010) and because they can control the size of their lateral sides to adopt either a columnar or a squamous shape (Rodriguez-Boulan and Macara 2014). Additionally, epithelial cells during development can orient their mitotic spindle in order to increase the amount of a certain population of cells, induce differentiation to generate a variety of cell types or give rise to a specific tissue architecture required for organ formation (Chen, Fingerhut, and Yamashita 2016; Morin and Bellaïche 2011). Another advantage of epithelial cells during development is their ability to lose their epithelial characteristics, transition to a mesenchymal phenotype and migrate to a different location where they regain the epithelial character (through epithelial-to-mesenchymal transition and mesenchymal-to-epithelial transition, respectively), for example, during kidney development (Carroll and Das 2011; Lim and Thiery 2012). All these capabilities require polarization. Epithelial cell polarity has been extensively studied in *C. elegans* and *D. melanogaster* (Rodriguez-Boulan and Macara 2014), but the mechanisms governing tubulogenesis and the *de novo* formation of lumina from a mass of epithelial cells have been mostly studied in cultures of epithelial cells embedded in 3D matrices (Overeem, Bryant, and van IJzendoorn 2015). The Madin-

Darby Canine Kidney (MDCK) cell line is one of the most used models. These cells, when cultured in a 3D matrix, form spherical epithelial monolayers surrounding a central lumen, named cysts (Montesano, Schaller, and Orci 1991).

The microtubule cytoskeleton suffers rearrangements during polarization in epithelial cells (Rodriguez-Boulan and Macara 2014). In polarizing MDCK cells, the centrioles move from an initial position close to the nucleus to directly below the apical membrane upon formation of cellular junctions (Buendia et al. 1990). There, the mother centriole generates the primary cilium (Figure 8). The primary cilium is a microtubule-based protrusion present on the surface of many cell types that acts as a hub for important signaling pathways (Goetz and Anderson 2010), which include Hedgehog (Bangs and Anderson 2017), Wnt (May-Simera and Kelley 2012), transforming growth factor β and platelet-derived growth factor receptor α signaling (Christensen et al. 2017). Also in MDCK cells, it has been shown that most of the microtubules are non-centrosomal and more stable in comparison with migratory cells, where microtubules emanate from the centrosomes and are less stable (Bré, Kreis, and Karsenti 1987). Some of this non-centrosomal microtubules anchor their minus ends to the zonula adherens and regulate the development of the apical junctional complex (Meng et al. 2008). Moreover, E-cadherin is able to stabilize the minus ends of a population of non-centrosomal microtubules (Chausovsky, Bershadsky, and Borisy 2000). In epithelial cells, cortical microtubules are oriented apicobasally (Figure 8), with their plus ends at the basal domain (Gilbert et al. 1991). End-binding protein 1 (EB1) is responsible for the localization of kinesin family 17 (KIF17) to microtubule plus ends, which in turn recruits APC and together they stabilize the microtubules (Jaulin and Kreitzer 2010). The organization of the microtubule cytoskeleton in epithelial cells is responsible for the characteristic supranuclear localization of the Golgi apparatus, common recycling endosomes (CREs) and apical recycling endosomes (AREs) and for the peripheral localization of apical and basolateral sorting endosomes (Figure 8) (Rodriguez-Boulan and Macara 2014). In mammary epithelial cells, microtubules that are attached to $\beta 1$ integrins at the basal membrane by the activity of the integrin-linked kinase (ILK) deliver apical proteins from the basal domain to the apical domain of the membrane (Akhtar and Streuli 2013). In the liver, hepatocytes have a unique microtubule organization

responsible for the formation of their apical domain interrupting the lateral membrane to form bile canaliculi. This special arrangement of epithelial polarity is achieved by high activity of Par1. MDCK cells in which Par1 activity is increased show a hepatic-like apical domain (Cohen et al. 2004), while hepatocytes with a lowered Par1 activity show columnar morphology (Lázaro-Diéguéz et al. 2013).

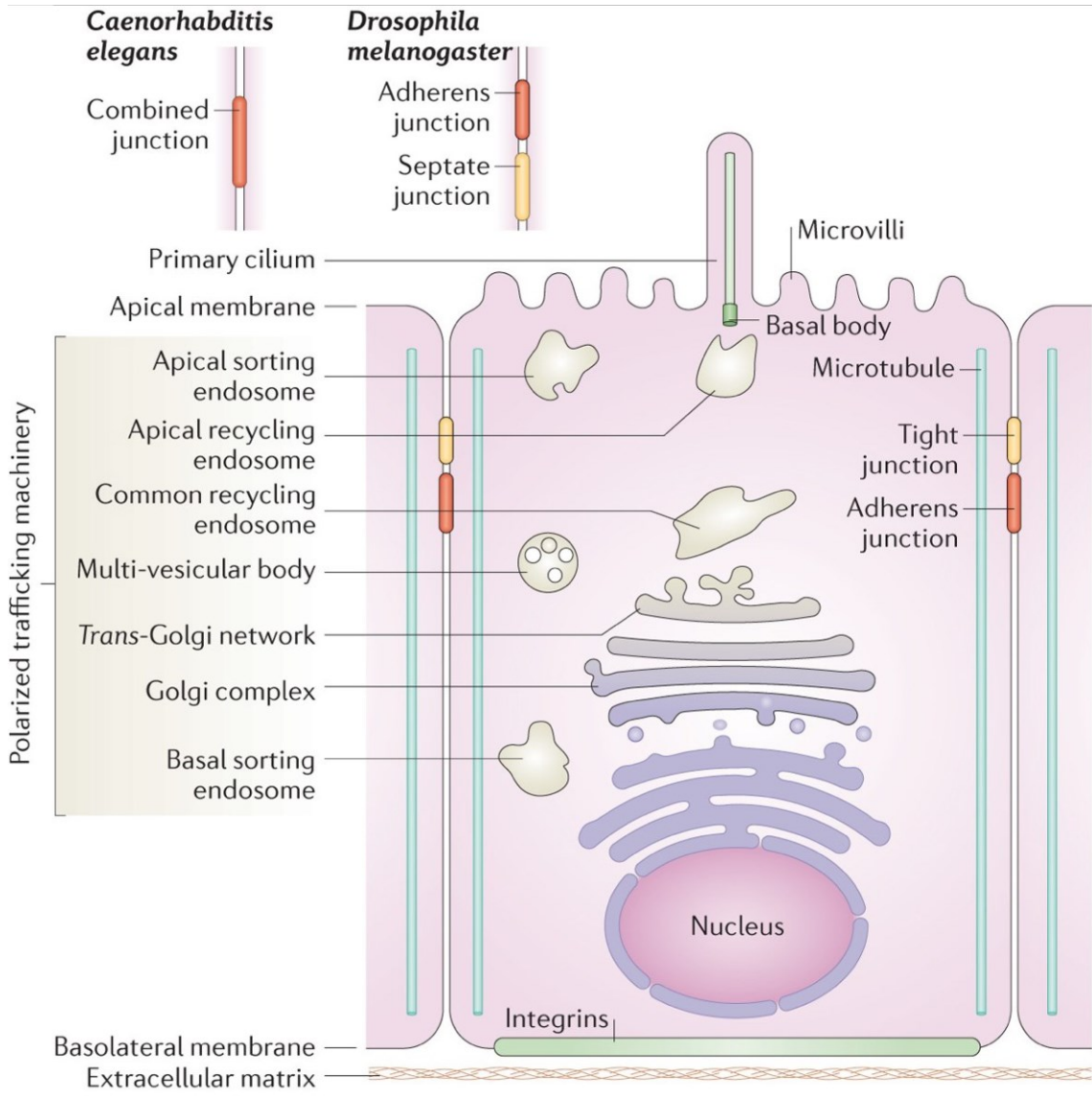


Figure 8. Epithelial polarity. Polarized organization of molecules, organelles and vesicle trafficking in epithelial cells (Rodriguez-Boulán and Macara 2014)

The actin cytoskeleton also reorganizes in epithelial cells, where it forms unique structures like the microvilli (Figure 8) at the apical membrane (Rodriguez-Boulán and Macara 2014). The formation of microvilli depends on 4.1 ezrin-radixin-moesin domain-containing proteins like ezrin in mammals and moesin in flies (Tepass 2009). At adherens junctions, the actin cytoskeleton organizes in bundles parallel to the contacting membrane (Hirokawa et al. 1983), a rearrangement that is regulated by E-cadherin through α -catenin (Drees et al. 2005). In turn, the actin cytoskeleton is involved in the formation and maintenance of junctional complexes (Nelson, Drees, and Yamada 2005). The perinuclear actin cytoskeleton is regulated by Cdc42 and controls vesicular transport from perinuclear endosomes and the trans-Golgi network (Erickson et al. 1996; Kroschewski, Hall, and Mellman 1999; Musch et al. 2001).

Epithelial cells express a high number of plasma membrane proteins that act as transporters or receptors, which are expressed with a characteristic apicobasal polarity, depending on the function of the tissue (Hediger et al. 2004). Their polarity is determined by intracellular sorting at the trans-Golgi network (TGN) and endosomes during biosynthetic and recycling routes (Rodriguez-Boulán, Kreitzer, and Müsch 2005).

The signals for apical sorting are N- and O-glycans in the extracellular domain (Scheiffele, Peränen, and Simons 1995; Yeaman et al. 1997), transmembrane domains such as that of the influenza haemagglutinin (HA) (Scheiffele, Roth, and Simons 1997), glycosyl-phosphatidyl-inositol (GPI) anchors (Lisanti et al. 1989) and motives in the intracellular domain (Tai et al. 1999; Takeda, Yamazaki, and Farquhar 2003). GPI anchors and proteins with specialized transmembrane sorting domains are believed to be preferentially incorporated to vesicles bound for the apical membrane because of their affinity to glycosphingolipid-enriched rafts (Simons and Gerl 2010; Puertollano et al. 1999). Lectins, like galectins 3, 4 and 9 have been shown to be involved in the apical targeting of N-glycosylated proteins (Stoops and Caplan 2014).

On the other hand, basolateral sorting signals are short amino acid sequences in the intracellular domain of the proteins, some of them very similar to endocytosis motifs, such as the tyrosine (NPxY or Yxx \emptyset , being X any amino acid and \emptyset a big hydrophobic amino acid) and dileucine (LL/LI) motifs (Gonzalez and Rodriguez-Boulán

2009), which can bind clathrin adaptor proteins. Therefore, basolateral sorting is believed to be clathrin-mediated (Deborde et al. 2008; Stoops and Caplan 2014).

Sorting of apical and basolateral proteins through the biosynthetic, recycling and transcytotic routes depends on production of post-Golgi vesicles and their polarized trafficking. Fission of apical transport vesicles from the TGN is mediated by dynamin 2 (Salvarezza et al. 2009), while fission of basolateral vesicles depends on protein kinase D (PKD) (Yeaman et al. 2004) and C-terminal-binding protein 1 (CtBP1) (Bonazzi et al. 2005). Dynamin 2 mediates the production of apical transport vesicles at the level of apical recycling endosomes (Thuenauer et al. 2014). The actin and microtubule cytoskeletons are implicated in the transport of these vesicles (Rodriguez-Boulan, Kreitzer, and Müsch 2005). Microtubule motors (like dyneins and kinesins) are mostly implicated in apical trafficking. For example, KIFC3, KIF5B and KIF16B (Noda et al. 2001; Jaulin et al. 2007; Perez Bay et al. 2013). Myosin II and myosin VI are involved in basolateral transport from the TGN (Müsch, Cohen, and Rodriguez-Boulan 1997; Au et al. 2007), while myosin V mediates apical transport from AREs (Roland et al. 2011).

Vesicle tethering at the apical or basolateral membrane requires the exocyst (Oztan et al. 2007), which resides at cell-cell junctions (Grindstaff et al. 1998). Additionally, vesicle trafficking is controlled by Rab GTPases. They are a family of small GTPases that have been shown to be master regulators of vesicle trafficking from the TGN or endosomes (Hutagalung and Novick 2011). Polarity proteins can also play a role in vesicle trafficking. E-cadherin vesicle transport in epithelial cells can be influenced by Cdc42. In the *Drosophila* embryo, the loss of Cdc42 blocks apical recycling and subsequently causes loss of the integrity of adherens junctions, since E-cadherin basolateral delivery depends on AREs (Lock and Stow 2005). Loss of Cdc42 can also cause a defect in E-cadherin endocytosis through alterations in the actin dynamics (Leibfried et al. 2008).

Polarity of epithelial cells also influences cell fate. In mouse embryos, cells are segregated in a single-layered trophoctoderm and an inner cell mass (Johnson 2009). Trophoctoderm cells have apicobasal polarity, while inner cell mass cells do not have an apical membrane (Yamanaka et al. 2006). The trophoctoderm will generate the placenta, while the inner cell mass will form the proper embryo. These cell fates are

determined by the Hippo pathway. In the trophectoderm the Par6-Par3-aPKC complex phosphorylates ezrin, which promotes Yap nuclear localization and Cdx2 expression. Cdx2 then suppresses the pluripotency gene Oct4. However, in the inner cell mass there is no apical membrane, thus preventing Yap to localize in the nucleus, which does not promote Cdx2 transcription and maintains Oct4 expression (Hirate et al. 2013).

1.4. Mitotic spindle orientation

Epithelial development, homeostasis and repair require a correct orientation of the cell division. This orientation is determined by the position of the mitotic spindle. The mitotic spindle is a structure formed by three types of microtubules nucleated from the centrosomes. Kinetochore microtubules bind the chromosomes and separate both genomes during anaphase. Interpolar microtubules form an antiparallel array that positions the mitotic furrow during cytokinesis. Astral microtubules anchor the spindle to the cortex (Morin and Bellaïche 2011).

Some of the processes for which a correct mitotic spindle orientation is necessary were mentioned above, for example, for the anterior-posterior axis determination during the first division of the *C. elegans* zygote (Siller and Doe 2009). During the development of the neural system in *Drosophila*, mitotic spindle orientation is critical to ensure the asymmetric division of neuroblasts (Morin and Bellaïche 2011). Also in mammals, in some tissues like the epidermis, switching the orientation of the mitotic spindle during development changes the division mode from symmetric, which is used to increase the surface of the epidermis, to asymmetric in order to produce stratification and induce differentiation (Xie and Zhou 2017).

The key components for the determination of the orientation of the mitotic spindle have been identified, although new mechanisms are still arising. The mitotic spindle gets in position through pulling forces that act on the plus end of the astral microtubules exerted by a dynein/dynactin motor complex (Kotak and Gönczy 2013; Okumura et al. 2018). In the next paragraphs I will go into detail of how mitotic spindle orientation is achieved, using some examples.

During the first division of the *C. elegans* zygote (Figure 9), the mitotic spindle aligns with the anterior-posterior axis, but it becomes closer to the posterior pole resulting in a big daughter cell and a small daughter cell (Siller and Doe 2009). This shift from the center of the zygote is caused by an increased activity of the “force generators” at the posterior pole (Grill et al. 2001, 2003). The Par complex formed by Par3, Par6 and aPKC locates at the anterior pole, while Par1 and Par2 locate at the posterior pole as discussed above. These Par proteins control the posterior accumulation of PI(4)P5-Kinase (PPK-1) through exclusion from the anterior pole by the casein kinase 1 (CSNK-1) (Figure 9), which results in GPR-1/2 (Pins in *Drosophila*, LGN in vertebrates) accumulation at the posterior pole during anaphase (Panbianco et al. 2008). GPR-1/2 is excluded from the lateral cortex by LET-99 (Park and Rose 2008). In this way, through the Par proteins and LET-99, three cortical domains are established: the anterior domain, a lateral domain and a posterior domain (Figure 9) (Krueger et al. 2010).

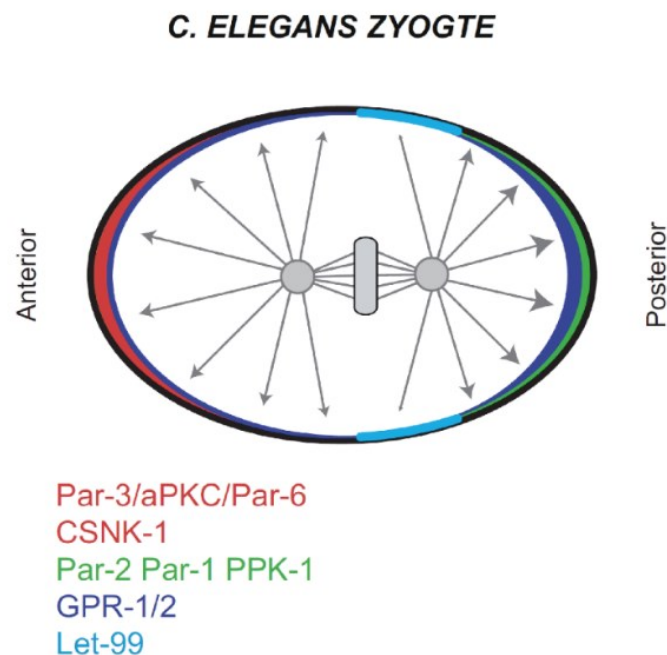


Figure 9. Alignment of the mitotic spindle with the anterior-posterior axis in the *C. elegans* zygote. For details, see text (Morin and Bellaïche 2011)

GPR-1/2 (LGN) binds through its GoLoco domain to GDP-bound G α anchored at the plasma membrane (Figure 10) (Morin and Bellaïche 2011). GPR-1/2 also binds to LIN-5 (Mud in *Drosophila*, NuMA in vertebrates) (Srinivasan et al. 2003), which interacts with the dynein/dynactin motor complex, also promoting its localization at the cell cortex (Nguyen-Ngoc, Afshar, and Gönczy 2007; Couwenbergs et al. 2007).

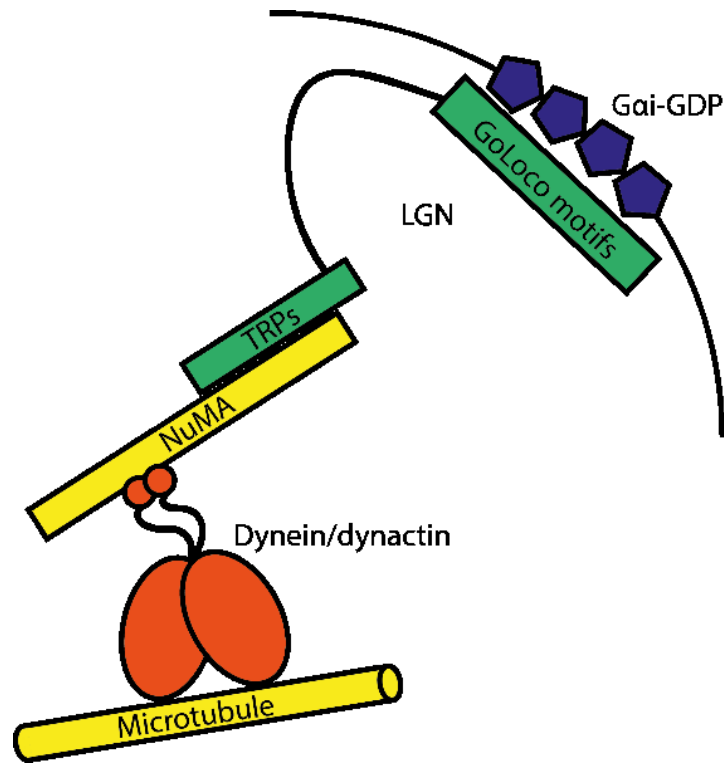


Figure 10. Model of mitotic spindle orientation by the Gai-LGN-NuMA complex. For details, see text. Adapted from Bergstralh, Haack, and St Johnston 2013

These proteins do not only position the mitotic spindle aligned to the anterior-posterior axis, but they can also align it to the apico-basal axis (Figure 11 A). During *Drosophila* development, neuroblasts delaminate from the neuroepithelium and divide asymmetrically along their apicobasal axis, to regenerate one neuroblast and produce the neurons of the larval nervous system (Kaltschmidt et al. 2000). In these cells, the Par complex formed by Baz-Par6-aPKC locates at the apical membrane during interphase and early prophase. Baz (Par 3) recruits Inscuteable to the apical membrane (Figure 11 A). Then, partner of Inscuteable (Pins, LGN in vertebrates) interacts through its GoLoco domain with GDP-bound G α and both are recruited to the apical membrane

by interaction of Pins with Insc through its tetratricopeptide repeats (TPR)(Yu, Kuo, and Jan 2006). Then Pins interacts with Mud (NuMA in vertebrates) at the apical pole also through its TPR domain (Bowman et al. 2006; Izumi et al. 2006; Siller, Cabernard, and Doe 2006). The apical localization of Mud also requires the adherens junction PDZ protein Canoe, which also associates with Pins (Speicher et al. 2008).

Pins has a linker domain between its GoLoco domain and its TPR domain. Through its linker domain, Pins can also control mitotic spindle orientation independently from Mud (Johnston et al. 2009). The mitotic spindle anchors to the edge of Pins localization: Pins binds to Dlg (Bellaïche et al. 2001), which binds to kinesin-73, a plus end microtubule motor (Siegrist and Doe 2005). This Pins linker activity is regulated by phosphorylation by the kinase Aurora A (Figure 11 A), which links Pins activity to cell cycle (Johnston et al. 2009).

Also in vertebrates, Gai, Pins, NuMA and Dynein are involved in apicobasal spindle orientation regulated by Insc (Morin and Bellaïche 2011). In mouse embryonic skin progenitors (Figure 11 B), it has been proved that mitotic spindle orientation along the apicobasal axis through the signaling cascade formed by mInsc-LGN-Gai-NuMA-dynein-dynactin is conserved (Lechler and Fuchs 2005). LGN localizes during interphase diffusively in the cytoplasm, but also at the cell cortex. During interphase, NuMA localizes in the nucleus, while during mitosis it has been observed at the cell cortex and at the mitotic spindle poles (Zhu et al. 2011). During mitosis along the apico-basal axis, mInsc, LGN and NuMA are located at the apical domain (Figure 11 B). This localization is controlled by β 1-integrin and α -catenin (Lechler and Fuchs 2005).

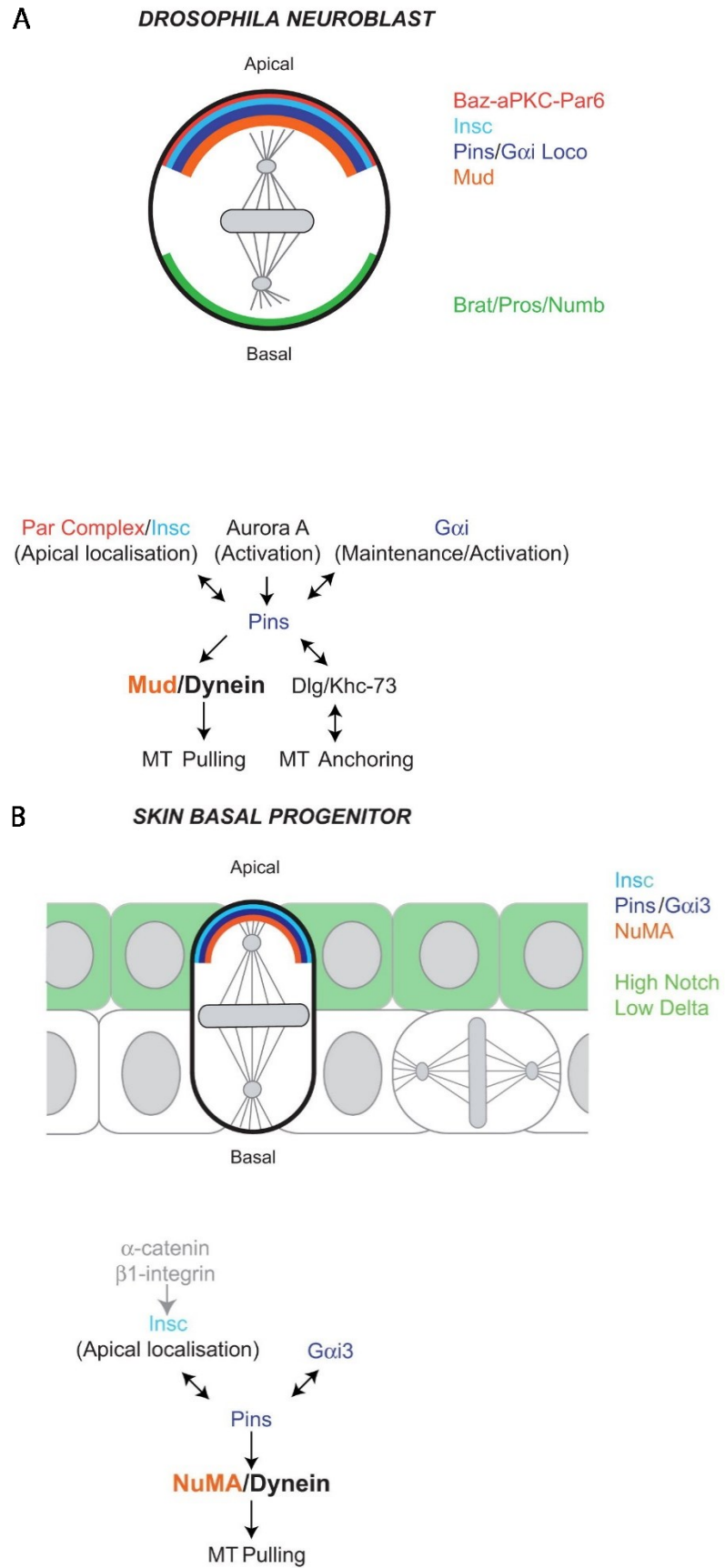


Figure 11. Mitotic spindle orientation along the apico-basal axis. Alignment during *Drosophila* neuroblast division (A) and mouse skin basal progenitor cell division (B) (Morin and Bellaïche 2011)

In planar cell divisions, like in the vertebrate neuronal progenitors (Figure 12 A), LGN and NuMA localize in a ring around the lateral cortex (Peyre et al. 2011). When the mitotic spindle forms, it rotates rapidly, until it finally aligns with the epithelial plane and locates just under the LGN-NuMA ring. Then, the spindle rotates in this plane until anaphase. Overexpression of Gai, makes LGN localize everywhere in the cell cortex making the spindle movements random (Peyre et al. 2011). This suggests that the Pins-NuMA complex is necessary for planar spindle orientation and at the same time is permissive for movement within this plane (Morin and Bellaïche 2011).

Planar cell divisions can also be controlled by planar cell polarity (Figure 12 B) so that they happen, for example, within the epithelial plane, but also along the anterior-posterior axis (Morin and Bellaïche 2011). During the *Drosophila* sensory organ precursor cell division (Figure 12 B), a pl cell divides to generate an anterior pllb cell and a posterior plla cell (Gho, Bellaïche, and Schweisguth 1999). Mud and Frizzled localize at the apical posterior membrane of the pl cell during cell division (Ségalen et al. 2010). This apical posterior localization of Mud is regulated by dishevelled, which binds Mud. Fz and Dsh signaling positions the Par proteins at the posterior-lateral membrane and Gai and Pins at the anterior-lateral cortex (Bellaïche et al. 2001).

Baz and Pins are not required for the alignment of the mitotic spindle with the anterior-posterior axis (David et al. 2005). However, loss of Pins tilts the spindle to a more apico-basal orientation, while Fz and Dsh mutants show a more planar orientation. Therefore, Fz and Dsh are responsible for the anterior-posterior orientation of the mitotic spindle, however tilting it towards the apico-basal axis. This is countered by the activity of Pins (Figure 12 B) (Morin and Bellaïche 2011).

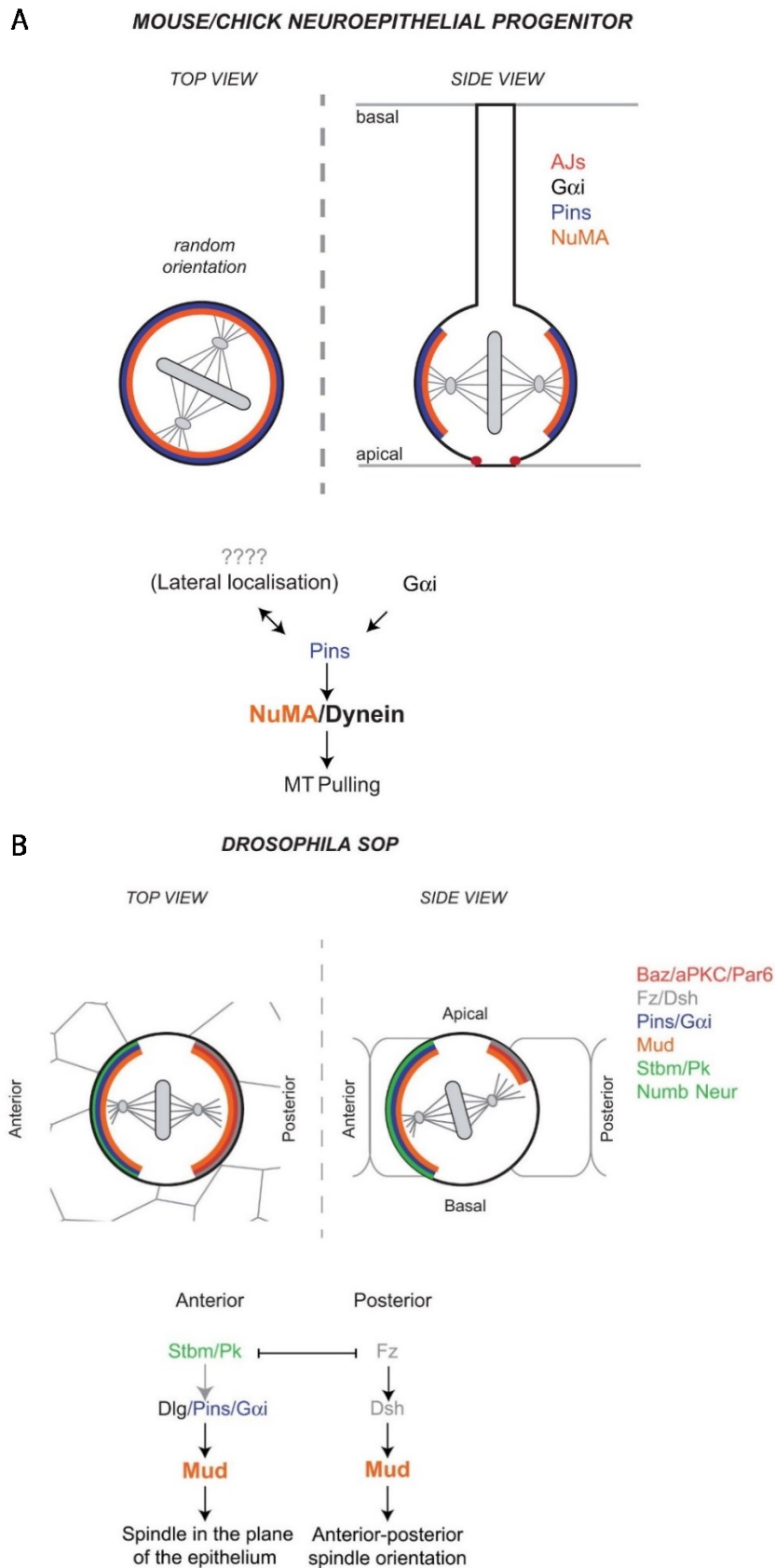


Figure 12. Alignment of the mitotic spindle with the epithelial plane. Planar cell polarity-independent alignment during vertebrate neuroepithelial progenitor cell division (A) and planar cell polarity-dependent orientation during the *Drosophila* sensory organ precursor cell division (B) (Morin and Bellaïche 2011)

In symmetric cell divisions during epithelial development, the daughter cells must remain in the epithelial plane. This is done by maintaining the mitotic spindle orientation within this plane (Morin and Bellaïche 2011). In dividing MDCK cells, G α i localizes everywhere at the cell cortex. LGN and NuMA, however, localize to the lateral membrane (Hao et al. 2010). LGN is phosphorylated by aPKC at the apical domain, which increases its affinity for a 14-3-3 protein. This creates a competition between 14-3-3 and GDP-bound G α i for LGN, resulting in the release of LGN from the apical membrane, to form a ring-like structure at the lateral cortex (Hao et al. 2010). There, LGN recruits NuMA through its TPR domain and NuMA exerts pulling forces on the astral microtubules to position the mitotic spindle through the dynein/dynactin motor complex, as described previously.

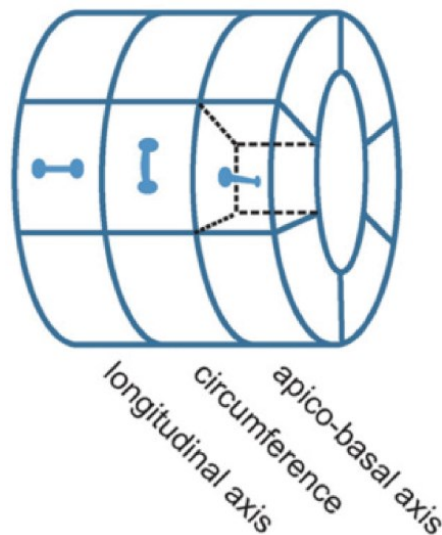


Figure 13. Different mitotic spindle orientation axes during tubular organ morphogenesis

In the mouse kidney *in vivo*, during postnatal nephron maturation, cell divisions in the renal tubular epithelial cells happen mostly in the direction of the renal tubule to increase its length without increasing its diameter (Fischer et al. 2006). Here, the Fat/Dachsous signaling pathway plays a role. Loss of the Fat4 gene results in mitotic spindle misorientation and enlarged tubules. This effect can be even more pronounced by removing Vangl2 (Saburi et al. 2008).

1.5. Semaphorin-plexin signaling

Semaphorins are a family of transmembrane, glycosylphosphatidylinositol-bound or secreted signaling proteins which were identified as axon guidance molecules (“Unified Nomenclature for the Semaphorins/Collapsins. Semaphorin Nomenclature Committee.” 1999). There are 20 described mammalian semaphorins divided in 5 classes (3-7) (Figure 14). They are characterized by having a Sema domain through which they interact with their receptors (Kolodkin, Matthes, and Goodman 1993). Semaphorins of the class 3 are secreted proteins, while semaphorins in the classes 4-6 are transmembrane and Semaphorin 7A is linked to the plasma membrane by GPI (Worzfeld and Offermanns 2014). Some transmembrane and GPI-bound semaphorins can be proteolytically cleaved and released, for example Sema4D, Sema5B or Sema7A (Elhabazi et al. 2001; Browne et al. 2012; Holmes et al. 2002). Among the vertebrate semaphorins, class 4, 5 and 6 have cytoplasmic domains (Gurrapu and Tamagnone 2016) that in some cases have been shown to interact with intracellular proteins (Sun et al. 2017).

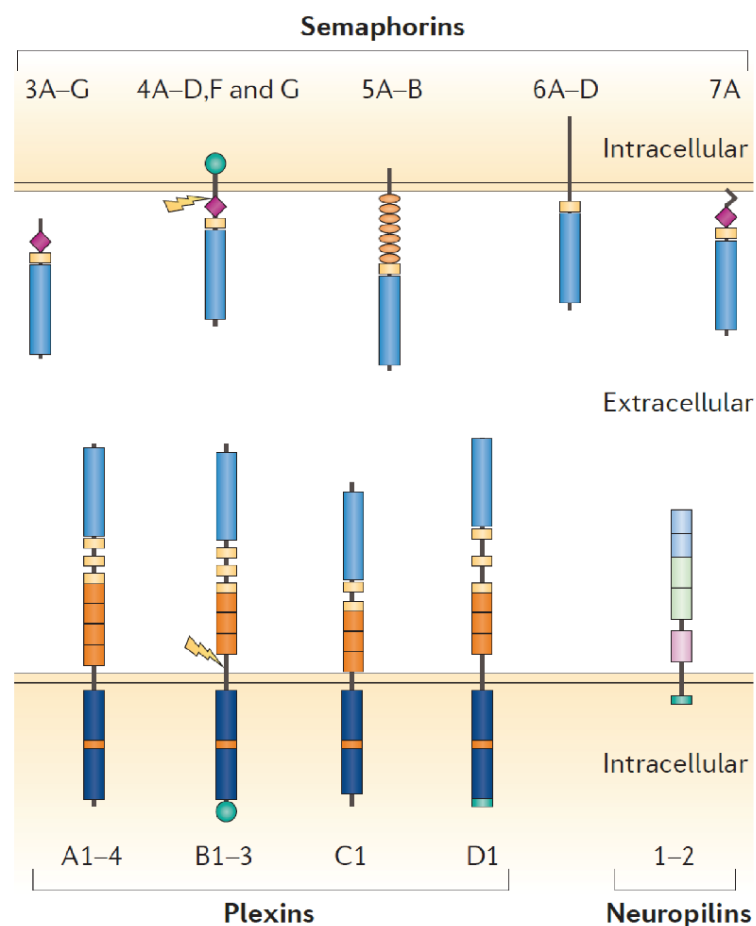


Figure 14. Semaphorin and plexin families. For details, see text (Worzfeld and Offermanns 2014)

Plexins are a family of transmembrane receptors for semaphorins (Tamagnone et al. 1999). In vertebrates there are 9 plexins divided in 4 classes (Plexin-A1-4, Plexin-B1-3, Plexin-C1 and Plexin-D1) (Figure 14). Plexins also have a Sema domain, which they use to bind semaphorins (Worzfeld and Offermanns 2014). Secreted class 3 semaphorins also interact with neuropilins (Neuropilin-1 and neuropilin-2, abbreviated as Nrp1 and Nrp2) (Figure 14) as co-receptors (Chen et al. 1997; Kolodkin et al. 1997; He and Tessier-Lavigne 1997). Plexins of the A subfamily are receptors for class 5 and class 6 semaphorins directly, but also for secreted class 3 semaphorins in necessary interaction with neuropilins. Plexins of the B subfamily are receptors for class 4 and class 5 semaphorins. Plexin-D1 binds Sema3E and Sema4A independently of neuropilins and several class 3 semaphorins with neuropilins as co-receptors. Lastly, Plexin-C1 is a receptor for Sema7A (Worzfeld and Offermanns 2014).

Even though semaphorins and plexins were initially described in the context of axon guidance (Tamagnone et al. 1999), many roles have been discovered in cell-cell communication for a variety of processes. In the nervous system, they play a role in synaptic plasticity and neural homeostasis (Pasterkamp and Giger 2009; Pasterkamp 2012; Koropouli and Kolodkin 2014). In the immune system they are involved in immune synapse formation, differentiation and migration (Kumanogoh and Kikutani 2013; Takamatsu and Kumanogoh 2012; Potiron et al. 2007). Semaphorin-plexin signaling has also been linked to bone remodelling and to osteoblast and osteoclast differentiation (Kang and Kumanogoh 2013; Negishi-Koga and Takayanagi 2012). Semaphorins and plexins have also been shown to play a role in vascular development, angiogenesis and cancer (Gu and Giraudo 2013; Sakurai et al. 2012; Neufeld et al. 2012). Furthermore, they have been proposed as therapeutical targets for a variety of diseases, including cancer (Tamagnone 2012; Worzfeld and Offermanns 2014; Zhang et al. 2018). Recently, Plexin-B2 has been shown to play a role in mitotic spindle orientation in the kidney epithelium (Xia et al. 2015), a role that will be discussed further in this section.

Apart from plexins and neuropilins, semaphorins have been shown to interact with other proteins as receptors, for example, Sema7A interacts with β 1 integrins (Pasterkamp et al. 2003) and in the immune system Sema4A and Sema4D interact with T-cell immunoglobulin and mucin domain-containing protein 2 (TIM2) and CD72,

respectively (Suzuki, Kumanogoh, and Kikutani 2008). Neural cell adhesion molecule L1 (L1CAM) has been shown to be part of a semaphorin receptor complex with neuropilin (Castellani et al. 2002). Also ErbB2 and MET, which interact with plexins of the B subfamily and Plexin-D1, are found in semaphorin receptor complexes (Swiercz, Kuner, and Offermanns 2004; Giordano et al. 2002; Casazza et al. 2010).

Some migrating cells and axons express simultaneously on their surface semaphorins and their respective plexin receptors (Winberg et al. 1998) and autocrine Semaphorin-Plexin signaling has been observed (Serini et al. 2003; Catalano et al. 2004). Furthermore, “reverse” signaling in which semaphorins act as receptors instead of ligands and start intracellular signaling cascades mediated by their cytoplasmic domains has been found exclusively for transmembrane semaphorins (Gurrapu and Tamagnone 2016). One example of this phenomenon can be observed during the trabeculation and expansion of the compact layer as part of the myocardium development, in which Sema6D reverse signaling recruits and activates the kinase Abelson (Abl), which phosphorylates Mena (an actin binding protein, also known as Enabled or VASP), promoting its dissociation from Sema6D and enhancing the migration of myocardial cells (Toyofuku, Zhang, Kumanogoh, Takegahara, Yabuki, et al. 2004).

Semaphorin-Plexin “forward” signaling acts through binding of a semaphorin dimer with two plexin receptors, each semaphorin interacting with only one plexin molecule, which brings them together forming a plexin dimer that becomes activated (Janssen et al. 2010). The cytoplasmic portion of plexins has two domains with a sequence similar to that of Ras GAPs that fold together to form a GAP-homologous domain (Rohm et al. 2000; Hu, Marton, and Goodman 2001). R-Ras and M-Ras inactivation was observed upon Semaphorin-Plexin signaling and consequently, Plexins were initially proposed as GAPs for R-Ras and M-Ras (Oinuma et al. 2004; Saito et al. 2009). However, it was later shown that they do not have a GAP activity towards Ras, but act in a non-canonical way to inactivate another Rho GTPase, Rap (Wang et al. 2012). Between the two sequences homologous to Ras GAPs lies a Rho GTPase-binding domain (RBD) that has been shown to bind active Rac1 and the constitutively active Rho GTPase Rnd1 (Driessens et al. 2001; Zanata et al. 2002). Even though plexins lack a direct GAP activity towards Ras, plexin-mediated inactivation of R-Ras and M-Ras through a

mechanism yet unknown requires binding to their semaphorin ligand and interaction with Rnd1 or active Rac1 through the RBD (Oinuma et al. 2004; Oinuma, Katoh, and Negishi 2004; Wang et al. 2012). However, the GAP activity towards Rap does not need binding of a Rho GTPase to the RBD (Wang et al. 2012).

The GAP-homologous domain of plexins is essential for Semaphorin-Plexin signaling, as point mutations in its sequence impair its axonal growth cone collapse function (Oinuma et al. 2004; Saito et al. 2009; Sakurai et al. 2010) and in some cases even result in the same phenotypic effects as their respective complete knockout (Worzfeld et al. 2014). It has been proposed that the inhibition of Ras by Semaphorin-Plexin signaling could be achieved by sequestering it rather than inactivating it (Sakurai et al. 2010), although another possibility would be that plexins interact with a Ras GAP. Plexins of the B family also contain a PDZ domain-binding motif, through which they interact with Rho GEFs (PDZ-RhoGEF and LARG) that activate RhoA and RhoC (Aurandt et al. 2002; Perrot, Vazquez-Prado, and Gutkind 2002; Swiercz et al. 2002). Mutations in the GAP-homologous domain of plexins does not impair RhoA activation and conversely, deletion of the PDZ domain-binding motif does not affect Ras inactivation (Oinuma et al. 2004), making these two effector cascades of Semaphorin-Plexin signaling independent of each other. Although some of the plexin signaling pathways are shared for several of the subclasses, there is also subclass-specific signaling (Jongbloets and Pasterkamp 2014).

Semaphorin-Plexin signaling controls integrin-dependent cell migration in a variety of cell types (Tamagnone and Comoglio 2004). R-Ras is able to regulate the activation of $\beta 1$ integrins (Zhang et al. 1996). Semaphorin-Plexin signaling has been shown to effectively reduce cell migration by inhibiting R-Ras and PI3K-mediated $\beta 1$ integrin activation/FAK signaling, for which the GAP-homologous domain of plexins and binding of Rnd1 to the RBD are required (Oinuma, Katoh, and Negishi 2006). However, promotion of cell migration and integrin signaling by semaphorins and plexins has also been observed (Basile, Gavard, and Gutkind 2007; Banu et al. 2006). Therefore, the role of Semaphorin-Plexin signaling in integrin-mediated cell adhesion and migration is not fully clear. During thymocyte maturation into T-lymphocytes at the thymic cortex, precise control of Plexin-D1 expression was shown to promote integrin clustering at the

thymocyte surface, while binding of Plexin-D1 to medullary-secreted Sema3E shortened the bond lifetime of integrin adhesion, thus constituting yet a different mechanism of Semaphorin-Plexin regulation of integrin-mediated cell adhesion and migration (Choi et al. 2014). Moreover, Rap has also been demonstrated to activate integrins (Gloerich and Bos 2011) and therefore, plexins could mediate integrin adhesion through Rap (Wang et al. 2012).

Rho can induce neurite retraction through its effector ROCK, which controls local actin dynamics (Dickson 2001). It has been shown that plexins of the B family can promote axonal growth cone collapse upon binding to their semaphorin ligand through PDZ-RhoGEF and LARG-mediated RhoA activation (Swiercz et al. 2002). The interaction between class I PDZ domain proteins and the C-terminus of proteins to which they bind happens through a conserved K/RxxxGLGF sequence in the PDZ domain and a xS/TxØ sequence in its target proteins (Doyle et al. 1996; Taya et al. 2001). In Plexins of the B subfamily, the carboxy-terminal VTDL amino acids constitute a PDZ domain binding motif (xS/TxØ) through which they interact with the PDZ domains of LARG and PDZ-RhoGEF (Aurandt et al. 2002; Perrot, Vazquez-Prado, and Gutkind 2002). Importantly, Plexin-B1 does not interact with the type I PDZ domain of Lin-7 (Aurandt et al. 2002) and neither Plexin-B1 nor Plexin-B2 interact with the PDZ domain of Tiam1 (Perrot, Vazquez-Prado, and Gutkind 2002), suggesting that the PDZ domain-binding motif of plexins of the B subfamily is specific for the class I PDZ domains of LARG and PDZ-RhoGEF. Binding to PDZ-RhoGEF and LARG has been shown to promote membrane localization of Plexin-B1 (Swiercz et al. 2002). Furthermore, Plexin-B1 interacts with ErbB2, which gets activated upon Sema4D binding to Plexin-B1, inducing ErbB2 autophosphorylation and phosphorylation of Plexin-B1, which was shown to be necessary for Plexin-B1-RhoA-mediated axonal growth cone collapse (Swiercz, Kuner, and Offermanns 2004).

Semaphorin-plexin signaling can be modulated to be able to elicit a variety of functions in a time- and space-controlled way. One of the mechanisms to achieve this is through co-receptor subunits (Pasterkamp 2012). For example, Sema5A is an attractive cue for axons expressing heparan sulphate proteoglycans, but for axons expressing chondroitin sulphate proteoglycans it acts as a repulsive signal (Kantor et al. 2004;

Hilario et al. 2009). Another mechanism by which one semaphorin or a semaphorin-plexin pair can mediate different responses is through the “reverse” signaling explained above. Semaphorin-Plexin signaling can be timely controlled by regulating receptor expression (Pasterkamp 2012). For example, Nrp1 and Nrp2 are transcriptionally repressed by the homeobox transcription factors DLX1, DLX2 and NKX2.1 in telencephalic interneurons to allow them enter the Sema3A- and Sema3F-expressing striatum (Le et al. 2007; Nóbrega-Pereira et al. 2008) or by COUP transcription factor 2 (COUP-TF2, also known as NR2F2) in mouse PAX-6 positive cells that migrate from the caudal ganglionic eminence to the amygdala (Tang et al. 2012). The cellular response to semaphorins is also controlled by semaphorin-plexin *cis* interactions (Pasterkamp 2012). Both dorsal root ganglion and sympathetic neurons express Plexin-A4, but repulsion by Sema6A only happens in sympathetic axonal growth cones, due to the fact that that dorsal root ganglion neurons express Sema6A themselves, which interacts with Plexin-A4 in *cis*, preventing interaction in *trans* (Haklai-Topper et al. 2010). Another example of this phenomenon occurs during hippocampal development. Mossy fibres expressing Plexin-A4 can enter the Sema6A-expressing stratum lucidum because pyramidal neurons of the stratum lucidum co-express Sema6A with Plexin-A2, which interact in *cis*, inhibiting the interaction in *trans* between their Sema6A and Plexin-A4 on mossy fibres (Suto et al. 2007).

Semaphorin signaling has several functions in the development of the nervous system that go beyond its role as an attractive or repulsive molecule (Pasterkamp 2012). As stated above, neurons are highly polarized cells that have distinct neurites: the axon and the dendrites. During polarization of neurons, axonal identity is specified by high levels of cAMP, while dendrite specification is promoted by elevated levels of cGMP (Shelly et al. 2010). Sema3A promotes dendrite specification in cooperation with Nrp1 by reducing the cAMP levels and increasing cGMP (Shelly et al. 2011). Semaphorin-Plexin signaling can also control where synapses are formed at the subcellular level by regulating the number and shape of dendritic spines in specific neurites (Koropouli and Kolodkin 2014). For example, Sema3F controls the distribution and morphology of dendritic spines in primary apical dendrites of cortical pyramidal neurons through a receptor complex formed by Nrp2 and Plexin-A3 (Tran et al. 2009). Semaphorins have

also been implicated in axonal pruning, a process consisting in the withdrawal of axon branches that make temporary connections during brain development (Bagri et al. 2003).

In the immune system Semaphorin-Plexin signaling plays different roles. Besides the above mentioned role of Sema3E and Plexin-D1 in thymocyte maturation, it has been shown that Plexin-A1 in cooperation with Nrp1 mediates dendritic cell transmigration between lymphatic endothelial cells in response to endothelial-secreted Sema3A through regulation of actomyosin contractility (Takamatsu et al. 2010). Moreover, Sema4D binding to Plexin-B1 and Plexin-B2 contributes to the adhesion between monocytes and endothelial cells (Luque et al. 2015). Semaphorin signaling not only plays a role in immune cell migration but also in immune cell-cell communication. For example, Sema4D is able to promote the activation of B and T cells and it is linked to antibody production and antigen-specific T cell responses (Shi et al. 2000). Sema7A is expressed in activated T cells and signals through $\alpha 1\beta 1$ integrins to stimulate monocytes and macrophages to produce interleukin 6 (IL-6) and tumor necrosis factor α (TNF α), which are proinflammatory cytokines (Suzuki et al. 2007). Moreover, Sema3A, expressed in T cells, dendritic cells and some tumor cells, binds to Nrp1-Plexin-A4 on T cells to inhibit their proliferation and immune responses (Catalano et al. 2006; Yamamoto et al. 2008).

In the bone, Semaphorin-Plexin signaling is involved in bone remodeling, that when altered can cause osteopenia, osteoporosis or osteopetrosis (Kang and Kumanogoh 2013). For example, Sema4D-Plexin-B1 signaling inhibits bone mineralization and induces osteoclast formation (a cell type specialized in bone resorption) (Negishi-Koga et al. 2011). Plexin-A1, stimulated by Sema6D, associates with triggering receptor expressed on myeloid cells 2 (Trem-2), which could result in promotion of osteoclastogenesis (Takegahara et al. 2006). Sema3A through Nrp1 and Plexin-A1 is involved in osteoprotection by simultaneously promoting osteoblast differentiation in a Rac1-mediated way and by inhibiting osteoclast precursor migration to the bone forming site in a RhoA-dependent manner (Hayashi et al. 2012).

Semaphorin-Plexin signaling also plays several roles in vasculogenesis. During development, Sema3E expressed in the somites signals through Plexin-D1 on

endothelial cells of intersomitic vessels to mediate repulsion and restrict vessel growth to the intersomitic space (Gu et al. 2005). Sema3E negatively regulates VEGF signaling (Gu and Giraudo 2013). For example, during the development of retinal vasculature, Sema3E produced by the retinal ganglion cells (RGCs) binds Plexin-D1 expressed on the surface of endothelial cells at the front of sprouting blood vessels to inhibit VEGF-mediated Dll4-Notch signaling (Kim et al. 2011). Semaphorin-Plexin signaling is also involved in tumor angiogenesis (Gu and Giraudo 2013). Tumor angiogenesis has been shown to be inhibited by Sema3A (Maione et al. 2009; Casazza et al. 2011), Sema3B (Varshavsky et al. 2008), Sema3D (Sabag et al. 2012), Sema3E (Sakurai et al. 2010) and Sema3F (Bielenberg et al. 2004; Kessler et al. 2004).

Through its role in tumor angiogenesis or by acting directly on cancer cells, Semaphorin-Plexin signaling has been shown to be involved in cancer progression. The first observation of this was that Sema3F constitutes a tumor suppressor in lung cancer, where it is frequently deleted (Roche et al. 1996; Xiang et al. 1996). In lung cancer cells, the highly expressed transcription repressor zinc finger E-box binding homeobox 1 (ZEB-1) inhibits Sema3F expression (Clarhaut et al. 2009). Sema3F also inhibits tumor growth and metastasis in mouse xenografts (Bielenberg et al. 2004). Sema3A through Nrp1 inhibits breast cancer migration and invasion in an autocrine manner (Bachelder et al. 2003; Pan and Bachelder 2010). Sema3B is deleted in lung cancer, similarly as Sema3F and it is also lost in neuroblastoma (Tomizawa et al. 2001; Nair et al. 2007). Sema3E binds Plexin-D1 promoting its association with ErbB2 and the activation of the latter in cancer cells (Casazza et al. 2010). Sema4D promotes tumor growth and angiogenesis of head and neck squamous cell carcinomas via Plexin-B1 expressed on endothelial cells (Basile et al. 2006). However, tumor angiogenesis is not inhibited in mice lacking Plexin-B1, which suggests that other class B plexins could compensate its loss (Fazzari et al. 2007). Sema4D has also been shown to trigger invasive growth upon binding to Plexin-B1 by activating scatter factor receptors Ron and Met, which induces their tyrosine kinase activity towards Plexin-B1 and themselves (Giordano et al. 2002; Conrotto et al. 2004). Interestingly, in breast cancer cells, Sema4D signaling through Met-associated Plexin-B1 inhibits cell migration, while signaling through ErbB2-associated Plexin-B1 promotes it (Swiercz, Worzfeld, and Offermanns 2008). Sema5A,

whose receptor is Plexin-B3, is upregulated in several types of cancer (Lu et al. 2010; Sadanandam et al. 2010). *Sema5A*, like *Sema4D*, has been shown to activate Met upon binding to Plexin-B3 (Artigiani et al. 2004). *Sema6D* receptor Plexin-A1 associates with VEGF tyrosine kinase receptor 2 (VEGFR-2) in mesothelioma cells (Catalano et al. 2009) and *Sema6D* has been shown to activate VEGFR-2 (Toyofuku, Zhang, Kumanogoh, Takegahara, Suto, et al. 2004). This activation promotes the anchorage-independent growth of mesothelioma cells (Catalano et al. 2009).

Epithelial-to-mesenchymal transition not only happens during development, but also in cancer cells, where it increases invasiveness, resistance to drugs and allows metastasis (Zhang and Weinberg 2018). Semaphorin signaling has also been linked to EMT (Gurrapu and Tamagnone 2019). For example, *Sema3A* (Maione et al. 2012; Wang et al. 2016) and *Sema3B* (Shahi et al. 2017) have been shown to inhibit EMT. Contrarily, *Sema3C* (Herman and Meadows 2007; Tam et al. 2017; Xu et al. 2017), *Sema3E* (Rehman et al. 2016; Tseng et al. 2011), *Sema4A* (Rokavec, Horst, and Hermeking 2017; Pan, Wang, and Ye 2016), *Sema4C* (Gurrapu et al. 2018) and *Sema7A* (Allegra et al. 2012; Garcia-Areas et al. 2017; Liu et al. 2018) have been found to promote EMT. Finally, *Sema5A* has been shown to promote (Pan, Zhang, et al. 2013; Pan, Zhu, et al. 2013) and inhibit (Saxena et al. 2018) EMT, so its effects could be cell type-specific.

Semaphorin-Plexin signaling also plays a role in epithelial cells in several processes, including polarity. *Sema4D* and Plexin-B1 have been shown to be expressed in mesenchymal-epithelial interfaces in many developing organs, with Plexin-B1 being frequently expressed in the epithelium and receiving *Sema4D* signals from the mesenchyma, which in the developing kidney was shown to inhibit epithelial branching of the ureteric tips (Korostylev et al. 2008). In *Drosophila* and zebrafish it has been shown that Semaphorin-Plexin signaling is involved in wound repair in epithelia (Yoo et al. 2016). Also in *Drosophila*, migrating follicular epithelial cells express *Sema5C* in a planar polarized manner at the leading edge of the basal membrane, promoting collective cell migration required for egg elongation by signaling through Plexin A and inhibiting protrusion formation at the rear edge of neighbouring cells (Stedden et al. 2019). During lung development, *Sema3C* and *Sema3F* promote epithelial branching and proliferation, while *Sema3A* signaling reduces the number of terminal pulmonary buds

(Kagoshima et al. 2001). Also during lung development, the Grainyhead-like transcription factor 2 (Grhl2), which regulates cell-cell adhesion molecule expression, also regulates the expression of Sema3B, Sema3C and their receptor Nrp2 (Varma et al. 2012). During the development of the cornea, Sema3A secreted by the corneal fibroblasts induces the membrane expression of E- and N-cadherins in corneal epithelial cells (Ko et al. 2010).

Interestingly, Semaphorin-Plexin signaling has also been shown to control mitotic spindle orientation. Sema3B released from the ventricle floor plate and nascent choroid plexus controls the apicobasal orientation of mitosis in neuroepithelial progenitors, but its loss does not alter apicobasal polarity and instead it is believed to act directly on mitotic spindle orientation through the regulation of the actin and microtubule cytoskeletons in a LIM kinase-1 (LIMK1)-cofilin- and glycogen-synthase kinase 3 β -collapsin response mediator 2 (CRMP2)-dependent way (Arbeille et al. 2015). A recent study from our group has shown that Plexin-B2 plays a role in mitotic spindle orientation during kidney development and repair, as well as in MDCK cyst formation (Xia et al. 2015). In that study, the knockdown of Plexin-B2 by shRNA and siRNA in MDCK cells yielded highly misorganized cysts with multiple lumina or with lumina filled with cells. *In vivo*, conditional knockout of Plexin-B2 in renal tubular epithelial cells showed normal kidney morphology, which was explained by a compensation mediated by the Plexin-B2 close homologue Plexin-B1, which is also expressed during development in the kidney. However, a Plexin-B1 and Plexin-B2 double conditional knockout showed multi-layered kidney tubules. Additionally, as opposed to control mice, Plexin-B2 knockout mice could not repair the kidney epithelium after an ischemic injury and developed multi-layered tubuli similar to those of Plexin-B1/Plexin-B2 double knockout mice. This result is possible because in the adult tubular epithelial cells Plexin-B1 is no longer expressed. Moreover, it was shown that the generation of multi-layered kidney tubules and abnormal MDCK cysts was the consequence of a shift in the mitotic spindle orientation from a position aligned with the epithelial plane to one perpendicular or oblique to it. It was also demonstrated that this role of Plexin-B2 in the control of mitotic spindle orientation is mediated by the Rho-GTPase Cdc42. The knockdown of Plexin-B2 in MDCK cells resulted in decreased activity of Cdc42. Furthermore, the abnormal lumen

phenotype of Plexin-B2-depleted MDCK cysts could be rescued by transfection of a constitutive active form of Cdc42. However, whether Plexin-B2 controls mitotic spindle regulators is still unknown.

1.6. CRISPR/Cas9 genome editing

In this work the CRISPR/Cas9 genome editing method was used to achieve Plexin-B2 deletion in kidney cell lines. CRISPR stands for Clustered Regularly Interspaced Short Palindromic Repeats. It constitutes an adaptive immune system in archaea and bacteria against foreign molecules of DNA (Mojica, Juez, and Rodriguez-Valera 1993; Horvath and Barrangou 2010). It is composed of CRISPR-associated genes (Cas), non-coding RNAs and an array of palindromic repeats interspaced by variable sequences which have a foreign origin (crRNA) (Makarova et al. 2011). The Cas proteins are nucleases that produce double strand breaks in the targeted foreign DNA molecules. The crRNA gets processed into several units and each short variable fragment directs the Cas nuclease to the target DNA (Garneau et al. 2010).

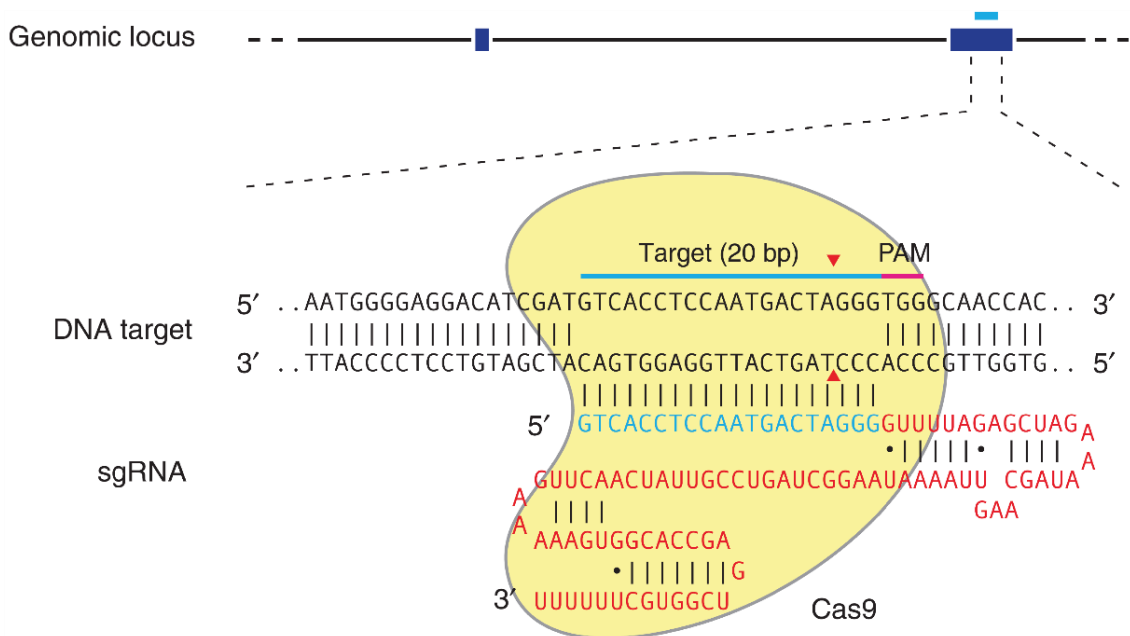


Figure 15. CRISPR/Cas9 system. Schematic of the genomic targeting of the Cas9 nuclease through a specific RNA sequence (Ran et al. 2013)

This system has been exploited to introduce modifications at desired locations in genomic DNA in the laboratory (Figure 15) by expressing a human codon-optimized Cas9 together with a single-guide RNA (sgRNA), consisting of a 20 nucleotide sequence targeted to a specific location of the genomic DNA and a scaffold sequence that interacts with the Cas9 (Ran et al. 2013). After the double strand break happens, two possible repair mechanisms could be activated. The Non-Homologous End Joining (NHEJ) repair mechanism deletes some bases before and after the double strand break and then ligates the DNA. With this method, deletions that cause a premature stop codon can be introduced to generate gene knockouts (Perez et al. 2008). This was the method used in this work. On the other hand, in proliferative cells, if a repair template is supplied, the cell could use the Homologous Recombination (HR) method. In this method the cell uses a template partially homologous to the damaged sequence to synthesize the damaged fragment (Saleh-Gohari and Helleday 2004). This method can be used to introduce specific changes in the nucleotide sequence of a gene or to introduce complete genes into a genome, like fluorescent proteins (Chen et al. 2011; Ran et al. 2013).

2. Aim of this study

The aim of this thesis was to investigate the molecular mechanisms underlying the control of mitotic spindle orientation by Plexin-B2.

3. Materials and Methods

3.1. Materials

Mouse lines

The Sema4B/Sema4D/Sema4G triple-knockout mouse line has been described previously (Xia et al. 2015).

Name	Genotype
Wildtype	C57BL/6 wildtype mice
Sema4BDG triple-Knockout	<i>sema4B^{-/-};sema4D^{-/-};sema4G^{-/-}</i>

Antibodies

Name	Manufacturer	Reference number	Dilution
Anti-armenian hamster-Cy3	Jackson ImmunoResearch	127-165-160	1:200
Anti-CD100 (Sema4D)	eBioscience	BMA12	1:200
Anti-E-cadherin	Cell Signaling	3195	1:200
Anti-E-cadherin	Invitrogen	13-1900	1:200
Anti-Mouse-Alexa Fluor 555	Invitrogen	A-21424	1:200
Anti-Plexin-B2	eBioscience	eBio3E7	1:500
Anti-Plexin-B2	R&D Systems	AF6836	1:1000
Anti-Rabbit-Alexa Fluor 488	Invitrogen	A-11008	1:200
Anti-Rabbit-HRP	Bio-Rad	1706515	1:5000
Anti-Rat-Alexa Fluor 488	Invitrogen	A-11006	1:200
Anti-Rat-Alexa Fluor 555	Invitrogen	A-21434	1:200
Anti-Sheep-HRP	Bio-Rad	172-1017	1:5000
Anti-ZO-1	Invitrogen	61-7300	1:200
Anti-ZO-1	Millipore	MABT11	1:200
Anti- α -Tubulin	Cell Signaling	2125	1:1000
Anti- β -catenin	BD Biosciences	610153	1:200

Devices

Device	Manufacturer
AE200	Mettler Toledo
AxioObserver.Z1	Zeiss
Axiovert 25	Zeiss
B6	Heraeus
Biofuge Pico	Heraeus
Biofuge Stratos	Heraeus
BioPhotometer 6131	Eppendorf
CSU-X1	Yokogawa
Eclipse Ti	Nikon
Evolve 512 EMCCD camera	Teledyne Photometrics
FACSCanto II 3L	BD Biosciences
FlexCycler ²	Analytik Jena
Gel Documentation System	PEQLAB
Heracell 1500	Heraeus
Herasafe	Heraeus
L610 D	Sartorius
Labofuge 400	Heraeus
Labogaz 206	Campingaz
LSM 700	Zeiss
MaxQ 4000	Thermo Scientific
Mi5 Processor	Jet X-Ray
MicroPulser	Bio-Rad
Micro Star 17R	VWR
Mini-PROTEAN Tetra Vertical Electrophoresis Cell	Bio-Rad
Nanodrop 1000	Thermo Scientific
PowerPac 300	Bio-Rad
RH Digital	IKA
RM5	Cat
S20 SevenEasy	Mettler Toledo
Sorvall RC-5B Plus	DuPont
Standard Power Pack P25 T	Biometra
Thermomixer C	Eppendorf
UV-transilluminator	PEQLAB
Varioklab 135 S	HP Medizintechnik
Vortex-Genie 2	Scientific Industries
CM3050 S	Leica
IQ5	Bio-Rad

Chemicals and reagents

Name	Manufacturer
Acetic acid	Carl Roth
Agarose	Carl Roth
Alcaline phosphatase	Fermentas
Alcaline phosphatase buffer	Fermentas
Ammonium persulfate	Merck
Bovine serum albumin (BSA)	Carl Roth
Calcium chloride	Carl Roth
Chloroform	Carl Roth
Crystal violet	Carl Roth
4',6-diamidino-2-phenylindole (DAPI)	Sigma Aldrich
Disodium phosphate	Carl Roth
Ethylenediaminetetracetic acid (EDTA)	Carl Roth
Ethanol	Carl Roth
Ethidium bromide	Sigma Aldrich
Fetal Calf Serum (FCS)	Invitrogen
Fluorescence Mounting Medium	Dako, Agilent
GeneRuler 1 Kb DNA ladder	Fermentas
GeneRuler 100 bp plus DNA ladder	Fermentas
Glutaraldehyde	Carl Roth
Glycine	Carl Roth
Isopropanol	Carl Roth
6X Loading dye	Fermentas
Milk powder	Carl Roth
NEBuffer 2	NEB
PageRuler Plus Prestained	Fermentas
Phosphate buffered saline (PBS)	Capricorn Scientific
Pepton/trypton	Carl Roth
Paraformaldehyde (PFA)	Carl Roth

PeqGOLD TriFast	VWR
Phenol/chloroform/isoamyl alcohol	Carl Roth
Potassium acetate	Carl Roth
Proteinase K	Thermo Scientific
RNase A	Sigma Aldrich
Rotiphorese Gel 30	Carl Roth
Sodium acetate	Carl Roth
Sodium dodecyl sulfate (SDS)	Carl Roth
Sodium chloride	Carl Roth
Sodium hydrogen phosphate	Carl Roth
Sodium hydroxide	Carl Roth
Sucrose	Carl Roth
T4 DNA ligase	Thermo Scientific
T7E1 endonuclease	NEB
10X T4 DNA ligase buffer	Thermo Scientific
Tetramethylethylenediamine (TEMED)	Carl Roth
Tissue-Tek OCT compound	Sakura
Tris	Carl Roth
Triton X 100	Carl Roth
Tween 20	AppliChem
Yeast extract	Carl Roth

Cell culture

Product	Manufacturer
N,N-bis(2-hydroxyethyl)-2-aminoethanesulfonic acid (BES)	Sigma Aldrich
Calcium chloride	Carl Roth
Dimethyl sulfoxide (DMSO)	Carl Roth
Dulbecco's modified Eagle medium (DMEM)	Capricorn Scientific
Dulbecco's modified Eagle medium/Nutrient mixture F12 (DMEM/F12)	Gibco

Materials and methods

Fetal calf serum (FCS)	Invitrogen
Lipofectamine LTX	Thermo Scientific
Matrigel	Corning
Millex-HV 33 mm PVDF filters of 0,45 µm pore size	Merck
Minimum essential medium (MEM)	Gibco
µ-slide 8 well	Ibidi
OptiMEM	Thermo Scientific
Penicillin/Streptomycin	Capricorn Scientific
Phosphate buffered saline (PBS)	Capricorn Scientific
Plus Reagent	Thermo Scientific
Polybrene	Sigma Aldrich
Puromycin	Invitrogen
SiR-Tubulin	Spirochrome
Trypsin-EDTA	Capricorn Scientific

Restriction enzymes and buffers

Name	Manufacturer
BamHI buffer	Fermentas
Buffer O	Fermentas
Buffer R	Fermentas
DraI	Fermentas
Eco47III	Fermentas
NotI	Fermentas
Sall	Fermentas

PCR reagents

Name	Manufacturer
dNTP Mix (10 mM each)	Thermo Scientific
5X GC buffer (Contains MgCl ₂)	Thermo Scientific
iQ SYBR Green Supermix	Bio-Rad
10X Long PCR buffer with 15 mM MgCl ₂	Thermo Scientific
Long PCR enzyme mix, 5 U/μl	Thermo Scientific
Magnesium chloride	Fermentas
Nuclease-free water	Fermentas
Phusion Hot Start II polymerase	Thermo Scientific
Random hexamer primer	Thermo Scientific
RevertAid Reverse Transcriptase	Thermo Scientific
RiboLock RNase inhibitor	Thermo Scientific
5X RT buffer	Thermo Scientific
SYBR Green Supermix	Bio-Rad
10X Taq Buffer + KCl - MgCl ₂	Fermentas
Taq DNA polymerase	Fermentas

Kits

Name	Manufacturer
NucleoSpin Gel and PCR clean-up	Macherey-Nagel
Propidium Iodide Flow Cytometry kit	Abcam
QIAamp MinElute Virus Spin kit	Qiagen
RNeasy Mini Kit	Qiagen
TURBO DNA-free Kit	Thermo Scientific

Vectors and plasmids

Name	Description
pcDNA3-3Xmyc-Plexin-B2	Non-viral, triple myc-tagged mouse Plexin-B2 mammalian expression plasmid
pEGFP-C1-LGN	Non-viral, EGFP-tagged chicken LGN mammalian expression plasmid
pEGFP-N1	Non-viral mammalian expression vector for C-terminal tagging of proteins with EGFP
pLNCX2	Retroviral expression vector by Clontech (Takara)
pLV-EGFP-hNuMA	VectorBuilder ID: VB171110-1111fye. Lentiviral, EGFP-tagged human NuMA mammalian expression plasmid
pSpCas9(BB)-2A-GFP (PX458)	Non-viral, CRISPR <i>S. pyogenes</i> Cas9 and 2A-GFP mammalian expression plasmid with cloning backbone for sgRNA
pSpCas9(BB)-2A-Puro (PX459 v2.0)	Non-viral, CRISPR <i>S. pyogenes</i> Cas9 and 2A-Puro mammalian expression plasmid with cloning backbone for sgRNA
pWPXL-H2B-mCherry	Lentiviral mCherry-tagged histone H2B mammalian expression plasmid
pWPXL-Tubulin-mCherry	Lentiviral mCherry-tagged Tubulin mammalian expression plasmid
PX459_mPB2_65	Non-viral, CRISPR <i>S. pyogenes</i> Cas9, 2A-Puro and mouse Plexin-B2 sgRNA 65 mammalian expression plasmid
PX459_mPB2_125	Non-viral, CRISPR <i>S. pyogenes</i> Cas9, 2A-Puro and mouse Plexin-B2 sgRNA 125 mammalian expression plasmid

PX459_mPB2_227	Non-viral, CRISPR <i>S. pyogenes</i> Cas9, 2A-Puro and mouse Plexin-B2 sgRNA 227 mammalian expression plasmid
PX459_mPB2_260	Non-viral, CRISPR <i>S. pyogenes</i> Cas9, 2A-Puro and mouse Plexin-B2 sgRNA 260 mammalian expression plasmid

Primers and oligos

Name	Sequence
sgRNA_mPB2_65_fwd	CACCGTGC GGAACTCTCCGGCTTT
sgRNA_mPB2_65_rev	AAACAAAGCCGGAGAGTTTCCGCAC
sgRNA_mPB2_125_fwd	AAACCGACATACACCACACCTGTGC
sgRNA_mPB2_125_rev	CACCGCACAGGTGTGGTGTATGTCTG
sgRNA_mPB2_227_fwd	AAACCAATGGGTGGTGTGCACTTC
sgRNA_mPB2_227_rev	CACCGAAGTGCACACCACCCATTG
sgRNA_mPB2_260_fwd	CACCGTGT CAGTGAGCACCGCTTCG
sgRNA_mPB2_260_rev	AAACCGAAGCGGTGCTCACTGACAC
T7_mPB2_uni_rev_1	CCAGCAGGCAGCAAATGGAG
T7_mPB2_uni_fwd_1	TCCGGCCATCTCTGCTGAAG
AfeI_NotI_mPB2_fwd	AAAAGCGCTGCGGCCGCATGGCTCTGCCACTCTGGGCC
Sall_mPB2 Δ C2_rev	AAAGTCGACGCCACCAAGTGCCACACGCG
Sall_mPB2 Δ RBDC2_rev	AAAGTCGACGCGGCATCGATCCCTTCATCCTG
Sall_mPB2 Δ C1RBDC2_rev	AAAGTCGACGCCCGCCGTGACTCAGGGATGT
NotI_EGFP_for	ATATATGCGGCCGCATGGTGAGCAAGGGCGAGGA
Sall_cLGN1_rev	ATATATGTCGACTCAGCTAGAACTTGGTCCTTTAATAG
Probe64_for	CTGCCAGGGTGGTCGTTA
Probe64_rev	ACCTCCTTGGACGTGGCTA
Probe89_for	CAAACACCAGGTGGAAAAGG
Probe89_rev	GCCTGTGTCATTGAGGGTGT

Bacterial culture

Name	Manufacturer
Ampicillin	Carl Roth
Agar	Carl Roth
ElectroMAX DH10B Cells	Invitrogen
Kanamycin	Carl Roth

Buffers, solutions and media

All buffers, solutions and media were prepared with double distilled water. Lysogeny Broth medium was autoclaved before use.

Name	Components
Lysogeny Broth (LB) bacterial growth medium	5 g/l yeast extract 10 g/l trypton 10 g/l NaCl
LB agar	15 g/l agar in LB medium
Buffer S1	50 mM tris pH 8,0 10 mM EDTA 0,1 mg/ml RNase A
Buffer S2	0,2 M NaOH 1 % SDS
Buffer S3	3 M sodium acetate pH 5,5
TE buffer	10 mM tris pH 8,0 1 mM EDTA pH 8,0
Lysis buffer	10 mM tris pH 7,7 10 mM EDTA pH 8,0 10 mM NaCl 0,5 % sarkosyl
Ethanol-NaCl mix	10 ml of 99,8 % ethanol 150 µl of 5 M NaCl
Quenching medium	50 % FCS in cell culture medium

Materials and methods

2X freezing medium	20 % DMSO in cell culture medium
4X Laemmli buffer	286 mM tris 10 mM EDTA 28 % glycerol 5,7 % SDS 0,35 % bromophenol blue 0,47 % β -mercaptoethanol
4X separation gel buffer	1,5 M tris pH 8,8 0,4 % SDS
4X stacking gel buffer	0,5 M tris pH 6,8 0,4 % SDS
Electrophoresis buffer	25 mM tris pH 8,3 192 mM glycine 0,1 % SDS
Transfer buffer	25 mM tris 192 mM glycine 10 % methanol 0,2 % SDS
Tris-buffered saline with Tween (TBS-T)	20 mM tris pH 7,5 500 mM NaCl 1 % Tween 20
2X BBS buffer	0,05 M BES 0,28 M NaCl 1,5 mM Na_2HPO_4

Sequencing

For sequencing of plasmids, Macrogen and SeqLab services were used.

Software and algorithms

Data obtained from flow cytometry was analysed and presented with FACSDiva from BD Biosciences. Microscopy images were processed using Fiji (ImageJ). DNA sequence alignments against databases were done using Blastn, DNA and protein pairwise sequence alignments were done using Serial Cloner and multiple protein sequence alignments were done using Clustal Omega. Design of PCRs, restriction digests and cloning of plasmids was done using Serial Cloner.

3.2. Methods

3.2.1. Immunofluorescence staining of murine tissue

Kidneys taken from euthanized adult mice or whole embryos were immediately washed after extraction with phosphate buffered saline (PBS) and fixed by fully submerging them in 0,2 % Paraformaldehyde (PFA) overnight without movement. In order to cryoprotect the specimens, they were subsequently transferred to a 30 % sucrose solution where they stayed overnight without agitation. The tissue was frozen down by carefully placing it on dry ice covered with aluminium foil. Afterwards, it was wrapped in plastic paraffin film and aluminium foil and stored at -80 °C until the time it was cut.

To make sections from the tissue, a cryostat was used. A cutting blade and a clean anti-roll plate were put in place and the chamber was allowed to cool down to the desired temperature. After reaching it, the frozen tissue was introduced in the chamber and allowed to warm up for 20 minutes. A few drops of OCT compound were added to the specimen stage and the tissue was placed on top, partially embedded in the OCT compound. The OCT compound was allowed to solidify. Individual kidneys and whole embryos were cut taking longitudinal sections of 35 µm of thickness, which were collected on slides. The sections were left to dry for 30 minutes at room temperature and then stored at -80 °C until the moment they were stained.

To stain the specimens, the sections were first allowed to dry for 30 minutes at room temperature. The tissue was further fixed by submerging the slides with the sections in 4 % ice-cold PFA for 10 minutes. PFA was inactivated by washing twice with

50 mM ice-cold glycine in PBS for 5 minutes each time. The slides were then washed with ice-cold PBS for 5 minutes. The tissue was permeabilized for 10 minutes with 0,2 % Triton X-100 in ice-cold PBS (PBS-T). Blocking was performed for 1 hour at room temperature with ice-cold PBS-T containing 4 % fetal calf serum (FCS). The slides were incubated with primary antibody overnight at 4 °C in PBS-T containing 2 % FCS. Next, they were washed 3 times, for 10 minutes each time, with ice-cold PBS containing 1 % FCS. Binding of secondary antibody was achieved by incubation for 1 hour at room temperature in ice-cold PBS containing 1,5 % FCS and 4',6-diamidino-2-phenylindole (DAPI). After that, the slides were washed for 10 minutes with ice-cold PBS containing 1 % FCS. Then, they were washed twice, for 10 minutes each time, with ice-cold PBS. Mounting was done placing glass coverslips over the tissue using a few drops of Dako mounting medium and the preparations were stored at 4 °C.

Genotype	Primary antibodies	Secondary antibodies
Wild type (adults and embryos)	Plexin-B2 (Hamster)	Anti-hamster-Cy3
	E-cadherin (Rabbit)	Anti-rabbit-Alexa Fluor 488
Wild type (adults and embryos)	Plexin-B2 (Hamster)	Anti-hamster-Cy3
	ZO-1 (Rabbit)	Anti-rabbit-Alexa Fluor 488
Wild type	Sema4D (Rat)	Anti-rat-Alexa Fluor 555
Sema4B ^{-/-} ;sema4D ^{-/-} ;sema4G ^{-/-}	Plexin-B2 (Hamster)	Anti-hamster-Cy3
	E-cadherin (Rabbit)	Anti-rabbit-Alexa Fluor 488
Sema4B ^{-/-} ;sema4D ^{-/-} ;sema4G ^{-/-}	Plexin-B2 (Hamster)	Anti-hamster-Cy3
	Anti-ZO-1 (Rabbit)	Anti-rabbit-Alexa Fluor 488

Table 1. Immunofluorescence stainings of murine tissue

The images were taken using the LSM 700 confocal microscope and then processed using Fiji.

3.2.2. Cell culture

2D cell culture

All culture media are supplemented with 10 % FCS and 1 % penicillin-streptomycin.

Name	Source, culture medium	References
MDCK II	Dog kidney, MEM	(Hansson, Simons, and van Meer 1986)
mIMCD-3	Mouse kidney, DMEM/F12	(Rauchman et al. 1993)
PT67	Mouse embryonic fibroblasts, DMEM	(Miller and Chen 1996)
HEK293T	Human embryonic kidney, DMEM	(DuBridg e et al. 1987)

Table 2. Cell lines used in the study with their origin, culture medium and bibliographic reference

In order to keep the different cell lines in culture, they were incubated with their corresponding cell culture medium in T25 flasks at 37 °C and 5 % CO₂. Each cell line was inspected every day using a bright-field microscope and split whenever the cells reached 80 % – 90 % confluence. The number of cells seeded after splitting was adjusted so that the cells would be split every other day. For that, the cell culture medium was first aspirated and the cells were washed with 5 ml of 37 °C PBS. Following the removal of the PBS, 1 ml of trypsin-EDTA was added and the cells were incubated until full detachment at 37 °C and 5 % CO₂. When the cells were completely detached and singled out, verified by observation under the bright-field microscope, they were resuspended in cell culture medium and counted using a Neubauer chamber. Finally, the desired amount of cells was added to a new T25 flask, diluted in cell culture medium to a final volume of 5 ml and incubated at 37 °C and 5 % CO₂.

3D cell culture

In order to model a monolayered kidney epithelium, MDCK and mIMCD-3 cells were cultured in 3D to generate cysts. These consisted of one layer of cells surrounding an empty lumen. These two cell types were able to generate such structures when they were cultured embedded in Matrigel. The process of cyst generation was similar for both

cell lines, but there were some differences regarding the culture medium, splitting technique and the time required until the cysts were formed completely. The day before seeding the cells on Matrigel they were split from the T25 flask where they were kept in culture to a 6-well plate, seeding $2,5 \times 10^5$ cells in the case of mIMCD-3 and $0,5 \times 10^6$ cells in the case of MDCK. They were incubated overnight at 37 °C and 5 % CO₂ in their respective cell culture medium (Table 2). On the next day, a frozen aliquot of Matrigel was taken and put on ice for one hour until it thawed. Once the Matrigel had thawed, the cells were taken out of the incubator, their medium was aspirated and they were washed with 2 ml of PBS. Next, the PBS was removed and 400 µl of trypsin-EDTA were added to each well. The cells were then incubated at 37 °C and 5 % CO₂ until they detached completely from the bottom of the wells. During this time, the next three steps were carried out. The bottom of each well of an ibidi µ-slide was covered spreading 6 – 8 µl of 100 % Matrigel by pipetting and spreading it with the pipette tip. The 8-well chambered slide was left on ice to prevent the Matrigel from solidifying. A solution containing 3 % Matrigel in cell culture medium was prepared. The cells were taken out of the incubator, 1.6 ml of cell culture medium were added to each well and they were resuspended and singled out by pipetting up and down several times. The 8-well chambered slide was taken away from the ice and left at room temperature for 5 minutes before seeding. The concentration of cells in each well was calculated by counting the cells using a Neubauer chamber under a bright field microscope. The cells were diluted in 3 % Matrigel-containing cell culture medium to a concentration of 10^4 cells per 250 µl. Next, 250 µl of the cell suspension were added on each of the Matrigel-coated wells of the 8-well chambered slide, distributing them evenly throughout its surface. The 8-well chambered slide was put in the incubator at 37 °C and 5 % CO₂. The cells were incubated until the day of imaging, exchanging the medium for fresh 3 % Matrigel-containing cell culture medium every other day. The cysts were inspected daily and they were fully formed after 3-4 days of incubation.

3.2.3. Immunofluorescence staining of 2D and 3D cell cultures

In order to perform immunofluorescent staining of proteins in mIMCD-3 cells, first they were seeded in ibidi µ-slides and cultured until they reached the desired degree of

confluence (2D) or until the cysts were formed (3D). Then, cell culture medium was removed and the cells were washed with PBS. Fixation was achieved using 4 % PFA for 20 minutes at room temperature. PFA was removed by washing the cells thrice with PBS. Cells were permeabilized with PBS containing 0,2 % triton X-100 and 0,1 % SDS for 10 minutes at room temperature. Then, they were washed twice with PBS. Blocking was performed with PBS containing 3 % BSA during 30 minutes at room temperature. Primary antibody was diluted to the desired concentration in the blocking solution described for the previous step and was added to the cells, which were incubated 1 hour at room temperature. Then, they were washed with PBS and incubated with secondary antibody and DAPI in blocking solution for 1 hour at room temperature. Finally, the cells were washed once with PBS and kept in PBS until imaging.

Experiment	Primary antibodies	Secondary antibodies
Plexin-B2 and E-cadherin in mIMCD-3 cells in 2D and 3D	Plexin-B2 (Hamster) E-cadherin (Rat)	Anti-hamster-Cy3 Anti-Rat-Alexa Fluor 488
Plexin-B2 and ZO-1 in mIMCD-3 cells in 2D and 3D	Plexin-B2 (Hamster) ZO-1 (Rat)	Anti-hamster-Cy3 Anti-Rat-Alexa Fluor 488
Lumen formation assay	β -catenin (Mouse) ZO-1 (Rat)	Anti-Mouse-Alexa Fluor 555 Anti-Rat-Alexa Fluor 488

Table 3. Immunostainings in mIMCD-3 cells growing in 2D and 3D

The LSM 700 confocal microscope was used to take the images that were then processed with Fiji.

3.2.4. Generation of fluorophore-labelled protein constructs in viral plasmids

In order to achieve stable transduction of cell lines, the coding sequences of the proteins of interest fused to fluorescent proteins were cloned into viral vectors as described in the following sections.

PCR and generation of serial deletion mutants of Plexin-B2

For the generation of the different constructs of Plexin-B2 fused to EGFP, the sequence that encodes Plexin-B2 or the different truncated versions were cloned without their stop codon into the multiple cloning site (MCS) of the pEGFP-N1 vector. The coding sequence of Plexin-B2 was obtained by PCR amplification from a plasmid containing a triple-myc-tagged version of Plexin-B2 in the pcDNA3 vector (pcDNA3-3Xmyc-Plexin-B2), previously generated in the lab. The 3 units of the myc tag were located after the signal peptide of Plexin-B2. The truncated versions of Plexin-B2 were generated by choosing a reverse primer that would anneal right before the sequences encoding the functional domains to be deleted. The forward primer contained an overhang with the restriction site for Eco47III (AfeI), while the reverse primer contained the restriction site for Sall, for the later integration of the amplified sequence into pEGFP-N1. Both primers contained some additional bases at the 5' end which help accommodate the polymerase during the reaction.

The reverse primers used were Sall_mPB2ΔC2_rev, Sall_mPB2ΔRBDC2_rev and Sall_mPB2ΔC1RBDC2_rev. The forward primer was AfeI_NotI_mPB2_fwd. The PCR reaction was run using the FlexCycler². After pipetting the reaction mixes into the PCR tubes, these were immediately placed in the already hot thermocycler, to carry out a hot start. The PCR products were purified from the reaction tubes using NucleoSpin gel and PCR clean-up kit following the instructions of the manufacturer. Before that, in a 0,8 % agarose gel containing 0,01 % ethidium bromide, 1 µl of every PCR reaction was loaded to verify the correct amplification. The electrophoresis was carried out during 1 hour at 100 V.

Digest of Plexin-B2 constructs and vector pEGFP-N1

The PCR products and the vector pEGFP-N1 were digested using Eco47III (AfeI) and Sall, in order to make cohesive ends for the insertion of the PCR products (Plexin-B2 wild type and serial deletion mutants) into pEGFP-N1. The digest was carried out in a final volume of 40 µl containing buffer O, all purified DNA for each PCR product or 1 µg of the pEGFP-N1 vector and enough units of each enzyme to achieve full digest at 37 °C in 1

hour. After the incubation, the digested DNA was loaded in a 0,8 % agarose gel containing 0,01 % ethidium bromide and an electrophoresis was carried out during 1 hour at 100 V. With the help of a transilluminator, the DNA bands of digested PCR products (inserts) and pEGFP-N1 vector were cut out from the gel and the DNA was purified using NucleoSpin gel and PCR clean-up kit, following the instructions of the manufacturer. The concentration of the purified inserts and vector was measured using the Nanodrop 1000 and verified by comparison to the bands of the DNA ladder after an agarose gel electrophoresis.

Ligation

For the ligation of the inserts to the vector, a series of mixes with different vector:insert ratios were prepared using the following equation:

$$\frac{\text{vector}}{\text{insert}} = \frac{m(\text{vector})/\text{length}(\text{vector})}{m(\text{insert})/\text{length}(\text{insert})}$$

The vector:insert ratios used were 1:1, 3:1, 1:3 and 1:6, always using a minimum amount of 50-100 ng of vector. Then, the ligase buffer and the T4 DNA ligase were added. The final volume for the ligations was 20 μ l. Ligations were carried out during 30 minutes at room temperature and protected from light.

Transformation of electrocompetent bacteria

Right after the ligation, 5 μ l of each reaction were mixed with 50 μ l of electrocompetent bacteria, pipetted in 1 mm electroporation cuvettes and kept on ice. Then, Lysogeny Broth (LB) bacterial growth medium without antibiotics was warmed up to 37 °C. The electrocompetent bacteria were transformed with the ligated plasmids containing the different Plexin-B2 variants in pEGFP-N1 by electroporation, placing the cuvettes between the electrodes of the MicroPulser and passing a pulse of 1,8 kV. Immediately after electroporation 1 ml of LB medium was carefully and slowly pipetted into the electroporation cuvette and the transformed bacteria were resuspended in it by gently pipetting up and down a couple of times. Then, they were transferred to 1,5 ml tubes

and incubated at 37 °C for a maximum of 1 hour with shaking. Finally, 100 µl from the bacterial precultures were spread on LB agar plates containing kanamycin, for the selection of successfully transformed bacteria. These plates were incubated at 37 °C overnight and the next day, the formation of single colonies on the plates was verified. Some of the colonies were picked and inoculated in 4 ml LB liquid cultures in 15 ml tubes containing kanamycin, which were incubated at 37 °C with shaking overnight.

Miniprep

On the next day, a miniprep protocol to isolate plasmid DNA was carried out: 2 ml of each of these overnight liquid cultures were transferred to 2 ml tubes and were spun down for 1 minute at 16.000 x g at room temperature. The supernatant was removed and the bacterial pellet was resuspended in 200 µl of buffer S1 containing RNase A by pipetting up and down several times. Then, 200 µl of buffer S2 were added and the tubes were inverted several times for mixing. After that, 200 µl of buffer S3 were added and the tubes were again inverted. Then, the tubes were placed on ice, where they were chilled for 5 minutes. The samples were centrifuged for 10 minutes at 16.000 x g and room temperature. The supernatant was pipetted in fresh 1,5 ml tubes and 0,5 ml of phenol/chloroform/isoamyl alcohol were added. The tubes were shaken harsh during 30 seconds and spun down for 5 minutes at 16.000 x g and room temperature. The upper phase containing the DNA was transferred to new 1,5 ml tubes and 0,5 ml of isopropanol were added. The tubes were shaken harsh for 30 seconds and stored at -20 °C for 10 minutes. Then, the samples were centrifuged for 10 minutes at 16.000 x g and room temperature. The supernatant was poured off, 0,5 ml of 80 % ethanol were added and the tubes were vortexed. The tubes were centrifuged for 5 minutes at 16.000 x g and room temperature. The supernatant was poured off and the remaining liquid was sucked with a pipette. The pellet was dried by placing the tubes with the lids open in a heat block at 56 °C for a couple of minutes. Then, the pellet was resuspended in 50 µl of TE buffer. The successful cloning was verified by a test digest with restriction enzymes followed by sequencing.

Digest of Plexin-B2-EGFP fusion constructs and pLNCX2

In order to transduce eukaryotic cells with the fluorescently labelled Plexin-B2 constructs, the sequences encoding the Plexin-B2 variants followed by EGFP were cut out from the pEGFP-N1 plasmids and inserted into the viral vector pLNCX2. In order to do that, 6 µg of the pEGFP-N1-Plexin-B2 plasmids were cut using NotI and DraI with twice the normal amount of enzyme in BamHI buffer (DraI was used to cut the backbone in smaller fragments that would allow to clearly identify the fragment corresponding to each Plexin-B2 variant fused to EGFP) and 1 µg of pLNCX2 was digested using NotI in a final volume of 40 µl with buffer O. Then, the digested DNA was separated using agarose gel electrophoresis. The bands corresponding to the Plexin-B2-EGFP fusions and pLNCX2 were cut from the gel and the DNA was isolated using NucleoSpin gel and PCR clean-up kit.

Alkaline phosphatase treatment

Since the vector was cut using only 1 restriction enzyme, alkaline phosphatase was used in order to prevent recircularization during ligation. The following mix was prepared:

Component	Amount per reaction
Linearized pLNCX2 (6,1 kb)	2 µg (~1 pmol termini)
10X alkaline phosphatase buffer	2 µl
FastAP alkaline phosphatase	1 µl
Nuclease-free water	Up to 20 µl

Table 4. Alkaline phosphatase reaction mix

The reaction was pipetted up and down a few times to mix the components and then incubated at 37 °C for 10 minutes. To inactivate the alkaline phosphatase and stop the reaction it was incubated at 75 °C for 5 minutes.

Ligation and plasmid isolation

After that, different mixes of insert and vector were prepared for ligation as described previously for the cloning of Plexin-B2 constructs into pEGFP-N1. Ligase buffer and the enzyme were added and ligation was carried out as described above. The new viral plasmids containing the different Plexin-B2 constructs fused to EGFP were transformed into bacteria by electroporation. Transformed bacteria were spread on LB agar plates containing ampicillin and incubated overnight at 37 °C. Growing single colonies were picked to inoculate small liquid LB cultures containing ampicillin that were incubated at 37 °C with shaking overnight. After that, plasmid DNA was isolated from 2 ml of the bacterial cultures following the miniprep protocol described for the cloning of the Plexin-B2 variants into pEGFP-N1. Since the sequence of each construct cloned into pLNCX2 is flanked by a NotI site, the correct orientation of the insertion was verified by a test restriction digest and sequencing.

Cloning of GFP-LGN into pLNCX2

In order to clone LGN fused to EGFP into a viral vector, it was PCR-amplified from a pEGFP-C1-LGN, which contains the sequence for chicken LGN N-terminally fused to EGFP, and then inserted in pLNCX2 using the restriction sites of NotI and Sall. The template used was pEGFP-C1-LGN. The primers used were NotI_EGFP_for and Sall_cLGN1_rev. After the PCR, 1 µl of each reaction was loaded in an agarose gel electrophoresis to verify the correct amplification. DNA was purified from the rest of the reactions using the NucleoSpin gel and PCR clean-up kit. The isolated PCR product and 1 µg of pLNCX2 were digested using the restriction enzymes NotI and Sall in buffer O during 1 hour at 37 °C. Then, the digested DNA was separated by agarose gel electrophoresis as described previously. The bands corresponding to the digested PCR product and the digested pLNCX2 vector were cut from the gel and the DNA was isolated using the NucleoSpin gel and PCR clean-up kit. After isolation, the concentration of the insert and the vector was determined using the Nanodrop 1000 and by loading a small amount of them in an agarose gel electrophoresis, where the intensity of the bands was compared to the DNA ladder of known concentration. Once the concentration of the

insert and the vector were estimated, mixes of different insert:vector ratios were prepared for ligation as described for the other cloning procedures above. Ligation was carried out in the same way as before and the new plasmids were transformed into electrocompetent bacteria by electroporation. After 1 hour of incubation in 1 ml liquid cultures at 37 °C, 100 µl of the transformed bacteria were spread on LB agar plates containing ampicillin and incubated overnight at 37 °C. The next day, some growing colonies were picked and inoculated into 4 ml liquid cultures containing ampicillin, which were incubated at 37 °C overnight. Then, plasmid DNA was isolated from the liquid cultures following the miniprep protocol described above. The correct generation of this new plasmid was verified by a test digest with restriction enzymes and sequencing.

3.2.5. Plexin-B1 and Plexin-B2 expression analysis

In order to investigate the role of Plexin-B2 in epithelial cell division by analysing the effect of its knockout, the expression levels of Plexin-B2 were assessed by qPCR. Due to the similarity of Plexin-B2 with Plexin-B1, the expression levels of the latter were also analysed to find out if it was necessary to knock it out as well in order to rule out a possible compensation mechanism in the absence of Plexin-B2. The expression levels were analysed for mIMCD-3 cells growing in 2D and in 3D as described in the following sections.

RNA isolation

First, mIMCD-3 cells were grown in a T25 flask until they reached 90 % confluence. The day before seeding them for 2D or 3D cultures, they were split from the flask to a 6-well plate, seeding $2,5 \times 10^5$ cells per well. They were incubated overnight at 37 °C and 5 % CO₂. The next day, Matrigel was thawed on ice for one hour. Then, the cells were detached and singled out as described previously. In the meantime, two 6-well plates were prepared for 2D or 3D cultures. The wells of the plate for 3D culture were coated with 50 µl of Matrigel and it was placed on ice to prevent its solidification. The mIMCD-3 cells were taken out of the incubator, resuspended in medium and counted using a

Neubauer chamber. For the 2D cell culture, $2,5 \times 10^5$ cells were seeded in each well of the 6-well plate and incubated at 37°C and $5\% \text{CO}_2$. The 6-well plate with its wells coated with Matrigel was taken from the ice and left at room temperature for 5 minutes before seeding. During that time, the cells were diluted in 3% Matrigel-containing cell culture medium to a concentration of 4.000 cells per $250 \mu\text{l}$. Then, 1 ml of the cell suspension was added to each well on top of the 100% Matrigel coating. The 6-well plate was incubated at 37°C and $5\% \text{CO}_2$. The medium was exchanged for fresh 3% Matrigel-containing medium every other day. The cysts were inspected daily and they were formed after 3-4 days of incubation.

The medium was removed from the wells of the 3D culture 6-well plate and $200 \mu\text{l}$ of trizol were added to each well. The cells were scraped with the pipette tip and collected in 2 ml tubes. They were briefly vortexed and centrifuged for 5 minutes at $17.000 \times g$ and 4°C , then the supernatant was transferred to a new tube and $200 \mu\text{l}$ of chloroform were added. The cells were vortexed and centrifuged for 10 minutes at $17.000 \times g$ and 4°C . After that, $400 \mu\text{l}$ of the upper phase were transferred to a new tube and $400 \mu\text{l}$ of isopropanol were added. The mix was incubated for 10 minutes at room temperature. The mix was loaded in a RNeasy Mini Kit column and centrifuged for 1 minute at $6.000 \times g$ at room temperature. Then, $700 \mu\text{l}$ of buffer RW1 were added and the mix was centrifuged at $6.000 \times g$ for 1 minute at room temperature. The flowthrough was discarded and $500 \mu\text{l}$ of buffer RPE were added to the column. It was then centrifuged for 1 minute at $6.000 \times g$ and room temperature. The flowthrough was discarded and the same step was repeated once more. The column was dried by centrifuging for 2 minutes at $17.000 \times g$ at room temperature. RNA was eluted by addition of $50 \mu\text{l}$ of nuclease-free water to the column and centrifugation for 1 minute at $9.500 \times g$ at room temperature.

The medium was also removed from the mIMCD-3 cells growing in 2D when they had reached 90% confluence and 1 ml of trizol was added to each well. The cells were detached and lysed by pipetting up and down several times. The samples were transferred to a $1,5 \text{ ml}$ tube and kept 5 minutes at room temperature. Then, $200 \mu\text{l}$ of chloroform were added and the mix was shaken harsh for 15 seconds. The samples were kept for 10 minutes at room temperature and then centrifuged for 15 minutes at

12.000 x g. The upper phase was transferred to a new tube, 500 µl of isopropanol were added and the mix was shaken for 15 seconds. The samples were incubated for 10 minutes on ice and then centrifuged for 10 minutes at 4 °C and 12.000 x g. The supernatant was discarded and the pellet was washed with 75 % ethanol by vortexing and centrifugation for 5 minutes at 7.500 x g and 4 °C. The pellet was air-dried and resuspended in nuclease-free water. The RNA isolated from 2D and 3D cell cultures was treated using TURBO DNA-free kit, following the instructions of the manufacturer.

cDNA synthesis

Reverse transcription was used to generate cDNA from 1 µg of DNA-free RNA isolated from mIMCD-3 cells cultured in 2D and 3D. First, the following mix was prepared:

Component	Amount per reaction
Total RNA	1 µg
Random hexamer	1 µl (100 pmol)
Nuclease-free water	Up to 12,5 µl

Table 5. Initial components of the reverse transcription mix

This mix was incubated at 65 °C for 5 minutes and then chilled on ice. Then, the following components were added:

Component	Amount per reaction
5X RT buffer	4 µl
RiboLock RNase inhibitor	0,5 µl
dNTPs	2 µl
Reverse transcriptase	1 µl

Table 6. Final components of the reverse transcription mix

The final volume was 20 µl. The following program was run using FlexCycler² to synthesize the cDNA by reverse transcription:

Temperature	Duration
25 °C	10 minutes
42 °C	60 minutes
70 °C	10 minutes
4 °C	∞

Table 7. Program for the reverse transcription

Quantitative PCR

In order to do an absolute quantification of the Plexin-B1 and Plexin-B2 expression, standard curves from known amounts of previously isolated mouse genomic DNA were generated. In a qPCR plate, 20 ng of the cDNA obtained from mIMCD-3 cells growing in 2D and 3D were pipetted, having two biological replicates for each of them and three technical replicates for each biological replicate. This was pipetted twice: once for Plexin-B1 and once for Plexin-B2. In the same plate, known amounts of genomic DNA for the generation of standard curves were also pipetted. For that, the amounts of 0,33 ng, 1 ng, 3 ng and 9 ng were used, pipetting 3 technical replicates for each. A master mix containing the primers, the SYBR Green supermix and water was prepared and pipetted in the wells. The primer pairs used were the Probe 64 for Plexin-B1 and the Probe 89 for Plexin-B2. The SYBR Green supermix already contains the polymerase, dNTPs, MgCl₂ and the SYBR Green dye. The final mix of components in each well of the qPCR plate was as follows:

Component	Amount
H ₂ O	7 µl
Primer mix	0,5 µl
SYBR Green supermix	12,5 µl
DNA	5 µl

Table 8. qPCR mix

The plate was then sealed with a protective adhesive plastic, introduced in the qPCR thermocycler and the reaction was carried out. After the reaction, some microliters were loaded on an agarose gel electrophoresis to verify the amplification. The data from the qPCR was exported to Excel where it was analysed, creating bar graphs and calculating statistical parameters.

3.2.6. CRISPR/Cas9 genome editing

In order to generate Plexin-B2 knockouts in mIMCD-3 cells the CRISPR/cas9 system was used. The knockout of Plexin-B2 was achieved by using the NHEJ repair method. A double strand break was introduced close to the beginning of the coding sequence, in the first exon. The NHEJ repair method caused small insertions or deletions, which led to a premature stop codon. This completely prevented the expression of functional Plexin-B2 proteins.

For the generation of Plexin-B2 knockouts in mIMCD-3 cells, sgDNA-Cas9 plasmids designed to target mouse Plexin-B2 were used, which were previously generated and already available in the lab. Those were produced by cloning four different sgDNA sequences (named 65, 125, 227 and 260) into the plasmid PX459 V2.0. For the analysis of the first exon to find adequate target sequences and the design of sgDNAs, the now unavailable Optimized CRISPR Design Tool was used (<http://tools.genome-engineering.org>)(Ran et al. 2013).

Transfection

For the transfection of the CRISPR plasmids $2,5 \times 10^5$ mIMCD-3 cells were seeded in each well of a 6-well plate the day before the transfection. One well was transfected with PX458 to control transfection by verifying GFP expression, another with PX459 V2.0 as a positive control for puromycin selection and each one of the other 4 wells was transfected with one of the CRISPR plasmids. For the transfection of 2,5 µg of plasmid per well, Lipofectamine LTX was used. First, 42 µl of Lipofectamine LTX were diluted in 1 ml of Opti-MEM. Then, for every transfection, 4 µg of the corresponding plasmid were

mixed with 4 μ l of PLUS reagent and diluted in Opti-MEM up to a final volume of 200 μ l. Next, 150 μ l of the Lipofectamine LTX dilution and 150 μ l of the plasmid dilution were mixed to prepare the transfection mixes. They were incubated at room temperature for 5 minutes and then 250 μ l of the transfection mix were added to the cells. The next day the transfection efficiency was verified using the Nikon Eclipse Ti and the selection with puromycin was started.

Antibiotic selection

The cells which were successfully transfected with PX459 V2.0 or the CRISPR plasmids derived from it expressed resistance to puromycin. Therefore, for the selection of cells transfected with the CRISPR plasmids, the day after the transfection, the old medium was removed, the cells were washed with PBS and new medium containing 8 μ g/ml of puromycin was added. The selection lasted for three days. Every day the cells were inspected, the medium was removed, the cells were washed with PBS to remove the dead ones and new medium with antibiotic was added. At the end of the selection, the cells in the wells transfected with the CRISPR plasmids were still growing, as well as the cells transfected with PX459 V2.0, which served as a positive control for the selection and to generate control clones. On the other hand, the cells transfected with PX458 had died, which served as a negative control for the selection and helped defining the finishing point of the selection period. The selected cells were allowed to grow until they could be subcultured.

Isolation of genomic DNA from bulk cells

When the cells expressing PX459_mPB2_65, PX459_mPB2_125, PX459_mPB2_227 and PX459_mPB2_260 had reached around 90 % confluence in the 6-well plate, they were split into T25 flasks and kept in culture. The next time of splitting, the remaining cell suspensions that were not seeded were transferred to 15 ml tubes and centrifuged at 500 rpm in the Biofuge Stratos for 3 minutes at room temperature. Then, the cells were washed with PBS repeating the centrifugation step. After removing the PBS, the cells were lysed at 56 $^{\circ}$ C in 300 μ l of lysis buffer containing 82 μ l/ml of proteinase K overnight

with shaking. After the addition of 280 μ l of phenol/chloroform/isoamyl alcohol, the samples were shaken for 30 seconds and centrifuged during 5 minutes at 20.000 x g and room temperature. Next, 280 μ l of supernatant were transferred to a new tube, 280 μ l of chloroform were added and the samples were shaken and centrifuged as before. This step was repeated, this time taking 250 μ l of supernatant mixed with 250 μ l of chloroform. Then, 200 μ l of supernatant were taken to a new tube and 20 μ l of sodium acetate were added. The tubes were inverted several times, 440 μ l of ice-cold 99,8 % ethanol were added, the samples were shaken lightly and centrifuged for 10 minutes at 20.000 x g at room temperature. Then, the supernatant was completely removed with a pipette and the pellet was air dried. Finally, the DNA was resuspended in 50 μ l of nuclease-free water.

Genomic PCR

To test the efficiency of the CRISPR/Cas9-mediated modification of the locus of Plexin-B2 with the T7 endonuclease assay, its genomic sequence was PCR-amplified. The forward primer used was T7_mPB2_uni_fwd_1 and the reverse primer was T7_mPB2_uni_rev_1. The mix was pipetted and they were kept on ice until the FlexCycler² reached the initial denaturation temperature, to begin the reactions from a hot start. After the PCR, a small volume of each reaction was loaded on an agarose gel electrophoresis to verify the correct amplification.

T7 endonuclease assay

In order to detect successful modification of the genomic DNA sequence of Plexin-B2 in the bulk of cells transfected with the CRISPR plasmids, the T7 endonuclease assay was used. The enzyme T7E1, cleaves double-strand DNA at the site of mismatches. When the product of the PCR described in the previous section was denatured and renatured again, wild type or modified homoduplexes were formed, but also heteroduplexes formed by a wild type strand and a modified strand. When this DNA was incubated with the T7E1 endonuclease, it cleaved the DNA at the site of the mismatches in the heteroduplexes, while leaving the homoduplexes intact. This was later visualized in an

agarose gel electrophoresis and gave an estimation of the efficiency of the CRISPR/cas9 genome modification in the bulk cells. To do this, 17 μ l of the PCR were mixed with 2 μ l of the buffer NEBuffer 2 and were put in a heat block that immediately started to increase its temperature from room temperature to 95 °C in order to denature the DNA. The remaining volume from the PCR reactions were loaded in an agarose gel electrophoresis to control the correct amplification of the PCR and the band size. The samples were incubated at 95 °C for 5 minutes. Then, the heat block was covered with aluminium foil and its temperature was slowly decreased until 37 °C, allowing the DNA to reanneal. After that, 1 μ l of the T7 enzyme was added and the samples were incubated at 37 °C for 30 minutes to cut the DNA at the site of mismatches. Then, the samples were loaded in an agarose gel electrophoresis to visualize the presence of digested PCR product that would confirm successful modification of the Plexin-B2 locus in the genomic DNA of the bulk cells.

Clonal expansion

The bulk cells transfected with the CRISPR plasmids were detached using trypsin as described above. Then, they were counted using a Neubauer chamber and seeded in 96-well plates, adding 130 μ l of cell suspension to each well, with a concentration of 0,5 cells per well. They were incubated at 37 °C and 5 % CO₂ and observed under the brightfield microscope daily to identify the wells where cells were growing from a single colony. Those wells were marked and when the cells reached approximately 90 % confluence they were split into three 96-well plates: one to isolate genomic DNA from them, one to freeze them and one to keep the cells in culture, working with them more comfortably.

Freezing of CRISPR clones

To freeze the CRISPR clones in a 96-well plate, first, quenching medium was prepared by mixing culture medium and FCS in a 1:1 proportion. Then, 2X freezing medium was prepared by mixing culture medium and DMSO in a 4:1 proportion. The medium was removed from the wells with the cells and they were washed with 100 μ l of PBS per well.

Then, the PBS was removed, 30 μ l of trypsin were added and the cells were incubated at 37 °C and 5 % CO₂ until they completely detached from the wells. Next, 70 μ l of quenching medium were added to each well and 30 μ l of this cell suspension were discarded. To the remaining cells, 70 μ l of 2X freezing medium were added per well, mixed and transferred to a 96-well plate with round bottom wells. The plate was wrapped with paper, sealed with plastic paraffin film, put in an expanded polystyrene box and kept at -80 °C.

Isolation of genomic DNA from cells in 96-well plates

The cells were washed with 100 μ l of PBS per well twice. Then, the PBS was removed and 50 μ l of lysis buffer were added to each well. The plate was wrapped in paper, sealed with plastic paraffin film and incubated overnight at 60 °C. The next day, 100 μ l of ice-cold ethanol-NaCl mix were added per well and the plate was incubated for 30 minutes at room temperature. During this time the plate was not moved. After the incubation, the liquid was poured off and the wells were washed thrice with 50 μ l of 70 % ethanol. Then, they were air dried and the pellets were resuspended in 20 μ l of TE buffer.

Indel PCR

In order to reduce the number of clones to be tested with western blot, a PCR based identification of possible knockout clones was used. To screen for potential indel mutations in the Plexin-B2 locus the PCR was designed in a way that either the forward or the reverse primer had its 3' end annealing in the region of the double strand break produced by the Cas9. That way, proper priming would not be possible for those clones with indel mutations in that area.

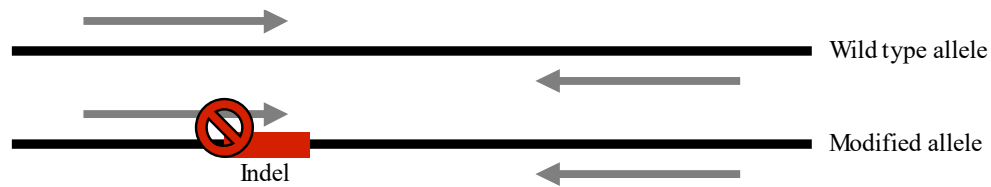


Figure 16. Principle of the indel PCR

The primers used to detect indels in clones coming from cells transfected with sgDNA 65 were sgRNA_mPB2_65_fwd and T7_mPB2_uni_rev_1, in clones coming from cells transfected with sgDNA 125 were T7_mPB2_uni_fwd_1 and sgRNA_mPB2_125_rev, in clones coming from cells transfected with sgDNA 227 were T7_mPB2_uni_fwd_1 and sgRNA_mPB2_227_rev and in clones coming from cells transfected with sgDNA 260 were sgRNA_mPB2_260_fwd and T7_mPB2_uni_rev_1. The amplification was verified by agarose gel electrophoresis.

Cell lysis and SDS-PAGE

Proteins from untreated mIMCD-3 cells, CRISPR clones and control clones were separated by SDS polyacrylamide gel electrophoresis (SDS-PAGE) as a previous step for western blot, for the detection of Plexin-B2. The clones suspected to be knockouts, the control clones and untreated mIMCD-3 cells were subcultured in 6-well plates to increase the amount of cells and, therefore, of its Plexin-B2 protein, in order to improve its detection. Once the cells were almost confluent, they were lysed by adding 200 μ l of 4X Laemmli buffer, scraping the cells with the pipette tip, pipetting up and down and transferring them to 1,5 ml tubes that were incubated for 5 minutes at 95 $^{\circ}$ C. Next, 5 % polyacrylamide gels of 1,5 mm of thickness were prepared by mixing 2,5 ml of acrylamide/bis-acrylamide (Rotiphorese Gel 30) with 3,75 ml of 4X separation gel buffer pH 8,8 containing tris and SDS, 8,75 ml of double-distilled water, 100 μ l of 10 % ammonium persulfate (APS) as a radical initiator and 20 μ l of the catalyst tetramethylethylenediamine (TEMED) and pouring the mix between 2 glass plates clamped in a stand. On top of the separating gel, the stacking gel was produced by mixing 1 ml of acrylamide/bis-acrylamide, 1,25 ml of 4X stacking gel buffer pH 6,8

containing tris and SDS, 3 ml of double-distilled water, 25 μ l of APS and 10 μ l of TEMED and pouring the mix on top of the already solidified separating gel. The gel pockets were created placing a comb in the stacking gel before it solidified and removing it when the polymerization was finished. The gels were placed in an electrophoresis chamber that was filled with electrophoresis buffer. Using a Hamilton syringe, 5 μ l of PageRuler Plus Prestained protein ladder were added to the leftmost well of each one of the gels and subsequently, using the Hamilton syringe, 50 μ l of the lysates from the untreated mIMCD-3 cells, control clones and CRISPR clones suspected to be Plexin-B2 knockouts were loaded in the pockets of the gels. Then, a voltage of 80 V was applied to the gels until the samples reached the end of the stacking gel. After that, the voltage was changed to 120 V for the rest of the electrophoresis until the protein marker was fully separated and the front of the electrophoresis reached the bottom of the gels.

Western blotting

In order to detect Plexin-B2 in the different samples, western blotting to nitrocellulose membranes was performed by electrotransfer using the separating gels from the SDS-PAGE. For that, each separating gel was placed on a stack formed by a foam pad, Whatman paper, the separating gel, a nitrocellulose membrane, another piece of Whatman paper and another foam pad. The whole stack was soaked in cold transfer buffer and all the air was removed from it by gently pressing the stack. The stack was placed in a cassette, which was inserted in the electrode assembly in the orientation in which the membrane was facing the side of the anode and the gel faced the side of the cathode. The electrode assemblies containing the stacks were placed in electrotransfer tanks filled with cold transfer buffer, along with an ice block and a stir magnet. The tanks were placed on trays full of ice on top of magnetic stirrers, to ensure that the buffer inside the tanks remains uniformly cold during the transfer. Then, a current of 350 mA was passed during 2 hours. During this time, the negatively charged proteins in the gels moved towards the positively charged anode, transferring to the nitrocellulose membranes. Then, the membranes were placed in a solution of 5 % milk powder in tris-buffered saline with tween (TBS-T) for blocking during 30 minutes. Primary antibody was diluted in 5 ml of blocking solution and transferred to a 50 ml tube. Since α -tubulin

was used as a loading control, the membranes were cut above the 70 kilodalton mark in the protein ladder to incubate each part of the membrane with a different primary antibody. After cutting the membranes, the upper part was incubated with the anti-Plexin-B2 antibody solution, while the lower part of the membrane was incubated with the anti- α -tubulin antibody solution by placing the membranes in the 50 ml tubes containing the antibody solutions and placing them on a tube roller overnight at 4 °C. Next, the membranes were washed thrice with TBS-T for 5 minutes each time. After that, they were incubated with the corresponding secondary antibody conjugated with horseradish peroxidase (HRP) in the same way they were incubated with the primary antibody but at room temperature and for 1 hour. Then, the membranes were washed again three times with TBS-T for 5 minutes each. ECL substrate was added on the membranes and they were placed in a cassette to expose a photographic film with the signal coming from the activity of the peroxidase on the ECL substrate. Finally, the films were developed using the Mi5 processor.

3.2.7. Generation of virally-transduced stable cell lines

MDCK and mIMCD-3 cell lines were transduced with the Plexin-B2 serial deletion mutants using the viral constructs generated. In this way a stable expression of the fusion protein was achieved, which allowed for the analysis of the localization of the protein still after several days. This was necessary in order to be able to assess the localization of the protein in the 3D context, as the cysts require 3-4 days to grow and a transient transfection would not be strong enough to do proper imaging at that time point. The same was the case for the analysis of the localization of mitotic spindle regulators LGN and NuMA in mIMCD-3 cysts, comparing wild type cysts with Plexin-B2 knockouts.

The Plexin-B2 deletion mutants transduced in mIMCD-3 and MDCK cells were cloned in the pLNCX2 backbone and the same was true for the mitotic spindle regulator LGN. The pLNCX2 system does not require any helper plasmids for viral production, but requires a special packaging cell line called PT67. The investigation of the localization of the Plexin-B2 mutants was done without co-transduction of any other construct.

However, in the case of the study of the localization of mitotic spindle regulators, mIMCD-3 CRISPR control or Plexin-2 knockout cells were also transduced with Tubulin fused to mCherry, in order to visualize the mitotic spindle. The transduction of LGN was similar to the one of the Plexin-B2 mutants as it is in the same viral vector backbone of pLNCX2. However, the plasmid used to express EGFP-tagged NuMA was constructed and packaged by VectorBuilder in a pLV vector backbone, while Tubulin and H2B were in a pWPXL backbone. All of these are lentiviral systems and they require a different protocol to that of pLNCX2. In the case of lentiviral systems, a co-transfection with the helper plasmids pMD2.G and psPAX2 was necessary. The following stable cell lines expressing fluorescently-labelled proteins were generated:

Target cell line	Transduced fluorescent proteins
mIMCD-3	Plexin-B2-EGFP
	Plexin-B2 Δ IC-EGFP
	Plexin-B2 Δ C1-RBD-C2-EGFP
	Plexin-B2 Δ RBD-C2-EGFP
	Plexin-B2 Δ C2-EGFP
MDCK	Plexin-B2-EGFP H2B-mCherry
	Plexin-B2-EGFP
	Plexin-B2 Δ IC-EGFP
	Plexin-B2 Δ C1-RBD-C2-EGFP
	Plexin-B2 Δ RBD-C2-EGFP
	Plexin-B2 Δ C2-EGFP
mIMCD-3 CRISPR control	EGFP-LGN
	EGFP-LGN Tubulin-mCherry
	EGFP-NuMA
mIMCD-3 CRISPR Plexin-B2 Knockouts	EGFP-LGN
	EGFP-LGN Tubulin-mCherry
	EGFP-NuMA

Table 9. Virally-transduced cell lines stably expressing fluorescently-labelled proteins

Retroviral transduction

For a retroviral infection using pLNCX2, the packaging cell line PT67 is necessary. The pLNCX2 vector carries the extended packaging signal Ψ^+ , but not the structural genes Gag, Pol and Env. These are encoded in the PT67 packaging cell line. For the transduction of cells using the pLNCX2 system, first, PT67 cells which were in culture were split and seeded in a 6-well plate one day before the transfection. The next day the cells were about 70 % confluent and ready for transfection with the calcium phosphate method. First, one sterile 2 ml tube was prepared for each one of the transfections. Then, 5 μg of the corresponding plasmid was added to the bottom of the tubes. These were filled up to 112,5 μl with sterile double distilled water. Next, the 2X BBS buffer was shaken vigorously before 125 μl were added to each tube. Quickly, 12,5 μl of CaCl_2 were added dropwise on top of each one of the mixes. Then, the tubes were closed, vortexed and left for incubation for 20 minutes. Next, the mixes were pipetted dropwise on the PT67 and these were incubated for 3 hours. After that, the medium was changed for the corresponding fresh cell culture medium. The cells were transferred to an S2 incubator and they were allowed to produce virus for 48 hours. One day before infection, the target cell lines were split into six well plates. On the day of the infection, the virus-containing supernatants were taken from the PT67 cells, were centrifuged at 900 RPM in the Labofuge 400 for 3 minutes and the supernatants were transferred to new tubes. Next, they were filtered using hydrophilic polyvinylidene fluoride (PVDF) filters of 0,45 μm pore size into fresh tubes. Polybrene was added to each viral supernatant to a final concentration of 8 $\mu\text{g}/\text{ml}$. Then, the medium was removed from the target cell lines and the viral supernatants were added to them. The cells were incubated with the viral supernatant for 24 hours and then the medium was replaced for fresh cell culture medium. The efficiency of the transduction was checked using the Nikon Eclipse Ti. The new stable cell lines were kept in culture and passaged in the S2 cell culture room until they were proved to be virus-free using the QIAamp MinElute Virus Spin kit, following the instructions of the manufacturer. Then, they were transferred to S1 cell culture and prepared for imaging.

Lentiviral transduction

For the transduction of the lentiviral constructs (EGFP-NuMA, H2B-mCherry and Tubulin-mCherry), HEK293T cells, which were in culture, were split and seeded in 6-well plates. The next day they were transfected with the transfer plasmids and additionally with the helper plasmids pMD2.G and psPAX2. The plasmid pMD2.G is the envelope plasmid, containing the VSV-G sequence. The plasmid psPAX2 contains the packaging genes Gag, Pol, Rev and Tat. Transfection was done by the calcium phosphate method as described for the pLNCX2 system, but using the HEK293T cells and transfecting 1 μ g of the target construct and 2 μ g of each one of the helper plasmids for every transfection. The collection of the viral supernatant and the infection of the target cells was done as described previously for the pLNCX2 system.

3.2.8. Lumen formation assay

In order to assess the role of Plexin-B2 in mitosis of epithelial cells in a 3D context, cyst formation was compared between wild type mIMCD-3 cells, CRISPR control clones transduced with either LGN or NuMA and two Plexin-B2 knockout clones transduced with LGN or NuMA. For that, the amount of normal and abnormal lumina was counted and compared between the different cells. A lumen was considered normal when it was a unique empty cavity inside the cysts. When this cavity was split into several empty spaces because of the presence of cells that divided into the lumen or when these completely filled the cyst, the lumen was considered abnormal. These virally transduced cell lines were used instead of the non-transduced CRISPR clones because the same cell lines would later be used to study the localization of LGN and NuMA in normal control cysts compared with abnormal Plexin-B2 knockout cysts.

This lumen formation experiment was done in a blind manner by asking a colleague to assign a code number to the different cell suspensions before seeding them on Matrigel and keeping the equivalency of the code secret until the recount was finished. The method for 3D culture was as described above. After 3 days the cysts were fixed and stained for β -catenin, ZO-1 and DAPI as explained before in order to identify the lateral membrane and the apical pole of the cells. Then, the cells were observed

under the confocal microscope and the number of cysts with normal or abnormal lumina were counted. In each experiment and for each cell line, twenty-five cysts were counted and the percentages of normal and abnormal lumina were calculated. Once the counting had been finished, the code was revealed to know which cell line corresponds to each ratio of normal/abnormal lumina. This assay was repeated 4 times and the average percentage of normal or abnormal lumina, as well as the statistical significance, was calculated for each cell line.

3.2.9. Cell counting and crystal violet staining

In order to see if the deletion of Plexin-B2 has a net effect on the cell proliferation/cell death of mIMCD-3 cells two experiments were carried out. In the first one, the number of mIMCD-3 cells, a CRISPR control clone and two CRISPR Plexin-B2 knockout clones was monitored every day while they were in culture. For that, 12.000 cells of each type were seeded in triplicates in 12-well plates. After that, every 24 hours the cells were detached from the plate using trypsin as described before and counted using a Neubauer cell counting chamber. Then, the average number of cells for each cell line was calculated for each day and the net cell growth resulting from proliferation and cell death was compared.

For the second experiment, a similar comparison was made by daily fixing and staining the cells with crystal violet and measuring absorbance at 595 nm after washing and destaining them. For that, 12.000 cells of an mIMCD-3 CRISPR control clone and two CRISPR Plexin-B2 knockouts were seeded in triplicates on four 12-well plates, one plate for each day of the experiment. They were kept in culture and every 24 hours one of the plates was taken out of the incubator and the cells were washed three times with PBS. Next, they were fixed with 5 % glutaraldehyde for 20 minutes at room temperature. Then, they were washed three times with double distilled water. After that, they were stained with 0,1 % crystal violet for 60 minutes at room temperature. After the staining, the cells were washed three times with double distilled water and the dye was solubilized by adding 10 % acetic acid on the cells for 5 minutes and light shaking. Finally, the absorbance of the supernatant was measured at 595 nm. The average absorbance

of the triplicates was calculated for each cell line and for each day and the results were compared.

3.2.10. Cell cycle analysis

To test whether the absence of Plexin-B2 has an effect on cell cycle in mIMCD-3 cells, the DNA of a CRISPR control clone and a Plexin-B2 knockout clone was stained with propidium iodide and the proportion of cells with different amounts of DNA were counted using a Flow cytometer. In order to do that, the cells were kept in culture and grown in a 10 cm dish, detached with trypsin as described above and counted using a Neubauer chamber. Approximately 50 million cells of each cell type were collected in 15 ml tubes by centrifugation at 500 rpm in the Biofuge Stratos for 3 minutes at room temperature and the supernatant was removed by aspiration. The cells were washed by adding 1 ml of PBS and gently resuspending. They were spun down again by centrifuging for 5 minutes at 500 x g at room temperature. Then, the cells were fixed in 66 % ethanol by resuspending them in 400 µl of ice-cold PBS and slowly adding 800 µl of ice-cold 100 % ethanol and mixing well. Next, the cells were kept at 4 °C for 2 hours. The cells were resuspended by inverting the tube several times and then pelleted by centrifugation at 500 x g for 5 minutes. The supernatant was carefully removed without disturbing the pellet and the cells were washed in 1 ml of PBS. Next, they were centrifuged again for 5 minutes at 500 x g and at room temperature and the supernatant was aspirated. Then, the cells were resuspended in 200 µl of 1X propidium iodide + RNase staining solution and incubated in the dark for 30 minutes at 37 °C. Next, the tubes were placed on ice and taken to the flow cytometer, where the cells were resuspended and counted with the appropriate settings for a propidium iodide cell cycle analysis. The results were analysed using the FACSDiva software.

3.2.11. Spinning disk microscopy

In order to visualize the localization of Plexin-B2 during mitosis in MDCK cysts, the localization of LGN during mitosis in mIMCD-3 wild type cysts compared to Plexin-B2 knockout cysts, the localization of NuMA during mitosis in Plexin-B2 knockout mIMCD-

3 cysts and the localization of the different generated Plexin-B2 deletion mutants in MDCK and mIMCD-3 cells growing in 2D and 3D, live-cell imaging was performed using spinning disk microscopy. The microscope used was a Zeiss AxioObserver.Z1 with the spinning disk unit CSU-X1 from Yokogawa and an incubator chamber with CO₂ supply. The images were taken with a 63x water/glycerine immersion objective with a numerical aperture of 1,3. The camera used was the Evolve 512 EMCCD camera. A spinning disk microscope is a special type of confocal microscope that does not scan the sample one point at a time with the laser. Instead, a wider laser beam illuminates a spinning disk consisting of an array of microlenses and pinholes that scan the sample multiple points at a time. This way the time needed to generate the image is shorter, which is very useful to record live processes like mitosis. For these experiments, the virally transduced, fluorescently labelled, generated stable cell lines described above were used. The cells were seeded in ibidi μ -slides, either in 2D or 3D as described before. During imaging the cells were incubated at 37 °C and 5 % CO₂. In the case of the videos of mitosis, each cyst was imaged for 1 to 3 hours and the high speed allowed to take a z-stack of the entire cyst every 5 minutes. The total z-distance was variable, as every cyst has a different size, but the distance between single slices was of 1-2 μ m. For the experiment to determine the localization of NuMA during mitosis in Plexin-B2 knockout mIMCD-3 cysts, the mitotic spindle was visualized using SiR-Tubulin. For that, SiR-Tubulin was diluted in cell culture medium to a final concentration of 50 nM. Then, the medium was removed from the cells and it was replaced with the SiR-Tubulin-containing medium. The cells were incubated with the SiR-Tubulin overnight. Before live-cell imaging, the staining medium was replaced with fresh normal medium.

4. Results

4.1. Plexin-B2 and its ligand sema4D localize to the basolateral membrane in the renal epithelium

The kidney is an excellent model organ to study epithelial polarity (Wilson 2011; Carroll and Das 2011; Carroll and Yu 2012; Fedeles and Gallagher 2013). First, in order to visualize the localization of Plexin-B2 at distinct plasma membrane domains, a series of immunofluorescence stainings was done on cryosections of kidneys from adult mice or embryos and analysed by confocal microscopy (Figure 17). Additionally, the tissue was stained for E-cadherin and ZO-1 to be able to better identify the lateral membrane and the lateral-apical border of the cells, respectively, which allows for a precise determination of the localization of Plexin-B2.

Also of interest was to assess the localization of one of the main transmembrane ligands of Plexin-B2 in the renal epithelium in order to verify whether it localizes in the same regions of the cells, which would allow for juxtacrine signaling. For that purpose, the adult kidney epithelium was also stained for sema4D.

These experiments revealed that Plexin-B2 is expressed in a strictly polarized manner at the basolateral membrane of renal epithelial cells (Figure 17) colocalizing with E-cadherin, consistent with previous work (Xia et al. 2015). Interestingly, this polarized localization of Plexin-B2 observable in adult tissue was already present in the developing epithelium of 15,5 day old embryos (Figure 17).

Sema4D localized to the basolateral membrane in adult renal epithelial cells as well. This demonstrated that both ligand and receptor localize in close proximity and that this polarized localization could have a functional meaning in the context of semaphorin-plexin signaling.

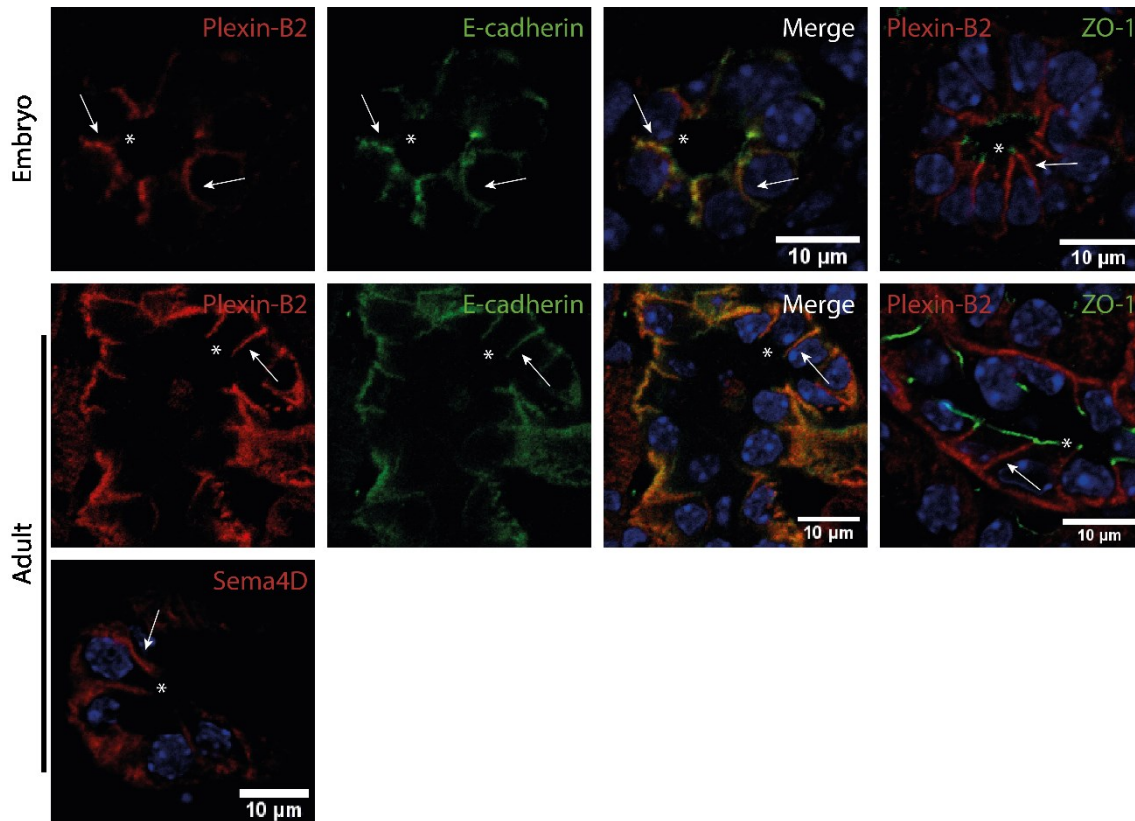


Figure 17. Confocal images of immunofluorescence stainings of Plexin-B2, Sema4D, E-cadherin and ZO-1 in embryonic and adult mouse renal epithelium. Arrows indicate cell-cell contacts. Stars show apical membranes

At the lateral membrane, cell-cell contacts occur. Since Sema4D is a transmembrane protein, this polarized localization of both ligand and receptor could be explained as a way of communication between cells adjacent to each other. The Sema4D on the lateral surface of one cell could bind the receptor Plexin-B2 present in the lateral membrane of the cell next to it. Therefore, in a later experiment, it was interesting to verify whether the presence of the ligand determines the position of the receptor (see section 4.4).

4.2. Plexin-B2 localizes to cell-cell contacts in mIMCD-3 cells in 2D and 3D cultures

Since the previous experiment showed that Plexin-B2 has a polarized expression in the renal epithelium, the next objective was to investigate the localization of Plexin-B2 in cell lines that could be used in cell culture to model the epithelium. Cell lines are much

easier to manipulate than mice and many more experiments can be done in a shorter span of time. In this work, in order to make a closer comparison with the previously analysed mouse kidney, the cell lines used to model the conditions of the kidney epithelium in cell culture were the dog MDCK (Madin-Darby canine kidney) and mouse mIMCD-3 cells (mouse inner medullary collecting duct-3), which are renal epithelial cell lines. MDCK cells are thought to be derived from the distal tubules or the collecting duct (Hansson, Simons, and van Meer 1986). Even though this cell line was generated to be a model for viral infection, it has been used for a long time as a mammalian model of epithelial cell biology (Hall, Farson, and Bissell 1982).

The downside of MDCK cells is that they are derived from dog. Most antibodies are generated to react against mouse or human proteins and few have cross reactivity with dog (Dukes, Whitley, and Chalmers 2011). Moreover, databases and online genetic tools are more focused on mouse and human genes. For this reason, the mouse kidney epithelial cell line mIMCD-3 was also used to model the epithelial tissue (Giles, Ajzenberg, and Jackson 2014).

In a first experiment, the localization of endogenous Plexin-B2 was determined by immunofluorescence staining in mIMCD-3 cells growing in 2D (Figure 18). For this, it was appropriate to study cells in a medium to low confluence level. In this setting, some cells show domains of the membrane forming cell-cell contacts with neighbouring cells and other domains facing empty spaces, representing different functional parts of the plasma membrane.

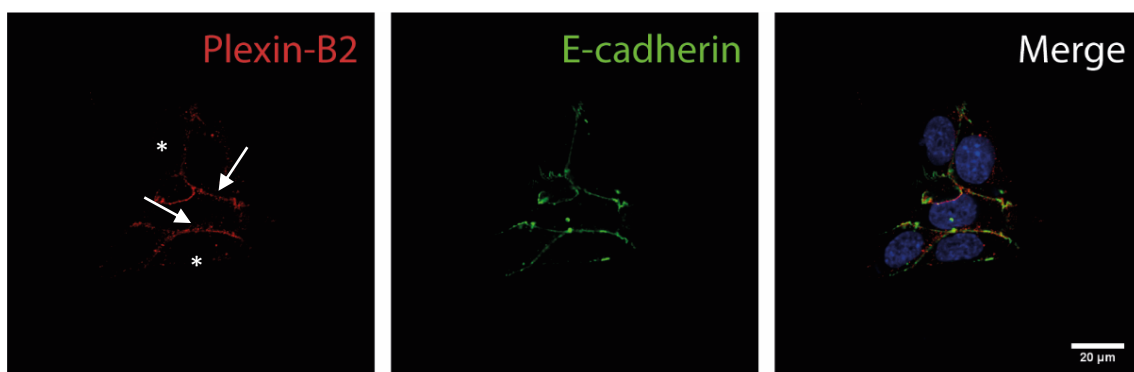


Figure 18. Confocal images of immunofluorescence staining of Plexin-B2 and E-cadherin in mIMCD-3 cells in two-dimensional culture. The arrows show accumulation of Plexin-B2 at cell-cell contacts. The stars show absence of Plexin-B2 where there are no cells in contact

In mIMCD-3 cells growing in 2D, Plexin-B2 localized to cell-cell contacts, coincidentally with the localization observed in the mouse kidney (Figure 18). This was clear when comparing the localization of Plexin-B2 with the localization of E-cadherin, which should only be present at cell-cell contacts. In the sections of murine kidney, Plexin-B2 was absent from the apical membrane, where no cell-cell contacts happen. In this experiment with mIMCD-3 cells, the same can be observed; in those regions where the plasma membrane was facing an empty space, Plexin-B2 did not localize. This further supported the idea that the localization of Plexin-B2 in these cells is determined by the interaction of adjacent cells and it could mean that it plays a role in communication between neighbouring cells.

However, this setting was insufficient to study the polarized expression of Plexin-B2 in epithelial cells, as apical-basal polarity is not evident unless a z-stack of the entire monolayer is performed. One of the reasons that the mIMCD-3 and MDCK cell lines were chosen to model the kidney epithelium was their ability to grow forming cysts when cultured in 3D. This setting allows for the investigation of the localization of Plexin-B2 in cells where apicobasal polarity is much easier to visualize.

The goal was to verify if endogenous Plexin-B2 localizes to the basolateral membrane in mIMCD-3 cysts as it does in the adult renal epithelium. For that, immunofluorescence stainings of Plexin-B2, E-cadherin and ZO-1 were performed in mIMCD-3 cells cultured in 3D. Plexin-B2 localized to the lateral membrane in mIMCD-3 cysts, colocalizing with E-cadherin (Figure 19). In this case, the distribution of the protein was reminiscent of that of the developing kidney, being Plexin-B2 absent from the apical and the basal membranes.

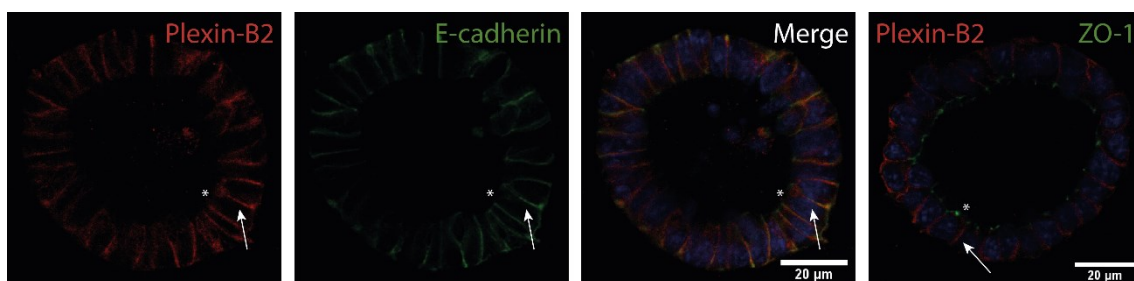


Figure 19. Confocal images of immunofluorescence staining of Plexin-B2, E-cadherin and ZO-1 in mIMCD-3 three-dimensional cysts. Arrows indicate lateral membranes. Stars show apical membranes

4.3. Plexin-B2 localizes to cell-cell contacts during mitosis in MDCK cysts

In every epithelium, cell division is a key process to maintain tissue homeostasis (Yang, Plikus, and Komarova 2015). During this process, some components of the cell redistribute or change localization and later reorganize in the two daughter cells. In previous work from our group it was shown that Plexin-B2 plays a role in mitotic spindle orientation (Xia et al. 2015). Whether the polarized expression of Plexin-B2 in epithelial cells is relevant for mitotic spindle orientation is yet unknown. Therefore, in the following experiment the goal was to determine the localization of Plexin-B2 during mitosis of epithelial cells. For that, the MDCK cell line was used.

With the purpose of visualizing the localization of Plexin-B2 throughout the entire mitotic process, live-cell imaging was performed with a spinning disk microscope and the entire cell division was recorded (Figure 20). After several attempts using transient plasmid transfections of an EGFP-tagged Plexin-B2, it was not possible to visualize the protein in living cells during mitosis. The construct was not expressed at sufficiently high levels by the time the MDCK cysts formed. Therefore, the MDCK cells were virally transduced to achieve stable expression of the fusion protein. In this construct, wild type Plexin-B2 is C-terminally tagged with EGFP (see methods) as shown in figure 24. The cells were also transduced with the histone H2B fused to the fluorophore mCherry in order to visualize the chromatin (Figure 20).

The main challenge of this experiment was to record mitosis from the beginning in cells expressing both transduced constructs, as this cell line grows slowly and the efficiency of transduction was not high. Because of this, it was easier to find cells that had just started mitosis and record the cell division until the two daughter cells reached interphase. Images of the cell divisions were taken every 5 minutes (Figure 20).

As shown in Figure 20, Plexin-B2 localized at cell-cell contacts in MDCK cells during mitosis when growing in 3D cysts, similarly to what was observed in neighbouring mIMCD-3 cells in interphase. When the new membrane formed, separating the two daughter cells, Plexin-B2 quickly localized there, maintaining the same polarized expression observed in the previous experiments. During the whole process, Plexin-B2 was absent from the apical domain of the membrane.

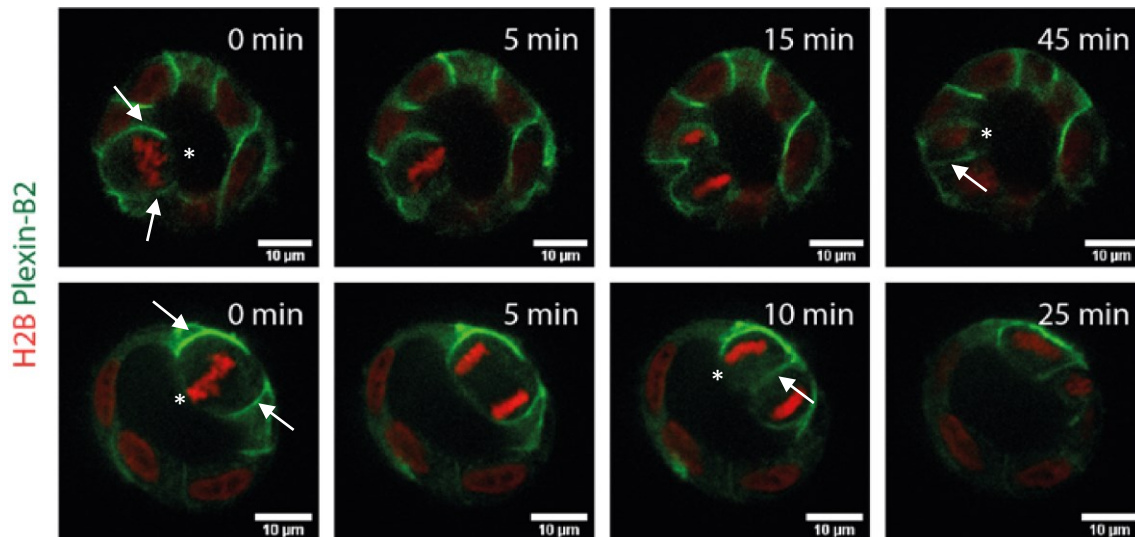


Figure 20. Spinning disk live-cell microscopy images of Plexin-B2-GFP and H2B-mCherry-expressing MDCK cells during mitosis in 3D cell culture. Every row shows a different time-course experiment. Arrows indicate the accumulation of Plexin-B2 at cell-cell contacts, while stars show absence of Plexin-B2 in the apical membrane

4.4. The basolateral localization of Plexin-B2 is ligand-independent

As explained in section 4.1, the polarized expression of Plexin-B2 and its ligand Sema4D could be due to their possible functional role in communication between adjacent cells through Semaphorin-Plexin juxtacrine signaling. The ligands of Plexin-B2 are Sema4A, Sema4B, Sema4C, Sema4D and Sema4G (Maier et al. 2011; Hirschberg et al. 2010; Masuda et al. 2004; Yukawa et al. 2010; Xia et al. 2015). However, Sema4C is not expressed in renal tubular epithelial cells and the expression of Sema4A is limited to the renal cortex (Xia et al. 2015). Therefore, to test whether the polarized expression of Plexin-B2 depends on the presence of its ligand, its localization was analysed in Sema4B^{-/-}; Sema4D^{-/-}; Sema4G^{-/-} triple-knockout mice by immunofluorescence stainings (Figure 21).

In the absence of its ligands, Plexin-B2 still localized to the basolateral membrane and colocalized with E-cadherin (Figure 21). This result suggested that the localization of Plexin-B2 is independent of the presence of its ligands.

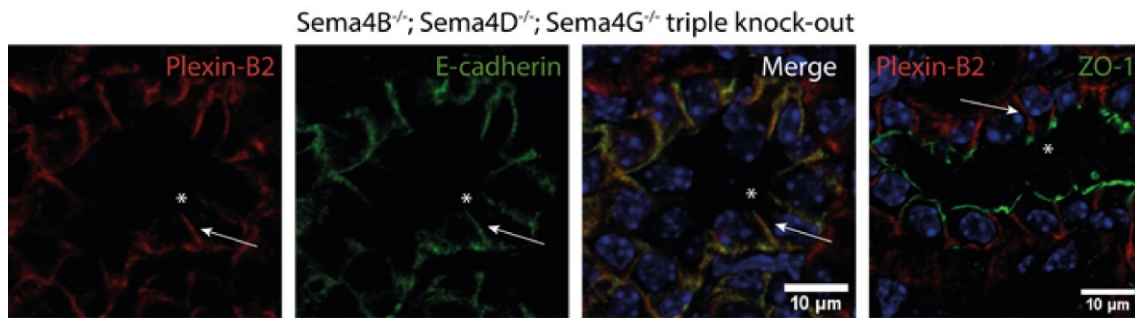


Figure 21. Confocal images of immunofluorescence staining of Plexin-B2, E-cadherin and ZO-1 in the renal epithelium of Sema4B, Sema4D and Sema4G triple deficient mice. Arrows indicate cell-cell contacts. Stars show apical membranes

To sum up, the results of the experiments explained above show how Plexin-B2 has a polarized expression at cell-cell contacts in renal epithelial cells both *in vivo* as in the MDCK and mIMCD-3 cell lines in interphase. Furthermore, it also localized at cell-cell contacts during mitosis in MDCK cells. Moreover, this targeting is independent of the expression of the ligand. Therefore, the reason of this polarized localization remained unknown. Among other possibilities, the localization of Plexin-B2 could depend on part of its sequence or one of its functional domains. For that reason, the sequences of the functional intracellular domains of Plexin-B2 were determined and analysed, to assess their possible role determining Plexin-B2 localization.

4.5. The localization of Plexin-B2 to cell-cell contacts is independent of its intracellular domain in MDCK and mIMCD-3 cells in 2D

As explained in the introduction, the basolateral localization of transmembrane proteins in epithelial cells can be determined by short sequences in their cytoplasmic domains that bind clathrin adaptors (Stoops and Caplan 2014). Therefore, it was interesting to see the effect of the deletion of the intracellular domain of Plexin-B2 on the localization of the protein. For that, a construct of Plexin-B2 lacking the entire intracellular domain and C-terminally fused to EGFP (Plexin-B2 Δ IC-EGFP) was stably expressed in MDCK cells. As shown in figure 22, Plexin-B2 lost its typical basolateral localization and was expressed at the apical membrane instead.

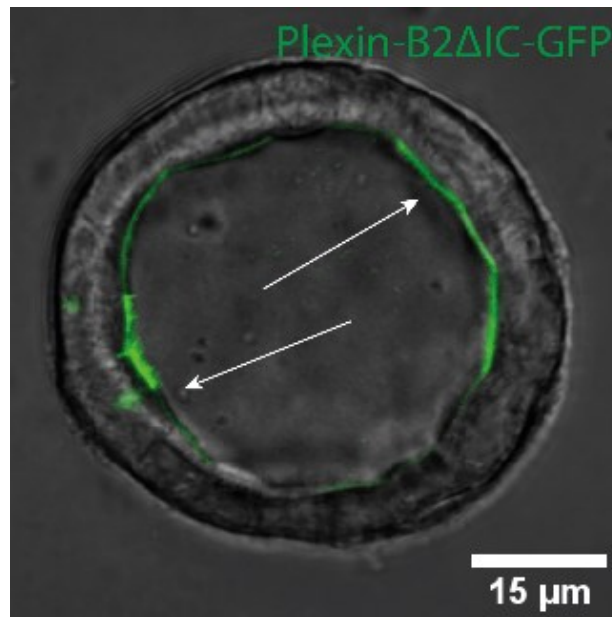


Figure 22. Confocal image of an MDCK cyst expressing Plexin-B2 Δ IC-GFP. Arrows indicate accumulation of the fusion protein at the apical membrane

One hypothesis is that the targeting of Plexin-B2 to the basolateral membrane is determined by a motif present in its cytoplasmic region. In order to narrow down the position of this motif within the sequence of Plexin-B2, sequential deletion mutants of the different domains present in the cytoplasmic region were generated. For that, first, the boundaries of the functional domains of murine Plexin-B2 had to be determined.

The cytoplasmic region of plexins has already been extensively studied. In human Plexin-A1 two subdomains of the intracellular portion show high level of sequence similarity to parts of the SynGAP and R-RasGAP proteins, which includes two conserved arginine residues that have been shown to be essential for GAP function (Rohm et al. 2000). These subdomains are named C1 and C2, and their boundaries have been unambiguously defined for mouse Plexin-A3 (He et al. 2009). It has been shown that the RBD domain is located between the C1 and C2 domains and the residues through which it interacts with the Rho-family GTPases Rac1 and Rnd1 have also been defined (Vikis et al. 2000; Driessens et al. 2001; Hu, Marton, and Goodman 2001; Zanata et al. 2002; Wang et al. 2011). Taken this information, the sequences of mouse Plexin-A3 and mouse Plexin-B2 were aligned to define the limits of each functional domain before designing the serial deletions to be generated (Figure 23).



Figure 23. Sequence alignment of mouse Plexin-A3 (residues 1242-1872) and mouse Plexin-B2 (residues 1123-1842). Conserved residues are shown in white letters and red background. The red boxes show the boundaries of the functional domains C1, RBD and C2

Based on this alignment, sequential deletion mutants of Plexin-B2 were generated by PCR, designing the reverse primers to anneal between the different domains of the cytoplasmic sequence. Then, they were C-terminally fused to EGFP to visualize the proteins in confocal and spinning disk microscopy.

In an initial experiment, the goal was to investigate whether the intracellular functional domains were required for the membrane targeting of Plexin-B2. For that, mIMCD-3 and MDCK cells were transduced with either one of three C-terminally EGFP-labelled constructs: wild type Plexin-B2 (Plexin-B2wt-EGFP), a deletion mutant lacking the whole cytoplasmic region (Plexin-B2 Δ IC-EGFP) or a deletion mutant lacking all the described functional domains (Plexin-B2 Δ C1-RBD-C2, hereafter shortened as Plexin-B2 Δ C1 in the figures), but retaining the juxtamembrane sequence. These stable cell lines were then cultured in a 2D monolayer. The domain structure of the constructs used is shown in Figure 24.

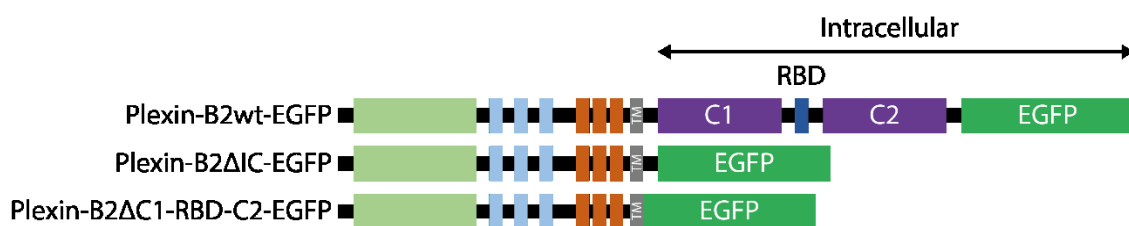


Figure 24. Domain structure of the EGFP-tagged Plexin-B2 wild type, complete cytoplasmic deletion mutant (Plexin-B2 Δ IC) and C1, RBD and C2 domains deletion mutant (Plexin-B2 Δ C1-RBD-C2)

As shown in Figure 25 and Figure 26, for both cell lines, Plexin-B2 wild type accumulated at cell-cell contacts, as expected. The deletion of the functional domains did not change the membrane targeting of Plexin-B2. Moreover, both deletion constructs still accumulated preferentially at the cell-cell contacts like the wild type. These results suggest that the targeting of Plexin-B2 to the membrane is independent of its intracellular domain in mIMCD-3 and MDCK cells in 2D.

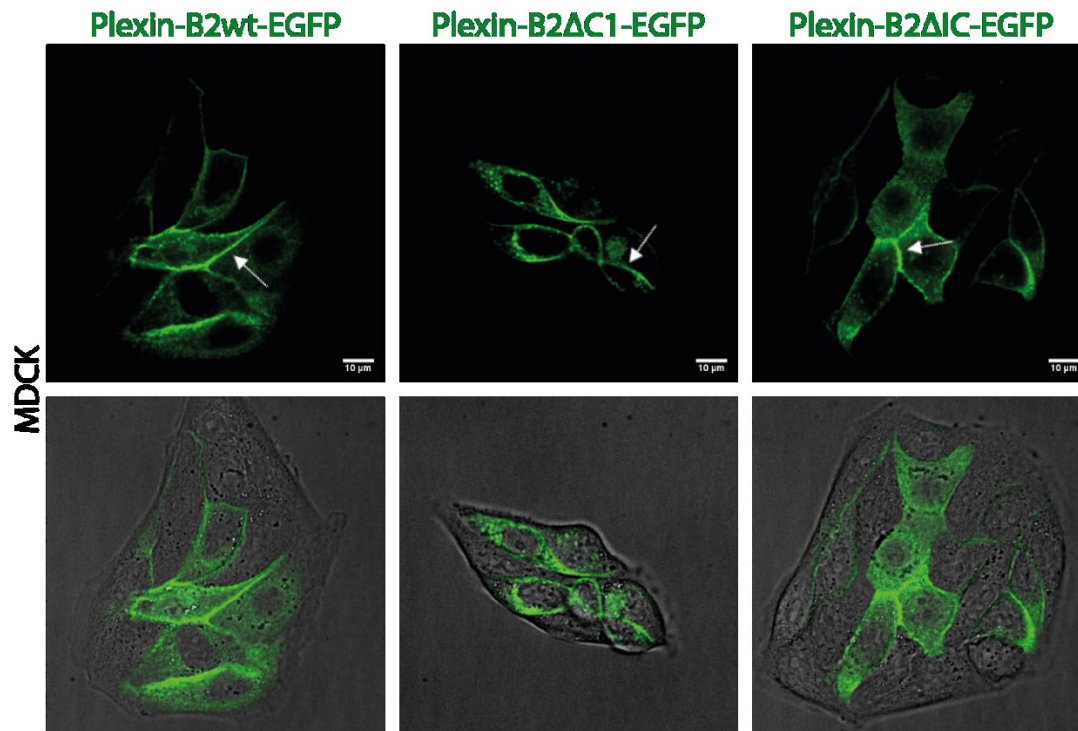


Figure 25. Confocal images of MDCK cells growing in 2D and expressing the Plexin-B2 constructs. Arrows indicate the accumulation of Plexin-B2 at the cell-cell contacts

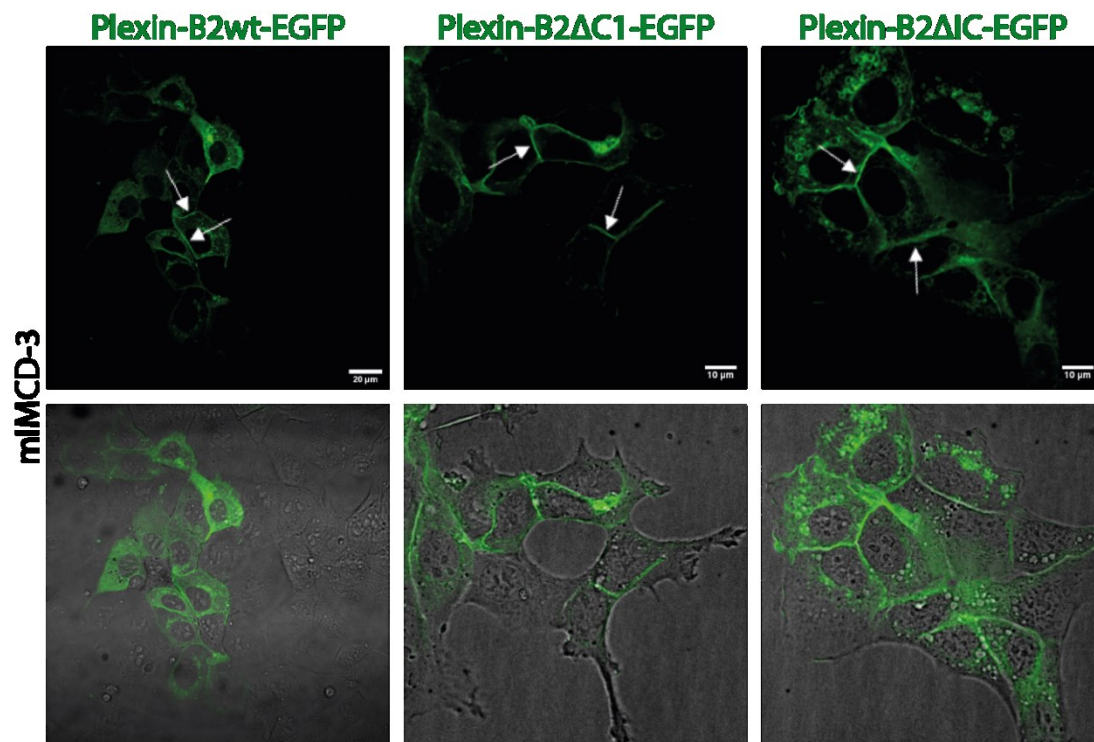


Figure 26. Confocal images of mIMCD-3 cells growing in 2D and expressing the Plexin-B2 constructs. Arrows indicate the accumulation of Plexin-B2 at the cell-cell contacts

However, to investigate whether the targeting of Plexin-B2 to the basolateral membrane in the kidney epithelium and in the cysts is dependent or not on the functional domains of the intracellular region of Plexin-B2, the 3D setting is much better suited than the culture of cells in a 2D monolayer. For that reason, the cells transduced with the constructs described before were cultured in 3D.

4.6. The localization of Plexin-B2 to the basolateral membrane in MDCK and mIMCD-3 cysts is dependent on its intracellular domain

In order to verify whether in a 3D context the functional domains of the cytoplasmic region of Plexin-B2 are relevant for its basolateral targeting, MDCK and mIMCD-3 cells were transduced with EGFP-tagged Plexin-B2 wild type and the two deletion mutants described above and cultured in 3D to form cysts, which were imaged with confocal microscopy. In Figure 27 it is shown that in MDCK cells Plexin-B2 wild type localized to cell cell contacts at the lateral plasma membrane, while the mutant lacking the whole intracellular domain shifted its localization to exclusively the apical membrane. The mutant lacking all of the functional domains in the cytoplasmic region, but retaining the juxtamembrane domain still localized to the basolateral membrane. Therefore, it is likely that the signal that is responsible for the basolateral targeting of Plexin-B2 is located in the short juxtamembrane sequence between the transmembrane domain and the C1 domain.

As shown in Figure 28, in mIMCD-3 cells, the deletion of the Plexin-B2 intracellular domains C1, RBD and C2 did not affect the basolateral localization of Plexin-B2 that can be observed for the wild type. However, the deletion of the whole intracellular domain of Plexin-B2, including the juxtamembrane domain, caused accumulation of the protein mainly at the apical membrane, similarly to what happened for MDCK cells. In the case of mIMCD-3 cells, this mutant did not localize exclusively at the apical membrane and some of the protein still remained at cell-cell contacts. These results further supported that the motif responsible for the correct localization of Plexin-B2 is located between the transmembrane and C1 domains.

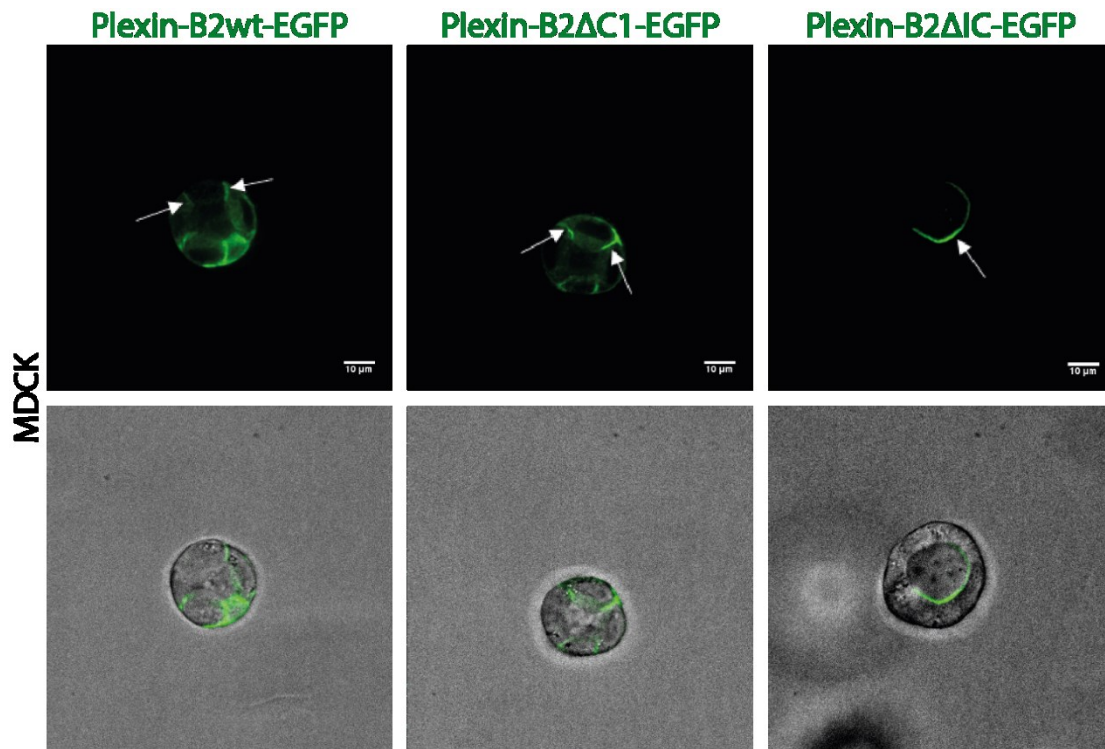


Figure 27. Confocal images of MDCK cells growing in 3D and expressing the Plexin-B2 constructs. Arrows indicate the accumulation of Plexin-B2

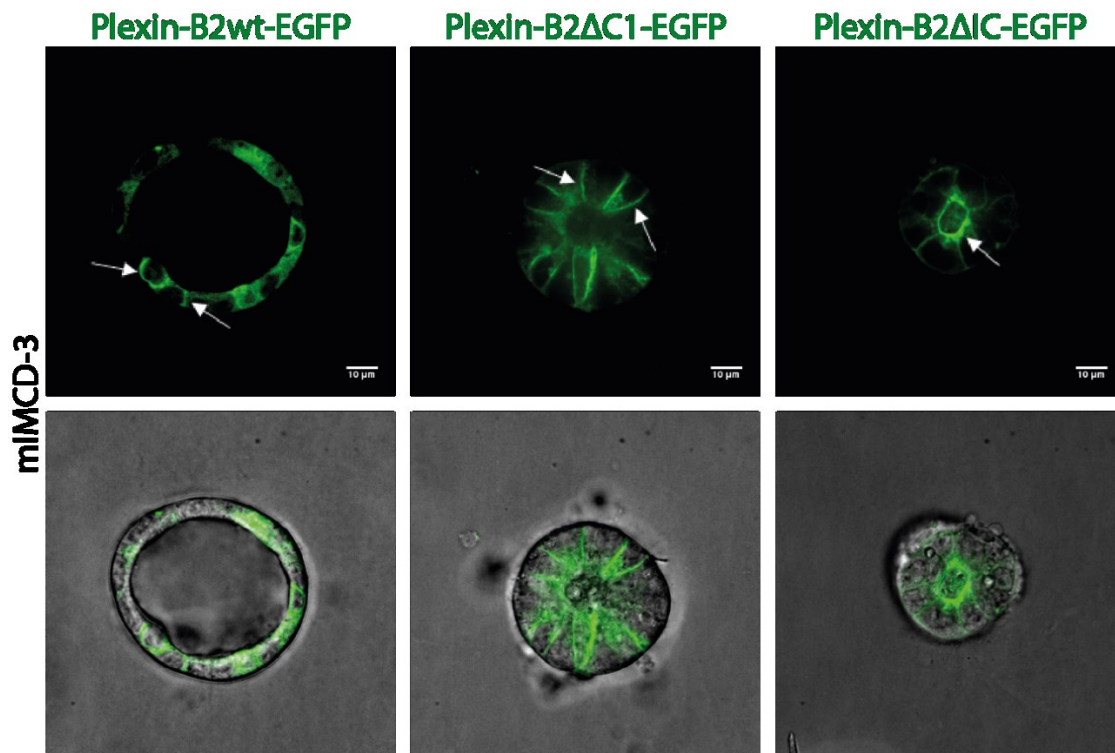


Figure 28. Confocal images of mIMCD-3 cells growing in 3D and expressing the Plexin-B2 constructs. Arrows indicate the accumulation of Plexin-B2

With these results the next step was to find a sequence of residues in the mentioned area of the protein, which would be known to make transmembrane proteins localize at the basolateral membrane.

4.7. Identification of a possible motif required for the sorting of Plexin-B2 to the lateral membrane

The most common basolateral targeting signals are the tyrosine-based (NPxY and YxxØ) or the dileucine motifs (D/ExxxLL). These are located in the cytoplasmic domain of the proteins and sometimes also serve as endocytosis signals. Other basolateral sorting signals contain only one leucine (EExxxL)(Stoops and Caplan 2014). As shown in Figure 29, in the region between the transmembrane domain and the C1 domain only one tyrosine-based domain can be found (YEKI), while the rest of the motifs do not appear.

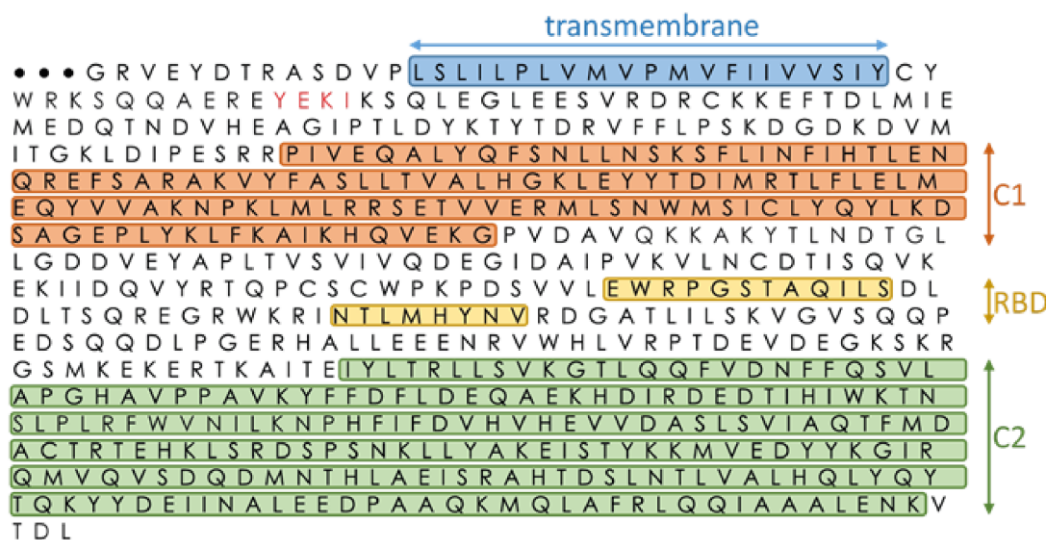


Figure 29. Potential lateral localization motif in the cytoplasmic domain of Plexin-B2. Part of the amino acid sequence of mouse Plexin-B2 showing the transmembrane domain, the C1 and C2 GAP domains and the RBD domain. The likely motif for lateral localization is highlighted in red (YEKI)

Next, the sequences of all mouse plexins were compared to see which ones of them had this motif. The sequence of human Plexin-B2 was also aligned to see if this motif was conserved between species. As shown in Figure 30, only the plexins of the B family have this motif, including the human Plexin-B2, which has the sequence fully conserved. In the case of mouse Plexin-B1 and mouse Plexin-B3, the hydrophobic residue changes from isoleucine to valine and the two residues between the tyrosine

and the hydrophobic residue change from glutamic acid-lysine to lysine-lysine and glutamine-lysine, respectively. However, for this sorting motif any residue can be at those positions.

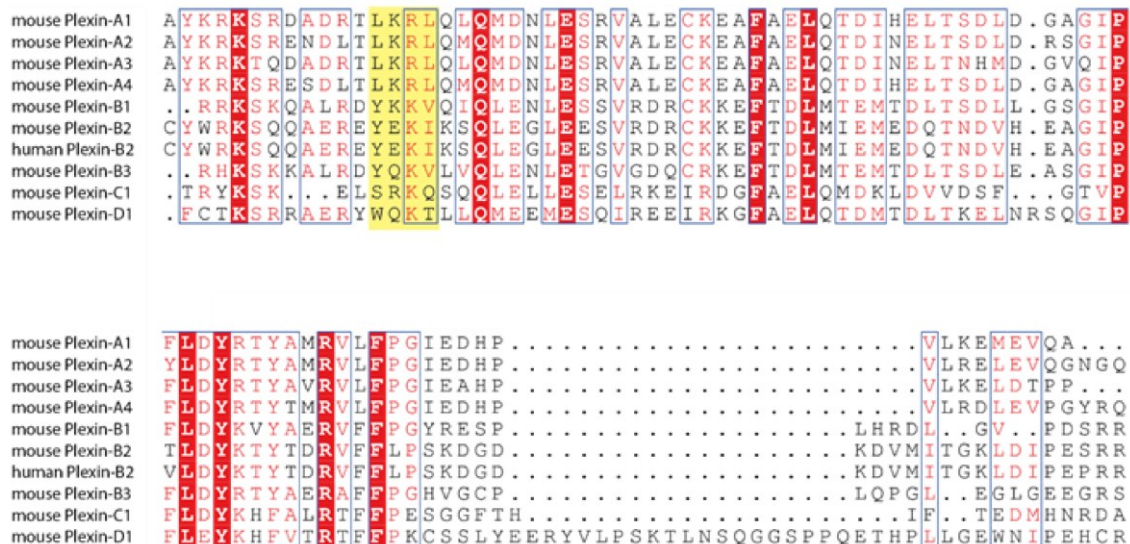


Figure 30. Alignment of all mouse plexins and human Plexin-B2. The alignment of the residues conforming the proposed basolateral localization signal is highlighted in yellow. Conserved residues are shown in white letters over red background

4.8. Generation of Plexin-B2-deficient mIMCD-3 cells by CRISPR/Cas9 genome editing

In a previous work from our group it was shown that signaling through Plexin-B2 controls mitotic spindle orientation via its GAP domain and Cdc42 (Xia et al. 2015). As explained in the introduction, the mitotic spindle is correctly oriented by a protein complex that includes NuMa exerting pulling forces on astral microtubules of the spindle and LGN linking NuMA to the appropriate region of the plasma membrane. However, it is unknown whether Plexin-B2 controls these critical regulators of mitotic spindle orientation and if so, how it does. Therefore, the next step was to test in mIMCD-3 cells what happens with the mitotic spindle regulators LGN and NuMA in the absence of Plexin-B2. There are different methods to abolish the expression of Plexin-B2 in mIMCD-3 cells, like knockout mediated by CRISPR/Cas9 genome editing or knockdown using shRNA or siRNA. Here, CRISPR/Cas9 genome editing was used to knock out Plexin-B2 from mIMCD-3 cells.

First, the expression levels of Plexin-B2 and its closely related homologue Plexin-B1, which could potentially compensate the loss of Plexin-B2, were verified. Expression levels were determined by qPCR in number of copies of the gene per nanogram of cDNA. Cells growing in 2D monolayers as well as cysts growing in 3D were analysed. The results showed that Plexin-B2 was expressed in these cells and that Plexin-B1 expression was much lower, although it could be detected (Figure 31).

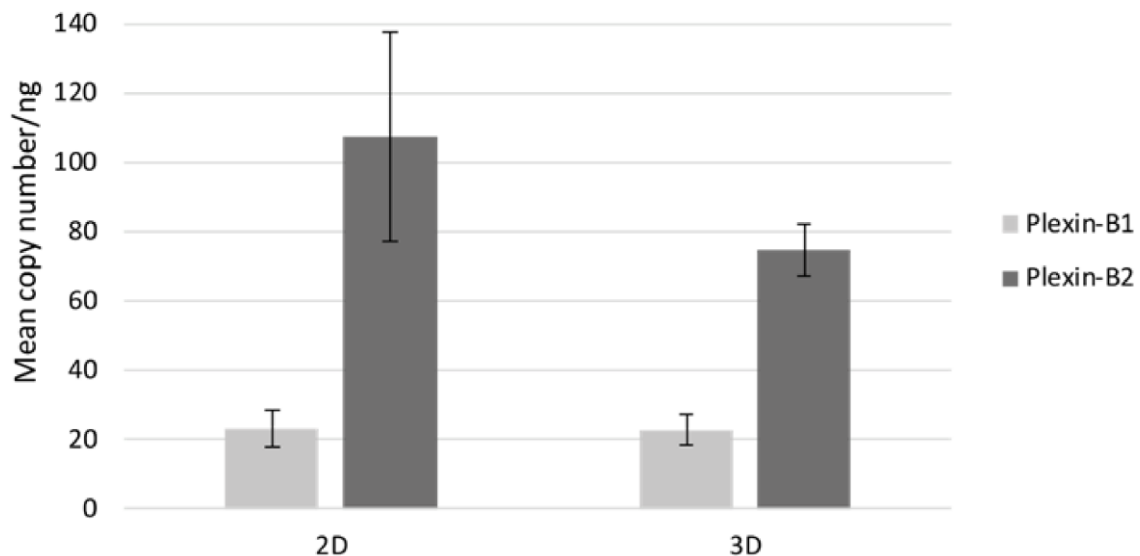


Figure 31. Expression levels of the Plexin-B1 and Plexin B2 genes in mIMCD-3 cells growing in 2D and 3D cultures assessed by qPCR

Because of these results, Plexin-B2 knockout clones were generated by CRISPR/Cas9 genome editing. This was only done for mIMCD-3 cells, as MDCK are dog cells and there was no available antibody for dog Plexin-B2. To control for the specificity of the results, different sgRNAs were used to target the Plexin-B2 locus. As controls for further experiments, untreated mIMCD-3 cells were used, but also CRISPR control cells, which underwent the same CRISPR treatment as the knockout clones, but were only transfected with the CRISPR plasmid without an sgRNA sequence. From all the clones generated, one control clone and two knockout clones were chosen to continue with further experiments. These knockout clones came from cells treated with different sgRNAs.

As shown in Figure 32, in the knockout clones, Plexin-B2 could not be detected by western blotting, confirming the successful modification of their genome. Plexin-B2 could still be detected in the CRISPR control clone in a level comparable with untreated mIMCD-3 cells, supporting that the procedures involved in the CRISPR/Cas9 genome editing method do not reduce the expression of the protein and that the absence of Plexin-B2 in the knockout clones is a consequence of the specific targeting of the sgRNAs.

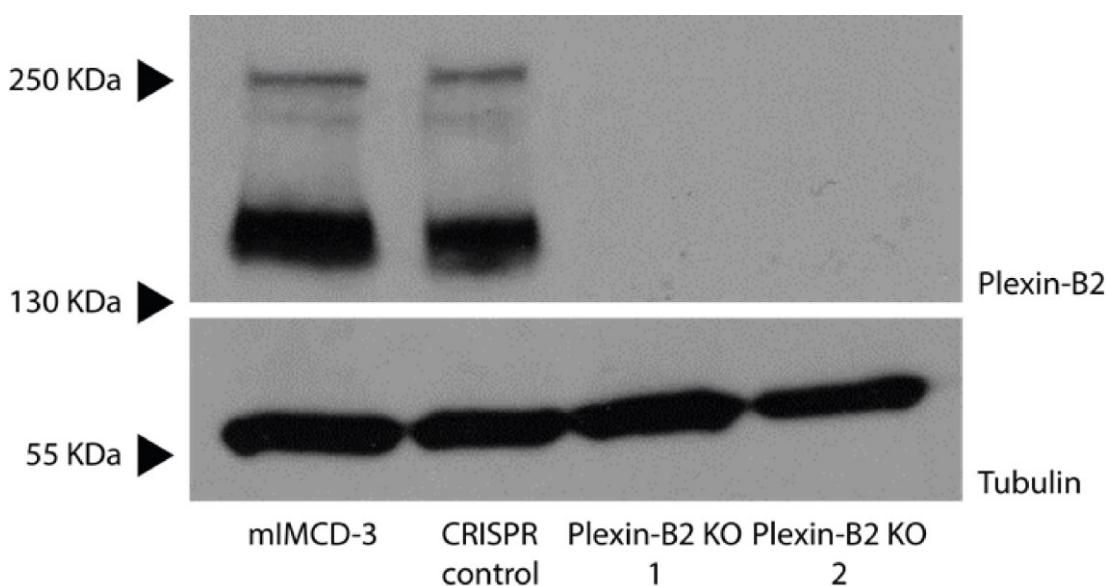


Figure 32. Western blot showing Plexin-B2 in mIMCD-3 cells and in control and knockout CRISPR clones

4.9. Knockout of Plexin-B2 impairs lumen formation in mIMCD-3 cysts

In order to investigate the impact of Plexin-B2-deficiency on the mitotic spindle regulators LGN and NuMA in mIMCD-3 cells, the CRISPR clones (control and knockout) were virally transduced with either EGFP-tagged LGN or EGFP-tagged NuMA, to visually analyse them with spinning disk microscopy. The cells transduced with LGN were also transduced with mCherry-tagged tubulin in order to visualize the mitotic spindle. However, this double transduction could not be achieved for the cells transduced with NuMA and in this case the mitotic spindle was visualized using the tubulin probe SiR-Tubulin.

First, to verify that the Plexin-B2 knockout has a mitotic orientation defect phenotype, the CRISPR control and knockout clones were cultured in 3D and stained for

β -catenin and ZO-1. If the orientation of mitosis is not altered, the daughter cells stay in the same plane and the structure of the cysts remains normal, with one layer of cells surrounding a single lumen. If cells divide perpendicularly or oblique to the plane, the daughter cells invade the lumen and split it in several cavities or completely fill it (Figure 33). Therefore, after seeding the CRISPR clones in a blind manner, when the cysts grew, the amount of cysts with normal and abnormal lumina were counted.

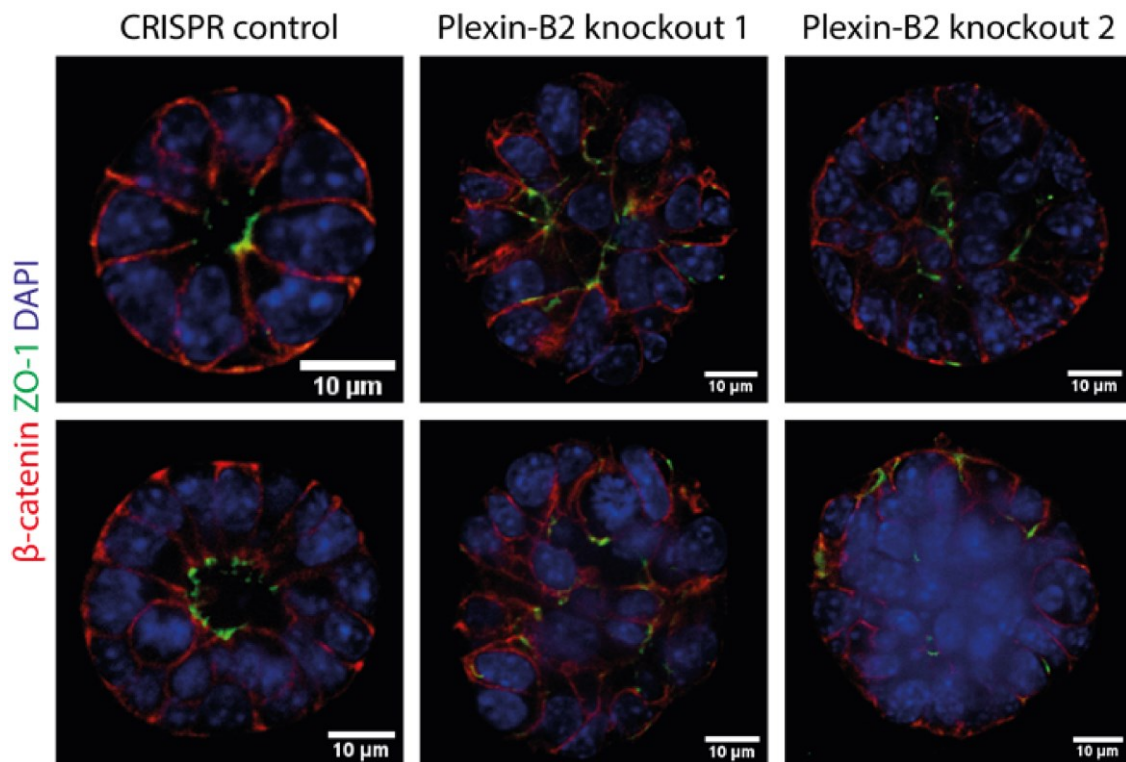


Figure 33. Confocal images of mIMCD-3 Plexin-B2 wild type (control) and Plexin-B2 knockout growing in 3D and stained for β -catenin, ZO-1 and DAPI. Each row shows an independent experiment

As shown in Figure 34, untreated mIMCD-3 cells and the control CRISPR clone for both transductions showed formation of mostly normal cysts with normal lumina. However, both Plexin-B2 knockout clones transduced with either of the mitotic spindle regulators showed an increased proportion of abnormal cysts with their lumen divided or filled with cells.

Lumen Quantification

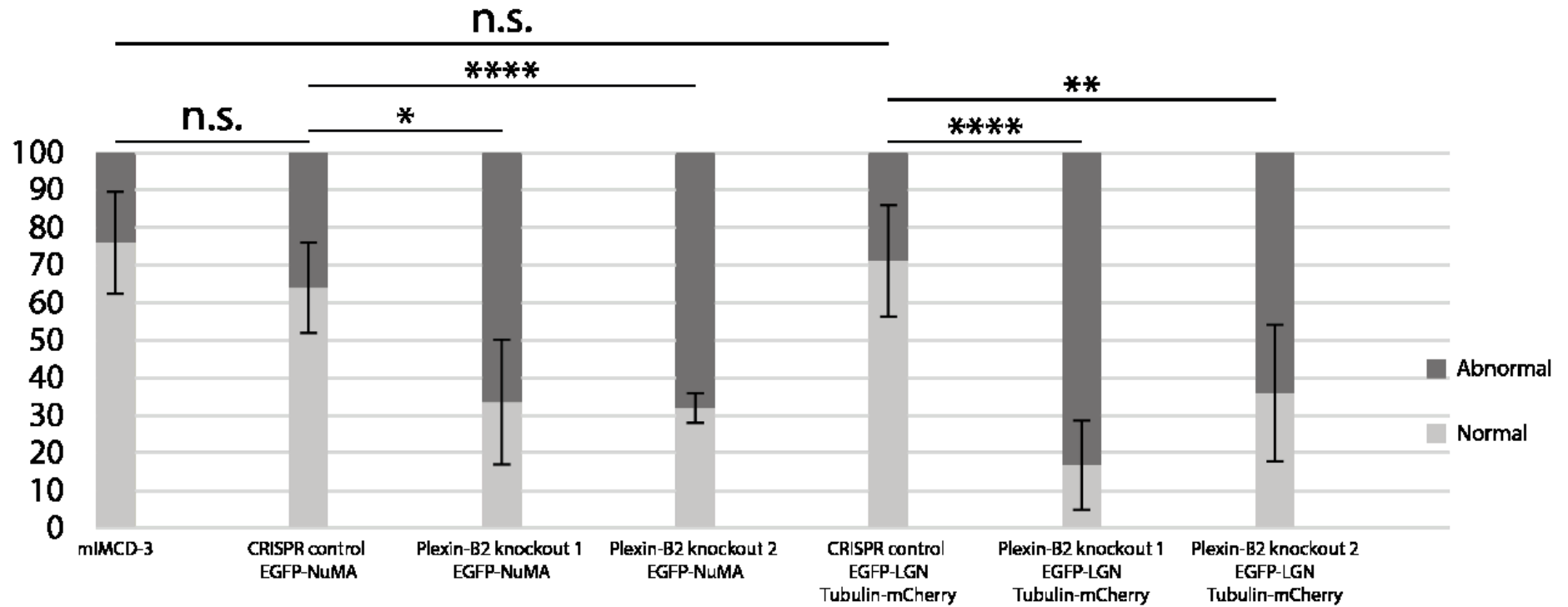


Figure 34. Quantification of normal and abnormal lumen formation in mIMCD-3 Plexin-B2 wild type and Plexin-B2 knockouts transduced with EGFP-NuMA or EGFP-LGN and tubulin-mCherry

4.10. Knockout of Plexin-B2 does not increase net proliferation of mIMCD-3 cells

During culture of the CRISPR control cells and Plexin-B2 knockouts there was an impression that they were forming bigger cysts in the same amount of time and it was also observed that the amount of dead cells floating in the medium in 2D cultures was higher. Therefore, it was verified if they were growing at a higher rate.

To test if the growth of the cells is affected in the knockout clones a counting experiment and a crystal violet staining experiment were done. Both experiments give an estimation of the growth of the cells in culture. For the cell counting experiment, untreated mIMCD-3 cells, a CRISPR control clone and the two Plexin-B2 knockout clones were seeded in equal numbers and counted every day for four days. After four days, the CRISPR control clone and the two Plexin-B2 knockout clones had a statistically significant higher growth compared to untreated mIMCD-3 cells (Figure 35, $p = 0,001$; $p = 0,04$ and $p = 0,01$; respectively). The CRISPR control also grew more than the knockout clone 2, but the difference with the knockout 1 was not significant ($p = 0,02$ and $p = 0,09$; respectively). However, the difference between both Plexin-B2 knockout clones was not significant ($p = 0,7$).

Another experiment to test the growth of the cells was the crystal violet staining. For that, the same number of CRISPR control cells and Plexin-B2 knockouts from both clones were seeded. Three wells were seeded for each time point and cell line to be analysed. Every day, the corresponding cells were stained with crystal violet. After washing away the excess of crystal violet, they were destained and the absorbance of the crystal violet-containing supernatant was measured. The bigger the amount of cells that were present in the wells, the more concentrated the crystal violet would be in the supernatant. Therefore, this was an indirect way of measuring growth.

As shown in Figure 36, Plexin-B2 knockout clones seemed to grow slightly more than CRISPR controls, but overall the growth levels were comparable. After four days, no statistical differences could be detected between any of the knockouts and the CRISPR control (knockout 1: $p = 0,6$; knockout 2: $p = 0,2$) nor between knockout 1 and knockout 2 cells ($p = 0,5$). These two experiments taken together suggest that the growth of mIMCD-3 cells is not significantly affected by the deletion of Plexin-B2.

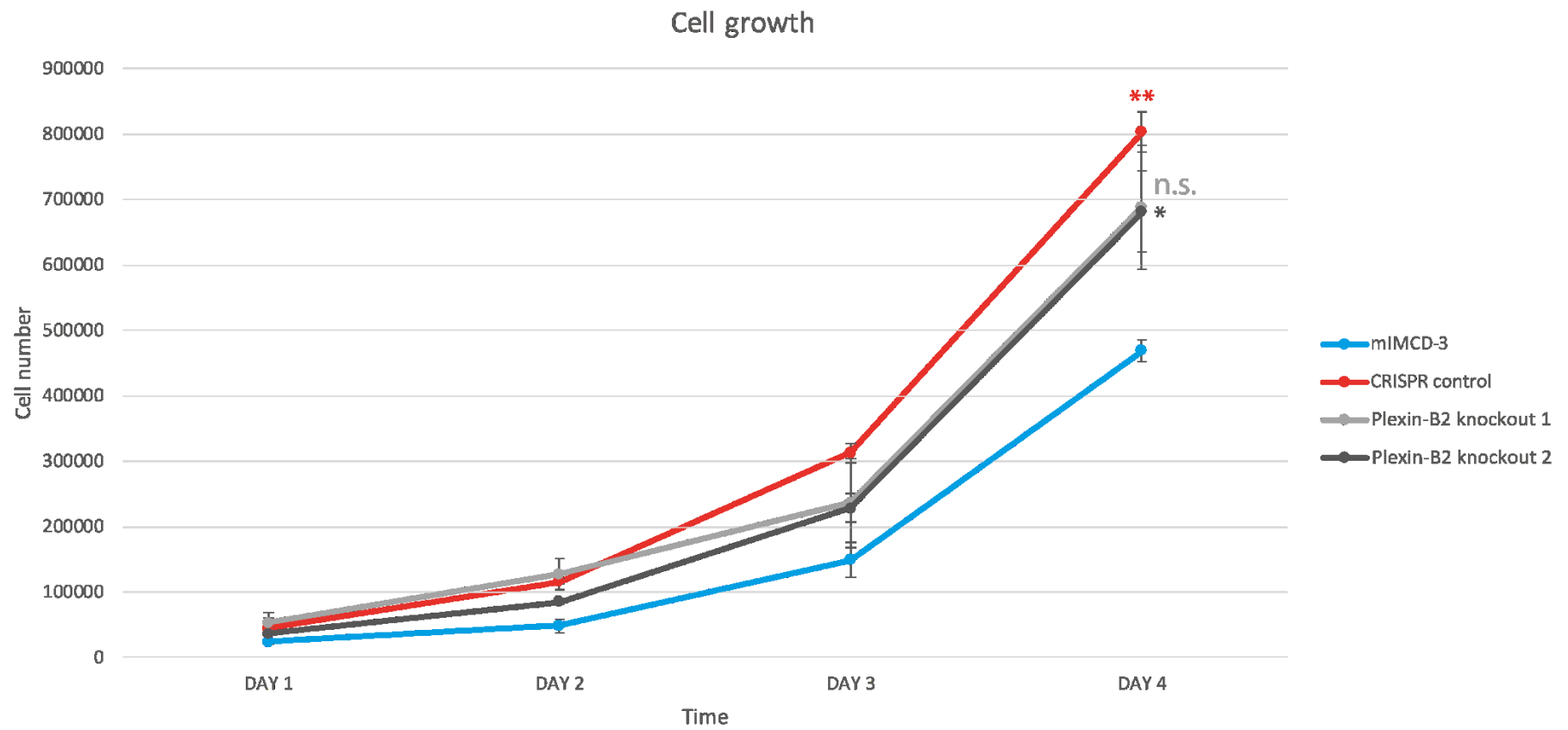


Figure 35. Growth of mIMCD-3 control cells and Plexin-B2 mutants. Number of cells counted every day after seeding control cells and Plexin-B2 knockouts

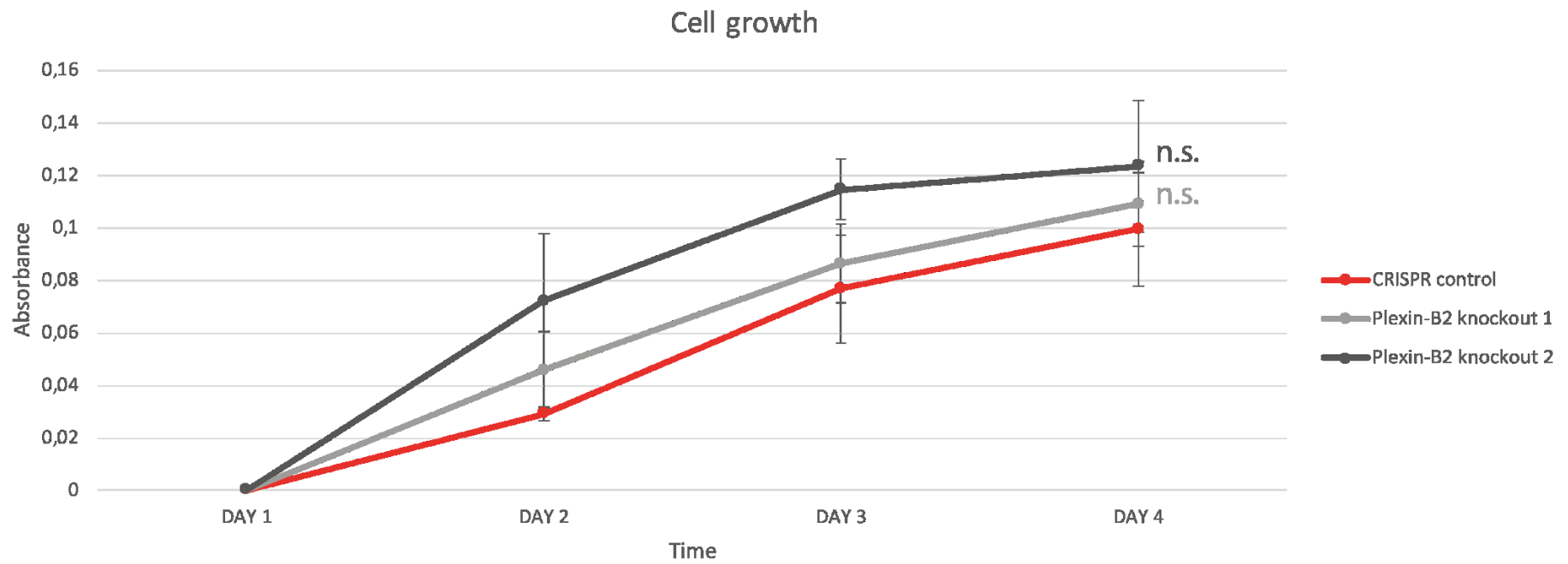


Figure 36. Crystal violet absorbance-based indirect measurement of growth of mIMCD-3 control cells and Plexin-B2 knockouts. Absorbance at 595 nm measured in the supernatant after destaining the crystal violet in CRISPR control cells and Plexin-B2 knockout clones 1, 2, 3 and 4 days after seeding

4.11. Knockout of Plexin-B2 increases the proportion of cells in the S and G2/M phases and aneuploidy in mIMCD-3 cells

After verifying that both Plexin-B2 knockout clones show the same phenotype and behave similarly, in further experiments, I focused on clone number 2. When imaging the Plexin-B2 knockout cysts transduced with EGFP-LGN and tubulin-mCherry, some aberrant mitosis with more than two poles were observed (Figure 37). For this reason, it was interesting to verify the occurrence of aneuploidy in Plexin-B2 knockout mIMCD-3 clones. For that, a cell cycle analysis with propidium iodide staining and flow cytometry was performed.

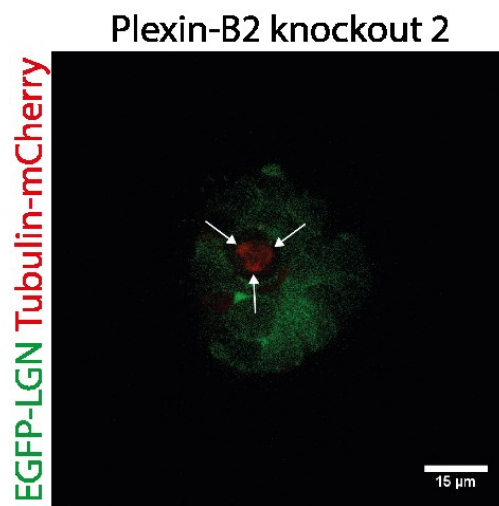


Figure 37. Aberrant mitosis in a Plexin-B2 knockout mIMCD-3 cell. Plexin-B2 knockout clone transduced with EGFP LGN and tubulin-mCherry in which a mitotic spindle with three poles could be observed

The amount of propidium iodide inside of a stained cell reflected the amount of DNA that it contained. In those cells where Plexin-B2 was knocked out, an increase of cells in the G2/M phase could be observed (Figure 38). This result taken together with the equal rate of growth when compared with the control cells could suggest that the Plexin-B2 knockout cells spend more time in the G2 or M phases of the cycle, thus increasing the proportion of the cells present in one of these phases. A striking result was the observed increase in the proportion of cells with aneuploidy in the Plexin-B2 knockout mIMCD-3 cells compared to the control. This could be a consequence of defects in mitosis.

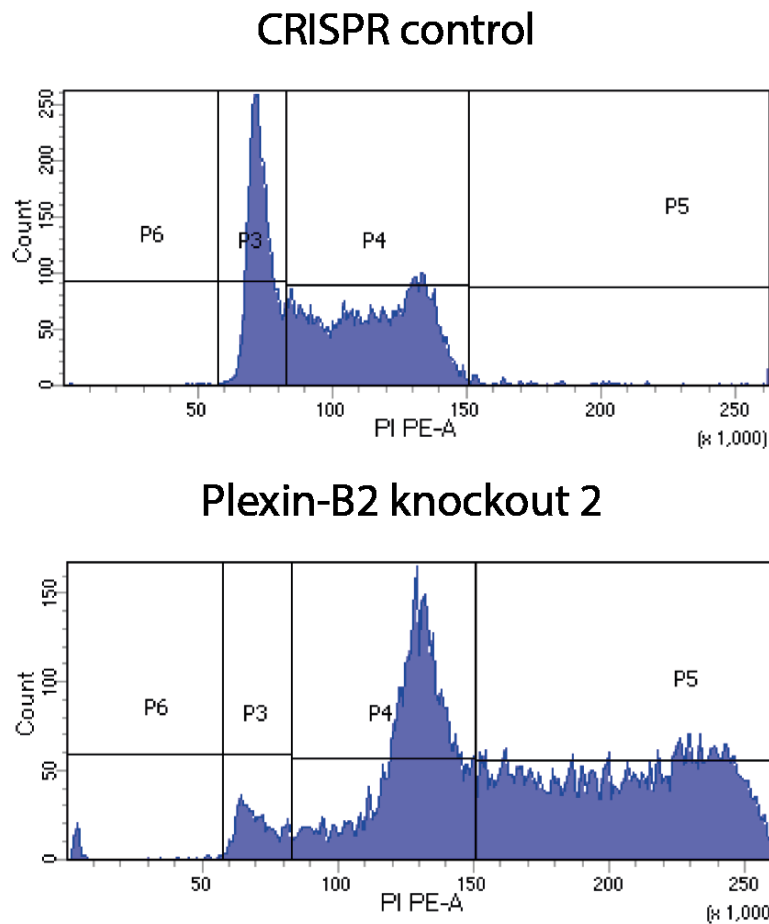


Figure 38. Cell cycle analysis of control and Plexin-B2 knockout mIMCD-3 cells. Cell count of cells containing different amounts of propidium iodide depending on their DNA content. P6: sub-G0. P3: G0/G1. P4: S and G2/M. P5: aneuploid cells

4.12. Knockout of Plexin-B2 does not change LGN and NuMA localization during mitosis

Since the knockout of Plexin-B2 impaired lumen formation in mIMCD-3 cysts, next, the mitotic spindle regulators LGN and NuMA were investigated. The goal was to verify if the localization of LGN and NuMA changes when Plexin-B2 is absent. For that, the CRISPR control clone and the two Plexin-B2 knockout clones, transduced with either EGFP-LGN or EGFP-NuMA, were cultured in 3D and live-cell imaging was performed using a spinning disk microscope. Tubulin was also labelled to visualize the mitotic spindle and be able to follow the process of mitosis, as well as identify the orientation of the cell division.

The goal was to image wild type and Plexin-B2 knockout cysts when they were still small and growing, so that it would be possible to see cells go from interphase into mitosis and record the entire cell division. However, very few cells were labelled for the mitotic spindle regulators and tubulin simultaneously and from those, none could be recorded going from interphase into mitosis. Instead, cells that had just started mitosis were recorded during the rest of the cell division. Another problem was that in the Plexin-B2 knockout cysts the lumen was filled with cells from a very early stage, which meant that the cells had contact with other cells in all directions and a potential mislocalization of LGN to the wrong membrane domains could not be investigated.

In the mIMCD-3 wild type cysts expressing Plexin-B2, the mitotic spindle regulator LGN localized to the lateral membrane, where the cell-cell contacts happened, positioning the mitotic spindle in parallel to the epithelial plane. In the Plexin-B2 knockout clones, LGN still localized at cell-cell contacts, but now these extended to the whole membrane. Furthermore, the orientation of cell division seemed to be random and sometimes cells divided perpendicularly or oblique to the epithelial plane (Figure 39).

As shown in Figure 40, in the absence of Plexin-B2, NuMA still localized normally, accumulating at the mitotic spindle poles during cell division (Hueschen et al. 2017; Kotak, Busso, and Gönczy 2014). These results taken together strongly suggest that the absence of Plexin-B2 does not affect the localization of the mitotic spindle regulators LGN and NuMA.

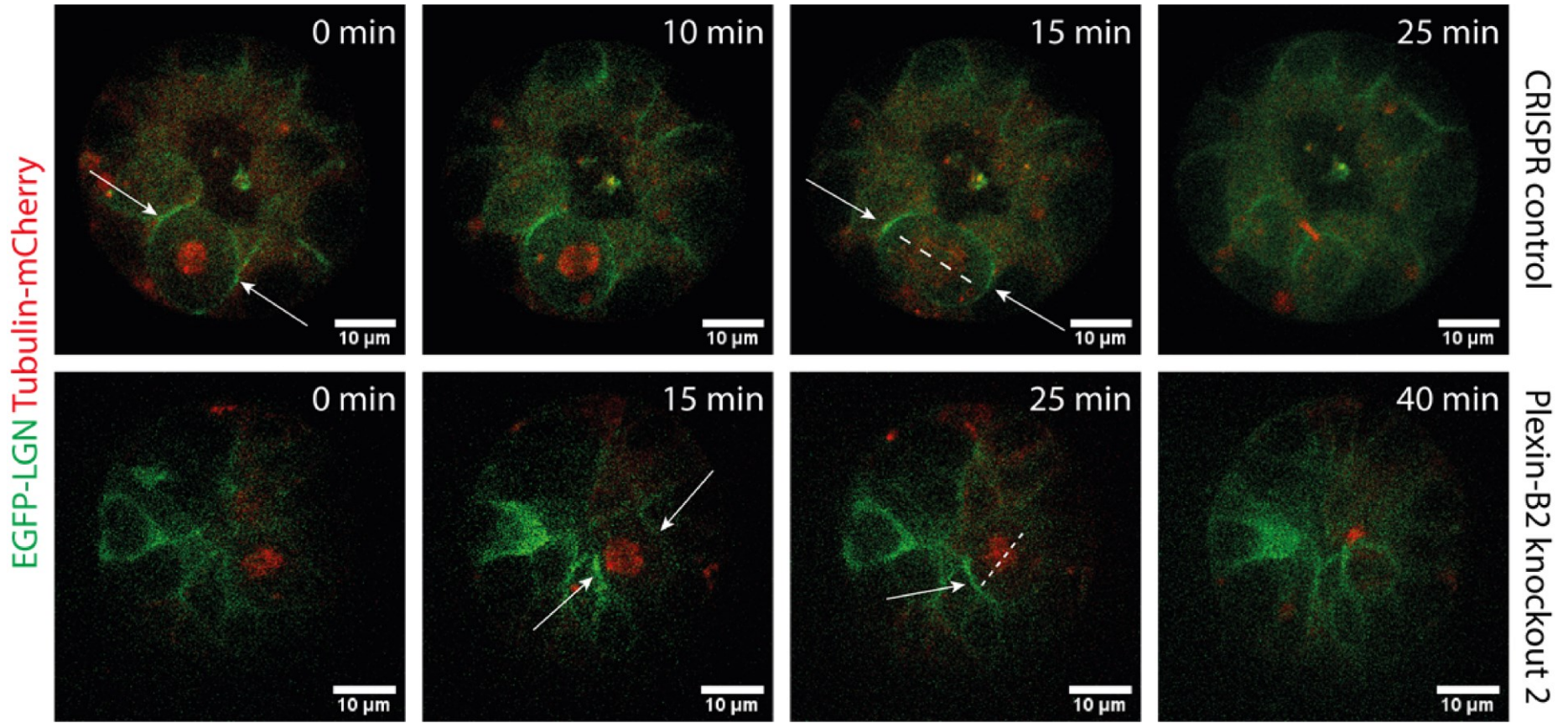


Figure 39. Spinning disk live-cell imaging of wild type and Plexin-B2 knockout cysts expressing EGFP-LGN and tubulin-mCherry during mitosis. Arrows indicate accumulation of LGN and dashed lines indicate the orientation of the mitotic spindle

mIMCD-3 Plexin-B2 knockout

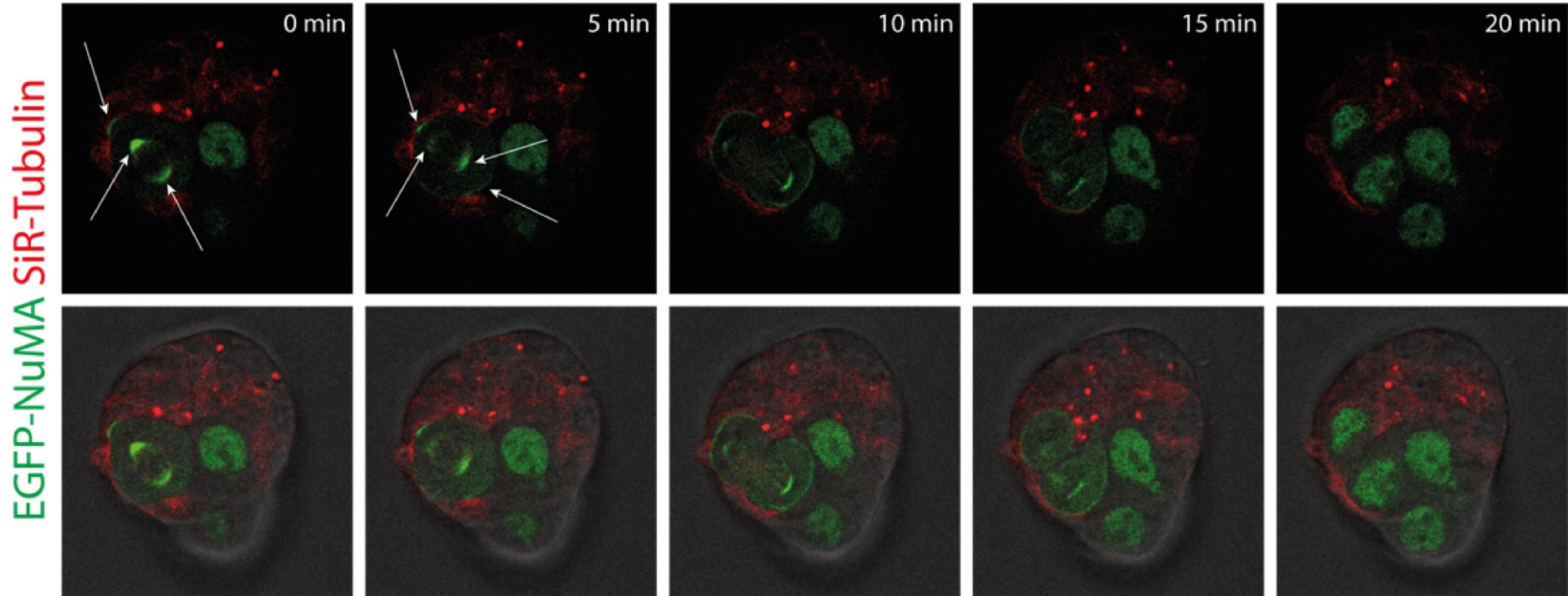


Figure 40. Spinning disk live-cell imaging of a Plexin-B2 knockout cyst expressing EGFP-NuMA and labelled with SiR-tubulin during mitosis. Arrows indicate NuMA accumulation

5. Discussion

Cell polarity is essential in order to maintain epithelial integrity and function. In epithelial cells, many components and processes show a polarized organization. One of them is the mitotic spindle, whose orientation is controlled to achieve precise tissue shaping, differentiation of progenitors or symmetrical division in stem cells. Plexins have been demonstrated to control mitotic spindle orientation during tissue morphogenesis. In this work I investigated the possible mechanism responsible for the polarized expression of Plexin-B2 in epithelial cells and the potential link between Plexin-B2 and the mitotic spindle regulators LGN and NuMA.

5.1. Polarized localization of Plexin-B2 in epithelia

First, I investigated the localization of Plexin-B2 in epithelial cells *in vivo*. I confirmed that in the mouse kidney Plexin-B2 is expressed in a strictly polarized manner to the basolateral membrane, while being absent from the luminal surface. At the embryonic stage, the expression of Plexin-B2 is restricted to cell-cell contacts in the developing kidney. On the other hand, in the adult, Plexin-B2 also localizes at the epithelial-extracellular matrix interface. This was demonstrated by immunofluorescence staining of endogenous Plexin-B2 in the embryonic and adult mouse kidney and comparison with staining of E-cadherin and ZO-1 (Figure 17).

This strict basolateral localization of Plexin-B2 was also observed by Xia et al. for the mouse kidney epithelium and also for other epithelia like the lung or the intestine (Xia et al. 2015). This hints that Plexin-B2 might exert similar functions in these epithelia. Interestingly, in the mid-secretory human endometrium, Plexin-B2 has been shown to localize in a polarized manner to the apical surface of luminal epithelial cells (Singh and Aplin 2015). These differences could reflect a different role of Plexin-B2 in these tissues. In fact, Fujiwara et al. showed that another axon guidance molecule, ephrin-A1, was also expressed at the apical membrane of luminal epithelial cells of the endometrium and proposed that it mediates the interaction between blastocysts and the endometrium (Fujiwara et al. 2002).

The basolateral localization of Plexin-B2 in the epithelium would permit juxtacrine Semaphorin-Plexin signaling with adjacent epithelial cells mediated by transmembrane semaphorin ligands. This is further supported by the fact that Sema4D, a Plexin-B2 transmembrane ligand, is also localized at the basolateral membrane of renal epithelial cells as shown by immunofluorescence staining of the endogenous protein (Figure 17). This way, Sema4D expressed on the lateral surface of one epithelial cell can bind Plexin-B2 on the lateral membrane of the adjacent cell. Therefore, in these cells, Sema4D-Plexin-B2 signaling is possible. On the other hand, an apical localization of the plexin would be required for paracrine signaling mediated by a secreted or a cleaved semaphorin released into the lumen. Indeed, Arbeille et al. showed that during the development of the central nervous system, Sema3B released to the brain ventricles and spinal cord canal, bound to neuropilins on the apical surface of mitotic progenitors (Arbeille et al. 2015). This suggests that the expression of plexins is polarized to the surfaces where they can bind their ligands. Both patterns of expression could hypothetically also be used for a semaphorin-independent role of plexins. For example, Plexin-D1 has recently been identified as a mechanosensor in endothelial cells, which signals independently from its semaphorin ligand in a complex with Nrp1 and VEGFR2 (Mehta et al. 2020).

Supporting the idea that the basolateral localization of Plexin-B2 in kidney epithelial cells is related to its role in juxtacrine cell-cell communication, Ogawa et al. showed that another molecule involved in cell-cell communication, ephrin-B1, localizes to the basolateral membrane of epithelial cells of the proximal tubules in the kidney cortex (Ogawa et al. 2006). Contrarily, another group of axon guidance receptors, Robo1 and Robo2, which use Slit as a ligand, have been shown to localize to the apical membrane of epithelial cells during lung development (Anselmo et al. 2003), although during a short period they were also observed at the basolateral membrane. This indicates that different families of axon guidance molecules exhibit sometimes the same subcellular distribution in epithelia, but other times the opposite one, probably related to their function in those tissues at specific times.

The fact that Plexin-B2 is also localized at the basal membrane next to the extracellular matrix in the adult, but not in the embryo, suggests that its targeting there

might have a functional relevance. This could be linked to integrin function, as Plexin-B1 has already been demonstrated to regulate integrin activity (Oinuma, Katoh, and Negishi 2006; Barberis et al. 2004; Basile, Gavard, and Gutkind 2007). Besides Plexin-B1, other plexins can also regulate integrin function (Banu et al. 2006; Choi et al. 2014). Integrin signaling is essential for the development of epithelial polarity and epithelial morphogenesis. On one hand, Integrin signaling through Rac1 upon binding to the extracellular matrix is necessary for laminin secretion and assembly of the basement membrane (O'Brien et al. 2001; Yu et al. 2005). Then, integrin binds the basement membrane and signals through ILK in order to polarize the plus end of non-centrosomal microtubules at the basal membrane, which correctly orients apicobasal polarity and allows lumen formation (Akhtar and Streuli 2013). However, whether plexins play a role in this process needs to be further investigated. It would also be interesting to determine the subcellular localization of Plexin-B2 and its ligands in other epithelial tissues where their role is already known. Additionally, it is important to assess the subcellular expression of other axon guidance and cell-cell communication molecules like ephrin-Eph and Slit-Robo in different epithelia and compare it with that of semaphorins and Plexins.

Next, I assessed the localization of Plexin-B2 in mIMCD-3 cells, which I used as a model. The expression of Plexin-B2 at cell-cell contacts in mIMCD-3 monolayers and 3D cysts, as demonstrated by immunofluorescence staining of the endogenous protein (Figures 18 and 19), further supported the possible role of Plexin-B2 in cell-cell communication in epithelial cells. Moreover, it validated mIMCD-3 cells as a model to study localization and function of Plexin-B2 in epithelial cells, as it recapitulated the situation observed *in vivo*.

The potential relevance of the localization at cell-cell contacts of axon guidance molecules in epithelial cells was also supported by the observation of EphA, a receptor for ephrin-A1, at cell-cell contacts in MDCK cells (Miao et al. 2003). It would be interesting to assess the localization of other axon guidance molecules, in particular other plexins and their semaphorin ligands, in mIMCD-3 cells in 2D and 3D.

5.2. Plexin-B2 localization during cell division

Since it is known that Plexin-B2 plays a role in mitotic spindle orientation (Xia et al. 2015), the next question was to find out where Plexin-B2 localizes during mitosis. Plexin-B2 is constantly expressed at the mitotic poles during cell division, even after cell rounding, as demonstrated by live-cell imaging (Figure 20). As soon as the new membrane divided both daughter cells, Plexin-B2 also localized there. This suggests that Plexin-B2 might indicate the site of anchorage of the mitotic spindle to the cell cortex. Since the mitotic spindle regulators LGN and NuMA localize forming a lateral ring in planar symmetric cell divisions (Hao et al. 2010), the polarized expression of Plexin-B2 at the mitotic poles could also mean that it interacts with the mitotic spindle machinery. A first step for the future investigation of these possibilities would be to visualize the localization of Plexin-B2 from a top or bottom view during cell division. This could be followed by co-IP studies to look for binding partners during cell division. It would also be interesting to observe the localization of Sema4D or other Plexin-B2 ligands during mitosis in these cells.

Although it has been observed that Eph signaling can also control mitotic spindle orientation *in vivo* (Franco and Carmena 2019), there is not sufficient evidence in the current literature about the subcellular expression of this axon guidance molecule during mitosis. Therefore, it would be interesting to assess the subcellular localization of other axon guidance molecules during cell division to hint to the potential mode of action of this group of molecules, including semaphorins and plexins, in their control of mitosis.

Plexins have been proposed to be adhesion molecules (Ohta et al. 1995). In a study by Gloerich et al., another adhesion molecule, E-cadherin, was involved in mitotic spindle orientation by positioning LGN at cell-cell contacts. In the same study it was shown that the loss of E-cadherin-mediated cell-cell adhesions produces the same phenotype demonstrated by Xia et al. in MDCK cysts and in the present study in mIMCD-3 cysts after knockout of Plexin-B2 (Gloerich et al. 2017). Interestingly, they further showed that E-cadherin localizes forming a lateral ring in MDCK cells during mitosis in a way similar to the observed for LGN and NuMA in planar symmetric cell divisions. Moreover, Desclozeaux et al. showed that Rab11 and the recycling endosome are required for E-cadherin trafficking to the basolateral membrane and that inhibiting

Rab11 caused aberrant MDCK cyst formation. Furthermore, ectopically expressing E-cadherin at the apical membrane produced the same phenotypical effects (Desclozeaux et al. 2008). These results, together with the ones that I present here and with the work of Xia et al. showing that the loss of Plexin-B2 causes aberrant mitotic spindle orientation, suggest that Plexin-B2-mediated cell-cell adhesion could represent a mechanism that positions Plexin-B2 at the mitotic poles, which could be important in order to control the orientation of cell division. However, this needs to be further investigated. One way to do this would be by disrupting Plexin-B2 homophilic interaction through mutation of the responsible extracellular domains. This homophilic interaction could also be investigated by co-culturing Plexin-B2 knockout cells with cells transduced with EGFP-labelled wild type Plexin-B2, which would be visualized during mitosis.

5.3. Plexin-B2 localization does not depend on binding to its ligand

Since the strictly polarized localization of Plexin-B2 in epithelial cells could be explained by its requirement for juxtacrine Semaphorin-Plexin signaling, I hypothesized whether the trafficking of Plexin-B2 to the basolateral membrane depended on binding to its ligand. As demonstrated by immunofluorescence staining of endogenous Plexin-B2 in ligand-deficient mouse kidney (Figure 21), the polarized expression of Plexin-B2 is not dependent on the presence of its ligand. This means that the basolateral localization of Plexin-B2 in epithelia does not require stabilization by binding to semaphorins on adjacent cells. Plexin-B2 might interact with other proteins at cell-cell contacts to prevent endocytosis. Another possibility is, as mentioned above, that Plexin-B2 acts as a cell-cell adhesion molecule by binding homophilically (Ohta et al. 1995), which could prevent its internalization. It would therefore be interesting to co-culture Plexin-B2 knockout cells with wild type cells in the absence of the ligands of Plexin-B2 and see if Plexin-B2 in the wild types still localizes to cell-cell contacts.

Interestingly, the kidney epithelium could develop normally in *sema4B^{-/-}*, *Sema4D^{-/-}* and *Sema4G^{-/-}* triple knockout mice (Xia et al. 2015). This suggests that another ligand of Plexin-B2 is expressed in renal tubular epithelial cells during

development and compensates the loss of the other three. For instance, Sema4A or Sema4C.

5.4. Identification of a basolateral sorting motif in the cytoplasmic domain of Plexin-B2

Considering that many membrane proteins are targeted basolaterally through intracellular peptide motifs (Stoops and Caplan 2014), I studied a cytoplasmic domain-deficient Plexin-B2 mutant. As demonstrated by expressing the EGFP-tagged intracellular deletion mutant of Plexin-B2 in MDCK cells (Figure 22), its cytoplasmic domain is required for its basolateral localization in epithelial cells in 3D. This result suggests the existence of a basolateral targeting motif within the intracellular sequence of Plexin-B2. Another possibility would be that Plexin-B2 gets recruited to the basolateral membrane by interacting with another protein localized at cell-cell contacts through its cytoplasmic region. Supporting this hypothesis, PDZ-RhoGEF has been shown to promote membrane localization of Plexin-B1, a close homologue of Plexin-B2 (Swiercz et al. 2002). However, this recruitment was not specific to cell-cell contacts, which could possibly require an additional interaction partner.

For another cell-cell adhesion molecule like E-cadherin, a dileucine motif was identified as being the responsible for its basolateral targeting. This motif was conserved in most of the cadherin family members, sometimes changing the second leucine for isoleucine (Miranda et al. 2001). The expression patterns of the Plexin-B2 sequential deletion mutants in 3D (Figures 27 and 28) showed that the basolateral targeting motif must reside between the transmembrane domain and the C1 domain of the GAP. In this region, no dileucine motive like the one in E-cadherin can be found. Instead, tyrosine-based lateral targeting motif appears (Figure 29). This motif is present in all mouse class B plexins and conserved in Plexin-B2 (Figure 30). The fact that this motif is conserved in plexins of the B subfamily but not in A, C or D subfamilies suggests that B plexins are targeted to the basolateral membrane while A, C and D plexins locate apically. However, there is no literature about their exact subcellular localization yet. Interestingly, Plexins of the A subfamily act as receptors for Sema3B, and their potential apical localization

could fit the neuropilin-mediated Sema3B signaling at the apical membrane of neuroepithelial progenitors observed by Arbeille et al.

In order to verify whether this motif is really responsible for Plexin-B2 polarized basolateral localization in epithelia, point mutants should be generated and their targeting analyzed. Of note, there are several point mutations described for Plexin-B1, but none of them in the suggested motif (Wong et al. 2007). In that study, those mutations were investigated in the roles of cell spreading, adhesion, migration and cell collapse, but their possible phenotypes in the subcellular localization of Plexin-B1 in epithelial cells in 3D were not investigated.

Interestingly, in MDCK and mIMCD-3 cells in 2D, the cytoplasmic domain of Plexin-B2 was not required for its targeting to cell-cell contacts. In this case, its localization to cell-cell contacts could be mediated by resistance to endocytosis by stabilization through homophilic interactions mediated by the extracellular domain (Ohta et al. 1995). As mentioned above, an experiment co-culturing these cells, expressing Plexin-B2 Δ IC, with Plexin-B2 knockouts would help solve this question.

5.5. Plexin-B2 in mitotic spindle orientation

Next, I further investigated the role of Plexin-B2 in mitotic spindle orientation. Interestingly, the apical localization of Plexin-B2 Δ IC in MDCK cells did not prevent the formation of normal cysts (Figures 22, 27 and 28). This can be explained by the fact that these cells are still expressing wild type Plexin-B2 endogenously. Considering that Xia et al. showed that the GAP domain of Plexin-B2 is required for mitotic spindle positioning, it can be concluded that Plexin-B2 Δ IC does not intervene in the orientation of the mitotic spindle. It would be interesting to ectopically express full-length Plexin-B2 at the apical membrane in these cells and observe its potential impact on cell division.

Plexin-B2 is required to correctly position the mitotic spindle also in mIMCD-3 cysts, as confirmed by deleting Plexin-B2 using CRISPR/Cas9 genome editing (Figures 33, 34 and 39). This is coincident with the results of Xia et al. in MDCK cysts and *in vivo*. Sema3B signaling was also demonstrated to control the positioning of the spindle in neuroepithelial mitotic progenitors (Arbeille et al. 2015), supporting the role of

Semaphorin-Plexin signaling in mitotic spindle orientation. Furthermore, another axon guidance receptor like Eph has been shown to control mitotic spindle orientation as well (Franco and Carmena 2019). Therefore, it seems likely that epithelial cells utilize cell-cell communication factors, like axonal guidance molecules, as extrinsic cues to position their mitotic spindle correctly.

In order to elucidate how this happens, I investigated the mitotic spindle regulators LGN and NuMA in Plexin-B2 knockout cells and compared them to wild type cells. It has been shown before that LGN and NuMA localize forming a lateral ring in planar dividing cells (Hao et al. 2010). Furthermore, NuMA also shows localization at the centrosomes during mitosis (Du and Macara 2004). The deletion of Plexin-B2 in mIMCD-3 cells did not alter the localization of LGN at cell-cell contacts during interphase (Figure 39). During mitosis, in control cysts, LGN localized at the mitotic poles of the cell cortex similarly to what was shown for Plexin-B2 (Figures 39 and 20). However, in Plexin-B2 knockout mutants, LGN localized all around the membrane (Figure 39). This result has to be interpreted with caution, as in both wild type and Plexin-B2 knockout cells, LGN localizes to cell-cell contacts during cell division. In the case of Plexin-B2 knockout cysts, at the time point of the analysis, the dividing cells are completely surrounded by other cells. In contrast, in wild type cysts, each cell only contacts other cells at its lateral sides. LGN could potentially still be excluded from the apical membrane in Plexin-B2 knockout cells, but since they do not show an apical domain, this could not be analysed. From this result it cannot be concluded whether Plexin-B2 controls the localization of LGN at cell-cell contacts. However, it is possible to confirm that Plexin-B2 is not required for the targeting of LGN to the membrane. It would be interesting to knockout or knockdown Plexin-B2 after the mIMCD-3 cells have been allowed to form normal cysts with a central lumen, for example by transducing the cells with an inducible shRNA construct. This way, the localization of LGN during mitosis could be observed in Plexin-B2 depleted cells that still show an apical domain.

In Plexin-B2 knockout mIMCD-3 cells, the mitotic spindle axis could be observed sometimes aligning normally (not shown), parallel to the outer surface of the cyst, but other times perpendicularly or oblique (Figure 39). Therefore, the localization of LGN in the whole cell cortex makes the orientation of the mitotic spindle random, causing

eventual cell divisions towards the centre of the cyst and generating multi-layered and luminal filling.

In this study, I encountered many difficulties to analyse the position of NuMA in Plexin-B2 knockout and wild type mIMCD-3 cysts due to its low transduction efficiency. From the example that could be analyzed (Figure 40), it can be concluded that the knockout of Plexin-B2 does not alter the localization of NuMA at the spindle poles. However, the deletion of Plexin-B2 alters the recruitment of NuMA to the correct membrane domain to ensure planar division. This is consistent with the fact that LGN does not influence the localization of NuMA to the centrosomes, but recruits it to the appropriate cortical domain (Du and Macara 2004).

How does Plexin-B2 control mitotic spindle orientation? Xia et al. showed that correct orientation of the spindle depended on Plexin-B2-mediated activation of Cdc42 (Xia et al. 2015). Interestingly, active Cdc42 has been shown to mediate the apical membrane determination in MDCK and Caco-2 cells in the first cell divisions during cyst formation (Martin-Belmonte et al. 2007; Jaffe et al. 2008). Therefore, Plexin-B2 might control the formation of the apical membrane and an initial lumen at the first cell divisions of MDCK and mIMCD-3 cysts, rather than regulate directly the position of LGN. This would be consistent with the results that I present here, where LGN still localizes to cell-cell contacts in Plexin-B2 knockout cysts, but no clear apical domain or central lumen is formed. Another possibility is that Plexin-B2 controls mitotic spindle orientation by regulating the cortical actin cytoskeleton. The observation that another axon guidance receptor like Eph controls mitotic spindle orientation by regulating myosin II supports this idea (Franco and Carmena 2019). However, Arbeille et al. showed the cortical actin cytoskeleton was unaltered in Sema3B-deficient neuroepithelial progenitors with mitotic spindle orientation defects. They propose that semaphorin signaling controls the positioning of the spindle through GSK3-mediated inhibition of the microtubule stabilizer CRMP2 (Arbeille et al. 2015). Therefore, further investigation needs to be done analysing the actin cytoskeleton in Plexin-B2 knockout cysts and pathways like GSK3-CRMP2. It would also be interesting to repeat the experiments done in this work during the first divisions of mIMCD-3 cells in order to elucidate if they ever form a central lumen.

5.6. Plexin-B2 and cell cycle

Due to the observation that Plexin-B2 knockout cysts were bigger than wild type cysts and also because of the finding of striking multipolar mitoses in Plexin-B2 knockout cells, the role of Plexin-B2 in the cell cycle was further investigated. By performing a propidium iodide staining followed by flow cytometry, a higher proportion of cells in the G2/M phases of the cell cycle could be observed in Plexin-B2 knockout cells. This could have various interpretations. It is possible that in Plexin-B2 knockout cells mitosis takes longer, causing an accumulation of cells in the G2/M phases. Indeed, this was the impression while recording mitosis in wild type and Plexin-B2 knockout cysts, but the duration of cell division has not been quantified in this work. This hypothesis is consistent with the results of a study on breast cancer cells, in which a G2/M transition block was found upon knockdown of either Plexin-B2 or its ligand Sema4C (Gurrapu et al. 2018). That block resulted in the increase of cells in the G2/M phases. Another possibility is that Plexin-B2 knockout cells proliferate more than wild types. As shown in Figure 35 and Figure 36, growth was comparable between wild types and Plexin-B2 knockouts. However, this could also mean that both cell proliferation as well as cell death are increased in Plexin-B2 knockout cells, keeping the net growth unchanged. In the study of Gurrapu et al. it was shown that knockdown of Sema4C or Plexin-B2 reduced proliferation of breast cancer cells, but not of normal immortalized human mammary epithelial cells. It would be interesting to measure cell death in mIMCD-3 Plexin-B2 knockout cells and compare it to that of the wild type or perform a more specific cell proliferation assessment. Besides the study of Gurrapu et al., other studies have shown that the depletion of Plexin-B2 or its close homologue Plexin-B1 decreased proliferation in several cell types, including cancer cells (Daviaud et al. 2016; Saha et al. 2012; Perälä et al. 2011; Cao et al. 2014). Contrarily, Eph deletion not only showed disrupted mitotic spindle orientation, but also promoted proliferation by a reduced Rho-dependent inactivation of the PI3K-Akt1 pathway (Franco and Carmena 2019). This suggests that Plexin-B2 could act in a similar way through its PDZ domain-binding motif and RhoA activation downstream effect. Interestingly, the altered proliferation observed in the study of Gurrapu et al. was attributable to a reduction in Plexin-B2-

mediated RhoA activation. Whether Plexin-B2 signaling enhances or inhibits proliferation in mIMCD-3 cells has to be further studied using Plexin-B2 knockout cells.

Even though multipolar mitoses were observed for Plexin-B2 knockout cells, strikingly, an increase of the Sub-G0 population was not found, but in fact there was a higher proportion of cells with excessive DNA content. An explanation for this phenomenon could be that too prolonged mitosis could lead to problems when finalizing cell division or to defects in cytokinesis as a consequence of the absence of Plexin-B2. This is consistent with the results of Gurrapu et al., who also observed a blockade of cytokinesis resulting in multinucleated cells. However, no experiments have been conducted in this thesis to investigate this possibility.

6. Acknowledgements

Coming to the end of my doctorate means the conclusion of a chapter of my life. This one has not been particularly easy, but now that I am nearing its culmination I realize how much I have learnt and how many people have been by my side to help me through it. I have been very lucky to have them all and to be able to learn from them.

First, I would like to thank Prof. Thomas Worzfeld for trusting me to carry out his project, giving me the opportunity to work in his lab, making corrections to this thesis and for his mentoring and support throughout my PhD. He has been a dedicated director and supervisor and I am grateful for his guidance.

Second, I thank all the members of the Worzfeld Lab for their support, helping me with my experiments and for their suggestions to my project. I learnt a lot of science from all of you. Specially, I would like to thank my office mates and friends Florian and Ivana. Thank you for all the great moments I have lived with you inside and outside of the lab during this time. You have been one of my greatest supports. Thank you for helping me overcome many problems and difficulties in my project with your scientific insights and suggestions, and thank you for helping me get my mind off the science in the evenings and weekends.

I would also like to thank the members of the Grosse Lab. I could always count on your help with my experiments. Thank you for the scientific discussions at lab meetings and for all your suggestions. In particular, I thank my friend and fellow Spaniard Laura. You have been supporting me from the very beginning. Thank you for helping me with my experiments and for being one of my best friends, also outside of the lab. I would also like to give special thanks to Jessica. At the beginning of my PhD you have seen some of my worst moments, when I felt that this was too much for me and almost gave up. You gave me support and encouragement to overcome those feelings and go on. Thank you for being a good friend and for all of the great moments outside of the lab.

I would like to thank all the members of the Institute of Pharmacology and the BPC in general for helping me overcome all the limitations and problems that I encountered during my research. Specially I would like to thank all the lab technicians,

who have helped me so much with my experiments. I am particularly grateful to Kathrin Stelter for helping me with the difficult cloning experiments. I would also like to thank the professors of our institute for the scientific discussions and suggestions. Special thanks to Tanja Pfeffer-Eckel for being an immense help, in particular during the first months when I had so much trouble finding a place to live and for helping me do all the daunting paperwork for the university and the city.

I thank the Philipps-Universität of Marburg for letting me use their facilities and their research resources. I would like to give special thanks to Katrin Roth for teaching me spinning disk microscopy and helping me solve many problems with my experiments. Many thanks to the DFG Research Training Group GRK 2213 for allowing me to participate in their activities and for the constructive discussion in our meetings.

During my entire PhD and particularly during the hardest phases, my biggest support have been my family and friends. I thank my parents for being supportive whenever I complained too much or had doubts. Thank you for your patience when I was going through hard times and thank you for not letting me give up. I thank my brother Luis and my sister Cristina. You have also given me support when I needed it most. I would like to thank the rest of my family for caring and asking me about the progress of my PhD.

I thank all my friends, those from Spain and the ones I have met in Marburg. I would like to thank in particular Alejandro, for being a good friend since our days in high school. I could always share my thoughts with you, no matter how stupid or crazy they were. You have always listened to my problems, given me sound advice and been present, though sometimes in the distance, for the most part of my life. You too have been a great support during my thesis. I thank also Michael and Claudia. You are among the nicest people I know. I feel very lucky to have met you and be your friend. Thank you for all you have done for me, from all the times you invited me over for dinner to helping me improve my German. I would also like to thank my two most outgoing friends, Natalia and Shankar. It is so much fun to be your friend. Thank you for all those party nights that always push me a little bit out of my comfort zone, but that I enjoy so much and helped me forget about the difficulties in the lab.

Acknowledgements

Lastly, I would like to thank all the people that I could not mention explicitly here, but have shared this time with me and have helped me in one way or another. Some of you have been also a critical support for me, being there from the beginning and giving me strength to keep pushing and accomplish this goal. This thesis is as much yours as it is mine. I am grateful to all of you.

7. List of academic professors

Alfredo de Bustos Rodríguez

Alfredo Prieto Martín

Armando del Romero Guerrero

Arturo Baz Ramos

Bartolomé Sabater García

Benito Fraile Laiz

Carlos Illana Esteban

Carmen Bartolomé Esteban

Eduardo Arilla Ferreiro

Emilio Jesús López Caballero

Esperanza Gutiérrez Redomero

Fernando San Segundo Barahona

Francisco Javier Martínez Gonzalez

Guillermo Bodega Magro

Ignacio Martínez Mendizábal

Inés Díaz-Laviada Marturet

Joaquín Royo Cárcamo

Jorge Pérez Serrano

José Carlos Díez Ballesteros

José Luis Copa Patiño

Josefa Isabel Belliure Ferrer

Juan Carlos Prieto Villapún

Juan M. González Triguero

Juan Soliveri de Carranza

Juana Rodríguez Bullido

Julio Pérez Márquez

Leonardo Mario Casano Mazza

Lilian Puebla Jiménez

Luis A. González Guijarro

Manuel Hernández Cutuli

Marcos Marvá Ruiz

María del Carmen Muñoz Moreno

María del Mar Royela García

María Esther Ferrer Cebrián

María Gloria Quintanilla López

María Isabel Arenas Jiménez

María Isabel Gegúndez Cámara

María Montserrat Araceli Fominaya Yagüe

María Tíscar Espigares Pinilla

Miguel Rubio Sáez

Nieves Casado Escribano

Pedro Villar Salvador

Ricardo Paniagua Gómez-Álvarez

8. References

- Adler, Paul N. 2002. "Planar Signaling and Morphogenesis in *Drosophila*." *Developmental Cell* 2 (5): 525–35. <http://www.ncbi.nlm.nih.gov/pubmed/12015961>.
- Akhtar, Nasreen, and Charles H. Streuli. 2013. "An Integrin–ILK–Microtubule Network Orients Cell Polarity and Lumen Formation in Glandular Epithelium." *Nature Cell Biology* 15 (1): 17–27. <https://doi.org/10.1038/ncb2646>.
- Allegra, Maryline, Andreas Zaragkoulias, Elena Vorgia, Marina Ioannou, Gabriele Litos, Hartmut Beug, and George Mavrothalassitis. 2012. "Semaphorin-7a Reverses the ERF-Induced Inhibition of EMT in Ras-Dependent Mouse Mammary Epithelial Cells." *Molecular Biology of the Cell* 23 (19): 3873–81. <https://doi.org/10.1091/mbc.E12-04-0276>.
- Anselmo, Mark A, Sussie Dalvin, Parthak Proadhan, Katsumi Komatsuzaki, Jeremy T Aidlen, Jay J Schnitzer, Jane Y Wu, and T Bernard Kinane. 2003. "Slit and Robo: Expression Patterns in Lung Development." *Gene Expression Patterns : GEP* 3 (1): 13–19. [https://doi.org/10.1016/s1567-133x\(02\)00095-9](https://doi.org/10.1016/s1567-133x(02)00095-9).
- Arbeille, Elise, Florie Reynaud, Isabelle Sanyas, Muriel Bozon, Karine Kindbeiter, Frédéric Causeret, Alessandra Pierani, Julien Falk, Frédéric Moret, and Valérie Castellani. 2015. "Cerebrospinal Fluid-Derived Semaphorin3B Orients Neuroepithelial Cell Divisions in the Apicobasal Axis." *Nature Communications* 6 (1): 6366. <https://doi.org/10.1038/ncomms7366>.
- Artigiani, Stefania, Paolo Conrotto, Pietro Fazzari, Giorgio F. Gilestro, Davide Barberis, Silvia Giordano, Paolo M. Comoglio, and Luca Tamagnone. 2004. "Plexin-B3 Is a Functional Receptor for Semaphorin 5A." *EMBO Reports* 5 (7): 710–14. <https://doi.org/10.1038/sj.embor.7400189>.
- Au, Josephine Sui-Yan, Claudia Puri, Gudrun Ihrke, John Kendrick-Jones, and Folma Buss. 2007. "Myosin VI Is Required for Sorting of AP-1B–Dependent Cargo to the Basolateral Domain in Polarized MDCK Cells." *The Journal of Cell Biology* 177 (1): 103–14. <https://doi.org/10.1083/jcb.200608126>.
- Aurandt, Jennifer, Haris G Vikis, J Silvio Gutkind, Natalie Ahn, and Kun-Liang Guan. 2002. "The Semaphorin Receptor Plexin-B1 Signals through a Direct Interaction with the Rho-Specific Nucleotide Exchange Factor, LARG." *Proceedings of the National Academy of Sciences of the United States of America* 99 (19): 12085–90. <https://doi.org/10.1073/pnas.142433199>.
- Axelrod, J D. 2001. "Unipolar Membrane Association of Dishevelled Mediates Frizzled Planar Cell Polarity Signaling." *Genes & Development* 15 (10): 1182–87. <https://doi.org/10.1101/gad.890501>.
- Bachelder, Robin E, Elizabeth A Lipscomb, Xuena Lin, Melissa A Wendt, Neil H Chadborn, Britta J Eickholt, and Arthur M Mercurio. 2003. "Competing Autocrine Pathways Involving Alternative Neuropilin-1 Ligands Regulate Chemotaxis of Carcinoma Cells." *Cancer Research* 63 (17): 5230–33.

- <http://www.ncbi.nlm.nih.gov/pubmed/14500350>.
- Bagri, Anil, Hwai Jong Cheng, Avraham Yaron, Samuel J. Pleasure, and Marc Tessier-Lavigne. 2003. "Stereotyped Pruning of Long Hippocampal Axon Branches Triggered by Retraction Inducers of the Semaphorin Family." *Cell* 113 (3): 285–99. [https://doi.org/10.1016/S0092-8674\(03\)00267-8](https://doi.org/10.1016/S0092-8674(03)00267-8).
- Bangs, Fiona, and Kathryn V. Anderson. 2017. "Primary Cilia and Mammalian Hedgehog Signaling." *Cold Spring Harbor Perspectives in Biology* 9 (5): a028175. <https://doi.org/10.1101/cshperspect.a028175>.
- Banu, Nazifa, Jason Teichman, Marya Dunlap-Brown, Guillermo Villegas, and Alda Tufro. 2006. "Semaphorin 3C Regulates Endothelial Cell Function by Increasing Integrin Activity." *FASEB Journal* 20 (12): 2150–52. <https://doi.org/10.1096/fj.05-5698fje>.
- Barberis, D., S. Artigiani, A. Casazza, S. Corso, S. Giordano, C. A. Love, E. Y. Jones, P. M. Comoglio, and Luca Tamagnone. 2004. "Plexin Signaling Hampers Integrin-Based Adhesion, Leading to Rho-Kinase Independent Cell Rounding, and Inhibiting Lamellipodia Extension and Cell Motility." *The FASEB Journal : Official Publication of the Federation of American Societies for Experimental Biology* 18 (3): 592–94. <https://doi.org/10.1096/fj.03-0957fje>.
- Basile, John R., Rogerio M. Castilho, Vanessa P. Williams, and J. Silvio Gutkind. 2006. "Semaphorin 4D Provides a Link between Axon Guidance Processes and Tumor-Induced Angiogenesis." *Proceedings of the National Academy of Sciences of the United States of America* 103 (24): 9017–22. <https://doi.org/10.1073/pnas.0508825103>.
- Basile, John R., Julie Gavard, and J. Silvio Gutkind. 2007. "Plexin-B1 Utilizes RhoA and Rho Kinase to Promote the Integrin-Dependent Activation of Akt and ERK and Endothelial Cell Motility." *Journal of Biological Chemistry* 282 (48): 34888–95. <https://doi.org/10.1074/jbc.M705467200>.
- Bastock, R., Helen Strutt, and David Strutt. 2003. "Strabismus Is Asymmetrically Localised and Binds to Prickle and Dishevelled during Drosophila Planar Polarity Patterning." *Development* 130 (13): 3007–14. <https://doi.org/10.1242/dev.00526>.
- Beaumont, Marie, Linda Akloul, Wilfrid Carré, Chloé Quélin, Hubert Journal, Laurent Pasquier, Mélanie Fradin, et al. 2019. "Targeted Panel Sequencing Establishes the Implication of Planar Cell Polarity Pathway and Involves New Candidate Genes in Neural Tube Defect Disorders." *Human Genetics* 138 (4): 363–74. <https://doi.org/10.1007/s00439-019-01993-y>.
- Bellaïche Y., A. Radovic, D. F. Woods, C. D. Hough, M. L. Parmentier, C. J. O’Kane, P. J. Bryant, and F. Schweisguth. 2001. "The Partner of Inscuteable/Discs-Large Complex Is Required to Establish Planar Polarity during Asymmetric Cell Division in Drosophila." *Cell* 106 (3): 355–66. [https://doi.org/10.1016/S0092-8674\(01\)00444-5](https://doi.org/10.1016/S0092-8674(01)00444-5).
- Benton, Richard, and Daniel St Johnston. 2003. "Drosophila PAR-1 and 14-3-3 Inhibit Bazooka/PAR-3 to Establish Complementary Cortical Domains in Polarized Cells." *Cell* 115 (6): 691–704. [https://doi.org/10.1016/S0092-8674\(03\)00938-3](https://doi.org/10.1016/S0092-8674(03)00938-3).

- Betschinger, Jörg, Karl Mechtler, and Juergen A. Knoblich. 2003. "The Par Complex Directs Asymmetric Cell Division by Phosphorylating the Cytoskeletal Protein Lgl." *Nature* 422 (6929): 326–30. <https://doi.org/10.1038/nature01486>.
- Bhanot, Purnima, Marcel Brink, Cindy Harryman Samos, Jen-Chih Hsieh, Yanshu Wang, Jennifer P. Macke, Deborah Andrew, Jeremy Nathans, and Roel Nusse. 1996. "A New Member of the Frizzled Family from *Drosophila* Functions as a Wingless Receptor." *Nature* 382 (6588): 225–30. <https://doi.org/10.1038/382225a0>.
- Bielenberg, Diane R., Yasuhiro Hida, Akio Shimizu, Arja Kaipainen, Michael Kreuter, Caroline Choi Kim, and Michael Klagsbrun. 2004. "Semaphorin 3F, a Chemorepellent for Endothelial Cells, Induces a Poorly Vascularized, Encapsulated, Nonmetastatic Tumor Phenotype." *The Journal of Clinical Investigation* 114 (9): 1260–71. <https://doi.org/10.1172/JCI21378>.
- Bilder, D., M. Li, and N. Perrimon. 2000. "Cooperative Regulation of Cell Polarity and Growth by *Drosophila* Tumor Suppressors." *Science* 289 (5476): 113–16. <https://doi.org/10.1126/science.289.5476.113>.
- Bilder, David, Markus Schober, and Norbert Perrimon. 2003. "Integrated Activity of PDZ Protein Complexes Regulates Epithelial Polarity." *Nature Cell Biology* 5 (1): 53–58. <https://doi.org/10.1038/ncb897>.
- Bonazzi, Matteo, Stefania Spanò, Gabriele Turacchio, Claudia Cericola, Carmen Valente, Antonino Colanzi, Hee Seok Kweon, et al. 2005. "CtBP3/BARS Drives Membrane Fission in Dynamin-Independent Transport Pathways." *Nature Cell Biology* 7 (6): 570–80. <https://doi.org/10.1038/ncb1260>.
- Bose, I., J. E. Irazoqui, J. J. Moskow, E. S. Bardes, T. R. Zyla, and D. J. Lew. 2001. "Assembly of Scaffold-Mediated Complexes Containing Cdc42p, the Exchange Factor Cdc24p, and the Effector Cla4p Required for Cell Cycle-Regulated Phosphorylation of Cdc24p." *The Journal of Biological Chemistry* 276 (10): 7176–86. <https://doi.org/10.1074/jbc.M010546200>.
- Bowman, Sarah K., Ralph A. Neumüller, Maria Novatchkova, Quansheng Du, and Juergen A. Knoblich. 2006. "The *Drosophila* NuMA Homolog Mud Regulates Spindle Orientation in Asymmetric Cell Division." *Developmental Cell* 10 (6): 731–42. <https://doi.org/10.1016/j.devcel.2006.05.005>.
- Boyd, L., S. Guo, D. Levitan, D. T. Stinchcomb, and K. J. Kemphues. 1996. "PAR-2 Is Asymmetrically Distributed and Promotes Association of P Granules and PAR-1 with the Cortex in *C. Elegans* Embryos." *Development (Cambridge, England)* 122 (10): 3075–84. <http://www.ncbi.nlm.nih.gov/pubmed/8898221>.
- Bré, M. H., T. E. Kreis, and E. Karsenti. 1987. "Control of Microtubule Nucleation and Stability in Madin-Darby Canine Kidney Cells: The Occurrence of Noncentrosomal, Stable Detyrosinated Microtubules." *The Journal of Cell Biology* 105 (3): 1283–96. <https://doi.org/10.1083/jcb.105.3.1283>.
- Brittle, Amy L., Ada Repiso, José Casal, Peter A. Lawrence, and David Strutt. 2010. "Four-Jointed Modulates Growth and Planar Polarity by Reducing the Affinity of Dachshous for Fat." *Current Biology* 20 (9): 803–10.

- <https://doi.org/10.1016/j.cub.2010.03.056>.
- Browne, Kristen, Wenyan Wang, Rachel Q. Liu, Matthew Piva, and Timothy P. O'Connor. 2012. "Transmembrane Semaphorin5B Is Proteolytically Processed into a Repulsive Neural Guidance Cue." *Journal of Neurochemistry* 123 (1): 135–46. <https://doi.org/10.1111/j.1471-4159.2012.07885.x>.
- Bryant, David M., Julie Rognot, Anirban Datta, Arend W. Overeem, Minji Kim, Wei Yu, Xiao Peng, et al. 2014. "A Molecular Switch for the Orientation of Epithelial Cell Polarization." *Developmental Cell* 31 (2): 171–87. <https://doi.org/10.1016/j.devcel.2014.08.027>.
- Bryant, David M., Anirban Datta, Alejo E. Rodríguez-Fraticelli, Johan Peränen, Fernando Martín-Belmonte, and Keith E. Mostov. 2010. "A Molecular Network for de Novo Generation of the Apical Surface and Lumen." *Nature Cell Biology* 12 (11): 1035–45. <https://doi.org/10.1038/ncb2106>.
- Buendia, B., M. H. Bré, G. Griffiths, and E. Karsenti. 1990. "Cytoskeletal Control of Centrioles Movement during the Establishment of Polarity in Madin-Darby Canine Kidney Cells." *The Journal of Cell Biology* 110 (4): 1123–35. <https://doi.org/10.1083/jcb.110.4.1123>.
- Butty, Anne-Christine, Nathalie Perrinjaquet, Audrey Petit, Malika Jaquenoud, Jeffrey E. Segall, Kay Hofmann, Catherine Zwahlen, and Matthias Peter. 2002. "A Positive Feedback Loop Stabilizes the Guanine-Nucleotide Exchange Factor Cdc24 at Sites of Polarization." *The EMBO Journal* 21 (7): 1565–76. <https://doi.org/10.1093/emboj/21.7.1565>.
- Cabernard, Clemens, and Chris Q. Doe. 2009. "Apical/Basal Spindle Orientation Is Required for Neuroblast Homeostasis and Neuronal Differentiation in Drosophila." *Developmental Cell* 17 (1): 134–41. <https://doi.org/10.1016/j.devcel.2009.06.009>.
- Campanale, Joseph P., Thomas Y. Sun, and Denise J. Montell. 2017. "Development and Dynamics of Cell Polarity at a Glance." *Journal of Cell Science* 130 (7): 1201–7. <https://doi.org/10.1242/jcs.188599>.
- Cao, Jiao, Chen Zhang, Ting Chen, Rong Tian, Shuhong Sun, Xianshui Yu, Chunying Xiao, et al. 2014. "Plexin-B1 and Semaphorin 4D Cooperate to Promote Cutaneous Squamous Cell Carcinoma Cell Proliferation, Migration and Invasion." *Journal of Dermatological Science* 79 (2): 127–36. <https://doi.org/10.1016/j.jdermsci.2015.05.002>.
- Carroll, Thomas J., and Amrita Das. 2011. "Planar Cell Polarity in Kidney Development and Disease." *Organogenesis* 7 (3): 180–90. <https://doi.org/10.4161/org.7.3.18320>.
- Carroll, Thomas J., and Jing Yu. 2012. "The Kidney and Planar Cell Polarity." *Current Topics in Developmental Biology* 101: 185–212. <https://doi.org/10.1016/B978-0-12-394592-1.00011-9>.
- Casazza, Andrea, Veronica Finisguerra, Lorena Capparuccia, Andrea Camperi, Jakub M.

- Swiercz, Sabrina Rizzolio, Charlotte Rolny, et al. 2010. "Sema3E-Plexin D1 Signaling Drives Human Cancer Cell Invasiveness and Metastatic Spreading in Mice." *Journal of Clinical Investigation* 120 (8): 2684–98. <https://doi.org/10.1172/JCI42118>.
- Casazza, Andrea, Xi Fu, Irja Johansson, Lorena Capparuccia, Fredrik Andersson, Alice Giustacchini, Mario Leonardo Squadrito, et al. 2011. "Systemic and Targeted Delivery of Semaphorin 3A Inhibits Tumor Angiogenesis and Progression in Mouse Tumor Models." *Arteriosclerosis, Thrombosis, and Vascular Biology* 31 (4): 741–49. <https://doi.org/10.1161/ATVBAHA.110.211920>.
- Castellani, V., E. De Angelis, S. Kenwrick, and G. Rougon. 2002. "Cis and Trans Interactions of L1 with Neuropilin-1 Control Axonal Responses to Semaphorin 3A." *The EMBO Journal* 21 (23): 6348–57. <https://doi.org/10.1093/emboj/cdf645>.
- Catalano, Alfonso, Paola Caprari, Simona Moretti, Monica Faronato, Luca Tamagnone, and Antonio Procopio. 2006. "Semaphorin-3A Is Expressed by Tumor Cells and Alters T-Cell Signal Transduction and Function." *Blood* 107 (8): 3321–29. <https://doi.org/10.1182/blood-2005-06-2445>.
- Catalano, Alfonso, Paola Caprari, Sabrina Rodilossi, Piergiacomo Betta, Mario Castellucci, Andrea Casazza, Luca Tamagnone, and Antonio Procopio. 2004. "Cross-Talk between Vascular Endothelial Growth Factor and Semaphorin-3A Pathway in the Regulation of Normal and Malignant Mesothelial Cell Proliferation." *The FASEB Journal : Official Publication of the Federation of American Societies for Experimental Biology* 18 (2): 358–60. <https://doi.org/10.1096/fj.03-0513fje>.
- Catalano, Alfonso, Raffaella Lazzarini, Silvia Di Nuzzo, Silvia Orciari, and Antonio Procopio. 2009. "The Plexin-A1 Receptor Activates Vascular Endothelial Growth Factor-Receptor 2 and Nuclear Factor- κ B to Mediate Survival and Anchorage-Independent Growth of Malignant Mesothelioma Cells." *Cancer Research* 69 (4): 1485–93. <https://doi.org/10.1158/0008-5472.CAN-08-3659>.
- Cestra, Gianluca, Adam Kwiatkowski, Marco Salazar, Frank Gertler, and Pietro De Camilli. 2005. "Tuba, A GEF for CDC42, Links Dynamin to Actin Regulatory Proteins." *Methods in Enzymology*, 404: 537–45. [https://doi.org/10.1016/S0076-6879\(05\)04047-4](https://doi.org/10.1016/S0076-6879(05)04047-4).
- Chausovsky, Alexander, Alexander D. Bershadsky, and Gary G. Borisy. 2000. "Cadherin-Mediated Regulation of Microtubule Dynamics." *Nature Cell Biology* 2 (11): 797–804. <https://doi.org/10.1038/35041037>.
- Chen, Cuie, Jaclyn M Fingerhut, and Yukiko M Yamashita. 2016. "The Ins(Ide) and Outs(Ide) of Asymmetric Stem Cell Division." *Current Opinion in Cell Biology* 43 (December): 1–6. <https://doi.org/10.1016/j.ceb.2016.06.001>.
- Chen, Fuqiang, Shondra M. Pruett-Miller, Yuping Huang, Monika Gjoka, Katarzyna Duda, Jack Taunton, Trevor N. Collingwood, Morten Frodin, and Gregory D. Davis. 2011. "High-Frequency Genome Editing Using SsDNA Oligonucleotides with Zinc-Finger Nucleases." *Nature Methods* 8 (9): 753–55. <https://doi.org/10.1038/nmeth.1653>.

- Chen, H., A. Chédotal, Z. He, C. S. Goodman, and M. Tessier-Lavigne. 1997. "Neuropilin-2, a Novel Member of the Neuropilin Family, Is a High Affinity Receptor for the Semaphorins Sema E and Sema IV but Not Sema III." *Neuron* 19 (3): 547–59. [https://doi.org/10.1016/s0896-6273\(00\)80371-2](https://doi.org/10.1016/s0896-6273(00)80371-2).
- Chen, Xinyu, and Ian G. Macara. 2005. "Par-3 Controls Tight Junction Assembly through the Rac Exchange Factor Tiam1." *Nature Cell Biology* 7 (3): 262–69. <https://doi.org/10.1038/ncb1226>.
- Chien, Yuan-Hung, Ray Keller, Chris Kintner, and David R. Shook. 2015. "Mechanical Strain Determines the Axis of Planar Polarity in Ciliated Epithelia." *Current Biology* 25 (21): 2774–84. <https://doi.org/10.1016/j.cub.2015.09.015>.
- Chiou, Jian-geng, Mohan K. Balasubramanian, and Daniel J. Lew. 2017. "Cell Polarity in Yeast." *Annual Review of Cell and Developmental Biology* 33 (1): 77–101. <https://doi.org/10.1146/annurev-cellbio-100616-060856>.
- Choi, Young I., Jonathan S. Duke-Cohan, Wei Chen, Baoyu Liu, Jérémie Rossy, Thibault Tabarin, Lining Ju, et al. 2014. "Dynamic Control of B1 Integrin Adhesion by the PlexinD1-Sema3E Axis." *Proceedings of the National Academy of Sciences of the United States of America* 111 (1): 379–84. <https://doi.org/10.1073/pnas.1314209111>.
- Christensen, Søren T., Stine K. Morthorst, Johanne B. Mogensen, and Lotte B. Pedersen. 2017. "Primary Cilia and Coordination of Receptor Tyrosine Kinase (RTK) and Transforming Growth Factor β (TGF- β) Signaling." *Cold Spring Harbor Perspectives in Biology* 9 (6): a028167. <https://doi.org/10.1101/cshperspect.a028167>.
- Chu, Chih-Wen, and Sergei Y. Sokol. 2016. "Wnt Proteins Can Direct Planar Cell Polarity in Vertebrate Ectoderm." *ELife* 5 (September): e16463. <https://doi.org/10.7554/eLife.16463>.
- Clarhaut, Jonathan, Robert M. Gemmill, Vincent A. Potiron, Slimane Ait-Si-Ali, Jean Imbert, Harry A. Drabkin, and Joëlle Roche. 2009. "ZEB-1, a Repressor of the Semaphorin 3F Tumor Suppressor Gene in Lung Cancer Cells." *Neoplasia (New York, N.Y.)* 11 (2): 157–66. <https://doi.org/10.1593/neo.81074>.
- Cohen, David, Patrick J. Brennwald, Enrique Rodriguez-Boulan, and Anne Mûsch. 2004. "Mammalian PAR-1 Determines Epithelial Lumen Polarity by Organizing the Microtubule Cytoskeleton." *The Journal of Cell Biology* 164 (5): 717–27. <https://doi.org/10.1083/jcb.200308104>.
- Conrotto, Paolo, Simona Corso, Sara Gamberini, Paolo Maria Comoglio, and Silvia Giordano. 2004. "Interplay between Scatter Factor Receptors and B Plexins Controls Invasive Growth." *Oncogene* 23 (30): 5131–37. <https://doi.org/10.1038/sj.onc.1207650>.
- Couwenbergs, Claudia, Jean-Claude Labbé, Morgan Goulding, Thomas Marty, Bruce Bowerman, and Monica Gotta. 2007. "Heterotrimeric G Protein Signaling Functions with Dynein to Promote Spindle Positioning in *C. Elegans*." *The Journal of Cell Biology* 179 (1): 15–22. <https://doi.org/10.1083/jcb.200707085>.

- Cuenca, A. A., Aaron Schetter, Donato Aceto, Kenneth Kemphues, and Geraldine Seydoux. 2003. "Polarization of the *C. Elegans* Zygote Proceeds via Distinct Establishment and Maintenance Phases." *Development* 130 (7): 1255–65. <https://doi.org/10.1242/dev.00284>.
- Curtin, John A., Elizabeth Quint, Vicky Tshipouri, Ruth M. Arkeel, Bruce Cattanach, Andrew J. Copp, Deborah J. Henderson, et al. 2003. "Mutation of *Celsr1* Disrupts Planar Polarity of Inner Ear Hair Cells and Causes Severe Neural Tube Defects in the Mouse." *Current Biology : CB* 13 (13): 1129–33. [https://doi.org/10.1016/s0960-9822\(03\)00374-9](https://doi.org/10.1016/s0960-9822(03)00374-9).
- Daulat, Avais M., and Jean-Paul Borg. 2017. "Wnt/Planar Cell Polarity Signaling: New Opportunities for Cancer Treatment." *Trends in Cancer* 3 (2): 113–25. <https://doi.org/10.1016/j.trecan.2017.01.001>.
- Daviaud, Nicolas, Karen Chen, Yong Huang, Roland H. Friedel, and Hongyan Zou. 2016. "Impaired Cortical Neurogenesis in Plexin-B1 and -B2 Double Deletion Mutant." *Developmental Neurobiology* 76 (8): 882–99. <https://doi.org/10.1002/dneu.22364>.
- David, Nicolas B., Charlotte A. Martin, Marion Segalen, François Rosenfeld, François Schweisguth, and Yohanns Bellaïche. 2005. "Drosophila Ric-8 Regulates Gai Cortical Localization to Promote Gai-Dependent Planar Orientation of the Mitotic Spindle during Asymmetric Cell Division." *Nature Cell Biology* 7 (11): 1083–90. <https://doi.org/10.1038/ncb1319>.
- Deborde, Sylvie, Emilie Perret, Diego Gravotta, Ami Deora, Susana Salvarezza, Ryan Schreiner, and Enrique Rodriguez-Boulan. 2008. "Clathrin Is a Key Regulator of Basolateral Polarity." *Nature* 452 (7188): 719–23. <https://doi.org/10.1038/nature06828>.
- Desclozeaux, Marion, Juliana Venturato, Fiona G. Wylie, Jason G. Kay, Shannon R. Joseph, Huong T. Le, and Jennifer L. Stow. 2008. "Active Rab11 and Functional Recycling Endosome Are Required for E-Cadherin Trafficking and Lumen Formation during Epithelial Morphogenesis." *American Journal of Physiology-Cell Physiology* 295 (2): C545–56. <https://doi.org/10.1152/ajpcell.00097.2008>.
- Devenport, Danelle. 2014. "The Cell Biology of Planar Cell Polarity." *The Journal of Cell Biology* 207 (2): 171–79. <https://doi.org/10.1083/jcb.201408039>.
- Dickson, B. J. 2001. "Rho GTPases in Growth Cone Guidance." *Current Opinion in Neurobiology* 11 (1): 103–10. [https://doi.org/10.1016/S0959-4388\(00\)00180-X](https://doi.org/10.1016/S0959-4388(00)00180-X).
- Donovan, Kirk W., and Anthony Bretscher. 2012. "Myosin-V Is Activated by Binding Secretory Cargo and Released in Coordination with Rab/Exocyst Function." *Developmental Cell* 23 (4): 769–81. <https://doi.org/10.1016/j.devcel.2012.09.001>.
- Doyle, D. A., A. Lee, J. Lewis, E. Kim, M. Sheng, and R. MacKinnon. 1996. "Crystal Structures of a Complexed and Peptide-Free Membrane Protein-Binding Domain: Molecular Basis of Peptide Recognition by PDZ." *Cell* 85 (7): 1067–76. [https://doi.org/10.1016/s0092-8674\(00\)81307-0](https://doi.org/10.1016/s0092-8674(00)81307-0).

- Drees, Frauke, Sabine Pokutta, Soichiro Yamada, W. James Nelson, and William I. Weis. 2005. "α-Catenin Is a Molecular Switch That Binds E-Cadherin-β-Catenin and Regulates Actin-Filament Assembly." *Cell* 123 (5): 903–15. <https://doi.org/10.1016/j.cell.2005.09.021>.
- Driessens, M. H., H. Hu, C. D. Nobes, A. Self, I. Jordens, C. S. Goodman, and A. Hall. 2001. "Plexin-B Semaphorin Receptors Interact Directly with Active Rac and Regulate the Actin Cytoskeleton by Activating Rho." *Current Biology : CB* 11 (5): 339–44. <http://www.ncbi.nlm.nih.gov/pubmed/11267870>.
- Du, Quansheng, and Ian G. Macara. 2004. "Mammalian Pins Is a Conformational Switch That Links NuMA to Heterotrimeric G Proteins." *Cell* 119 (4): 503–16. <https://doi.org/10.1016/j.cell.2004.10.028>.
- DuBridge, R. B., P. Tang, H. C. Hsia, P. M. Leong, J. H. Miller, and M. P. Calos. 1987. "Analysis of Mutation in Human Cells by Using an Epstein-Barr Virus Shuttle System." *Molecular and Cellular Biology* 7 (1): 379–87. <http://www.ncbi.nlm.nih.gov/pubmed/3031469>.
- Dukes, Joseph D., Paul Whitley, and Andrew D. Chalmers. 2011. "The MDCK Variety Pack: Choosing the Right Strain." *BMC Cell Biology* 12 (1): 43. <https://doi.org/10.1186/1471-2121-12-43>.
- Elhabazi, Abdellah, Stéphanie Delaire, Armand Bensussan, Laurence Boumsell, and Georges Bismuth. 2001. "Biological Activity of Soluble CD100. I. The Extracellular Region of CD100 Is Released from the Surface of T Lymphocytes by Regulated Proteolysis." *The Journal of Immunology* 166 (7): 4341–47. <https://doi.org/10.4049/jimmunol.166.7.4341>.
- Erickson, Jon W., Chun-jiang Zhang, Richard A. Kahn, Tony Evans, and Richard A. Cerione. 1996. "Mammalian Cdc42 Is a Brefeldin A-Sensitive Component of the Golgi Apparatus." *Journal of Biological Chemistry* 271 (43): 26850–54. <https://doi.org/10.1074/jbc.271.43.26850>.
- Etemad-Moghadam, Bijan, Su Guo, and Kenneth J. Kemphues. 1995. "Asymmetrically Distributed PAR-3 Protein Contributes to Cell Polarity and Spindle Alignment in Early C. Elegans Embryos." *Cell* 83 (5): 743–52. [https://doi.org/10.1016/0092-8674\(95\)90187-6](https://doi.org/10.1016/0092-8674(95)90187-6).
- Fazzari, Pietro, Junia Penachioni, Sara Gianola, Ferdinando Rossi, Britta J. Eickholt, Flavio Maina, Lena Alexopoulou, et al. 2007. "Plexin-B1 Plays a Redundant Role during Mouse Development and in Tumour Angiogenesis." *BMC Developmental Biology* 7 (May): 55. <https://doi.org/10.1186/1471-213X-7-55>.
- Fedeles, Sorin, and Anna Rachel Gallagher. 2013. "Cell Polarity and Cystic Kidney Disease." *Pediatric Nephrology* 28: 1161–72. <https://doi.org/10.1007/s00467-012-2337-z>.
- Feiguin, F., M. Hannus, M. Mlodzik, and S. Eaton. 2001. "The Ankyrin Repeat Protein Diego Mediates Frizzled-Dependent Planar Polarization." *Developmental Cell* 1 (1): 93–101. <http://www.ncbi.nlm.nih.gov/pubmed/11703927>.

- Feng, Wei, Hao Wu, Ling-Nga Chan, and Mingjie Zhang. 2008. "Par-3-Mediated Junctional Localization of the Lipid Phosphatase PTEN Is Required for Cell Polarity Establishment." *Journal of Biological Chemistry* 283 (34): 23440–49. <https://doi.org/10.1074/jbc.M802482200>.
- Fischer, Evelyne, Emilie Legue, Antonia Doyen, Faridabano Nato, Jean-François Nicolas, Vicente Torres, Moshe Yaniv, and Marco Pontoglio. 2006. "Defective Planar Cell Polarity in Polycystic Kidney Disease." *Nature Genetics* 38 (1): 21–23. <https://doi.org/10.1038/ng1701>.
- Franco, Maribel, and Ana Carmena. 2019. "Eph Signaling Controls Mitotic Spindle Orientation and Cell Proliferation in Neuroepithelial Cells." *Journal of Cell Biology* 218 (4): 1200–1217. <https://doi.org/10.1083/jcb.201807157>.
- Fujiwara, Hiroshi, Shinya Yoshioka, Keiji Tatsumi, Kenzo Kosaka, Yukiyasu Satoh, Yoshihiro Nishioka, Miho Egawa, Toshihiro Higuchi, and Shingo Fujii. 2002. "Human Endometrial Epithelial Cells Express Ephrin A1: Possible Interaction between Human Blastocysts and Endometrium via Eph-Ephrin System." *The Journal of Clinical Endocrinology & Metabolism* 87 (12): 5801–7. <https://doi.org/10.1210/jc.2002-020508>.
- Gallo, C. M., J. T. Wang, F. Motegi, and G. Seydoux. 2010. "Cytoplasmic Partitioning of P Granule Components Is Not Required to Specify the Germline in *C. Elegans*." *Science* 330 (6011): 1685–89. <https://doi.org/10.1126/science.1193697>.
- Garcia-Areas, R., S. Libreros, M. Simoes, C. Castro-Silva, N. Gazaniga, S. Amat, J. Jaczewska, et al. 2017. "Suppression of Tumor-Derived Semaphorin 7A and Genetic Ablation of Host-Derived Semaphorin 7A Impairs Tumor Progression in a Murine Model of Advanced Breast Carcinoma." *International Journal of Oncology* 51 (5): 1395–1404. <https://doi.org/10.3892/ijo.2017.4144>.
- Garneau, Josiane E., Marie-Ève Dupuis, Manuela Villion, Dennis A. Romero, Rodolphe Barrangou, Patrick Boyaval, Christophe Fremaux, Philippe Horvath, Alfonso H. Magadán, and Sylvain Moineau. 2010. "The CRISPR/Cas Bacterial Immune System Cleaves Bacteriophage and Plasmid DNA." *Nature* 468 (7320): 67–71. <https://doi.org/10.1038/nature09523>.
- Genevet, Alice, and Nicolas Tapon. 2011. "The Hippo Pathway and Apico–Basal Cell Polarity." *Biochemical Journal* 436 (2): 213–24. <https://doi.org/10.1042/BJ20110217>.
- Gho, M., Y. Bellaïche, and F. Schweisguth. 1999. "Revisiting the *Drosophila* Microchaete Lineage: A Novel Intrinsically Asymmetric Cell Division Generates a Glial Cell." *Development (Cambridge, England)* 126 (16): 3573–84. <http://www.ncbi.nlm.nih.gov/pubmed/10409503>.
- Gilbert, T., A. Le Bivic, A. Quaroni, and E. Rodriguez-Boulan. 1991. "Microtubular Organization and Its Involvement in the Biogenetic Pathways of Plasma Membrane Proteins in Caco-2 Intestinal Epithelial Cells." *The Journal of Cell Biology* 113 (2): 275–88. <https://doi.org/10.1083/jcb.113.2.275>.
- Giles, Rachel H., Henry Ajzenberg, and Peter K. Jackson. 2014. "3D Spheroid Model of

- MIMCD3 Cells for Studying Ciliopathies and Renal Epithelial Disorders." *Nature Protocols* 9 (12): 2725–31. <https://doi.org/10.1038/nprot.2014.181>.
- Gillies, Taryn E., and Clemens Cabernard. 2011. "Cell Division Orientation in Animals." *Current Biology* 21 (15): R599–609. <https://doi.org/10.1016/j.cub.2011.06.055>.
- Giordano, Silvia, Simona Corso, Paolo Conrotto, Stefania Artigiani, Giorgio Gilestro, Davide Barberis, Luca Tamagnone, and Paolo M. Comoglio. 2002. "The Semaphorin 4D Receptor Controls Invasive Growth by Coupling with Met." *Nature Cell Biology* 4 (9): 720–24. <https://doi.org/10.1038/ncb843>.
- Gloerich, Martijn, Julie M. Bianchini, Kathleen A. Siemers, Daniel J. Cohen, and W. James Nelson. 2017. "Cell Division Orientation Is Coupled to Cell–Cell Adhesion by the E-Cadherin/LGN Complex." *Nature Communications* 8 (January): 13996. <https://doi.org/10.1038/ncomms13996>.
- Gloerich, Martijn, and Johannes L. Bos. 2011. "Regulating Rap Small G-Proteins in Time and Space." *Trends in Cell Biology* 21 (10): 615–23. <https://doi.org/10.1016/j.tcb.2011.07.001>.
- Goetz, Sarah C., and Kathryn V. Anderson. 2010. "The Primary Cilium: A Signalling Centre during Vertebrate Development." *Nature Reviews Genetics* 11 (5): 331–44. <https://doi.org/10.1038/nrg2774>.
- Gong, Ying, Chunhui Mo, and Scott E. Fraser. 2004. "Planar Cell Polarity Signalling Controls Cell Division Orientation during Zebrafish Gastrulation." *Nature* 430 (7000): 689–93. <https://doi.org/10.1038/nature02796>.
- Gonzalez, Alfonso, and Enrique Rodriguez-Boulan. 2009. "Clathrin and AP1B: Key Roles in Basolateral Trafficking through Trans-Endosomal Routes." *FEBS Letters* 583 (23): 3784–95. <https://doi.org/10.1016/j.febslet.2009.10.050>.
- Grill, S. W., Jonathon Howard, Erik Schäffer, Ernst H K Stelzer, and Anthony A Hyman. 2003. "The Distribution of Active Force Generators Controls Mitotic Spindle Position." *Science* 301 (5632): 518–21. <https://doi.org/10.1126/science.1086560>.
- Grill, Stephan W., Pierre Gönczy, Ernst H. K. Stelzer, and Anthony A. Hyman. 2001. "Polarity Controls Forces Governing Asymmetric Spindle Positioning in the *Caenorhabditis Elegans* Embryo." *Nature* 409 (6820): 630–33. <https://doi.org/10.1038/35054572>.
- Grinberg-Bleyer, Yenkel, Rachel Caron, John J. Seeley, Nilushi S. De Silva, Christian W. Schindler, Matthew S. Hayden, Ulf Klein, and Sankar Ghosh. 2018. "The Alternative NF- κ B Pathway in Regulatory T Cell Homeostasis and Suppressive Function." *Journal of Immunology (Baltimore, Md. : 1950)* 200 (7): 2362–71. <https://doi.org/10.4049/jimmunol.1800042>.
- Grindstaff, K. K., C. Yeaman, N. Anandasabapathy, S. C. Hsu, E. Rodriguez-Boulan, R. H. Scheller, and W. J. Nelson. 1998. "Sec6/8 Complex Is Recruited to Cell-Cell Contacts and Specifies Transport Vesicle Delivery to the Basal-Lateral Membrane in Epithelial Cells." *Cell* 93 (5): 731–40. [https://doi.org/10.1016/s0092-8674\(00\)81435-x](https://doi.org/10.1016/s0092-8674(00)81435-x).

- Gu, Chenghua, and Enrico Giraud. 2013. "The Role of Semaphorins and Their Receptors in Vascular Development and Cancer." *Experimental Cell Research* 319 (9): 1306–16. <https://doi.org/10.1016/j.yexcr.2013.02.003>.
- Gu, Chenghua, Yutaka Yoshida, Jean Livet, Dorothy V. Reimert, Fanny Mann, Janna Merte, Christopher E. Henderson, Thomas M. Jessell, Alex L. Kolodkin, and David D. Ginty. 2005. "Semaphorin 3E and Plexin-D1 Control Vascular Pattern Independently of Neuropilins." *Science* 307 (5707): 265–68. <https://doi.org/10.1126/science.1105416>.
- Gubb, D., and A. García-Bellido. 1982. "A Genetic Analysis of the Determination of Cuticular Polarity during Development in *Drosophila Melanogaster*." *Journal of Embryology and Experimental Morphology* 68 (April): 37–57. <http://www.ncbi.nlm.nih.gov/pubmed/6809878>.
- Guirao, Boris, Alice Meunier, Stéphane Mortaud, Andrea Aguilar, Jean-Marc Corsi, Laetitia Strehl, Yuki Hirota, et al. 2010. "Coupling between Hydrodynamic Forces and Planar Cell Polarity Orients Mammalian Motile Cilia." *Nature Cell Biology* 12 (4): 341–50. <https://doi.org/10.1038/ncb2040>.
- Guo, N., C. Hawkins, and J. Nathans. 2004. "From The Cover: Frizzled6 Controls Hair Patterning in Mice." *Proceedings of the National Academy of Sciences* 101 (25): 9277–81. <https://doi.org/10.1073/pnas.0402802101>.
- Guo, Su, and Kenneth J. Kemphues. 1995. "Par-1, a Gene Required for Establishing Polarity in *C. Elegans* Embryos, Encodes a Putative Ser/Thr Kinase That Is Asymmetrically Distributed." *Cell* 81 (4): 611–20. [https://doi.org/10.1016/0092-8674\(95\)90082-9](https://doi.org/10.1016/0092-8674(95)90082-9).
- Gurrapu, Sreeharsha, Emanuela Pupo, Giulia Franzolin, Letizia Lanzetti, and Luca Tamagnone. 2018. "Sema4C/PlexinB2 Signaling Controls Breast Cancer Cell Growth, Hormonal Dependence and Tumorigenic Potential." *Cell Death and Differentiation* 25 (7): 1259–75. <https://doi.org/10.1038/s41418-018-0097-4>.
- Gurrapu, Sreeharsha, and Luca Tamagnone. 2016. "Transmembrane Semaphorins: Multimodal Signaling Cues in Development and Cancer." *Cell Adhesion and Migration* 10 (6): 675–91. <https://doi.org/10.1080/19336918.2016.1197479>.
- . 2019. "Semaphorins as Regulators of Phenotypic Plasticity and Functional Reprogramming of Cancer Cells." *Trends in Molecular Medicine* 25 (4): 303–14. <https://doi.org/10.1016/j.molmed.2019.01.010>.
- Haklai-Topper, Liat, Guy Mlechkovich, Dana Savariego, Irena Gokhman, and Avraham Yaron. 2010. "Cis Interaction between Semaphorin6A and Plexin-A4 Modulates the Repulsive Response to Sema6A." *EMBO Journal* 29 (15): 2635–45. <https://doi.org/10.1038/emboj.2010.147>.
- Hall, H. G., D. A. Farson, and M. J. Bissell. 1982. "Lumen Formation by Epithelial Cell Lines in Response to Collagen Overlay: A Morphogenetic Model in Culture." *Proceedings of the National Academy of Sciences of the United States of America* 79 (15): 4672–76. <http://www.ncbi.nlm.nih.gov/pubmed/6956885>.

- Hansson, G. C., K. Simons, and G. van Meer. 1986. "Two Strains of the Madin-Darby Canine Kidney (MDCK) Cell Line Have Distinct Glycosphingolipid Compositions." *The EMBO Journal* 5 (3): 483–89. <http://www.ncbi.nlm.nih.gov/pubmed/3519211>.
- Hao, Yi, Quansheng Du, Xinyu Chen, Zhen Zheng, Jeremy L. Balsbaugh, Sushmit Maitra, Jeffrey Shabanowitz, Donald F. Hunt, and Ian G. Macara. 2010. "Par3 Controls Epithelial Spindle Orientation by APC-Mediated Phosphorylation of Apical Pins." *Current Biology* 20 (20): 1809–18. <https://doi.org/10.1016/j.cub.2010.09.032>.
- Harris, Tony J.C., and Mark Peifer. 2005. "The Positioning and Segregation of Apical Cues during Epithelial Polarity Establishment in *Drosophila*." *The Journal of Cell Biology* 170 (5): 813–23. <https://doi.org/10.1083/jcb.200505127>.
- Hayashi, Mikihito, Tomoki Nakashima, Masahiko Taniguchi, Tatsuhiko Kodama, Atsushi Kumanogoh, and Hiroshi Takayanagi. 2012. "Osteoprotection by Semaphorin 3A." *Nature* 485 (7396): 69–74. <https://doi.org/10.1038/nature11000>.
- He, Huawei, Taehong Yang, Jonathan R. Terman, and Xuewu Zhang. 2009. "Crystal Structure of the Plexin A3 Intracellular Region Reveals an Autoinhibited Conformation through Active Site Sequestration." *Proceedings of the National Academy of Sciences of the United States of America* 106 (37): 15610–15. <https://doi.org/10.1073/pnas.0906923106>.
- He, Z., and M. Tessier-Lavigne. 1997. "Neuropilin Is a Receptor for the Axonal Chemorepellent Semaphorin III." *Cell* 90 (4): 739–51. [https://doi.org/10.1016/S0092-8674\(00\)80534-6](https://doi.org/10.1016/S0092-8674(00)80534-6).
- Hediger, Matthias A., Michael F. Romero, Ji-Bin Peng, Andreas Rolfs, Hitomi Takanaga, and Elspeth A. Bruford. 2004. "The ABCs of Solute Carriers: Physiological, Pathological and Therapeutic Implications of Human Membrane Transport Proteins." *Pflügers Archiv: European Journal of Physiology* 447 (5): 465–68. <https://doi.org/10.1007/s00424-003-1192-y>.
- Herman, Jeffery G., and Gary G. Meadows. 2007. "Increased Class 3 Semaphorin Expression Modulates the Invasive and Adhesive Properties of Prostate Cancer Cells." *International Journal of Oncology* 30 (5): 1231–38. <https://doi.org/10.3892/ijo.30.5.1231>.
- Hilario, Jona D., Louise R. Rodino-Klapac, Chunping Wang, and Christine E. Beattie. 2009. "Semaphorin 5A Is a Bifunctional Axon Guidance Cue for Axial Motoneurons in Vivo." *Developmental Biology* 326 (1): 190–200. <https://doi.org/10.1016/j.ydbio.2008.11.007>.
- Hirate, Yoshikazu, Shino Hirahara, Ken-ichi Inoue, Atsushi Suzuki, Vernadeth B. Alarcon, Kazunori Akimoto, Takaaki Hirai, et al. 2013. "Polarity-Dependent Distribution of Angiomotin Localizes Hippo Signaling in Preimplantation Embryos." *Current Biology* 23 (13): 1181–94. <https://doi.org/10.1016/j.cub.2013.05.014>.
- Hirokawa, N., T. C. Keller, R. Chasan, and M. S. Mooseker. 1983. "Mechanism of Brush Border Contractility Studied by the Quick-Freeze, Deep-Etch Method." *The Journal of Cell Biology* 96 (5): 1325–36. <https://doi.org/10.1083/jcb.96.5.1325>.

- Hirschberg, A., S. Deng, A. Korostylev, E. Paldy, M. R. Costa, T. Worzfeld, P. Vodrazka, et al. 2010. "Gene Deletion Mutants Reveal a Role for Semaphorin Receptors of the Plexin-B Family in Mechanisms Underlying Corticogenesis." *Molecular and Cellular Biology* 30 (3): 764–80. <https://doi.org/10.1128/MCB.01458-09>.
- Hodge, Richard G., and Anne J. Ridley. 2016. "Regulating Rho GTPases and Their Regulators." *Nature Reviews Molecular Cell Biology* 17 (8): 496–510. <https://doi.org/10.1038/nrm.2016.67>.
- Holmes, S., A.-M. Downs, A. Fosberry, P. D. Hayes, D. Michalovich, P. Murdoch, K. Moores, et al. 2002. "Sema7A Is a Potent Monocyte Stimulator." *Scandinavian Journal of Immunology* 56 (3): 270–75. <https://doi.org/10.1046/j.1365-3083.2002.01129.x>.
- Horvath, Philippe, and Rodolphe Barrangou. 2010. "CRISPR/Cas, the Immune System of Bacteria and Archaea." *Science* 327 (5962): 167–70. <https://doi.org/10.1126/science.1179555>.
- Hu, H., T. F. Marton, and C. S. Goodman. 2001. "Plexin B Mediates Axon Guidance in Drosophila by Simultaneously Inhibiting Active Rac and Enhancing RhoA Signaling." *Neuron* 32 (1): 39–51. <http://www.ncbi.nlm.nih.gov/pubmed/11604137>.
- Hueschen, Christina L., Samuel J. Kenny, Ke Xu, and Sophie Dumont. 2017. "NuMA Recruits Dynein Activity to Microtubule Minus-Ends at Mitosis." *ELife* 6 (November): e29328. <https://doi.org/10.7554/eLife.29328>.
- Hung, T. J., and K. J. Kemphues. 1999. "PAR-6 Is a Conserved PDZ Domain-Containing Protein That Colocalizes with PAR-3 in Caenorhabditis Elegans Embryos." *Development (Cambridge, England)* 126 (1): 127–35. <http://www.ncbi.nlm.nih.gov/pubmed/9834192>.
- Hurd, Toby W., Lin Gao, Michael H. Roh, Ian G. Macara, and Ben Margolis. 2003. "Direct Interaction of Two Polarity Complexes Implicated in Epithelial Tight Junction Assembly." *Nature Cell Biology* 5 (2): 137–42. <https://doi.org/10.1038/ncb923>.
- Hurov, Jonathan B., Janis L. Watkins, and Helen Piwnicka-Worms. 2004. "Atypical PKC Phosphorylates PAR-1 Kinases to Regulate Localization and Activity." *Current Biology* 14 (8): 736–41. <https://doi.org/10.1016/j.cub.2004.04.007>.
- Hutagalung, Alex H., and Peter J. Novick. 2011. "Role of Rab GTPases in Membrane Traffic and Cell Physiology." *Physiological Reviews* 91 (1): 119–49. <https://doi.org/10.1152/physrev.00059.2009>.
- Hutterer, Andrea, Joerg Betschinger, Mark Petronczki, and Juergen A. Knoblich. 2004. "Sequential Roles of Cdc42, Par-6, APKC, and Lgl in the Establishment of Epithelial Polarity during Drosophila Embryogenesis." *Developmental Cell* 6 (6): 845–54. <https://doi.org/10.1016/j.devcel.2004.05.003>.
- Iden, Sandra, and John G. Collard. 2008. "Crosstalk between Small GTPases and Polarity Proteins in Cell Polarization." *Nature Reviews Molecular Cell Biology* 9

- (11): 846–59. <https://doi.org/10.1038/nrm2521>.
- Izumi, Yasushi, Nao Ohta, Kanako Hisata, Thomas Raabe, and Fumio Matsuzaki. 2006. “Drosophila Pins-Binding Protein Mud Regulates Spindle-Polarity Coupling and Centrosome Organization.” *Nature Cell Biology* 8 (6): 586–93. <https://doi.org/10.1038/ncb1409>.
- Jaffe, Aron B., Noriko Kaji, Joanne Durgan, and Alan Hall. 2008. “Cdc42 Controls Spindle Orientation to Position the Apical Surface during Epithelial Morphogenesis.” *Journal of Cell Biology* 183 (4): 625–33. <https://doi.org/10.1083/jcb.200807121>.
- Janssen, Bert J. C., Ross A. Robinson, Francesc Pérez-Brangulí, Christian H. Bell, Kevin J. Mitchell, Christian Siebold, and E. Yvonne Jones. 2010. “Structural Basis of Semaphorin–Plexin Signalling.” *Nature* 467 (7319): 1118–22. <https://doi.org/10.1038/nature09468>.
- Jaulin, Fanny, and Geri Kreitzer. 2010. “KIF17 Stabilizes Microtubules and Contributes to Epithelial Morphogenesis by Acting at MT plus Ends with EB1 and APC.” *The Journal of Cell Biology* 190 (3): 443–60. <https://doi.org/10.1083/jcb.201006044>.
- Jaulin, Fanny, Xiaoxiao Xue, Enrique Rodriguez-Boulan, and Geri Kreitzer. 2007. “Polarization-Dependent Selective Transport to the Apical Membrane by KIF5B in MDCK Cells.” *Developmental Cell* 13 (4): 511–22. <https://doi.org/10.1016/j.devcel.2007.08.001>.
- Jessen, Jason R., Jacek Topczewski, Stephanie Bingham, Diane S. Sepich, Florence Marlow, Anand Chandrasekhar, and Lilianna Solnica-Krezel. 2002. “Zebrafish Trilobite Identifies New Roles for Strabismus in Gastrulation and Neuronal Movements.” *Nature Cell Biology* 4 (8): 610–15. <https://doi.org/10.1038/ncb828>.
- Johnson, Jayme M., Meng Jin, and Daniel J. Lew. 2011. “Symmetry Breaking and the Establishment of Cell Polarity in Budding Yeast.” *Current Opinion in Genetics & Development* 21 (6): 740–46. <https://doi.org/10.1016/j.gde.2011.09.007>.
- Johnson, Martin H. 2009. “From Mouse Egg to Mouse Embryo: Polarities, Axes, and Tissues.” *Annual Review of Cell and Developmental Biology* 25 (1): 483–512. <https://doi.org/10.1146/annurev.cellbio.042308.113348>.
- Johnston, Christopher A., Keiko Hirono, Kenneth E. Prehoda, and Chris Q. Doe. 2009. “Identification of an Aurora-A/PinsLINKER/ Dlg Spindle Orientation Pathway Using Induced Cell Polarity in S2 Cells.” *Cell* 138 (6): 1150–63. <https://doi.org/10.1016/j.cell.2009.07.041>.
- Jongbloets, B. C., and R. J. Pasterkamp. 2014. “Semaphorin Signalling during Development.” *Development* 141 (17): 3292–97. <https://doi.org/10.1242/dev.105544>.
- Kagoshima, Masako, Takaaki Ito, Hitoshi Kitamura, and Yoshio Goshima. 2001. “Diverse Gene Expression and Function of Semaphorins in Developing Lung: Positive and Negative Regulatory Roles of Semaphorins in Lung Branching Morphogenesis.” *Genes to Cells* 6 (6): 559–71. <https://doi.org/10.1046/j.1365-2443.2001.00441.x>.
- Kaltschmidt, Julia A., Catherine M. Davidson, Nicholas H. Brown, and Andrea H. Brand.

2000. "Rotation and Asymmetry of the Mitotic Spindle Direct Asymmetric Cell Division in the Developing Central Nervous System." *Nature Cell Biology* 2 (1): 7–12. <https://doi.org/10.1038/71323>.
- Kang, Sujin, and Atsushi Kumanogoh. 2013. "Semaphorins in Bone Development, Homeostasis, and Disease." *Seminars in Cell & Developmental Biology* 24 (3): 163–71. <https://doi.org/10.1016/j.semcdb.2012.09.008>.
- Kantor, David B., Onanong Chivatakarn, Katherine L. Peer, Stephen F. Oster, Masaru Inatani, Michael J. Hansen, John G. Flanagan, et al. 2004. "Semaphorin 5A Is a Bifunctional Axon Guidance Cue Regulated by Heparan and Chondroitin Sulfate Proteoglycans." *Neuron* 44 (6): 961–75. <https://doi.org/10.1016/j.neuron.2004.12.002>.
- Kemphues, K. J., J. R. Priess, D. G. Morton, and N. S. Cheng. 1988. "Identification of Genes Required for Cytoplasmic Localization in Early C. Elegans Embryos." *Cell* 52 (3): 311–20. [https://doi.org/10.1016/s0092-8674\(88\)80024-2](https://doi.org/10.1016/s0092-8674(88)80024-2).
- Kessler, Ofra, Niva Shraga-Heled, Tali Lange, Noga Gutmann-Raviv, Edmond Sabo, Limor Baruch, Marcelle Machluf, and Gera Neufeld. 2004. "Semaphorin-3F Is an Inhibitor of Tumor Angiogenesis." *Cancer Research* 64 (3): 1008–15. <https://doi.org/10.1158/0008-5472.can-03-3090>.
- Kibar, Zoha, Elena Torban, Jonathan R. McDearmid, Annie Reynolds, Joanne Berghout, Melissa Mathieu, Irena Kirillova, et al. 2007. "Mutations in *VANGL1* Associated with Neural-Tube Defects." *New England Journal of Medicine* 356 (14): 1432–37. <https://doi.org/10.1056/NEJMoa060651>.
- Kibar, Zoha, Kyle J. Vogan, Normand Groulx, Monica J. Justice, D. Alan Underhill, and Philippe Gros. 2001. "Ltap, a Mammalian Homolog of Drosophila Strabismus/Van Gogh, Is Altered in the Mouse Neural Tube Mutant Loop-Tail." *Nature Genetics* 28 (3): 251–55. <https://doi.org/10.1038/90081>.
- Kim, Jiha, Won-Jong Oh, Nicholas Gaiano, Yutaka Yoshida, and Chenghua Gu. 2011. "Semaphorin 3E-Plexin-D1 Signaling Regulates VEGF Function in Developmental Angiogenesis via a Feedback Mechanism." *Genes & Development* 25 (13): 1399–1411. <https://doi.org/10.1101/gad.2042011>.
- Klein, Thomas J., and Marek Mlodzik. 2005. "PLANAR CELL POLARIZATION: An Emerging Model Points in the Right Direction." *Annual Review of Cell and Developmental Biology* 21 (1): 155–76. <https://doi.org/10.1146/annurev.cellbio.21.012704.132806>.
- Knoblich, Juergen A. 2001. "Asymmetric Cell Division during Animal Development." *Nature Reviews Molecular Cell Biology* 2 (1): 11–20. <https://doi.org/10.1038/35048085>.
- Ko, Ji-Ae, Yasumiko Akamatsu, Ryoji Yanai, and Teruo Nishida. 2010. "Effects of Semaphorin 3A Overexpression in Corneal Fibroblasts on the Expression of Adherens-Junction Proteins in Corneal Epithelial Cells." *Biochemical and Biophysical Research Communications* 396 (4): 781–86. <https://doi.org/10.1016/j.bbrc.2010.04.029>.

- Kolodkin, A. L., D. V. Levensgood, E. G. Rowe, Y. T. Tai, R. J. Giger, and D. D. Ginty. 1997. "Neuropilin Is a Semaphorin III Receptor." *Cell* 90 (4): 753–62. [https://doi.org/10.1016/s0092-8674\(00\)80535-8](https://doi.org/10.1016/s0092-8674(00)80535-8).
- Kolodkin, A. L., D. J. Matthes, and C. S. Goodman. 1993. "The Semaphorin Genes Encode a Family of Transmembrane and Secreted Growth Cone Guidance Molecules." *Cell* 75 (7): 1389–99. [https://doi.org/10.1016/0092-8674\(93\)90625-z](https://doi.org/10.1016/0092-8674(93)90625-z).
- Koropouli, Eleftheria, and Alex L. Kolodkin. 2014. "Semaphorins and the Dynamic Regulation of Synapse Assembly, Refinement, and Function." *Current Opinion in Neurobiology* 27 (August): 1–7. <https://doi.org/10.1016/j.conb.2014.02.005>.
- Korostylev, Alexander, Thomas Worzfeld, Suhua Deng, Roland H. Friedel, Jakub M. Swiercz, Peter Vodrazka, Viola Maier, et al. 2008. "A Functional Role for Semaphorin 4D/Plexin B1 Interaction in Epithelial Branching Morphogenesis during Organogenesis." *Development* 135 (20): 3333–43. <https://doi.org/10.1242/dev.019760>.
- Kotak, Sachin, Coralie Busso, and Pierre Gönczy. 2014. "NuMA Interacts with Phosphoinositides and Links the Mitotic Spindle with the Plasma Membrane." *The EMBO Journal* 33 (16): 1815–30. <https://doi.org/10.15252/embj.201488147>.
- Kotak, Sachin, and Pierre Gönczy. 2013. "Mechanisms of Spindle Positioning: Cortical Force Generators in the Limelight." *Current Opinion in Cell Biology* 25 (6): 741–48. <https://doi.org/10.1016/j.ceb.2013.07.008>.
- Kozubowski, Lukasz, Koji Saito, Jayme M. Johnson, Audrey S. Howell, Trevin R. Zyla, and Daniel J. Lew. 2008. "Symmetry-Breaking Polarization Driven by a Cdc42p GEF-PAK Complex." *Current Biology* 18 (22): 1719–26. <https://doi.org/10.1016/j.cub.2008.09.060>.
- Kroschewski, Ruth, Alan Hall, and Ira Mellman. 1999. "Cdc42 Controls Secretory and Endocytic Transport to the Basolateral Plasma Membrane of MDCK Cells." *Nature Cell Biology* 1 (1): 8–13. <https://doi.org/10.1038/8977>.
- Krueger, Lori E., Jui-Ching Wu, Meng-Fu Bryan Tsou, and Lesilee S. Rose. 2010. "LET-99 Inhibits Lateral Posterior Pulling Forces during Asymmetric Spindle Elongation in *C. Elegans* Embryos." *The Journal of Cell Biology* 189 (3): 481–95. <https://doi.org/10.1083/jcb.201001115>.
- Kumanogoh, Atsushi, and Hitoshi Kikutani. 2013. "Immunological Functions of the Neuropilins and Plexins as Receptors for Semaphorins." *Nature Reviews. Immunology* 13 (11): 802–14. <http://www.ncbi.nlm.nih.gov/pubmed/24319778>.
- Laprise, Patrick, Kimberly M. Lau, Kathryn P. Harris, Nancy F. Silva-Gagliardi, Sarah M. Paul, Slobodan Beronja, Greg J. Beitel, C. Jane McGlade, and Ulrich Tepass. 2009. "Yurt, Coracle, Neurexin IV and the Na⁺,K⁺-ATPase Form a Novel Group of Epithelial Polarity Proteins." *Nature* 459 (7250): 1141–45. <https://doi.org/10.1038/nature08067>.
- Lawrence, P. A., and P. M. Shelton. 1975. "The Determination of Polarity in the Developing Insect Retina." *Journal of Embryology and Experimental Morphology*

- 33 (2): 471–86. <http://www.ncbi.nlm.nih.gov/pubmed/1176856>.
- Lawrence, Peter A., Gary Struhl, and José Casal. 2007. “Planar Cell Polarity: One or Two Pathways?” *Nature Reviews Genetics* 8 (7): 555–63. <https://doi.org/10.1038/nrg2125>.
- Lawson, Campbell D., and Anne J. Ridley. 2018. “Rho GTPase Signaling Complexes in Cell Migration and Invasion.” *The Journal of Cell Biology* 217 (2): 447–57. <https://doi.org/10.1083/jcb.201612069>.
- Lázaro-Diéguez, Francisco, David Cohen, Dawn Fernandez, Louis Hodgson, Sven C.D. van IJzendoorn, and Anne Müsch. 2013. “Par1b Links Lumen Polarity with LGN–NuMA Positioning for Distinct Epithelial Cell Division Phenotypes.” *The Journal of Cell Biology* 203 (2): 251–64. <https://doi.org/10.1083/jcb.201303013>.
- Le, Trung N., Guoyan Du, Mario Fonseca, Qing-Ping Zhou, Jeffrey T. Wigle, and David D. Eisenstat. 2007. “Dlx Homeobox Genes Promote Cortical Interneuron Migration from the Basal Forebrain by Direct Repression of the Semaphorin Receptor Neuropilin-2.” *The Journal of Biological Chemistry* 282 (26): 19071–81. <https://doi.org/10.1074/jbc.M607486200>.
- Lechler, Terry, and Elaine Fuchs. 2005. “Asymmetric Cell Divisions Promote Stratification and Differentiation of Mammalian Skin.” *Nature* 437 (7056): 275–80. <https://doi.org/10.1038/nature03922>.
- Lee, Cheng-Yu, Brian D. Wilkinson, Sarah E. Siegrist, Robin P. Wharton, and Chris Q. Doe. 2006. “Brat Is a Miranda Cargo Protein That Promotes Neuronal Differentiation and Inhibits Neuroblast Self-Renewal.” *Developmental Cell* 10 (4): 441–49. <https://doi.org/10.1016/j.devcel.2006.01.017>.
- Leibfried, Andrea, Robert Fricke, Matthew J. Morgan, Sven Bogdan, and Yohanns Bellaiche. 2008. “Drosophila Cip4 and WASp Define a Branch of the Cdc42-Par6-APKC Pathway Regulating E-Cadherin Endocytosis.” *Current Biology* 18 (21): 1639–48. <https://doi.org/10.1016/j.cub.2008.09.063>.
- Li, Zhouhua, Liwei Wang, Thomas S. Hays, and Yu Cai. 2008. “Dynein-Mediated Apical Localization of Crumbs Transcripts Is Required for Crumbs Activity in Epithelial Polarity.” *The Journal of Cell Biology* 180 (1): 31–38. <https://doi.org/10.1083/jcb.200707007>.
- Lim, J., and J. P. Thiery. 2012. “Epithelial-Mesenchymal Transitions: Insights from Development.” *Development* 139 (19): 3471–86. <https://doi.org/10.1242/dev.071209>.
- Lisanti, M. P., I. W. Caras, M. A. Davitz, and E. Rodriguez-Boulán. 1989. “A Glycophospholipid Membrane Anchor Acts as an Apical Targeting Signal in Polarized Epithelial Cells.” *The Journal of Cell Biology* 109 (5): 2145–56. <https://doi.org/10.1083/jcb.109.5.2145>.
- Liu, T. J., J. L. Guo, H. K. Wang, and X. Xu. 2018. “Semaphorin-7A Contributes to Growth, Migration and Invasion of Oral Tongue Squamous Cell Carcinoma through TGF- β -Mediated EMT Signaling Pathway.” *European Review for Medical and*

- Pharmacological Sciences* 22 (4): 1035–43.
https://doi.org/10.26355/eurev_201802_14386.
- Lo, Priscilla, Hannah Hawrot, and Marios Georgiou. 2012. “Apicobasal Polarity and Its Role in Cancer Progression.” *BioMolecular Concepts* 3 (6): 505–21.
<https://doi.org/10.1515/bmc-2012-0020>.
- Lock, John G., and Jennifer L. Stow. 2005. “Rab11 in Recycling Endosomes Regulates the Sorting and Basolateral Transport of E-Cadherin.” *Molecular Biology of the Cell* 16 (4): 1744–55. <https://doi.org/10.1091/mbc.e04-10-0867>.
- Lodish, Harvey, Arnold Berk, S. Lawrence Zipursky, Paul Matsudaira, David Baltimore, and James Darnell. 2000. “Overview of Neuron Structure and Function.” *Molecular Cell Biology. 4th Edition*: 912–6.
<https://www.ncbi.nlm.nih.gov/books/NBK21535/>.
- Lu, B., M. Rothenberg, L. Y. Jan, and Y. N. Jan. 1998. “Partner of Numb Colocalizes with Numb during Mitosis and Directs Numb Asymmetric Localization in Drosophila Neural and Muscle Progenitors.” *Cell* 95 (2): 225–35.
[https://doi.org/10.1016/s0092-8674\(00\)81753-5](https://doi.org/10.1016/s0092-8674(00)81753-5).
- Lu, Tzu Pin, Mong Hsun Tsai, Jang Ming Lee, Chung Ping Hsu, Pei Chun Chen, Chung Wu Lin, Jin Yuan Shih, et al. 2010. “Identification of a Novel Biomarker, SEMA5A, for Non-Small Cell Lung Carcinoma in Nonsmoking Women.” *Cancer Epidemiology Biomarkers and Prevention* 19 (10): 2590–97.
<https://doi.org/10.1158/1055-9965.EPI-10-0332>.
- Luque, Maria Carolina A., Paulo S. Gutierrez, Victor Debbas, Jorge Kalil, and Beatriz S. Stolf. 2015. “CD100 and Plexins B2 and B1 Mediate Monocyte-Endothelial Cell Adhesion and Might Take Part in Atherogenesis.” *Molecular Immunology* 67 (2): 559–67. <https://doi.org/10.1016/j.molimm.2015.07.028>.
- Ma, Dali, Chung-hui Yang, Helen McNeill, Michael A. Simon, and Jeffrey D. Axelrod. 2003. “Fidelity in Planar Cell Polarity Signalling.” *Nature* 421 (6922): 543–47.
<https://doi.org/10.1038/nature01366>.
- Machacek, Matthias, Louis Hodgson, Christopher Welch, Hunter Elliott, Olivier Pertz, Perihan Nalbant, Amy Abell, Gary L. Johnson, Klaus M. Hahn, and Gaudenz Danuser. 2009. “Coordination of Rho GTPase Activities during Cell Protrusion.” *Nature* 461 (7260): 99–103. <https://doi.org/10.1038/nature08242>.
- Maier, Viola, Christine Jolicoeur, Helen Rayburn, Noriko Takegahara, Atsushi Kumanogoh, Hitoshi Kikutani, Marc Tessier-Lavigne, Wolfgang Wurst, and Roland H. Friedel. 2011. “Semaphorin 4C and 4G Are Ligands of Plexin-B2 Required in Cerebellar Development.” *Molecular and Cellular Neuroscience* 46 (2): 419–31.
<https://doi.org/10.1016/j.mcn.2010.11.005>.
- Maione, Federica, Stefania Capano, Donatella Regano, Lorena Zentilin, Mauro Giacca, Oriol Casanovas, Federico Bussolino, Guido Serini, and Enrico Giraud. 2012. “Semaphorin 3A Overcomes Cancer Hypoxia and Metastatic Dissemination Induced by Antiangiogenic Treatment in Mice.” *Journal of Clinical Investigation* 122 (5): 1832–48. <https://doi.org/10.1172/JCI58976>.

- Maione, Federica, Fabiola Molla, Claudia Meda, Roberto Latini, Lorena Zentilin, Mauro Giacca, Giorgio Seano, Guido Serini, Federico Bussolino, and Enrico Giraudo. 2009. "Semaphorin 3A Is an Endogenous Angiogenesis Inhibitor That Blocks Tumor Growth and Normalizes Tumor Vasculature in Transgenic Mouse Models." *Journal of Clinical Investigation* 119 (11): 3356–72. <https://doi.org/10.1172/JCI36308>.
- Makarova, Kira S., Daniel H. Haft, Rodolphe Barrangou, Stan J. J. Brouns, Emmanuelle Charpentier, Philippe Horvath, Sylvain Moineau, et al. 2011. "Evolution and Classification of the CRISPR–Cas Systems." *Nature Reviews Microbiology* 9 (6): 467–77. <https://doi.org/10.1038/nrmicro2577>.
- Margolis, B., and Jean-Paul Borg. 2005. "Apicobasal Polarity Complexes." *Journal of Cell Science* 118 (22): 5157–59. <https://doi.org/10.1242/jcs.02597>.
- Martin-Belmonte, Fernando, Ama Gassama, Anirban Datta, Wei Yu, Ursula Rescher, Volker Gerke, and Keith Mostov. 2007. "PTEN-Mediated Apical Segregation of Phosphoinositides Controls Epithelial Morphogenesis through Cdc42." *Cell* 128 (2): 383–97. <https://doi.org/10.1016/j.cell.2006.11.051>.
- Masuda, Kenta, Tatsuo Furuyama, Mizue Takahara, Shiho Fujioka, Hitomi Kurinami, and Shinobu Inagaki. 2004. "Sema4D Stimulates Axonal Outgrowth of Embryonic DRG Sensory Neurons." *Genes to Cells* 9 (9): 821–29. <https://doi.org/10.1111/j.1365-2443.2004.00766.x>.
- Matakatsu, H., and Seth S Blair. 2004. "Interactions between Fat and Dachshous and the Regulation of Planar Cell Polarity in the Drosophila Wing." *Development* 131 (15): 3785–94. <https://doi.org/10.1242/dev.01254>.
- Matis, M., and J. D. Axelrod. 2013. "Regulation of PCP by the Fat Signaling Pathway." *Genes & Development* 27 (20): 2207–20. <https://doi.org/10.1101/gad.228098.113>.
- May-Simera, Helen L., and Matthew W. Kelley. 2012. "Cilia, Wnt Signaling, and the Cytoskeleton." *Cilia* 1 (1): 7. <https://doi.org/10.1186/2046-2530-1-7>.
- Mehta, Vedanta, Kar Lai Pang, Daniel Rozbesky, Katrin Nather, Adam Keen, Dariusz Lachowski, Youxin Kong, et al. 2020. "The Guidance Receptor Plexin D1 Is a Mechanosensor in Endothelial Cells." *Nature* 578 (7794): 290–95. <https://doi.org/10.1038/s41586-020-1979-4>.
- Meng, Wenxiang, Yoshimi Mushika, Tetsuo Ichii, and Masatoshi Takeichi. 2008. "Anchorage of Microtubule Minus Ends to Adherens Junctions Regulates Epithelial Cell-Cell Contacts." *Cell* 135 (5): 948–59. <https://doi.org/10.1016/j.cell.2008.09.040>.
- Miao, Hui, Christian H. Nickel, Lloyd G. Cantley, Leslie A. Bruggeman, Laura N. Bennardo, and Bingcheng Wang. 2003. "EphA Kinase Activation Regulates HGF-Induced Epithelial Branching Morphogenesis." *Journal of Cell Biology* 162 (7): 1281–92. <https://doi.org/10.1083/jcb.200304018>.
- Miller, A. D., and F. Chen. 1996. "Retrovirus Packaging Cells Based on 10A1 Murine Leukemia Virus for Production of Vectors That Use Multiple Receptors for Cell

- Entry." *Journal of Virology* 70 (8): 5564–71.
<http://www.ncbi.nlm.nih.gov/pubmed/8764070>.
- Miranda, K. C., T. Khromykh, P. Christy, T. L. Le, C. J. Gottardi, A. S. Yap, J. L. Stow, and R. D. Teasdale. 2001. "A Dileucine Motif Targets E-Cadherin to the Basolateral Cell Surface in Madin-Darby Canine Kidney and LLC-PK1 Epithelial Cells." *The Journal of Biological Chemistry* 276 (25): 22565–72.
<https://doi.org/10.1074/jbc.M101907200>.
- Mojica, F. J. M., G. Juez, and F. Rodriguez-Valera. 1993. "Transcription at Different Salinities of *Haloferax Mediterranei* Sequences Adjacent to Partially Modified PstI Sites." *Molecular Microbiology* 9 (3): 613–21.
<https://doi.org/10.1111/j.1365-2958.1993.tb01721.x>.
- Montcouquiol, Mireille, Rivka A. Rachel, Pamela J. Lanford, Neal G. Copeland, Nancy A. Jenkins, and Matthew W. Kelley. 2003. "Identification of Vangl2 and Scrb1 as Planar Polarity Genes in Mammals." *Nature* 423 (6936): 173–77.
<https://doi.org/10.1038/nature01618>.
- Montesano, R., G. Schaller, and L. Orci. 1991. "Induction of Epithelial Tubular Morphogenesis in Vitro by Fibroblast-Derived Soluble Factors." *Cell* 66 (4): 697–711. [https://doi.org/10.1016/0092-8674\(91\)90115-f](https://doi.org/10.1016/0092-8674(91)90115-f).
- Morais-de-Sá, Eurico, Vincent Mirouse, and Daniel St Johnston. 2010. "APKC Phosphorylation of Bazooka Defines the Apical/Lateral Border in *Drosophila* Epithelial Cells." *Cell* 141 (3): 509–23. <https://doi.org/10.1016/j.cell.2010.02.040>.
- Morin, Xavier, and Yohanns Bellaïche. 2011. "Mitotic Spindle Orientation in Asymmetric and Symmetric Cell Divisions during Animal Development." *Developmental Cell* 21 (1): 102–19. <https://doi.org/10.1016/j.devcel.2011.06.012>.
- Morton, Diane G., Diane C. Shakes, Staci Nugent, Daryl Dichoso, Wenfu Wang, Andy Golden, and Kenneth J. Kemphues. 2002. "The *Caenorhabditis Elegans* Par-5 Gene Encodes a 14-3-3 Protein Required for Cellular Asymmetry in the Early Embryo." *Developmental Biology* 241 (1): 47–58. <https://doi.org/10.1006/dbio.2001.0489>.
- Motegi, Fumio, Seth Zonies, Yingsong Hao, Adrian A. Cuenca, Erik Griffin, and Geraldine Seydoux. 2011. "Microtubules Induce Self-Organization of Polarized PAR Domains in *Caenorhabditis Elegans* Zygotes." *Nature Cell Biology* 13 (11): 1361–67. <https://doi.org/10.1038/ncb2354>.
- Munro, Edwin, Jeremy Nance, and James R. Priess. 2004. "Cortical Flows Powered by Asymmetrical Contraction Transport PAR Proteins to Establish and Maintain Anterior-Posterior Polarity in the Early *C. Elegans* Embryo." *Developmental Cell* 7 (3): 413–24. <https://doi.org/10.1016/j.devcel.2004.08.001>.
- Musch, A., D. Cohen, G. Kreitzer, and E. Rodriguez-Boulan. 2001. "Cdc42 Regulates the Exit of Apical and Basolateral Proteins from the Trans-Golgi Network." *The EMBO Journal* 20 (9): 2171–79. <https://doi.org/10.1093/emboj/20.9.2171>.
- Müsch, Anne, David Cohen, and Enrique Rodriguez-Boulan. 1997. "Myosin II Is Involved in the Production of Constitutive Transport Vesicles from the TGN." *The Journal of*

- Cell Biology* 138 (2): 291–306. <https://doi.org/10.1083/jcb.138.2.291>.
- Nagai-Tamai, Yoko, Keiko Mizuno, Tomonori Hirose, Atsushi Suzuki, and Shigeo Ohno. 2002. “Regulated Protein-Protein Interaction between APKC and PAR-3 Plays an Essential Role in the Polarization of Epithelial Cells.” *Genes to Cells* 7 (11): 1161–71. <https://doi.org/10.1046/j.1365-2443.2002.00590.x>.
- Nair, Prakash N., Linda McArdle, John Cornell, Susan L. Cohn, and Raymond L. Stallings. 2007. “High-Resolution Analysis of 3p Deletion in Neuroblastoma and Differential Methylation of the SEMA3B Tumor Suppressor Gene.” *Cancer Genetics and Cytogenetics* 174 (2): 100–110. <https://doi.org/10.1016/j.cancergencyto.2006.11.017>.
- Negishi-Koga, Takako, Masahiro Shinohara, Noriko Komatsu, Haruhiko Bito, Tatsuhiko Kodama, Roland H. Friedel, and Hiroshi Takayanagi. 2011. “Suppression of Bone Formation by Osteoclastic Expression of Semaphorin 4D.” *Nature Medicine* 17 (11): 1473–80. <https://doi.org/10.1038/nm.2489>.
- Negishi-Koga, Takako, and Hiroshi Takayanagi. 2012. “Bone Cell Communication Factors and Semaphorins.” *BoneKEy Reports* 1 (September): 183. <https://doi.org/10.1038/BONEKEY.2012.183>.
- Nelson, W. James, Frauke Drees, and Soichiro Yamada. 2005. “Interaction of Cadherin with the Actin Cytoskeleton.” *Novartis Foundation Symposium* 269: 159–68; discussion 168–77, 223–30. <http://www.ncbi.nlm.nih.gov/pubmed/16358407>.
- Neufeld, Gera, Adi D. Sabag, Noa Rabinovicz, and Ofra Kessler. 2012. “Semaphorins in Angiogenesis and Tumor Progression.” *Cold Spring Harbor Perspectives in Medicine* 2 (1): a006718. <https://doi.org/10.1101/cshperspect.a006718>.
- Nguyen-Ngoc, Tu, Katayoun Afshar, and Pierre Gönczy. 2007. “Coupling of Cortical Dynein and Gα Proteins Mediates Spindle Positioning in *Caenorhabditis Elegans*.” *Nature Cell Biology* 9 (11): 1294–1302. <https://doi.org/10.1038/ncb1649>.
- Nikolopoulou, Evanthia, Gabriel L. Galea, Ana Rolo, Nicholas D. E. Greene, and Andrew J. Copp. 2017. “Neural Tube Closure: Cellular, Molecular and Biomechanical Mechanisms.” *Development* 144 (4): 552–66. <https://doi.org/10.1242/dev.145904>.
- Nishimura, Tamako, Hisao Honda, and Masatoshi Takeichi. 2012. “Planar Cell Polarity Links Axes of Spatial Dynamics in Neural-Tube Closure.” *Cell* 149 (5): 1084–97. <https://doi.org/10.1016/j.cell.2012.04.021>.
- Nóbrega-Pereira, Sandrina, Nicoletta Kessarlis, Tonggong Du, Shioko Kimura, Stewart A. Anderson, and Oscar Marín. 2008. “Postmitotic Nkx2-1 Controls the Migration of Telencephalic Interneurons by Direct Repression of Guidance Receptors.” *Neuron* 59 (5): 733–45. <https://doi.org/10.1016/j.neuron.2008.07.024>.
- Noda, Yasuko, Yasushi Okada, Nobuhito Saito, Mitsutoshi Setou, Ying Xu, Zheizeng Zhang, and Nobutaka Hirokawa. 2001. “KIFC3, a Microtubule Minus End-Directed Motor for the Apical Transport of Annexin XIIIb-Associated Triton-Insoluble Membranes.” *The Journal of Cell Biology* 155 (1): 77–88.

- <https://doi.org/10.1083/jcb.200108042>.
- Nunes de Almeida, Francisca, Rhian F. Walther, Mary T. Pressé, Evi Vlassaks, and Franck Pichaud. 2019. "Cdc42 Defines Apical Identity and Regulates Epithelial Morphogenesis by Promoting Apical Recruitment of Par6-APKC and Crumbs." *Development (Cambridge, England)* 146 (15). <https://doi.org/10.1242/dev.175497>.
- O'Brien, Lucy Erin, Tzuu-Shuh Jou, Anne L. Pollack, Qihang Zhang, Steen H. Hansen, Peter Yurchenco, and Keith E. Mostov. 2001. "Rac1 Orientates Epithelial Apical Polarity through Effects on Basolateral Laminin Assembly." *Nature Cell Biology* 3 (9): 831–38. <https://doi.org/10.1038/ncb0901-831>.
- Ogawa, Kazushige, Hiroki Wada, Noriyoshi Okada, Itsuki Harada, Takayuki Nakajima, Elena B. Pasquale, and Shingo Tsuyama. 2006. "EphB2 and Ephrin-B1 Expressed in the Adult Kidney Regulate the Cytoarchitecture of Medullary Tubule Cells through Rho Family GTPases." *Journal of Cell Science* 119 (3): 559–70. <https://doi.org/10.1242/jcs.02777>.
- Ohta, Kunimasa, Akihito Mizutani, Atsushi Kawakami, Yasunori Murakami, Yasuyo Kasuya, Shin Takagi, Hideaki Tanaka, and Hajime Fujisawa. 1995. "Plexin: A Novel Neuronal Cell Surface Molecule That Mediates Cell Adhesion via a Homophilic Binding Mechanism in the Presence of Calcium Ions." *Neuron* 14 (6): 1189–99. [https://doi.org/10.1016/0896-6273\(95\)90266-X](https://doi.org/10.1016/0896-6273(95)90266-X).
- Oinuma, I., Yukio Ishikawa, Hironori Katoh, and Manabu Negishi. 2004. "The Semaphorin 4D Receptor Plexin-B1 Is a GTPase Activating Protein for R-Ras." *Science* 305 (5685): 862–65. <https://doi.org/10.1126/science.1097545>.
- Oinuma, I., Hironori Katoh, and Manabu Negishi. 2004. "Molecular Dissection of the Semaphorin 4D Receptor Plexin-B1-Stimulated R-Ras GTPase-Activating Protein Activity and Neurite Remodeling in Hippocampal Neurons." *Journal of Neuroscience* 24 (50): 11473–80. <https://doi.org/10.1523/JNEUROSCI.3257-04.2004>.
- Oinuma, Izumi, Hironori Katoh, and Manabu Negishi. 2006. "Semaphorin 4D/Plexin-B1-Mediated R-Ras GAP Activity Inhibits Cell Migration by Regulating Beta(1) Integrin Activity." *The Journal of Cell Biology* 173 (4): 601–13. <https://doi.org/10.1083/jcb.200508204>.
- Okumura, Masako, Toyoaki Natsume, Masato T. Kanemaki, and Tomomi Kiyomitsu. 2018. "Dynein–Dynactin–NuMA Clusters Generate Cortical Spindle-Pulling Forces as a Multiarm Ensemble." *ELife* 7 (May): e36559. <https://doi.org/10.7554/eLife.36559>.
- Ooshio, T., N. Fujita, A. Yamada, T. Sato, Y. Kitagawa, R. Okamoto, S. Nakata, A. Miki, K. Irie, and Y. Takai. 2007. "Cooperative Roles of Par-3 and Afadin in the Formation of Adherens and Tight Junctions." *Journal of Cell Science* 120 (14): 2352–65. <https://doi.org/10.1242/jcs.03470>.
- Osmani, Naël, Nicolas Vitale, Jean-Paul Borg, and Sandrine Etienne-Manneville. 2006. "Scrib Controls Cdc42 Localization and Activity to Promote Cell Polarization during

- Astrocyte Migration." *Current Biology* 16 (24): 2395–2405.
<https://doi.org/10.1016/j.cub.2006.10.026>.
- Overeem, Arend W., David M. Bryant, and Sven C.D. van IJzendoorn. 2015.
 "Mechanisms of Apical–Basal Axis Orientation and Epithelial Lumen Positioning."
Trends in Cell Biology 25 (8): 476–85. <https://doi.org/10.1016/j.tcb.2015.04.002>.
- Oztan, Asli, Mark Silvis, Ora A. Weisz, Neil A. Bradbury, Shu-Chan Hsu, James R.
 Goldenring, Charles Yeaman, and Gerard Apodaca. 2007. "Exocyst Requirement
 for Endocytic Traffic Directed Toward the Apical and Basolateral Poles of Polarized
 MDCK Cells." Edited by Keith Mostov. *Molecular Biology of the Cell* 18 (10): 3978–
 92. <https://doi.org/10.1091/mbc.e07-02-0097>.
- Pan, Guoqing, Xiangling Zhang, Junyu Ren, Jianbo Lu, Wenliang Li, Hongmei Fu,
 Shufang Zhang, and Jun Li. 2013. "Semaphorin 5A, an Axon Guidance Molecule,
 Enhances the Invasion and Metastasis of Human Gastric Cancer through
 Activation of MMP9." *Pathology and Oncology Research* 19 (1): 11–18.
<https://doi.org/10.1007/s12253-012-9550-8>.
- Pan, Guoqing, Zhu Zhu, Jian Huang, Chenggang Yang, Ying Yang, Yingxia Wang, Xiaoyu
 Tuo, et al. 2013. "Semaphorin 5A Promotes Gastric Cancer Invasion/Metastasis
 via Urokinase-Type Plasminogen Activator/Phosphoinositide 3-Kinase/Protein
 Kinase B." *Digestive Diseases and Sciences* 58 (8): 2197–2204.
<https://doi.org/10.1007/s10620-013-2666-1>.
- Pan, Hongjie, and Robin E. Bachelder. 2010. "Autocrine Semaphorin3A Stimulates
 Eukaryotic Initiation Factor 4E-Dependent RhoA Translation in Breast Tumor
 Cells." *Experimental Cell Research* 316 (17): 2825–32.
<https://doi.org/10.1016/j.yexcr.2010.07.012>.
- Pan, Jie Xue, Fang Wang, and Long Yun Ye. 2016. "Doxorubicin-Induced Epithelial–
 Mesenchymal Transition through SEMA 4A in Hepatocellular Carcinoma."
Biochemical and Biophysical Research Communications 479 (4): 610–14.
<https://doi.org/10.1016/j.bbrc.2016.09.167>.
- Panbianco, Costanza, David Weinkove, Esther Zanin, David Jones, Nullin Divecha,
 Monica Gotta, and Julie Ahringer. 2008. "A Casein Kinase 1 and PAR Proteins
 Regulate Asymmetry of a PIP2 Synthesis Enzyme for Asymmetric Spindle
 Positioning." *Developmental Cell* 15 (2): 198–208.
<https://doi.org/10.1016/j.devcel.2008.06.002>.
- Papakrivopoulou, Eugenia, Elisavet Vasilopoulou, Maja T. Lindenmeyer, Sabrina
 Pacheco, Hortensja Ł. Brzóška, Karen L. Price, Maria Kolatsi-Joannou, et al. 2018.
 "Vangl2, a Planar Cell Polarity Molecule, Is Implicated in Irreversible and
 Reversible Kidney Glomerular Injury." *The Journal of Pathology* 246 (4): 485–96.
<https://doi.org/10.1002/path.5158>.
- Park, Dae Hwi, and Lesilee S. Rose. 2008. "Dynamic Localization of LIN-5 and GPR-1/2
 to Cortical Force Generation Domains during Spindle Positioning." *Developmental
 Biology* 315 (1): 42–54. <https://doi.org/10.1016/j.ydbio.2007.11.037>.
- Pasterkamp, R. Jeroen. 2012. "Getting Neural Circuits into Shape with Semaphorins."

- Nature Reviews Neuroscience* 13 (9): 605–18. <https://doi.org/10.1038/nrn3302>.
- Pasterkamp, R. Jeroen, Jacques J. Peschon, Melanie K. Spriggs, and Alex L. Kolodkin. 2003. “Semaphorin 7A Promotes Axon Outgrowth through Integrins and MAPKs.” *Nature* 424 (6947): 398–405. <https://doi.org/10.1038/nature01790>.
- Pasterkamp, R. Jeroen, and Roman J. Giger. 2009. “Semaphorin Function in Neural Plasticity and Disease.” *Current Opinion in Neurobiology* 19 (3): 263–74. <https://doi.org/10.1016/j.conb.2009.06.001>.
- Pegtel, D. Michiel, Saskia I.J. Ellenbroek, Alexander E.E. Mertens, Rob A. van der Kammen, Johan de Rooij, and John G. Collard. 2007. “The Par-Tiam1 Complex Controls Persistent Migration by Stabilizing Microtubule-Dependent Front-Rear Polarity.” *Current Biology* 17 (19): 1623–34. <https://doi.org/10.1016/j.cub.2007.08.035>.
- Peng, Juan, Aline Awad, Sokhavuth Sar, Ola Hamze Komaiha, Romina Moyano, Amel Rayal, Didier Samuel, et al. 2015. “Phosphoinositide 3-Kinase P110 δ Promotes Lumen Formation through the Enhancement of Apico-Basal Polarity and Basal Membrane Organization.” *Nature Communications* 6 (1): 5937. <https://doi.org/10.1038/ncomms6937>.
- Perälä, Nina, Madis Jakobson, Roxana Ola, Pietro Fazzari, Junia Y. Penachioni, Mariann Nymark, Tiina Tanninen, Tiina Immonen, Luca Tamagnone, and Hannu Sariola. 2011. “Sema4C-Plexin B2 Signalling Modulates Ureteric Branching in Developing Kidney.” *Differentiation* 81 (2): 81–91. <https://doi.org/10.1016/j.diff.2010.10.001>.
- Perez Bay, Andres E., Ryan Schreiner, Francesca Mazzoni, Jose M. Carvajal-Gonzalez, Diego Gravotta, Emilie Perret, Guillermo Lehmann Mantaras, Yuan-Shan Zhu, and Enrique J. Rodriguez-Boulan. 2013. “The Kinesin KIF16B Mediates Apical Transcytosis of Transferrin Receptor in AP-1B-Deficient Epithelia.” *The EMBO Journal* 32 (15): 2125–39. <https://doi.org/10.1038/emboj.2013.130>.
- Perez, Elena E., Jianbin Wang, Jeffrey C. Miller, Yann Jouvenot, Kenneth A. Kim, Olga Liu, Nathaniel Wang, et al. 2008. “Establishment of HIV-1 Resistance in CD4+ T Cells by Genome Editing Using Zinc-Finger Nucleases.” *Nature Biotechnology* 26 (7): 808–16. <https://doi.org/10.1038/nbt1410>.
- Perrot, Valerie, Jose Vazquez-Prado, and J. Silvio Gutkind. 2002. “Plexin B Regulates Rho through the Guanine Nucleotide Exchange Factors Leukemia-Associated Rho GEF (LARG) and PDZ-RhoGEF.” *The Journal of Biological Chemistry* 277 (45): 43115–20. <https://doi.org/10.1074/jbc.M206005200>.
- Peyre, Elise, Florence Jaouen, Mehdi Saadaoui, Laurence Haren, Andreas Merdes, Pascale Durbec, and Xavier Morin. 2011. “A Lateral Belt of Cortical LGN and NuMA Guides Mitotic Spindle Movements and Planar Division in Neuroepithelial Cells.” *The Journal of Cell Biology* 193 (1): 141–54. <https://doi.org/10.1083/jcb.201101039>.
- Poobalasingam, Thanushiyan, Laura L. Yates, Simone A. Walker, Miguel Pereira, Nina Y. Gross, Akmol Ali, Maria Kolatsi-Joannou, et al. 2017. “Heterozygous *Vangl2*^{Looptail} Mice Reveal Novel Roles for the Planar Cell Polarity Pathway in Adult Lung

- Homeostasis and Repair." *Disease Models & Mechanisms* 10 (4): 409–23.
<https://doi.org/10.1242/dmm.028175>.
- Potiron, Vincent, Patrick Nasarre, Joëlle Roche, Cynthia Healy, and Laurence Boumsell. 2007. "Semaphorin Signaling in the Immune System." *Semaphorins: Receptor and Intracellular Signaling Mechanisms* 600: 132–44.
https://doi.org/10.1007/978-0-387-70956-7_11.
- Pruyne, David W., Daniel H. Schott, and Anthony Bretscher. 1998. "Tropomyosin-Containing Actin Cables Direct the Myo2p-Dependent Polarized Delivery of Secretory Vesicles in Budding Yeast." *The Journal of Cell Biology* 143 (7): 1931–45.
<https://doi.org/10.1083/JCB.143.7.1931>.
- Puertollano, Rosa, Fernando Martín-Belmonte, Jaime Millán, María del Carmen de Marco, Juan P. Albar, Leonor Kremer, and Miguel A. Alonso. 1999. "The MAL Proteolipid Is Necessary for Normal Apical Transport and Accurate Sorting of the Influenza Virus Hemagglutinin in Madin-Darby Canine Kidney Cells." *The Journal of Cell Biology* 145 (1): 141–51. <https://doi.org/10.1083/jcb.145.1.141>.
- Qiao, X., Y. Liu, P. Li, Z. Chen, H. Li, X. Yang, R. H. Finnell, et al. 2016. "Genetic Analysis of Rare Coding Mutations in CELSR1-3 in Chinese Congenital Heart and Neural Tube Defects." *Clinical Science* 130 (24): 2329–40.
<https://doi.org/10.1042/CS20160686>.
- Qin, Yi, Walter H. Meisen, Yi Hao, and Ian G. Macara. 2010. "Tuba, a Cdc42 GEF, Is Required for Polarized Spindle Orientation during Epithelial Cyst Formation." *The Journal of Cell Biology* 189 (4): 661–69. <https://doi.org/10.1083/jcb.201002097>.
- Ran, F Ann, Patrick D Hsu, Jason Wright, Vineeta Agarwala, David A Scott, and Feng Zhang. 2013. "Genome Engineering Using the CRISPR-Cas9 System." *Nature Protocols* 8 (11): 2281–2308. <https://doi.org/10.1038/nprot.2013.143>.
- Rasmussen, J. P., S. S. Reddy, and J. R. Priess. 2012. "Laminin Is Required to Orient Epithelial Polarity in the C. Elegans Pharynx." *Development* 139 (11): 2050–60.
<https://doi.org/10.1242/dev.078360>.
- Rauchman, M. I., S. K. Nigam, E. Delpire, and S. R. Gullans. 1993. "An Osmotically Tolerant Inner Medullary Collecting Duct Cell Line from an SV40 Transgenic Mouse." *American Journal of Physiology-Renal Physiology* 265 (3): F416–24.
<https://doi.org/10.1152/ajprenal.1993.265.3.F416>.
- Rehman, Michael, Sreeharsha Gurrupu, Gabriella Cagnoni, Lorena Capparuccia, and Luca Tamagnone. 2016. "PlexinD1 Is a Novel Transcriptional Target and Effector of Notch Signaling in Cancer Cells." *PLoS ONE* 11 (10): e0164660.
<https://doi.org/10.1371/journal.pone.0164660>.
- Richardson, Helena E., and Marta Portela. 2017. "Tissue Growth and Tumorigenesis in Drosophila: Cell Polarity and the Hippo Pathway." *Current Opinion in Cell Biology* 48 (October): 1–9. <https://doi.org/10.1016/j.ceb.2017.03.006>.
- Ridley, Anne J., Martin A. Schwartz, Keith Burridge, Richard A. Firtel, Mark H. Ginsberg, Gary Borisy, J. Thomas Parsons, and Alan Rick Horwitz. 2003. "Cell Migration:

- Integrating Signals from Front to Back." *Science (New York, N.Y.)* 302 (5651): 1704–9. <https://doi.org/10.1126/science.1092053>.
- Riga, Amalia, Victoria G. Castiglioni, and Mike Boxem. 2020. "New Insights into Apical-Basal Polarization in Epithelia." *Current Opinion in Cell Biology* 62 (February): 1–8. <https://doi.org/10.1016/j.ceb.2019.07.017>.
- Roche, J., F. Boldog, M. Robinson, L. Robinson, M. Varella-Garcia, M. Swanton, B. Waggoner, et al. 1996. "Distinct 3p21.3 Deletions in Lung Cancer and Identification of a New Human Semaphorin." *Oncogene* 12 (6): 1289–97. <http://www.ncbi.nlm.nih.gov/pubmed/8649831>.
- Rodriguez-Boulán, Enrique, Geri Kreitzer, and Anne Műsch. 2005. "Organization of Vesicular Trafficking in Epithelia." *Nature Reviews Molecular Cell Biology* 6 (3): 233–47. <https://doi.org/10.1038/nrm1593>.
- Rodriguez-Boulán, Enrique, and Ian G. Macara. 2014. "Organization and Execution of the Epithelial Polarity Programme." *Nature Reviews Molecular Cell Biology* 15 (4): 225–42. <https://doi.org/10.1038/nrm3775>.
- Rodriguez-Fraticelli, Alejo E., and Fernando Martin-Belmonte. 2014. "Picking up the Threads: Extracellular Matrix Signals in Epithelial Morphogenesis." *Current Opinion in Cell Biology* 30 (October): 83–90. <https://doi.org/10.1016/j.ceb.2014.06.008>.
- Rohm, Beate, Belquis Rahim, Bedriska Kleiber, Iiris Hovatta, and Andreas W. Pűschel. 2000. "The Semaphorin 3A Receptor May Directly Regulate the Activity of Small GTPases." *FEBS Letters* 486 (1): 68–72. [https://doi.org/10.1016/S0014-5793\(00\)02240-7](https://doi.org/10.1016/S0014-5793(00)02240-7).
- Roignot, Julie, Xiao Peng, and Keith Mostov. 2013. "Polarity in Mammalian Epithelial Morphogenesis." *Cold Spring Harbor Perspectives in Biology* 5 (2): a013789. <https://doi.org/10.1101/cshperspect.a013789>.
- Rokavec, Matjaz, David Horst, and Heiko Hermeking. 2017. "Cellular Model of Colon Cancer Progression Reveals Signatures of MRNAs, MiRNA, LncRNAs, and Epigenetic Modifications Associated with Metastasis." *Cancer Research* 77 (8): 1854–67. <https://doi.org/10.1158/0008-5472.CAN-16-3236>.
- Roland, J. T., D. M. Bryant, A. Datta, A. Itzen, K. E. Mostov, and J. R. Goldenring. 2011. "Rab GTPase-Myo5B Complexes Control Membrane Recycling and Epithelial Polarization." *Proceedings of the National Academy of Sciences* 108 (7): 2789–94. <https://doi.org/10.1073/pnas.1010754108>.
- Sabag, Adi D., Julia Bode, Dorit Fink, Boaz Kigel, Wilfried Kugler, and Gera Neufeld. 2012. "Semaphorin-3D and Semaphorin-3E Inhibit the Development of Tumors from Glioblastoma Cells Implanted in the Cortex of the Brain." *PLoS ONE* 7 (8): e42912. <https://doi.org/10.1371/journal.pone.0042912>.
- Saburi, Sakura, Ian Hester, Evelyne Fischer, Marco Pontoglio, Vera Eremina, Manfred Gessler, Sue E. Quaggin, Robert Harrison, Richard Mount, and Helen McNeill. 2008. "Loss of Fat4 Disrupts PCP Signaling and Oriented Cell Division and Leads to

- Cystic Kidney Disease." *Nature Genetics* 40 (8): 1010–15.
<https://doi.org/10.1038/ng.179>.
- Sadanandam, Anguraj, Michelle L. Varney, Seema Singh, Abdelkader E. Ashour, Nicolas Moniaux, Shonali Deb, Subodh M. Lele, Surinder K. Batra, and Rakesh K. Singh. 2010. "High Gene Expression of Semaphorin 5A in Pancreatic Cancer Is Associated with Tumor Growth, Invasion and Metastasis." *International Journal of Cancer* 127 (6): 1373–83. <https://doi.org/10.1002/ijc.25166>.
- Sagot, Isabelle, Saskia K. Klee, and David Pellman. 2002. "Yeast Formins Regulate Cell Polarity by Controlling the Assembly of Actin Cables." *Nature Cell Biology* 4 (1): 42–50. <https://doi.org/10.1038/ncb719>.
- Saha, Bhaskar, Athéna R. Ypsilanti, Camille Boutin, Harold Cremer, and Alain Chédotal. 2012. "Plexin-B2 Regulates the Proliferation and Migration of Neuroblasts in the Postnatal and Adult Subventricular Zone." *The Journal of Neuroscience : The Official Journal of the Society for Neuroscience* 32 (47): 16892–905.
<https://doi.org/10.1523/JNEUROSCI.0344-12.2012>.
- Saitakis, Michael, Stéphanie Dogniaux, Christel Goudot, Nathalie Bufi, Sophie Asnacios, Mathieu Maurin, Clotilde Randriamampita, Atef Asnacios, and Claire Hivroz. 2017. "Different TCR-Induced T Lymphocyte Responses Are Potentiated by Stiffness with Variable Sensitivity." *ELife* 6 (June): e23190.
<https://doi.org/10.7554/eLife.23190>.
- Saito, Yasuhiro, Izumi Oinuma, Satoshi Fujimoto, and Manabu Negishi. 2009. "Plexin-B1 Is a GTPase Activating Protein for M-Ras, Remodelling Dendrite Morphology." *EMBO Reports* 10 (6): 614–21. <https://doi.org/10.1038/embor.2009.63>.
- Sakurai, Atsuko, Colleen Doci, and J. Silvio Gutkind. 2012. "Semaphorin Signaling in Angiogenesis, Lymphangiogenesis and Cancer." *Cell Research* 22 (1): 23–32.
<https://doi.org/10.1038/cr.2011.198>.
- Sakurai, Atsuko, Julie Gavard, Yuliya Annas-Linhares, John R. Basile, Panomwat Amornphimoltham, Todd R. Palmbly, Hiroshi Yagi, et al. 2010. "Semaphorin 3E Initiates Antiangiogenic Signaling through Plexin D1 by Regulating Arf6 and R-Ras." *Molecular and Cellular Biology* 30 (12): 3086–98.
<https://doi.org/10.1128/MCB.01652-09>.
- Saleh-Gohari, N., and Thomas Helleday. 2004. "Conservative Homologous Recombination Preferentially Repairs DNA Double-Strand Breaks in the S Phase of the Cell Cycle in Human Cells." *Nucleic Acids Research* 32 (12): 3683–88.
<https://doi.org/10.1093/nar/gkh703>.
- Salvarezza, Susana B., Sylvie Deborde, Ryan Schreiner, Fabien Campagne, Michael M. Kessels, Britta Qualmann, Alfredo Caceres, Geri Kreitzer, and Enrique Rodriguez-Boulan. 2009. "LIM Kinase 1 and Cofilin Regulate Actin Filament Population Required for Dynamin-Dependent Apical Carrier Fission from the Trans -Golgi Network." Edited by Sandra L. Schmid. *Molecular Biology of the Cell* 20 (1): 438–51. <https://doi.org/10.1091/mbc.e08-08-0891>.
- Sawyer, Jacob M., Jessica R. Harrell, Gidi Shemer, Jessica Sullivan-Brown, Minna Roh-

- Johnson, and Bob Goldstein. 2010. "Apical Constriction: A Cell Shape Change That Can Drive Morphogenesis." *Developmental Biology* 341 (1): 5–19. <https://doi.org/10.1016/j.ydbio.2009.09.009>.
- Saxena, Sugandha, Abhilasha Purohit, Michelle L. Varney, Yuri Hayashi, and Rakesh K. Singh. 2018. "Semaphorin-5A Maintains Epithelial Phenotype of Malignant Pancreatic Cancer Cells." *BMC Cancer* 18 (1): 1283. <https://doi.org/10.1186/s12885-018-5204-x>.
- Schaefer, M., A. Shevchenko, A. Shevchenko, and J. A. Knoblich. 2000. "A Protein Complex Containing Inscuteable and the Galpha-Binding Protein Pins Orients Asymmetric Cell Divisions in Drosophila." *Current Biology : CB* 10 (7): 353–62. [https://doi.org/10.1016/s0960-9822\(00\)00401-2](https://doi.org/10.1016/s0960-9822(00)00401-2).
- Scheiffele, P., M. G. Roth, and K. Simons. 1997. "Interaction of Influenza Virus Haemagglutinin with Sphingolipid-Cholesterol Membrane Domains via Its Transmembrane Domain." *The EMBO Journal* 16 (18): 5501–8. <https://doi.org/10.1093/emboj/16.18.5501>.
- Scheiffele, Peter, Johan Peränen, and Kai Simons. 1995. "N-Glycans as Apical Sorting Signals in Epithelial Cells." *Nature* 378 (6552): 96–98. <https://doi.org/10.1038/378096a0>.
- Schubert, C. M., R. Lin, C. J. de Vries, R. H. Plasterk, and J. R. Priess. 2000. "MEX-5 and MEX-6 Function to Establish Soma/Germline Asymmetry in Early C. Elegans Embryos." *Molecular Cell* 5 (4): 671–82. [https://doi.org/10.1016/s1097-2765\(00\)80246-4](https://doi.org/10.1016/s1097-2765(00)80246-4).
- Ségalen, Marion, Christopher A. Johnston, Charlotte A. Martin, Julien G. Dumortier, Kenneth E. Prehoda, Nicolas B. David, Chris Q. Doe, and Yohanns Bellaïche. 2010. "The Fz-Dsh Planar Cell Polarity Pathway Induces Oriented Cell Division via Mud/NuMA in Drosophila and Zebrafish." *Developmental Cell* 19 (5): 740–52. <https://doi.org/10.1016/j.devcel.2010.10.004>.
- Serini, Guido, Donatella Valdembri, Sara Zanivan, Giulia Morterra, Constanze Burkhardt, Francesca Caccavari, Luca Zammataro, et al. 2003. "Class 3 Semaphorins Control Vascular Morphogenesis by Inhibiting Integrin Function." *Nature* 424 (6947): 391–97. <https://doi.org/10.1038/nature01784>.
- Seward, Matthew E., Eric Swanson, Andrés Norambuena, Anja Reimann, J. Nicholas Cochran, Rong Li, Erik D. Roberson, and George S. Bloom. 2013. "Amyloid- β Signals through Tau to Drive Ectopic Neuronal Cell Cycle Re-Entry in Alzheimer's Disease." *Journal of Cell Science* 126 (Pt 5): 1278–86. <https://doi.org/10.1242/jcs.1125880>.
- Shahi, P., C. Y. Wang, J. Chou, C. Hagerling, H. Gonzalez Velozo, A. Ruderisch, Y. Yu, M. D. Lai, and Z. Werb. 2017. "GATA3 Targets Semaphorin 3B in Mammary Epithelial Cells to Suppress Breast Cancer Progression and Metastasis." *Oncogene* 36 (40): 5567–75. <https://doi.org/10.1038/onc.2017.165>.
- Shelly, Maya, Laura Cancedda, Byung Kook Lim, Andrei T. Popescu, Pei-lin Cheng, Hongfeng Gao, and Mu-ming Poo. 2011. "Semaphorin3A Regulates Neuronal

- Polarization by Suppressing Axon Formation and Promoting Dendrite Growth.” *Neuron* 71 (3): 433–46. <https://doi.org/10.1016/j.neuron.2011.06.041>.
- Shelly, Maya, Byung Kook Lim, Laura Cancedda, Sarah C. Heilshorn, Hongfeng Gao, and Mu Ming Poo. 2010. “Local and Long-Range Reciprocal Regulation of CAMP and CGMP in Axon/Dendrite Formation.” *Science* 327 (5965): 547–52. <https://doi.org/10.1126/science.1179735>.
- Shi, Wei, Atsushi Kumanogoh, Chie Watanabe, Junji Uchida, Xiaosong Wang, Teruhito Yasui, Kazunori Yukawa, et al. 2000. “The Class IV Semaphorin CD100 Plays Nonredundant Roles in the Immune System: Defective B and T Cell Activation in CD100-Deficient Mice.” *Immunity* 13 (5): 633–42. [https://doi.org/10.1016/S1074-7613\(00\)00063-7](https://doi.org/10.1016/S1074-7613(00)00063-7).
- Shimada, Y., T. Usui, S. Yanagawa, M. Takeichi, and T. Uemura. 2001. “Asymmetric Colocalization of Flamingo, a Seven-Pass Transmembrane Cadherin, and Dishevelled in Planar Cell Polarization.” *Current Biology : CB* 11 (11): 859–63. [https://doi.org/10.1016/s0960-9822\(01\)00233-0](https://doi.org/10.1016/s0960-9822(01)00233-0).
- Siegrist, Sarah E., and Chris Q. Doe. 2005. “Microtubule-Induced Pins/Gai Cortical Polarity in Drosophila Neuroblasts.” *Cell* 123 (7): 1323–35. <https://doi.org/10.1016/j.cell.2005.09.043>.
- Siller, Karsten H., Clemens Cabernard, and Chris Q. Doe. 2006. “The NuMA-Related Mud Protein Binds Pins and Regulates Spindle Orientation in Drosophila Neuroblasts.” *Nature Cell Biology* 8 (6): 594–600. <https://doi.org/10.1038/ncb1412>.
- Siller, Karsten H., and Chris Q. Doe. 2009. “Spindle Orientation during Asymmetric Cell Division.” *Nature Cell Biology* 11 (4): 365–74. <https://doi.org/10.1038/ncb0409-365>.
- Simon, M. A. 2004. “Planar Cell Polarity in the Drosophila Eye Is Directed by Graded Four-Jointed and Dachshous Expression.” *Development* 131 (24): 6175–84. <https://doi.org/10.1242/dev.01550>.
- Simon, Michael A., Aiguo Xu, Hiroyuki O. Ishikawa, and Kenneth D. Irvine. 2010. “Modulation of Fat:Dachshous Binding by the Cadherin Domain Kinase Four-Jointed.” *Current Biology* 20 (9): 811–17. <https://doi.org/10.1016/j.cub.2010.04.016>.
- Simons, Kai, and Mathias J. Gerl. 2010. “Revitalizing Membrane Rafts: New Tools and Insights.” *Nature Reviews Molecular Cell Biology* 11 (10): 688–99. <https://doi.org/10.1038/nrm2977>.
- Simons, Matias, Joachim Gloy, Athina Ganner, Axel Bullerkotte, Mikhail Bashkurov, Corinna Krönig, Bernhard Schermer, et al. 2005. “Inversin, the Gene Product Mutated in Nephronophthisis Type II, Functions as a Molecular Switch between Wnt Signaling Pathways.” *Nature Genetics* 37 (5): 537–43. <https://doi.org/10.1038/ng1552>.
- Simons, Matias, and Marek Mlodzik. 2008. “Planar Cell Polarity Signaling: From Fly

- Development to Human Disease." *Annual Review of Genetics* 42 (1): 517–40.
<https://doi.org/10.1146/annurev.genet.42.110807.091432>.
- Singh, H., and J.D. Aplin. 2015. "Endometrial Apical Glycoproteomic Analysis Reveals Roles for Cadherin 6, Desmoglein-2 and Plexin B2 in Epithelial Integrity." *MHR: Basic Science of Reproductive Medicine* 21 (1): 81–94.
<https://doi.org/10.1093/molehr/gau087>.
- Sokol, Sergei Y. 2015. "Spatial and Temporal Aspects of Wnt Signaling and Planar Cell Polarity during Vertebrate Embryonic Development." *Seminars in Cell & Developmental Biology* 42 (June): 78–85.
<https://doi.org/10.1016/j.semcdb.2015.05.002>.
- Spana, E. P., and C. Q. Doe. 1995. "The Prospero Transcription Factor Is Asymmetrically Localized to the Cell Cortex during Neuroblast Mitosis in *Drosophila*." *Development (Cambridge, England)* 121 (10): 3187–95.
<http://www.ncbi.nlm.nih.gov/pubmed/7588053>.
- Speicher, Stephan, Anja Fischer, Juergen Knoblich, and Ana Carmena. 2008. "The PDZ Protein Canoe Regulates the Asymmetric Division of *Drosophila* Neuroblasts and Muscle Progenitors." *Current Biology* 18 (11): 831–37.
<https://doi.org/10.1016/j.cub.2008.04.072>.
- Srinivasan, Dayalan G., Ridgely M. Fisk, Huihong Xu, and Sander van den Heuvel. 2003. "A Complex of LIN-5 and GPR Proteins Regulates G Protein Signaling and Spindle Function in *C. Elegans*." *Genes & Development* 17 (10): 1225–39.
<https://doi.org/10.1101/gad.1081203>.
- St Johnston, Daniel, and Julie Ahringer. 2010. "Cell Polarity in Eggs and Epithelia: Parallels and Diversity." *Cell* 141 (5): 757–74.
<https://doi.org/10.1016/j.cell.2010.05.011>.
- Stedden, Claire G., William Menegas, Allison L. Zajac, Audrey M. Williams, Shouqiang Cheng, Engin Özkan, and Sally Horne-Badovinac. 2019. "Planar-Polarized Semaphorin-5c and Plexin A Promote the Collective Migration of Epithelial Cells in *Drosophila*." *Current Biology* 29 (6): 908-920.e6.
<https://doi.org/10.1016/j.cub.2019.01.049>.
- Stein, W. von, Andreas Ramrath, Alexandra Grimm, Marion Müller-Borg, and Andreas Wodarz. 2005. "Direct Association of Bazooka/PAR-3 with the Lipid Phosphatase PTEN Reveals a Link between the PAR/APKC Complex and Phosphoinositide Signaling." *Development* 132 (7): 1675–86. <https://doi.org/10.1242/dev.01720>.
- Stoops, Emily H., and Michael J. Caplan. 2014. "Trafficking to the Apical and Basolateral Membranes in Polarized Epithelial Cells." *Journal of the American Society of Nephrology : JASN* 25 (7): 1375. <https://doi.org/10.1681/ASN.2013080883>.
- Straight, Samuel W., Kunyoo Shin, Vanessa C. Fogg, Shuling Fan, Chia-Jen Liu, Michael Roh, and Ben Margolis. 2004. "Loss of PALS1 Expression Leads to Tight Junction and Polarity Defects." *Molecular Biology of the Cell* 15 (4): 1981–90.
<https://doi.org/10.1091/mbc.e03-08-0620>.

- Strutt, David. 2003. "Frizzled Signalling and Cell Polarisation in *Drosophila* and Vertebrates." *Development* 130 (19): 4501–13. <https://doi.org/10.1242/dev.00695>.
- Sulston, J.E., E. Schierenberg, J.G. White, and J.N. Thomson. 1983. "The Embryonic Cell Lineage of the Nematode *Caenorhabditis Elegans*." *Developmental Biology* 100 (1): 64–119. [https://doi.org/10.1016/0012-1606\(83\)90201-4](https://doi.org/10.1016/0012-1606(83)90201-4).
- Sun, Tianliang, Lida Yang, Harmandeep Kaur, Jenny Pestel, Mario Looso, Hendrik Nolte, Cornelius Krasel, et al. 2017. "A Reverse Signaling Pathway Downstream of Sema4A Controls Cell Migration via Scrib." *The Journal of Cell Biology* 216 (1): 199–215. <https://doi.org/10.1083/jcb.201602002>.
- Suto, Fumikazu, Miu Tsuboi, Haruyuki Kamiya, Hidenobu Mizuno, Yuji Kiyama, Shoji Komai, Masayuki Shimizu, et al. 2007. "Interactions between Plexin-A2, Plexin-A4, and Semaphorin 6A Control Lamina-Restricted Projection of Hippocampal Mossy Fibers." *Neuron* 53 (4): 535–47. <https://doi.org/10.1016/j.neuron.2007.01.028>.
- Suzuki, Atsushi, Maki Hirata, Katsusi Kamimura, Rika Maniwa, Tomoyuki Yamanaka, Keiko Mizuno, Masaru Kishikawa, et al. 2004. "APKC Acts Upstream of PAR-1b in Both the Establishment and Maintenance of Mammalian Epithelial Polarity." *Current Biology* 14 (16): 1425–35. <https://doi.org/10.1016/j.cub.2004.08.021>.
- Suzuki, Kazuhiro, Atsushi Kumanogoh, and Hitoshi Kikutani. 2008. "Semaphorins and Their Receptors in Immune Cell Interactions." *Nature Immunology* 9 (1): 17–23. <https://doi.org/10.1038/ni1553>.
- Suzuki, Kazuhiro, Tatsusada Okuno, Midori Yamamoto, R. Jeroen Pasterkamp, Noriko Takegahara, Hyota Takamatsu, Tomoe Kitao, et al. 2007. "Semaphorin 7A Initiates T-Cell-Mediated Inflammatory Responses through Alpha1beta1 Integrin." *Nature* 446 (7136): 680–84. <https://doi.org/10.1038/nature05652>.
- Swiercz, Jakub M., Rohini Kuner, Jürgen Behrens, and Stefan Offermanns. 2002. "Plexin-B1 Directly Interacts with PDZ-RhoGEF/LARG to Regulate RhoA and Growth Cone Morphology." *Neuron* 35 (1): 51–63. [https://doi.org/10.1016/S0896-6273\(02\)00750-X](https://doi.org/10.1016/S0896-6273(02)00750-X).
- Swiercz, Jakub M., Rohini Kuner, and Stefan Offermanns. 2004. "Plexin-B1/RhoGEF-Mediated RhoA Activation Involves the Receptor Tyrosine Kinase ErbB-2." *The Journal of Cell Biology* 165 (6): 869–80. <https://doi.org/10.1083/jcb.200312094>.
- Swiercz, Jakub M., Thomas Worzfeld, and Stefan Offermanns. 2008. "ErbB-2 and Met Reciprocally Regulate Cellular Signaling via Plexin-B1." *Journal of Biological Chemistry* 283 (4): 1893–1901. <https://doi.org/10.1074/jbc.M706822200>.
- Tabuse, Y., Y. Izumi, F. Piano, K. J. Kemphues, J. Miwa, and S. Ohno. 1998. "Atypical Protein Kinase C Cooperates with PAR-3 to Establish Embryonic Polarity in *Caenorhabditis Elegans*." *Development (Cambridge, England)* 125 (18): 3607–14. <http://www.ncbi.nlm.nih.gov/pubmed/9716526>.
- Tada, M., and J. C. Smith. 2000. "Xwnt11 Is a Target of *Xenopus* Brachyury: Regulation of Gastrulation Movements via Dishevelled, but Not through the Canonical Wnt

- Pathway." *Development (Cambridge, England)* 127 (10): 2227–38.
<http://www.ncbi.nlm.nih.gov/pubmed/10769246>.
- Tai, A. W., J. Z. Chuang, C. Bode, U. Wolfrum, and C. H. Sung. 1999. "Rhodopsin's Carboxy-Terminal Cytoplasmic Tail Acts as a Membrane Receptor for Cytoplasmic Dynein by Binding to the Dynein Light Chain Tctex-1." *Cell* 97 (7): 877–87.
[https://doi.org/10.1016/s0092-8674\(00\)80800-4](https://doi.org/10.1016/s0092-8674(00)80800-4).
- Takamatsu, Hyota, and Atsushi Kumanogoh. 2012. "Diverse Roles for Semaphorin–plexin Signaling in the Immune System." *Trends in Immunology* 33 (3): 127–35. <https://doi.org/10.1016/j.it.2012.01.008>.
- Takamatsu, Hyota, Noriko Takegahara, Yukinobu Nakagawa, Michio Tomura, Masahiko Taniguchi, Roland H. Friedel, Helen Rayburn, et al. 2010. "Semaphorins Guide the Entry of Dendritic Cells into the Lymphatics by Activating Myosin II." *Nature Immunology* 11 (7): 594–600. <https://doi.org/10.1038/ni.1885>.
- Takeda, Tetsuro, Hajime Yamazaki, and Marilyn G. Farquhar. 2003. "Identification of an Apical Sorting Determinant in the Cytoplasmic Tail of Megalin." *American Journal of Physiology-Cell Physiology* 284 (5): C1105–13.
<https://doi.org/10.1152/ajpcell.00514.2002>.
- Takegahara, Noriko, Hyota Takamatsu, Toshihiko Toyofuku, Tohru Tsujimura, Tatsusada Okuno, Kazunori Yukawa, Masayuki Mizui, et al. 2006. "Plexin-A1 and Its Interaction with DAP12 in Immune Responses and Bone Homeostasis." *Nature Cell Biology* 8 (6): 615–22. <https://doi.org/10.1038/ncb1416>.
- Tam, Kevin J., Daniel H.F. Hui, Wilson W. Lee, Mingshu Dong, Tabitha Tombe, Ivy Z.F. Jiao, Shahram Khosravi, et al. 2017. "Semaphorin 3 C Drives Epithelial-to-Mesenchymal Transition, Invasiveness, and Stem-like Characteristics in Prostate Cells." *Scientific Reports* 7 (1): 11501.
<https://doi.org/10.1038/s41598-017-11914-6>.
- Tamagnone, L., S. Artigiani, H. Chen, Z. He, G. I. Ming, H. Song, A. Chedotal, et al. 1999. "Plexins Are a Large Family of Receptors for Transmembrane, Secreted, and GPI-Anchored Semaphorins in Vertebrates." *Cell* 99 (1): 71–80.
<http://www.ncbi.nlm.nih.gov/pubmed/10520995>.
- Tamagnone, Luca. 2012. "Emerging Role of Semaphorins as Major Regulatory Signals and Potential Therapeutic Targets in Cancer." *Cancer Cell* 22 (2): 145–52.
<https://doi.org/10.1016/j.ccr.2012.06.031>.
- Tamagnone, Luca, and Paolo M. Comoglio. 2004. "To Move or Not to Move? Semaphorin Signalling in Cell Migration." *EMBO Reports* 5 (4): 356–61.
<https://doi.org/10.1038/sj.embor.7400114>.
- Tanentzapf, Guy, and Ulrich Tepass. 2003. "Interactions between the Crumbs, Lethal Giant Larvae and Bazooka Pathways in Epithelial Polarization." *Nature Cell Biology* 5 (1): 46–52. <https://doi.org/10.1038/ncb896>.
- Tang, Ke, John L. R. Rubenstein, Sophia Y. Tsai, and Ming-Jer Tsai. 2012. "COUP-TFII Controls Amygdala Patterning by Regulating Neuropilin Expression." *Development*

- (Cambridge, England) 139 (9): 1630–39. <https://doi.org/10.1242/dev.075564>.
- Taya, Shinichiro, Naoyuki Inagaki, Hiroaki Sengiku, Hiroshi Makino, Akihiro Iwamatsu, Itaru Urakawa, Kenji Nagao, Shiro Kataoka, and Kozo Kaibuchi. 2001. “Direct Interaction of Insulin-like Growth Factor-1 Receptor with Leukemia-Associated RhoGEF.” *Journal of Cell Biology* 155 (5): 809–19. <https://doi.org/10.1083/jcb.200106139>.
- Tepass, U., C. Theres, and E. Knust. 1990. “Crumbs Encodes an EGF-like Protein Expressed on Apical Membranes of Drosophila Epithelial Cells and Required for Organization of Epithelia.” *Cell* 61 (5): 787–99. [https://doi.org/10.1016/0092-8674\(90\)90189-l](https://doi.org/10.1016/0092-8674(90)90189-l).
- Tepass, Ulrich. 2009. “FERM Proteins in Animal Morphogenesis.” *Current Opinion in Genetics & Development* 19 (4): 357–67. <https://doi.org/10.1016/j.gde.2009.05.006>.
- Thomas, Chloe, and David Strutt. 2012. “The Roles of the Cadherins Fat and Dachous in Planar Polarity Specification in Drosophila.” *Developmental Dynamics* 241 (1): 27–39. <https://doi.org/10.1002/dvdy.22736>.
- Thuenauer, R., Y.-C. Hsu, J. M. Carvajal-Gonzalez, S. Deborde, J.-Z. Chuang, W. Romer, A. Sonnleitner, E. Rodriguez-Boulan, and C.-H. Sung. 2014. “Four-Dimensional Live Imaging of Apical Biosynthetic Trafficking Reveals a Post-Golgi Sorting Role of Apical Endosomal Intermediates.” *Proceedings of the National Academy of Sciences* 111 (11): 4127–32. <https://doi.org/10.1073/pnas.1304168111>.
- Tissir, Fadel, Yibo Qu, Mireille Montcouquiol, Libing Zhou, Kouji Komatsu, Dongbo Shi, Toshihiko Fujimori, et al. 2010. “Lack of Cadherins Celsr2 and Celsr3 Impairs Ependymal Ciliogenesis, Leading to Fatal Hydrocephalus.” *Nature Neuroscience* 13 (6): 700–707. <https://doi.org/10.1038/nn.2555>.
- Tomizawa, Yoshio, Yoshitaka Sekido, Masashi Kondo, Boning Gao, Jun Yokota, Joëlle Roche, Harry Drabkin, Michael I. Lerman, Adi F. Gazdar, and John D. Minna. 2001. “Inhibition of Lung Cancer Cell Growth and Induction of Apoptosis after Reexpression of 3p21.3 Candidate Tumor Suppressor Gene SEMA3B.” *Proceedings of the National Academy of Sciences of the United States of America* 98 (24): 13954–59. <https://doi.org/10.1073/pnas.231490898>.
- Toyofuku, Toshihiko, Hong Zhang, Atsushi Kumanogoh, Noriko Takegahara, Fumikazu Suto, Junko Kamei, Kazuhiro Aoki, et al. 2004. “Dual Roles of Sema6D in Cardiac Morphogenesis through Region-Specific Association of Its Receptor, Plexin-A1, with off-Track and Vascular Endothelial Growth Factor Receptor Type 2.” *Genes and Development* 18 (4): 435–47. <https://doi.org/10.1101/gad.1167304>.
- Toyofuku, Toshihiko, Hong Zhang, Atsushi Kumanogoh, Noriko Takegahara, Masanori Yabuki, Koichiro Harada, Masatsugu Hori, and Hitoshi Kikutani. 2004. “Guidance of Myocardial Patterning in Cardiac Development by Sema6D Reverse Signalling.” *Nature Cell Biology* 6 (12): 1204–11. <https://doi.org/10.1038/ncb1193>.
- Tran, Tracy S., Maria E. Rubio, Roger L. Clem, Dontais Johnson, Lauren Case, Marc Tessier-Lavigne, Richard L. Haganir, David D. Ginty, and Alex L. Kolodkin. 2009.

- “Secreted Semaphorins Control Spine Distribution and Morphogenesis in the Postnatal CNS.” *Nature* 462 (7276): 1065–69.
<https://doi.org/10.1038/nature08628>.
- Tree, David R. P., Joshua M. Shulman, Raphaël Rousset, Matthew P. Scott, David Gubb, and Jeffrey D. Axelrod. 2002. “Prickle Mediates Feedback Amplification to Generate Asymmetric Planar Cell Polarity Signaling.” *Cell* 109 (3): 371–81.
[https://doi.org/10.1016/s0092-8674\(02\)00715-8](https://doi.org/10.1016/s0092-8674(02)00715-8).
- Tseng, Chun Hsien, Karl D. Murray, Mu Fan Jou, Su Ming Hsu, Hwai Jong Cheng, and Pei Hsin Huang. 2011. “Sema3E/Plexin-D1 Mediated Epithelial-to-Mesenchymal Transition in Ovarian Endometrioid Cancer.” *PLoS ONE* 6 (4): e19396.
<https://doi.org/10.1371/journal.pone.0019396>.
- “Unified Nomenclature for the Semaphorins/Collapsins. Semaphorin Nomenclature Committee.” 1999. *Cell* 97 (5): 551–52.
<https://www.ncbi.nlm.nih.gov/pubmed/10367884>.
- Usui, T., Y. Shima, Y. Shimada, S. Hirano, R. W. Burgess, T. L. Schwarz, M. Takeichi, and T. Uemura. 1999. “Flamingo, a Seven-Pass Transmembrane Cadherin, Regulates Planar Cell Polarity under the Control of Frizzled.” *Cell* 98 (5): 585–95.
[https://doi.org/10.1016/s0092-8674\(00\)80046-x](https://doi.org/10.1016/s0092-8674(00)80046-x).
- VanderVorst, Kacey, Jason Hatakeyama, Anastasia Berg, Hyun Lee, and Kermit L. Carraway. 2018. “Cellular and Molecular Mechanisms Underlying Planar Cell Polarity Pathway Contributions to Cancer Malignancy.” *Seminars in Cell & Developmental Biology* 81 (September): 78–87.
<https://doi.org/10.1016/j.semcdb.2017.09.026>.
- Varma, Saaket, Yuxia Cao, Jean-Bosco Tagne, Meenakshi Lakshminarayanan, Jun Li, Thomas B. Friedman, Robert J. Morell, David Warburton, Darrell N. Kotton, and Maria I. Ramirez. 2012. “The Transcription Factors Grainyhead-like 2 and NK2-Homeobox 1 Form a Regulatory Loop That Coordinates Lung Epithelial Cell Morphogenesis and Differentiation.” *The Journal of Biological Chemistry* 287 (44): 37282–95. <https://doi.org/10.1074/jbc.M112.408401>.
- Varshavsky, Asya, Ofra Kessler, Sivan Abramovitch, Boaz Kigel, Shelly Zaffryar, Gal Akiri, and Gera Neufeld. 2008. “Semaphorin-3B Is an Angiogenesis Inhibitor That Is Inactivated by Furin-like pro-Protein Convertases.” *Cancer Research* 68 (17): 6922–31. <https://doi.org/10.1158/0008-5472.CAN-07-5408>.
- Veeman, Michael T., Jeffrey D. Axelrod, and Randall T. Moon. 2003. “A Second Canon. Functions and Mechanisms of Beta-Catenin-Independent Wnt Signaling.” *Developmental Cell* 5 (3): 367–77.
<http://www.ncbi.nlm.nih.gov/pubmed/12967557>.
- Vikis, H. G., W. Li, Z. He, and K. L. Guan. 2000. “The Semaphorin Receptor Plexin-B1 Specifically Interacts with Active Rac in a Ligand-Dependent Manner.” *Proceedings of the National Academy of Sciences of the United States of America* 97 (23): 12457–62. <https://doi.org/10.1073/pnas.220421797>.
- Vladar, Eszter K., Roy D. Bayly, Ashvin M. Sangoram, Matthew P. Scott, and Jeffrey D.

- Axelrod. 2012. "Microtubules Enable the Planar Cell Polarity of Airway Cilia." *Current Biology* 22 (23): 2203–12. <https://doi.org/10.1016/j.cub.2012.09.046>.
- Wallingford, John B. 2012. "Planar Cell Polarity and the Developmental Control of Cell Behavior in Vertebrate Embryos." *Annual Review of Cell and Developmental Biology* 28 (1): 627–53. <https://doi.org/10.1146/annurev-cellbio-092910-154208>.
- Wallingford, John B., Brian A. Rowning, Kevin M. Vogeli, Ute Rothbächer, Scott E. Fraser, and Richard M. Harland. 2000. "Dishevelled Controls Cell Polarity during *Xenopus* Gastrulation." *Nature* 405 (6782): 81–85. <https://doi.org/10.1038/35011077>.
- Wang, H.-R., Yue Zhang, Barish Ozdamar, Abiodun A. Ogunjimi, Evguenia Alexandrova, Gerald H. Thomsen, and Jeffrey L. Wrana. 2003. "Regulation of Cell Polarity and Protrusion Formation by Targeting RhoA for Degradation." *Science* 302 (5651): 1775–79. <https://doi.org/10.1126/science.1090772>.
- Wang, Hui, Prasanta K. Hota, Yufeng Tong, Buren Li, Limin Shen, Lyudmila Nedyalkova, Susmita Borthakur, et al. 2011. "Structural Basis of Rnd1 Binding to Plexin Rho GTPase Binding Domains (RBDs)." *Journal of Biological Chemistry* 286 (29): 26093–106. <https://doi.org/10.1074/jbc.M110.197053>.
- Wang, Y., H. He, N. Srivastava, S. Vikarunnessa, Y.-b. Chen, J. Jiang, C. W. Cowan, and X. Zhang. 2012. "Plexins Are GTPase-Activating Proteins for Rap and Are Activated by Induced Dimerization." *Science Signaling* 5 (207): ra6. <https://doi.org/10.1126/scisignal.2002636>.
- Wang, Y., and J. Nathans. 2007. "Tissue/Planar Cell Polarity in Vertebrates: New Insights and New Questions." *Development* 134 (4): 647–58. <https://doi.org/10.1242/dev.02772>.
- Wang, Zhao, Jie Chen, Wei Zhang, Yang Zheng, Zilu Wang, Laikui Liu, Heming Wu, et al. 2016. "Axon Guidance Molecule Semaphorin3A Is a Novel Tumor Suppressor in Head and Neck Squamous Cell Carcinoma." *Oncotarget* 7 (5): 6048–62. <https://doi.org/10.18632/oncotarget.6831>.
- Wedlich-Soldner, Roland, Stephanie C. Wai, Thomas Schmidt, and Rong Li. 2004. "Robust Cell Polarity Is a Dynamic State Established by Coupling Transport and GTPase Signaling." *The Journal of Cell Biology* 166 (6): 889–900. <https://doi.org/10.1083/jcb.200405061>.
- Wilson, Patricia D. 2011. "Apico-Basal Polarity in Polycystic Kidney Disease Epithelia." *Biochimica et Biophysica Acta (BBA) - Molecular Basis of Disease* 1812 (10): 1239–48. <https://doi.org/10.1016/j.bbadis.2011.05.008>.
- Winberg, Margaret L., Jasprina N. Noordermeer, Luca Tamagnone, Paolo M. Comoglio, Melanie K. Spriggs, Marc Tessier-Lavigne, and Corey S. Goodman. 1998. "Plexin A Is a Neuronal Semaphorin Receptor That Controls Axon Guidance." *Cell* 95 (7): 903–16. [https://doi.org/10.1016/S0092-8674\(00\)81715-8](https://doi.org/10.1016/S0092-8674(00)81715-8).
- Wirtz-Peitz, Frederik, Takashi Nishimura, and Juergen A. Knoblich. 2008. "Linking Cell Cycle to Asymmetric Division: Aurora-A Phosphorylates the Par Complex to

- Regulate Numb Localization." *Cell* 135 (1): 161–73.
<https://doi.org/10.1016/j.cell.2008.07.049>.
- Wodarz, Andreas, Uwe Hinz, Martin Engelbert, and Elisabeth Knust. 1995. "Expression of Crumbs Confers Apical Character on Plasma Membrane Domains of Ectodermal Epithelia of *Drosophila*." *Cell* 82 (1): 67–76.
[https://doi.org/10.1016/0092-8674\(95\)90053-5](https://doi.org/10.1016/0092-8674(95)90053-5).
- Wong, Oscar Gee Wan, Tharani Nitkunan, Izumi Oinuma, Chun Zhou, Veronique Blanc, Richard S.D. Brown, Simon R.J. Bott, et al. 2007. "Plexin-B1 Mutations in Prostate Cancer." *Proceedings of the National Academy of Sciences of the United States of America* 104 (48): 19040–45. <https://doi.org/10.1073/pnas.0702544104>.
- Worzfeld, Thomas, and Stefan Offermanns. 2014. "Semaphorins and Plexins as Therapeutic Targets." *Nature Reviews Drug Discovery* 13 (8): 603–21.
<https://doi.org/10.1038/nrd4337>.
- Worzfeld, Thomas, and Markus Schwaninger. 2016. "Apicobasal Polarity of Brain Endothelial Cells." *Journal of Cerebral Blood Flow & Metabolism* 36 (2): 340–62.
<https://doi.org/10.1177/0271678X15608644>.
- Worzfeld, Thomas, Jakub M. Swiercz, Aycan Sentürk, Berit Genz, Alexander Korostylev, Suhua Deng, Jingjing Xia, et al. 2014. "Genetic Dissection of Plexin Signaling in Vivo." *Proceedings of the National Academy of Sciences of the United States of America* 111 (6): 2194–99. <https://doi.org/10.1073/pnas.1308418111>.
- Wu, Jun, Angel-Carlos Roman, Jose Maria Carvajal-Gonzalez, and Marek Mlodzik. 2013. "Wg and Wnt4 Provide Long-Range Directional Input to Planar Cell Polarity Orientation in *Drosophila*." *Nature Cell Biology* 15 (9): 1045–55.
<https://doi.org/10.1038/ncb2806>.
- Xia, Jingjing, Jakub M. Swiercz, Inmaculada Bañón-Rodríguez, Ivana Matković, Giuseppina Federico, Tianliang Sun, Timo Franz, et al. 2015. "Semaphorin-Plexin Signaling Controls Mitotic Spindle Orientation during Epithelial Morphogenesis and Repair." *Developmental Cell* 33 (3): 299–313.
<https://doi.org/10.1016/j.devcel.2015.02.001>.
- Xiang, Rui Hua, Charles H. Hensel, Dawn K. Garcia, Helene C. Carlson, Klaas Kok, Maria C. Daly, Karen Kerbacher, et al. 1996. "Isolation of the Human Semaphorin III/F Gene (SEM A3F) at Chromosome 3p21, a Region Deleted in Lung Cancer." *Genomics* 32 (1): 39–48. <https://doi.org/10.1006/geno.1996.0074>.
- Xie, Wei, and Jun Zhou. 2017. "Regulation of Mitotic Spindle Orientation during Epidermal Stratification." *Journal of Cellular Physiology* 232 (7): 1634–39.
<https://doi.org/10.1002/jcp.25750>.
- Xu, Xuejun, Zhiping Zhao, Shixiang Guo, Jian Li, Songsong Liu, Yu You, Bing Ni, Huaizhi Wang, and Ping Bie. 2017. "Increased Semaphorin 3c Expression Promotes Tumor Growth and Metastasis in Pancreatic Ductal Adenocarcinoma by Activating the ERK1/2 Signaling Pathway." *Cancer Letters* 397 (July): 12–22.
<https://doi.org/10.1016/j.canlet.2017.03.014>.

- Yamamoto, Midori, Kazuhiro Suzuki, Tatsusada Okuno, Takehiro Ogata, Noriko Takegahara, Hyota Takamatsu, Masayuki Mizui, et al. 2008. "Plexin-A4 Negatively Regulates T Lymphocyte Responses." *International Immunology* 20 (3): 413–20. <https://doi.org/10.1093/intimm/dxn006>.
- Yamanaka, Tomoyuki, Yosuke Horikoshi, Yuki Sugiyama, Chikako Ishiyama, Atsushi Suzuki, Tomonori Hirose, Akihiro Iwamatsu, Azusa Shinohara, and Shigeo Ohno. 2003. "Mammalian Lgl Forms a Protein Complex with PAR-6 and APKC Independently of PAR-3 to Regulate Epithelial Cell Polarity." *Current Biology : CB* 13 (9): 734–43. [https://doi.org/10.1016/s0960-9822\(03\)00244-6](https://doi.org/10.1016/s0960-9822(03)00244-6).
- Yamanaka, Yojiro, Amy Ralston, Robert O. Stephenson, and Janet Rossant. 2006. "Cell and Molecular Regulation of the Mouse Blastocyst." *Developmental Dynamics* 235 (9): 2301–14. <https://doi.org/10.1002/dvdy.20844>.
- Yang, Chung-hui, Jeffrey D. Axelrod, and Michael A. Simon. 2002. "Regulation of Frizzled by Fat-like Cadherins during Planar Polarity Signaling in the Drosophila Compound Eye." *Cell* 108 (5): 675–88. [https://doi.org/10.1016/s0092-8674\(02\)00658-x](https://doi.org/10.1016/s0092-8674(02)00658-x).
- Yang, Jienian, Maksim V. Plikus, and Natalia L. Komarova. 2015. "The Role of Symmetric Stem Cell Divisions in Tissue Homeostasis." *PLoS Computational Biology* 11 (12): e1004629. <https://doi.org/10.1371/JOURNAL.PCBI.1004629>.
- Yates, Laura L., Carsten Schnatwinkel, Jennifer N. Murdoch, Debora Bogani, Caroline J. Formstone, Stuart Townsend, Andy Greenfield, Lee A. Niswander, and Charlotte H. Dean. 2010. "The PCP Genes *Celsr1* and *Vangl2* Are Required for Normal Lung Branching Morphogenesis." *Human Molecular Genetics* 19 (11): 2251–67. <https://doi.org/10.1093/hmg/ddq104>.
- Yeaman, Charles, M. Inmaculada Ayala, Jessica R. Wright, Frederic Bard, Carine Bossard, Agnes Ang, Yusuke Maeda, et al. 2004. "Protein Kinase D Regulates Basolateral Membrane Protein Exit from Trans-Golgi Network." *Nature Cell Biology* 6 (2): 106–12. <https://doi.org/10.1038/ncb1090>.
- Yeaman, Charles, Annick H. Le Gall, Anne N. Baldwin, Laure Monlauzeur, Andre Le Bivic, and Enrique Rodriguez-Boulan. 1997. "The O-Glycosylated Stalk Domain Is Required for Apical Sorting of Neurotrophin Receptors in Polarized MDCK Cells." *The Journal of Cell Biology* 139 (4): 929–40. <https://doi.org/10.1083/jcb.139.4.929>.
- Yoo, Sa Kan, Heath G. Pascoe, Telmo Pereira, Shu Kondo, Antonio Jacinto, Xuewu Zhang, and Iswar K. Hariharan. 2016. "Plexins Function in Epithelial Repair in Both Drosophila and Zebrafish." *Nature Communications* 7 (July): 12282. <https://doi.org/10.1038/ncomms12282>.
- Yu, F., X. Morin, Y. Cai, X. Yang, and W. Chia. 2000. "Analysis of Partner of Inscuteable, a Novel Player of Drosophila Asymmetric Divisions, Reveals Two Distinct Steps in Inscuteable Apical Localization." *Cell* 100 (4): 399–409. [https://doi.org/10.1016/s0092-8674\(00\)80676-5](https://doi.org/10.1016/s0092-8674(00)80676-5).
- Yu, Fengwei, Chay T. Kuo, and Yuh Nung Jan. 2006. "Drosophila Neuroblast

- Asymmetric Cell Division: Recent Advances and Implications for Stem Cell Biology." *Neuron* 51 (1): 13–20. <https://doi.org/10.1016/j.neuron.2006.06.016>.
- Yu, Wei, Anirban Datta, Pascale Leroy, Lucy Erin O'Brien, Grace Mak, Tzoo-Shuh Jou, Karl S. Matlin, Keith E. Mostov, and Mirjam M.P. Zegers. 2005. "B1-Integrin Orients Epithelial Polarity via Rac1 and Laminin." *Molecular Biology of the Cell* 16 (2): 433–45. <https://doi.org/10.1091/mbc.e04-05-0435>.
- Yukawa, Kazunori, Tetsuji Tanaka, Kenji Yoshida, Noriko Takeuchi, Takuji Ito, Hyota Takamatsu, Hitoshi Kikutani, and Atsushi Kumanogoh. 2010. "Sema4A Induces Cell Morphological Changes through B-Type Plexin-Mediated Signaling." *International Journal of Molecular Medicine* 25 (2): 225–30. https://doi.org/10.3892/ijmm_00000334.
- Zanata, Silvio M., Iiris Hovatta, Beate Rohm, and Andreas W. Püschel. 2002. "Antagonistic Effects of Rnd1 and RhoD GTPases Regulate Receptor Activity in Semaphorin 3A-Induced Cytoskeletal Collapse." *Journal of Neuroscience* 22 (2): 471–77. <https://doi.org/10.1523/JNEUROSCI.22-02-00471.2002>.
- Zhang, Chen, Chunying Xiao, Erle Dang, Jiao Cao, Zhenlai Zhu, Meng Fu, Xu Yao, et al. 2018. "CD100–Plexin-B2 Promotes the Inflammation in Psoriasis by Activating NF- κ B and the Inflammasome in Keratinocytes." *Journal of Investigative Dermatology* 138 (2): 375–83. <https://doi.org/10.1016/j.jid.2017.09.005>.
- Zhang, Yun, and Robert A. Weinberg. 2018. "Epithelial-to-Mesenchymal Transition in Cancer: Complexity and Opportunities." *Frontiers of Medicine* 12 (4): 361–73. <https://doi.org/10.1007/s11684-018-0656-6>.
- Zhang, Z., K. Vuori, H. Wang, J. C. Reed, and E. Ruoslahti. 1996. "Integrin Activation by R-Ras." *Cell* 85 (1): 61–69. [https://doi.org/10.1016/s0092-8674\(00\)81082-x](https://doi.org/10.1016/s0092-8674(00)81082-x).
- Zhu, Jinwei, Wenyu Wen, Zhen Zheng, Yuan Shang, Zhiyi Wei, Zhuoni Xiao, Zhu Pan, Quansheng Du, Wenning Wang, and Mingjie Zhang. 2011. "LGN/MInsc and LGN/NuMA Complex Structures Suggest Distinct Functions in Asymmetric Cell Division for the Par3/MInsc/LGN and Gai/LGN/NuMA Pathways." *Molecular Cell* 43 (3): 418–31. <https://doi.org/10.1016/j.molcel.2011.07.011>.
- Zihni, Ceniz, Peter M.G. Munro, Ahmed Elbediwy, Nicholas H. Keep, Stephen J. Terry, John Harris, Maria S. Balda, and Karl Matter. 2014. "Dbl3 Drives Cdc42 Signaling at the Apical Margin to Regulate Junction Position and Apical Differentiation." *The Journal of Cell Biology* 204 (1): 111–27. <https://doi.org/10.1083/jcb.201304064>.
- Ziomek, C., and M. H. Johnson. 1980. "Cell Surface Interaction Induces Polarization of Mouse 8-Cell Blastomeres at Compaction." *Cell* 21 (3): 935–42. [https://doi.org/10.1016/0092-8674\(80\)90457-2](https://doi.org/10.1016/0092-8674(80)90457-2).